MACROPHAGE – *CRYPTOCOCCUS* INTERACTIONS DURING CRYPTOCOCCOSIS

by

Kerstin Voelz, Diplom-Biologist

A thesis submitted to

The University of Birmingham

for the degree of DOCTOR OF PHILOSOPHY

College of Life and Environmental Sciences

School of Biosciences

University of Birmingham

September 2010

“Das Leben is wert gelebt zu werden,

sagt die Kunst, die Schönste aller Verführerin;

das Leben ist wert, erkannt zu werden,

sagt die Wissenschaft.”

“Life is worth living,

says art, the beautiful temptress;

life is worth knowing,

says science.”

Friedrich Nietzsche

The human fungal pathogens *Cryptococcus neoformans* and *C. gattii* cause life-threatening infections of the central nervous system. One of the major characteristics of cryptococcal disease is the ability of the pathogen to parasitise upon phagocytic immune effector cells. *Cryptococcus* can survive and proliferate within macrophages, and is also able to escape into the extracellular environment via a non-lytic mechanism ('expulsion') and can be transferred directly from one cell to another (lateral transfer).

It is well established that the host's cytokine profile dramatically affects the outcome of cryptococcal infections. Patients exhibiting a so-called 'Th1' response have a significantly better clinical prognosis than those exhibiting a 'Th2' response. In the first part of this thesis, it is demonstrated that enhanced Th2, but not Th1, cytokine levels lead to increased intracellular cryptococcal proliferation but lower levels of cryptococcal expulsion. Thus, Th2 responses favor cryptococcal survival and dissemination leading to fatal infections of the central nervous system. These results help to explain the observed poor prognosis associated with the dominant Th2 cytokine profile (e.g. in HIV-infected patients).

Despite the importance of phagocyte/*Cryptococcus* interactions to disease progression, current methods for assaying virulence in the macrophage system are both time consuming and low throughput. In the second part of the thesis, the first stable and fully characterised GFP-expressing derivates of two widely used cryptococcal strains: *C. neoformans* serotype A type strain H99 and *C. gattii* serotype B type strain R265 are introduced and their use in the development of a method to effectively and rapidly investigate macrophage parasitism by flow cytometry, a technique that preserves the accuracy of current approaches but offers four-fold improvement in speed, is reported.

In addition, work to examine how *Cryptococcus*-macrophage interaction relates to a novel outbreak of cryptococcosis in immunocompetent individuals has been extended. Isolates from an ongoing outbreak on Vancouver Island, Canada, share an increased ability to proliferate within macrophages that correlates with a characteristic tubular morphology of cryptococcal mitochondria. The third part of the thesis dissects cellular conditions within the host as inducer of tubular morphology, describes the early onset of mitochondrial tubularisation upon encounter of the intracellular niche in a hypervirulent isolate and the first steps towards a comparative mitochondrial genome sequencing approach to identify molecular mechanisms.

There are so many people who have contributed to this piece of work, many of them might not even be aware of how much support they provided. I would like to thank everyone around me for his or her contribution in the last three years and would like to take this chance to acknowledge several people who had a particular strong impact during my PhD studies in the next few lines.

First of all, I would like to express my deep gratitude to my supervisor Robin May. Robin, you have provided fantastic support and guidance throughout the last three years and I believe I can say I could have not asked for a better supervisor. You supported me in my development as an independent researcher by believing in me and giving me the freedom to follow my own ideas whilst making sure that I stayed on track. Your door was always open to come in for a chat. Thank you for giving me the chance to do my PhD in your lab and for the continuing support you have been offering.

On my scientific way, I encountered many challenges and many people helped me to live up to these: Tony Lammas who showed me how to master primary human macrophages helping me to publish my first paper, Julian Rutherford and Robert Panting who hosted me for two months in Newcastle and taught me biolistic transformation laying the foundation of a second publication and Teun Boekhout and Ferry Hagen who gave me the opportunity to work with them for three weeks at the CBS in the Netherlands helping me to extract DNA and to beat DNA contaminations I had been struggling with for a long time. I would like to thank all of you for your help.

Not only Robin, the whole May-lab: Elizabeth, Nicola, Hansong, Rhiannon, Leanne and Simon offered me constant support. It has been an honour working with you and you guys are not only colleagues – you have become friends. Simon, thanks for all your patience when I couldn't figure out how to use the microscopes and the great GFP project we did together – it was great fun.

I have been incredibly fortunate to have a great circle of friends around that stood by me. I want to mention Elizabeth and Nicola, together with my dear neighbour Femy, who helped me through a very difficult personal time and always had an open ear and dried many tears. I hope you know how much you helped me to enjoy and love life again. I would also like to mention my wonderful and dearest housemates Angela Joyce and Lu Chen who patiently dealt with a lot of stressing out and self-doubt on my side but always encouraged me to keep going when things seemed tough. Last but not least, I want to thank Phil, Charlie, Cathy and Serena for keeping the ropes together in the last year. I love our little adventures together and hope they keep coming.

Die letzten Zeilen möchte ich zwei besonderen Menschen widmen – meinen Eltern. Ein besonderer Dank kommt Euch zu teil: schweren Herzen habt ihr mich ziehen lassen um meinen akademischen Traum des Doktortitels zu erfüllen. Obwohl keiner von euch beiden die Erfahrung einer universitären Ausbildung machen konnte, habt ihr mich auf meinem Weg unterstützt und standet hinter mir selbst wenn ihr meine Entscheidungen nicht immer verstanden habt. Vielen Dank!

Opportunistic pathogens have become of increasing medical importance over the last decade due to the AIDS pandemic. Cryptococcosis is not only the fourth most common fatal infectious disease in sub-Saharan Africa, but *Cryptococcus* is also an emerging pathogen of immunocompetent individuals. The interaction between the yeast and macrophages, specialized cells of the host's immune system, is a major determinant for the outcome of disease. *Cryptococcus* can survive and proliferate within these cells, and is also able to escape into the extracellular environment via a non-lytic mechanism ('expulsion') and can be transferred directly from one cell to another (lateral transfer). Further definition of cryptococcal interaction with macrophages may improve cryptococcosis treatment by highlighting potentially novel therapeutic approaches.

This thesis was written in a traditional style with introduction (chapter 1), material and methods (chapter 2), results and discussion (chapter 3-6). As three different projects are presented in this thesis, the discussion of each project immediately follows the results to better explain the data.

Chapter 3 analyses the effect of cytokine signaling on the outcome of macrophage parasitism by *Cryptococcus neoformans*. It is demonstrated that enhanced Th2, but not Th1, cytokine levels lead to increased intracellular cryptococcal proliferation but lower levels of cryptococcal expulsion.

Chapter 4 is a technical chapter describing the production and characterisation of GFP-tagged cryptococcal strains and subsequent development of a flow cytometry based approach for accurate and high throughput quantification of parameters such as cryptococcal phagocytosis and intracellular proliferation to describe macrophage parasitism.

Chapter 5 analyses the involvement of mitochondria in enhanced macrophage parasitism in isolates causing cryptococcosis in immunocompetent individuals. It describes the effect of different stress conditions encountered within the host and environment on mitochondrial morphology and the preliminary work for a comparative mitochondrial genome sequencing approach to decipher the underlying mechanism of the increased virulence. This is a currently ongoing project.

Chapter 6 describes an attempt to decipher the role of a sterol signaling pathway in cryptococcal adaptation to low oxygen conditions.

TABLE OF CONTENTS

TABLE OF FIGURES

TABLE OF TABLES

ABBREVIATIONS

AFLP	amplified fragment length polymorphism
AIDS	acquired immune deficiency syndrome
ANOVA	analysis-of-variance
ATP	adenosine-5'-triphosphate
BBB	blood brain barrier
Blast	basic local alignment search tool
bp	base pair
BSA	bovine serum albumin
CBS	Centraalbureau voor Schimmelcultures
CFU	colony forming unit
CIAP	calf intestinal alkaline phosphatase
CMI	cell mediated immunity
CNS	central nervous system
CR	complement receptor
CSF	cerebrospinal fluid
DAG	diacyglycerol
DC	dendritic cell
DMEM	Dulbecco's modified Eagle's medium
DMSO	dimethyl sulfoxide
DNA	deoxyribonucleic acid
EDTA	ethylenediaminetetraacetic acid
EGTA	ethylene glycol tetraacetic acid
ERK	extracellular signal-regulated kinase
FBS	fetal bovine serum
GFP	green fluorescent protein
GlcCer	glucosylceramide
GM-CSF	granulocyte-macrophage colony-stimulating factor
GTP	guanosine 5′-triphosphate
GXM	glucuronoxylomannan
HAART	highly active antiretroviral therapy
HIV	human immunodeficiency virus
HSD	honestly significant difference
IFN-γ	interferon gamma
IgG	immunoglobulin G
IL	interleukin
IPR	intracellular proliferation rate
kb	kilo bases

LB broth	Luria-Bertani broth
Mb	mega bases
MIT	Massachusetts Institue of Technology
MLST	multilocus sequence typing
NADPH	nicotinamide adenine dinucleotide phosphate
NCBI	National Centre for Biotechnology Information
NK cell	natural killer cell
OD	optical density
ORF	open reading frame
PBS	phosphate buffered saline
PCR	polymerase chain reaction
PEG	polyethylene glycol
PFP	pore forming protein
pH	potential of hydrogen
PI3K	phosphoinositide 3-kinase
PMA	phorbol myristic acetate
rcf	relative centrifugal force
RFLP	restriction fragment length polymorphism
RNA	ribonucleic acid
ROS	reactive oxygen species
rpm	revolutions per minute
RPMI-1640	Roswell Park Memorial Institute-1640 (medium)
SCAP	SREBP cleavage-activating protein
SD	synthetic defined
SDS	sodium dodecyl sulfate
SREBP	sterol regulatory element binding protein
STAT	signal transduction and activator of transcription
STET	sucrose- Tris-HCl-EDTA- Triton-X
UV	ultra violet
TAE	tris-acetate-EDTA
TBE	tris-borate-EDTA
T cell	thymus cell
Th	T-helper
TNF-α	tumor necrosis factor alpha
TRIS	hydroxymethylaminomethane
VIO	Vancouver Island Outbreak
YPD	yeast peptone dextrose

CHAPTER 1

INTRODUCTION

Major parts of this chapter have been published:

Voelz, K. and R. C. May. 2010. Cryptococcal interactions with the host immune system. Eukaryotic Cell **9:** 835-846. (Voelz *et al.*, 2010b).

Voelz, K, S. A. Johnston and R. C. May. 2010. Intracellular replication and exit strategies. *Cryptococcus*: from human pathogen to model yeast. (In press) (Voelz *et al.*, 2010a).

1.1 THE *CRYPTOCOCCUS* SPECIES COMPLEX

Opportunistic pathogens have become of increasing medical importance over the last decade due to the AIDS pandemic. Cryptococcosis is not only the fourth most common fatal infectious disease in sub-Saharan Africa, but *Cryptococcus* is also an emerging pathogen of immunocompetent individuals. The following section will give an introduction to the genus *Cryptococcus* and the related disease cryptococcosis.

1.1.1 *CRYPTOCOCCUS* SP.

The basidiomycetous genus *Cryptococcus* includes more than 70 species. In the 1890s, Buschke and Busse first indentified *C. neoformans* as human pathogen (Busse, 1894, Buschke, 1895) and to date, two species are predominantly considered as causative agents of cryptococcosis: *C. neoformans* and *C. gattii* (Casadevall *et al.*, 1998). Clinical isolates appear predominantly in their vegetative haploid form as spherical yeast with a characteristic polysaccharide capsule (Figure 1) (Mitchell *et al.*, 1995). Due to the varying size of the yeast capsule, cell

diameter can vary from 2 μm in poorly encapsulated strains up to 80 μm in heavily encapsulated strains (Casadevall *et al.*, 1998).

Based on differential antibody recognition of the capsule polysaccharide, the two medically important species are classified into *C. neoformans* serotypes A (*C. neoformans* var. *grubii*), D (*C. neoformans* var. *neoformans*) and A/D, and *C. gattii* serotypes B and C (formerly *C. neoformans* var. *gattii*) (Mitchell *et al.*, 1995, Franzot *et al.*, 1999, Kwon-Chung *et al.*, 1982). Advances in molecular typing techniques such as electrophoretic karyotyping by pulse-field electrophoresis, random amplification of polymorphic DNA, restriction fragment length polymorphism (RFLP), DNA hybridization studies, amplified fragment length polymorphism (AFLP), polymerase chain reaction (PCR) fingerprinting and multi locus sequence typing (MLST) in recent years have allowed this classification to be further defined into nine major genotypes: *C. neoformans* var. *grubii* molecular types VNI, VNII and VNB; *C. neoformans* var. *neoformans* molecular type VNIV; serotype A/D molecular type VNIII and *C. gattii* molecular types VGI, VGII, VGIII and VGIV (Figure 2) (Varma *et al.*, 1992b, Ruma *et al.*, 1996, Meyer *et al.*, 1999, Litvintseva *et al.*, 2006, Currie *et al.*, 1994, Brandt *et al.*, 1995, Boekhout *et al.*, 1997, Boekhout *et al.*, 2001).

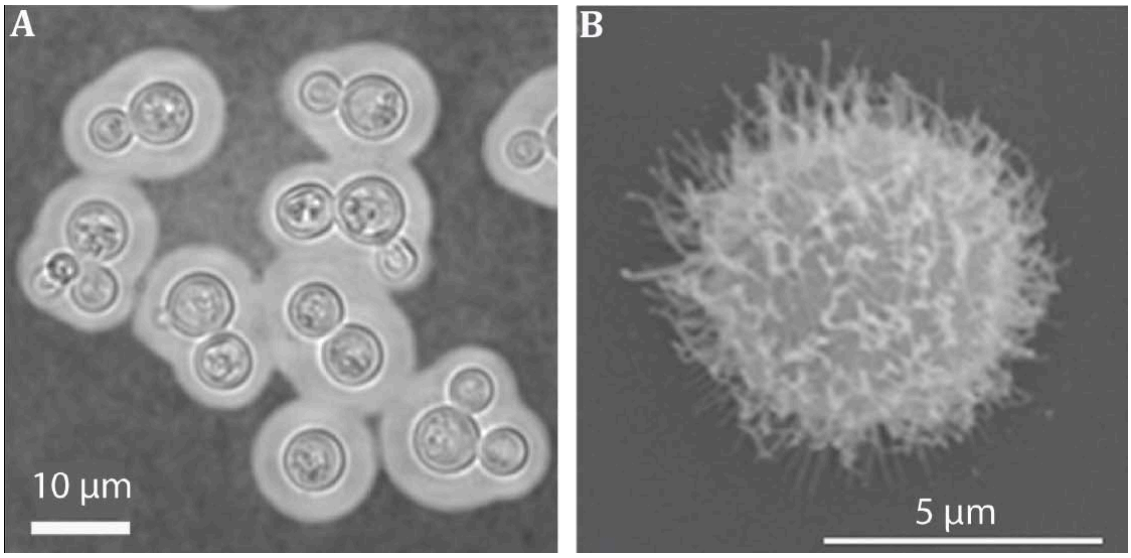

Figure 1: Cryptococcal capsule after India ink staining. Images were taken (A) under light microscope and (B) scanning electron microscope. (Taken and modified from Zaragoza *et al.* 2010 (Zaragoza *et al.*, 2010))

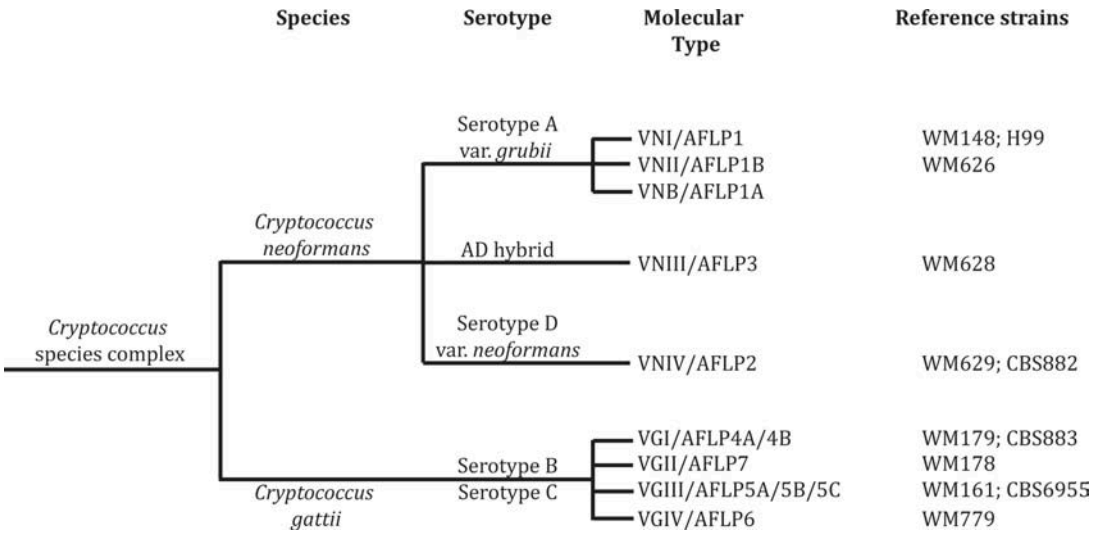

Figure 2: Schematic phylogeny of the *Cryptococcus* species complex. Diagram includes species, serotype, molecular type and reference strains. The species complex consists of two species; *C. neoformans* and *C. gattii*. *C. Neoformans* is further divided into the serotype a variety *grubii* with the molecular types VNI, VNII, VNB, the AD hybrids (VNIII) and the serotype D variety *neoformans* molecular type VNIV. The second species *C. gattii* comprises the serotypes B and C with the molecular types VGI, VGII, VGIII and VGIV (Bovers *et al.*, 2008, Lin *et al.*, 2006, Meyer *et al.*, 2003, Findley *et al.*, 2009).

1.1.1.1 *CRYPTOCOCCUS NEOFORMANS* AND *CRYPTOCOCCUS GATTII*

Historically, all pathogenic serotypes used to be considered as varieties of the species *C. neoformans*. However, due to their genetic variability and the lack of evidence for sexual recombination between *C. neoformans* and *C. gattii*, the latter is now regarded as an individual species (Kwon-Chung *et al.*, 2002). Further differences between both species can be found in their geographical distribution, epidemiology and clinical manifestation (Casadevall *et al.*, 1998).

C. neoformans is globally distributed and has been isolated from various natural sources with particularly high concentrations in avian guano, rotting vegetables and soil. In contrast, *C. gattii*, besides also being distributed worldwide, shows geographical hot spots in tropical and subtropical regions, with the notable exception of British Columbia. In tropical and subtropical regions it has been found to be associated with the eucalyptus tree species *Eucalyptus camaldulensis*, *E. tereticornis*, *E. rudis* and *E. gomphocephala* (Sorrell *et al.*, 1997, Harrison, 2000, Ellis *et al.*, 1990b, Pfeiffer *et al.*, 1992).

C. neoformans mainly causes opportunistic infections of immunocompromised patients with underlying conditions such as HIV, leukemia and other cancers or those taking corticosteroid medication (Mitchell *et al.*, 1995). Serotype A is responsible for the majority (95 %) of cryptococcosis cases in the immunocompromised host (Hull *et al.*, 2002). *C. gattii* mainly affects immunocompetent individuals. Although it only causes 0.94 cases per million population per year even in endemic areas such as Australia (Chen *et al.*, 2000, Sorrell, 2001), a recent and ongoing cryptococcosis outbreak in healthy individuals on Vancouver Island, British Columbia, Canada has highlighted the potential of *C. gattii* to act as an emerging pathogen (Kidd *et al.*, 2007, Kidd *et al.*, 2004, MacDougall *et al.*, 2007). The outbreak started in 1999 showing incidence rates of up to 36 cases per million population per year on Vancouver Island during 2002-2005 (MacDougall *et al.*, 2007). Moreover, there is evidence that the outbreak has since spread to mainland British Columbia and the Pacific Northwest (Byrnes *et al.*, 2009a, Byrnes *et al.*, 2009c, Byrnes *et al.*, 2009b, Datta *et al.*, 2009, Bartlett *et al.*,

2008, MacDougall *et al.*, 2007). Interestingly, most clinical isolates belong to the *C. gattii* genotype VGII (Kidd *et al.*, 2004). Isolates from this genotype have been separated into three subtypes: a VGIIa cluster containing hypervirulent clinical isolates, a VGIIb cluster containing mainly environmental isolates and a VGIIc cluster containing hypervirulent isolates recovered in Oregon (Kidd *et al.*, 2005, Kidd *et al.*, 2004, Byrnes *et al.*, 2009a).

In addition, other non-*neoformans*/non-*gattii* species, such as *C. laurentii* and *C. albidus* have recently started to emerge as potential human pathogens. However, as most of the non-*neoformans*/non-*gattii* species are not able to survive at human body temperature, infections are generally rare. Twenty cases of *C. laurentii* and 18 cases of *C. albidus* induced cryptococcosis have been reported to date (reviewed in (Khawcharoenporn *et al.*, 2007)).

1.1.1.2 THE CRYPTOCOCCAL LIFE CYCLE

Although *Cryptococcus* is predominantly found as budding yeast in patients and in the environment it can also appear in its filamentous form during mating and monokaryotic fruiting. During sexual reproduction, haploid yeast cells of the two opposite mating types a and α fuse and produce dikaryotic filaments. A basidium develops after migration of the parental nuclei to the ultimate hyphal cell. The nuclei fuse and undergo meiosis followed by mitosis and production of haploid basidiospores by budding on four characteristic chains. *Cryptococcus* can also respond to nutrient limitation by monokaryotic fruiting. Diploid monokaryotic hyphae result from endoduplication or cell and nuclear fusion of yeast cells of the same mating type. Meiosis occurs during basidium development, haploid basidiospores are produced shortly afterwards. Mature basidiospores are dispersed in the environment and germinate to haploid yeast cells (Figure 3) (Idnurm *et al.*, 2005, Hull *et al.*, 2002).

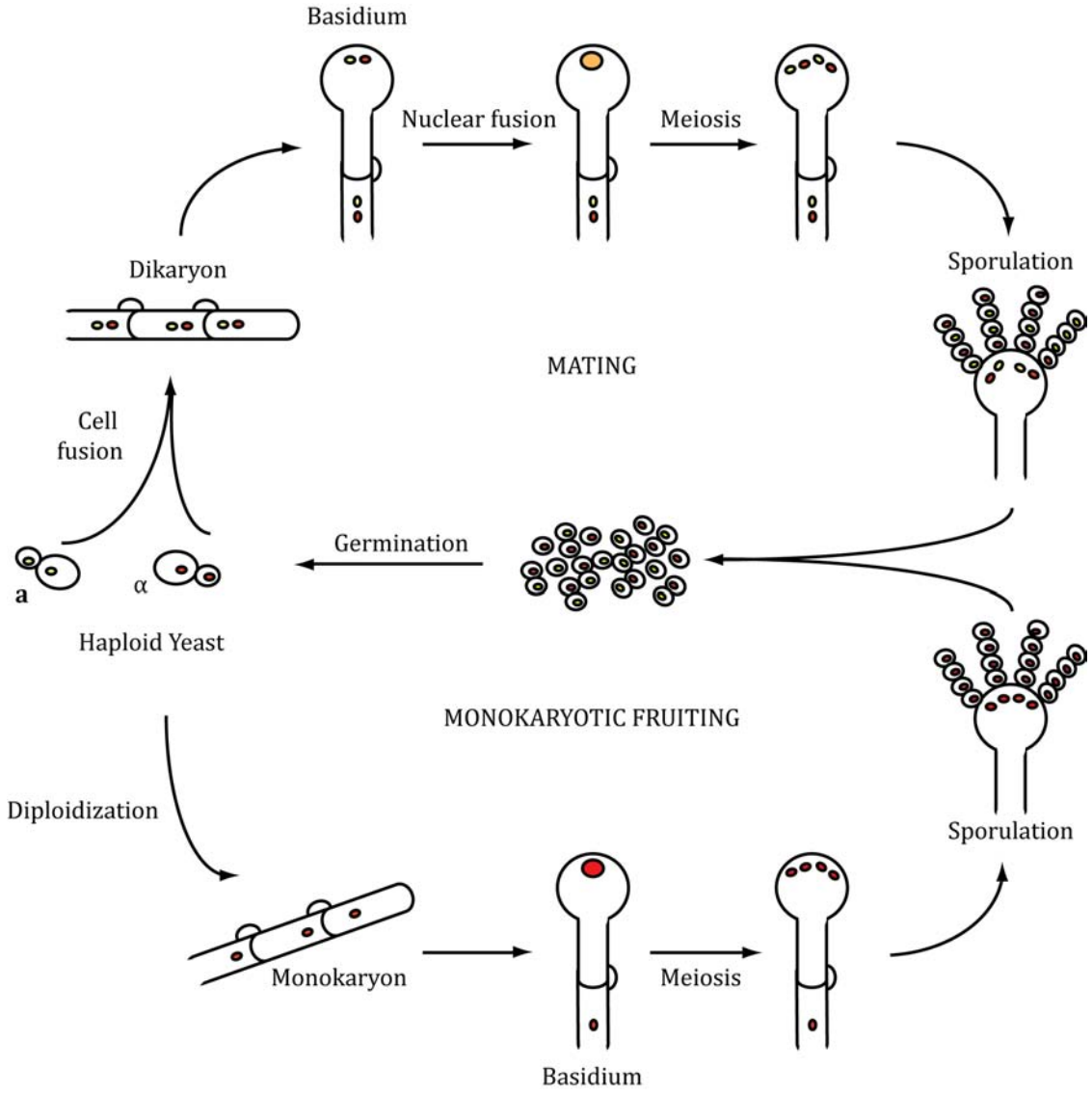

Figure 3: Schematic life cycle of *Cryptococcus neoformans*. Nutrient limitation can lead to mating and monokaryotic fruiting. During sexual reproduction, opposite mating partners fuse to a dikaryotic filament. After formation of a basidium, nuclear fusion and meiosis/mitosis occur eventually resulting in production of basidiospores by budding. During monokaryotic fruiting, yeast cells of one mating type form monokaryotic diploid hyphae that develop into basidia and sporulate following meiosis and mitosis.

1.1.1.3 THE *CRYPTOCOCCUS* GENOME SEQUENCING PROJECT

To date, seven cryptococcal genomes have been sequenced: *C. neoformans* serotype A strain H99; *C. neoformans* serotype D strains JEC21 and B3501A and *C. gattii* serotype B strains R265, CBS7750, WM276 and R272 (genome information summarized in table 1). The JEC21 genome project yielded 19 megabases (Mb) of sequence information organized in 14 chromosomes that is predicted to encode 6,572 protein-like genes rich in alternatively spliced and antisense messages. Genes have on average 6.3 exons of 255 base pairs (bp) and 5.3 introns of 67 bp length; the average transcript is 1.9 kilo bases (kb) long and contains 15 % noncoding sequence (Loftus *et al.*, 2005). Furthermore, the genome data indicates karyotype instability and phenotypic variation due to its richness in repetitive elements; 5 % of the JEC21 genome has been identified to be transposons that cluster in centromere-like regions (Loftus *et al.*, 2005).

The availability of sequence data within the genus *Cryptococcus* enables comparative genome studies and microarray studies to explore virulence genes and understand the molecular basis of pathogenicity mechanisms during cryptococcal disease (Fan *et al.*, 2005, Kraus *et al.*, 2004, Ma *et al.*, 2009a). Alternative splicing and antisense mechanisms have been identified for 277 and 53 genes, respectively, indicating both being widespread and regulatory in *C. neoformans* JEC21 (Loftus *et al.*, 2005). The *C. neoformans* strain B3501A differs remarkably in its phenotypic features from the closely related strain JEC21. Besides B3501A being more thermotolerant and more virulent in the mouse model, most of the genes of both strains show > 98 % sequence identity. However, four JEC21 specific genes could be identified (Loftus *et al.*, 2005).

Table 1: Summary of available cryptococcal genome sequences.

Strain	Serotype	Sequencing and Status	Genome Size	Chromosomes	Predicted number of protein-coding genes
C. neoformans H99	A	Broad Institute Assembly and annotation released http://www.broadinstitute.org/annotation/genome/cryptococcus_neoformans/MultiHome.html	19 Mb	14 nuclear 1 mitochondrial	6,967 nuclear 13 mitochondrial
C. neoformans JEC21	D	TIGR/Stanford University Published in (Loftus *et al.*, 2005)	19 Mb	14 nuclear	6,572 nuclear
C. neoformans B3501A	D	Stanford University Published in (Loftus *et al.*, 2005)	18.5 Mb	14 linked scaffolds	
C. gattii R265	B	Broad Institute Assembly and annotation released http://www.broadinstitute.org/annotation/genome/cryptococcus_neoformans_b/MultiHome.html	18 Mb	28 scaffolds	6,210 nuclear 13 mitochondrial
C. gattii CBS7750	B	Boekhout Lab. CBS , Netherlands Sequence unpublished	-	-	-
C. gattii WM276	B	Kronstad Lab, University of British Columbia, Canada Sequence unpublished	-	-	-
C. gattii R272	B	Heitman Lab, Duke University, USA Sequence unpublished	-	-	-

1.1.2 CRYPTOCOCCOSIS

Cryptococcal infection can be asymptomatic, chronic or acute. Typically, an initial pulmonary infection can spread systemically, with a particular predilection for the central nervous system (CNS). Pulmonary infections are in most cases asymptomatic. However, they can involve coughing, pleuritic chest pain, fever, dyspnoea, weight loss and malaise. Pneumonia and acute respiratory distress syndrome have mainly been reported for immunocompromised patients (Nadrous *et al.*, 2003, Campbell, 1966). Cryptococcosis of the CNS is life threatening and presents as meningitis or meningo-encephalitis with symptoms such as headache, increased intracranial pressure, fever, lethargy, coma, personality changes and memory loss. Less common are secondary infections of the skin, lungs, prostate and the eye (Mitchell *et al.*, 1995). A recent publication estimated 957,900 cases of cryptococcal meningitis resulting in 624,700 deaths globally each year (Park *et al.*, 2009). Cryptococcosis is an important cause of death in HIV infected individuals with an incidence of 15 % and a mortality of 30-60 %. The mortality rate in transplant patients is even higher at 20-100 % (Centre for Disease Control and Prevention)(Mitchell *et al.*, 1995).

Initial infection with *Cryptococcus* occurs via inhalation of airborne propagules and subsequent colonization of the respiratory tract (Casadevall *et al.*, 1998). It is believed that yeast cells with a diameter of 4-10 μm and additional polysaccharide capsule are too big to be the infectious particle. Instead, small basidiospores (1-2 μm), produced during mating or monokaryotic fruiting, or desiccated yeast cells are rather thought to be the infectious propagule (Ellis *et al.*, 1990a, Velagapudi *et al.*, 2009). In mouse and rat model systems, *C. neoformans* is internalized by alveolar macrophages shortly after inhalation (Diamond *et al.*, 1973a, Bulmer *et al.*, 1975, Goldman *et al.*, 2000, Feldmesser *et al.*, 2000, Swenson *et al.*, 1978, Mitchell *et al.*, 1972). RFLP analyses suggests that initial infection with *C. neoformans* often occurs in early childhood and can be followed by a long latent phase, most likely in macrophages, in immunocompetent individuals (Garcia-Hermoso *et al.*, 1999). In this context, two recent publications suggest a specific giant cell form of *Cryptococcus* as the dormant form within the human body (Okagaki *et al.,* Zaragoza

et al., 2010). However, *C. neoformans* is generally capable of disseminating to other organs within the human body, in particular to the CNS (Figure 4) (Chang *et al.*, 2004, Charlier *et al.*, 2009).

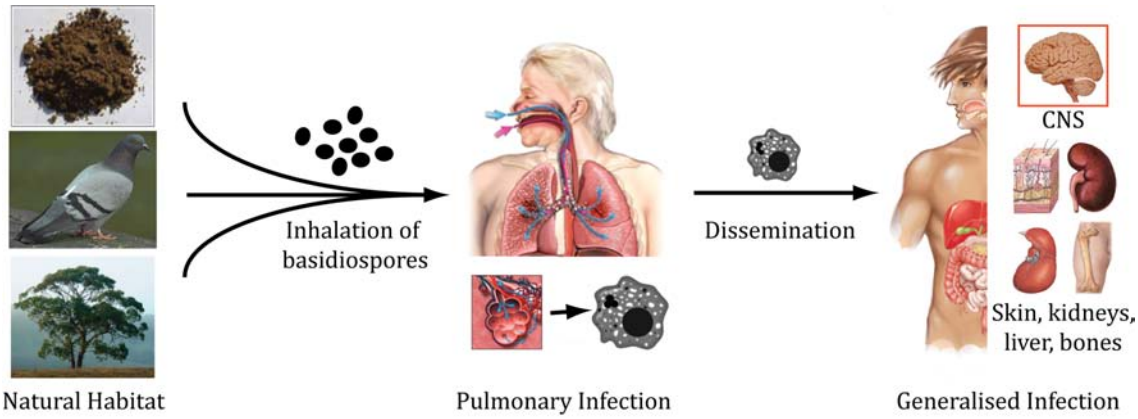

Figure 4: Schematic pathogenesis of cryptococcal disease. Infection is believed to occur by inhalation of basidiospores establishing a primary infection in the lungs. *Cryptococcus* cells are taken up by alveolar macrophages and can either go into a latent phase, likely within macrophages, but can also be reactivated and disseminate within the human body, in particular to the central nervous system but also to other organs such as the skin, kidneys, liver or bones.

Images were taken and modified from:
http://naturescrusaders.files.wordpress.com/2008/11/eucalyptus_tree_2_220.jpg
http://naturescrusaders.files.wordpress.com/2008/11/eucalyptus_tree_2_220.jpg
http://www.depiazzi.com.au/images/soil_mixes/soil_mixes_big/lawn_mix.jpg
http://www.aurorahealthcare.org/healthgate/images/lung_aspiration.jpg
http://fc03.deviantart.net/fs48/f/2009/196/2/3/Centrinova_Human_Body_System_by_Pegahoul.jpg
http://www.hivandhepatitis.com/0_images_2008/kidney2.jpg
http://www.nlm.nih.gov.ezproxyd.bham.ac.uk/medlineplus/ency/images/ency/fullsize/9734.jpg
http://www.epidemic.org/theFacts/essentials/images/liverDiagram1.jpg

1.1.2.1 ANTICRYPTOCOCCAL THERAPY

Cryptococcal meningitis is uniformly fatal without clinical intervention (Mwaba *et al.*, 2001). Standard therapy consists of amphotericin B, flucytosine and fluconazole. Amphotericin B and the triazole fluconazole both target the fungal membrane and disturb membrane integrity. The former associates with ergosterol, an essential component of the fungal plasma membrane, leading to formation of pores and increased permeability for protons and cations (Brajtburg *et al.*, 1990). The latter inhibits the cytochrome P450 enzyme 14α-demethylase and thus the conversion of lanosterol to ergosterol during membrane synthesis (Pasko *et al.*, 1990). Flucytosine, after conversion to 5-fluorouracil, functions as pyrimidine antagonist inhibiting RNA biosynthesis (Reviewed in Vermes *et al.*, 2000).

Treatment regimes, however, are dependent on the patient cohort and comprehensive guidelines have been published recently in Perfect *et al.* 2010 (Perfect *et al.*, 2010). For HIV-infected individuals with cryptococcal meningoencephalitis it is recommended to initiate therapy with a combination of 0.7-1.0 mg/kg of Amphotericin B per day intravenously and 100 mg/kg flucytosine per day orally for a minimum of two weeks, followed by 400 mg fluconazole per day orally for at least eight weeks (Perfect *et al.*, 2010). The length of primary therapy with amphotericin B and flucytosine is suggested to be prolonged to at least four to six weeks in non-HIV/non-transplant patients (Perfect *et al.*, 2010).

To date, treatment of cryptococcosis remains a challenge. Even with immediate treatment, patients show high mortality rates and therapy is associated with toxic side effects and low cost-effiency (Centre for Disease Control and Prevention). Especially in developing countries, amphotericin B, the most effective anticryptococcal medication, is too expensive and requires intravenous administration. Hence, treatment is focused on the cheaper and orally taken antifungal fluconazole (Jarvis *et al.*, 2007) which is better suited for maintenance therapy but less effective for initial treatment (Powderly, 1992, Bozzette *et al.*, 1991).

Although antifungal resistance does not seem to be a clinical problem currently (Witt *et al.*, 1996, Aller *et al.*, 2000), there have been recent concerns about *C. neoformans* and *C. gattii* heteroresistance towards fluconazole (Witt *et al.*, 1996, Aller *et al.*, 2000, Mondon *et al.*, 1999, Sionov *et al.*, 2009, Varma *et al.* 2010). This might be an additional challenge for African countries where treatment relies on the cheaper antifungal fluconazole. A small retrospective analysis has already shown that in 27 patients 67 % of reoccurring cryptococcosis episodes were related to reduced susceptibility to fluconazole (Bicanic *et al.*, 2006).

To date, cryptococcosis is a continuously increasing medical problem: in developing countries due to the high incidence in HIV-infected individuals and in developed countries because of the emergence of highly virulent strains affecting healthy individuals. The scientific challenge is to understand the pathogenesis mechanisms applied by *C. neoformans* and *C. gattii* in the interaction with the human host with the goal to prevent infection and disease or to improve treatment.

1.2 CRYPTOCOCCAL INTERACTIONS WITH THE HOST IMMUNE SYSTEM

The dramatic course of *Cryptococcus* infections in immunocompromised individuals shows the importance of an intact immune response to the pathogen. This section will consider both the host's innate and adaptive immune response to *C. neoformans* and *C. gattii* together with how current knowledge might be applied in improving anticryptococcal therapy.

1.2.1 THE INNATE IMMUNE RESPONSE TO *CRYPTOCOCCUS*

A variety of innate factors interfere with the establishment of cryptococcal infection. Beside physical barriers such as the skin and the nasal mucosa, the anticryptococcal activity of human serum and saliva has been described repeatedly (Szilagyi *et al.*, 1966, Nassar *et al.*, 1995, Igel *et al.*, 1966, Hendry *et al.*, 1969, Baum *et al.*, 1961a, Baum *et al.*, 1961b, Baum *et al.*, 1963). However, the complement system and phagocytic effector cells are the major players in the non-specific host immune response to *Cryptococcus*.

1.2.1.1 THE COMPLEMENT RESPONSE TO *CRYPTOCOCCUS*

The complement system is an anti-pathogen cascade of serum proteins that can be activated by the classical (antibody mediated), lectin or alternative (microbial surface mediated) pathway. All pathways eventually converge in the formation of the C3-convertase and cleavage of C3 into C3a and C3b. C3b either facilitates pathogen opsonization and thus enhances uptake by phagocytic cells or enables cleavage of C5 into C5a and C5b. C5a functions, together with C3a, as a mediator of inflammatory responses and attracts phagocytic effector cells, whereas C5b initiates the formation of the membrane attack complex (C5b, C6, C7, C8, C9) (Janeway *et al.*, 2001).

Observations from animal model systems and human patients have repeatedly shown the importance of complement system during cryptococcal infections (Figure 5). The survival time of *C. neoformans*-infected guinea pigs and mice treated with cobra venom to deplete late complement components (C3 to C9) is shortened and the ability to clear *C. neoformans* from extraneural sites reduced (Diamond *et al.*, 1973b). Mice deficient in C5 are more susceptible to intravenously injected *C. neoformans* and succumb three times quicker than C5 positive mice due to acute and fatal pneumonia (Rhodes, 1985, Rhodes *et al.*, 1980). Furthermore, patients presenting with cryptococcal fungaemia show reduced levels of C3 and alternative complement factor B (Macher *et al.*, 1978) and brain sections from patients with cryptococcal meningitis do not show C3 binding to the yeast (Truelsen *et al.*, 1992). In contrast, however, C4-deficient guinea pigs are not altered in their survival time after infection with *C. neoformans*, indicating that the alternative activation pathway is the major protective complement pathway during infections with *C. neoformans* (Diamond *et al.*, 1973b).

This finding is supported by results from *in vitro* analysis of the complement binding dynamics of *C. neoformans*. Diamond *et al*. (Diamond *et al.*, 1974) reported the consumption of complement components by *C. neoformans* when incubated with normal or C4-deficient guinea pig serum, whilst *C. neoformans* dependent activation of the complement cascade can be reconstituted from six proteins

(factor D, factor B, factor H, factor I, C3 and properdin) belonging to the alternative pathway (Kozel *et al.*, 1989). It was estimated that approximately 10^7 to 10^8 C3 fragments bind to an encapsulated cryptococcal cell and, dependent on the source of serum, localize inside and at the outer edge of the capsule (Gates *et al.*, 2006, Zaragoza *et al.*, 2003, Kozel *et al.*, 1988, Kozel, 1993a). The binding of C3 starts characteristically with a lag phase of four to six minutes followed by rapid accumulation of C3 fragments to the encapsulated yeast cell when incubated in normal human serum (Kozel *et al.*, 1991). Incubation with Mg-EGTA to chelate calcium that is required for classical pathway activation did not change the C3 binding dynamics supporting the dominant role of the alternative complement pathway during cryptococcosis (Kozel *et al.*, 1991). According to the complement model, the activation of the alternative pathway relies on spontaneous decomposition of C3 to C3b and Bb upon pathogen interaction. Similarly, closer examination of the binding process of C3 to the yeast cell by immunofluorescence revealed an initial slow C3 deposition in small loci with following expansion to larger areas after a lag (Kozel *et al.*, 1991). Investigation into the molecular form of bound C3 by SDS-page of eluted radioactive labeled fragments revealed a rapid decay of the C3 hydrolysis product C3b into the inactive form iC3b, which in turn, is the dominant fragment bound to the cryptococcal capsule (Kozel *et al.*, 1986, Pfrommer *et al.*, 1993).

The two major functions of the complement system during cryptococcosis are to stimulate the chemotaxis of phagocytic effector cells and enhance the uptake of cryptococcal cells by these phagocytes. Early evidence for the involvement of complement in opsonization of *C. neoformans* was drawn from phagocytosis assays with heat-inactivated serum (Diamond *et al.*, 1972). Assays with phagocytic cells and serum, depleted in specific components of the complement pathways, revealed the requirement of the complement pathway for phagocytosis of cryptococci by neutrophils (Diamond *et al.*, 1974), polymorphonuclear leukocytes and monocytes in an antibody free situation (Davies *et al.*, 1982). However, although the alternative pathway is sufficient for yeast opsonization, the classical pathway is required for optimal opsonization kinetics (Diamond *et al.*, 1974). Laxalt and Kozel

(1979) and Diamond and Erickson (1982) observed the chemotactic potential of serum; serum-opsonized encapsulated or non-encapsulated *C. neoformans* are both able to chemotactically attract neutrophils and monocytes *in vitro* (Laxalt *et al.*, 1979, Diamond *et al.*, 1982). However, C5-deficient mice are more susceptible to cryptococcosis (Rhodes, 1985, Rhodes *et al.*, 1980) and closer investigations revealed a lack of neutrophil accumulation in pulmonary vessels due to a lack of C5a, the C5 cleavage product that seems to be the chemotactic active component (Figure 5) (Lovchik *et al.*, 1993).

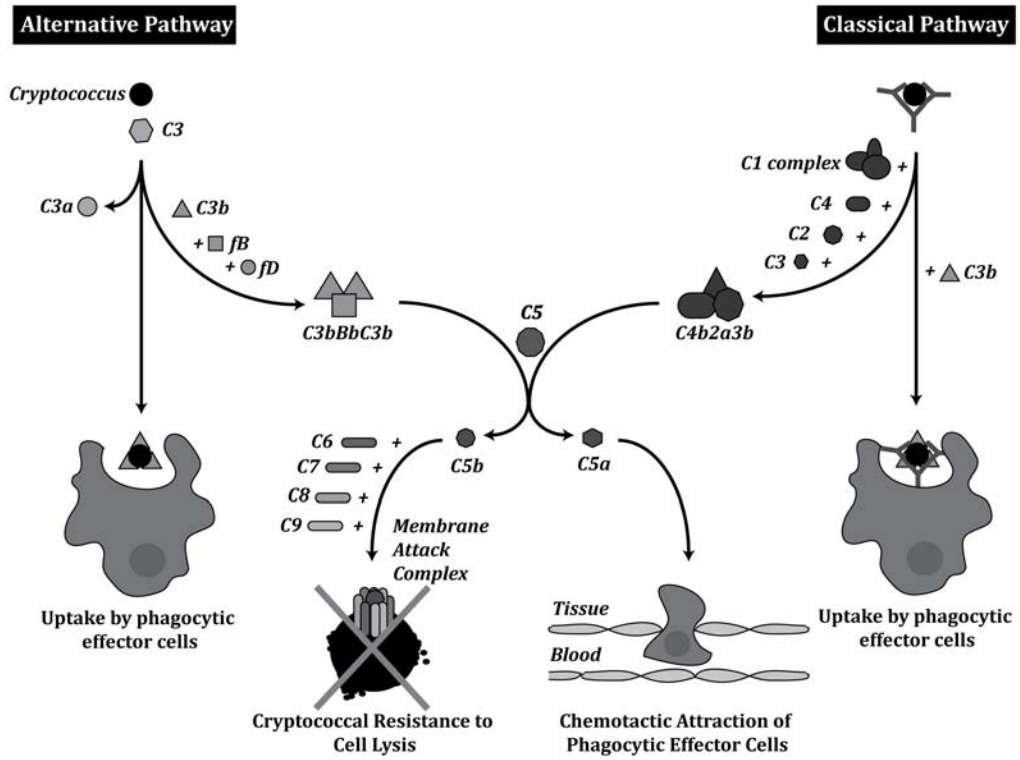

Figure 5: Summary of the complement pathways activated upon infection with *Cryptococcus neoformans*. The yeast can activate the classical (antibody mediated), and alternative (microbial surface mediated) pathway. Both pathways eventually converge in the formation of the C3-convertase and cleavage of C3 into C3a and C3b. C3b either facilitates pathogen opsonization and enhances uptake by phagocytic cells or enables cleavage of C5 into C5a and C5b. C5a functions as a mediator of inflammatory responses and attracts phagocytic effector cells, whereas C5b initiates the formation of the membrane attack complex (C5b, C6, C7, C8, C9). However, *C. neoformans* is resistant to pore formation and cell lysis by MAC (Shapiro *et al.*, 2002).

The cryptococcal polysaccharide capsule is a well-known factor required for the pathogen's virulence, e.g. by inhibiting phagocytosis (reviewed in (Zaragoza *et al.*, 2009)). *C. neoformans* mutants with a capsule-deficient phenotype are avirulent in mice (Chang *et al.*, 1994, Kwon-Chung *et al.*, 1986). Several studies with encapsulated and nonencapsulated *C. neoformans* strains also showed a difference in complement activation dependent on capsulation. The capsule inhibits the binding of mannan binding lectin and thus the activation of the complement system via the lectin pathway in *C. neoformans* (Panepinto *et al.*, 2007). The total number of bound C3 molecules is similar in different cryptococcal strains independent of the capsule size (Kozel *et al.*, 1988). However, a comparison of the deposition of C3 on the *C. neoformans* strain 145 grown under capsule inducing and non-capsule inducing conditions indicates a relationship between capsule diameter and C3 density under high yeast cell concentrations. The small capsule variant bound more C3 molecules per μm^3 capsule than the population with a large capsule (Kozel *et al.*, 1996). In contrast, the non-capsular strain 602 accumulates significantly less C3 on the cellular surface than capsulated strains (Kozel *et al.*, 1991, Kozel, 1993a, Kozel *et al.*, 1992). The decay rate of C3b to iC3b is lower in nonencapsulated *C. neoformans* than in capsulated forms (70 % versus 100 % respectively, after 20 minutes incubation with Factor H and I) (Kozel *et al.*, 1986, Pfrommer *et al.*, 1993). Furthermore, the acapsular strain 602 activates not only the alternative but also the classical complement pathway (Kozel *et al.*, 1991). C3 binding to the acapsular strain occurs immediately without any lag phase and rather than the characteristic small C3 deposition sites in encapsulated strains, sudden and rapid binding of C3 to the entire cell surface can be observed. This accumulation is ongoing and does not stop after eight minutes as seen in encapsulated *C. neoformans*. However, the dynamics described for capsular strains can be re-induced by treatment with Mg-EGTA (Kozel *et al.*, 1991). Interestingly, there seems to be a species-specific difference in activation of the complement system. Although the binding efficiency of C3 to *C. gattii* serotype B and C strains is higher than *C. neoformans* serotype A and D strains (Sahu *et al.*, 1994), total accumulation is only half of the latter (Washburn *et al.*, 1991, Young *et al.*, 1993).

The complement system is the first line of defense against *Cryptococcus* in the bloodstream and, by opsonising the pathogen and attracting immune effector cells, performs important preparations for the subsequent host defense response. The capsule probably functions as an inhibitor of complement related host responses, such as uptake by phagocytosis, by inhibiting the classical pathway and constriction of C3-convertase activity by efficient removal of C3b (in form of iC3b), an essential part of the alternative C3-convertase, thus limiting activity amplification. Differences in complement activation between *C. neoformans* and *C. gattii* might be important for the increased virulence of certain serotype B strains. In addition, recent data from Factor B- or C3-deficient mice survival assays after *C. gattii* infection have suggested that complement pathways other than the alternative activation pathway contribute to the host's protection (Mershon *et al.*, 2009).

1.2.1.2 PHAGOCYTIC EFFECTOR CELLS IN THE HOST IMMUNE RESPONSE TO *CRYPTOCOCCUS*

Research over the last few decades has shown the importance of phagocytic effector cells during the host's immune response to cryptococcal infections. This section will describe how the yeast cells are taken up and discuss the interaction with the different types of phagocytes.

1.2.1.2.1 PHAGOCYTOSIS

Uptake of cryptococcal cells has been shown repeatedly by a variety of leukocytes (Bulmer *et al.*, 1967) such as rat and mouse peritoneal macrophages (Mitchell *et al.*, 1972, Griffin, 1981, Kozel *et al.*, 1981), guinea pig pulmonary macrophages (Bulmer *et al.*, 1975), human neutrophils and macrophages (Dong *et al.*, 1997) and swine microglia (Lipovsky *et al.*, 1997). Phagocytosis is triggered by direct recognition of the yeast or by receptor-mediated recognition via complement or antibodies (Mitchell *et al.*, 1995). Conserved structures such as the components of

the cryptococcal capsule can be directly recognized by pattern recognition receptors. *C. neoformans* glucuronoxylomannan (GXM) can bind to Toll-like receptor 4 (Shoham *et al.*, 2001), the mannose receptor of dendritic cells binds to mannoproteins expressed on the yeast's surface (Pietrella *et al.*, 2005) and in the absence of complement to CD18, a subunit of the complement receptors (Dong *et al.*, 1997). Serum opsonized (i3Cb) *C. neoformans* are recognized either by the complement receptor CR1 (CD35) or by the heteromeric β2-integrins CR3 (CD11b/CD18) and CR4 (CD11c/CD35) (Levitz *et al.*, 1991, Zaragoza *et al.*, 2003). Studies with the receptors heterologously expressed in Chinese hamster ovary cells indicate that binding occurs independently to any of the receptors, with the greatest binding avidity being shown to CR3 followed by CR1 and CR4 (Levitz *et al.*, 1997b). Antibody-opsonized yeast cells are recognized by Fcγ receptor molecules expressed on the surface of macrophages, neutrophils and dendritic cells (Griffin, 1981, Luo *et al.*, 2006, Monari *et al.*, 1999, Syme *et al.*, 2002).

1.2.1.2.2 DENDRITIC CELLS (DCS)

Cryptococcus neoformans is phagocytosed by human primary dendritic cells *in vitro* (Syme *et al.*, 2002, Kelly *et al.*, 2005) and also in the mouse model (Wozniak *et al.*, 2006). Dendritic cells function as major antigen presenting cells that constantly monitor the current antigen population and modulate adaptive immune responses accordingly (Crowley *et al.*, 1990). During cryptococcal infections DCs are thought to be the major initiators of protective cell-mediated immunity (CMI) (Bauman *et al.*, 2000, Osterholzer *et al.*, 2009a). Not only are major antigens (e.g. mannoproteins and glycoantigens) for the activation of anticryptococcal T-cell responses dominantly presented by DCs (Mansour *et al.*, 2006, Levitz *et al.*, 2006) but the induction of T-cell responses by DCs is also much more efficient than by alveolar or peritoneal macrophages (Mansour *et al.*, 2006, Syme *et al.*, 2002).

1.2.1.2.3 NEUTROPHILS

Neutrophils are thought to contribute strongly to the innate immune response to cryptococcosis. Upon cryptococcal challenge, the number of polymorphonuclear cells increases at the site of infection in animal models (Gadebusch *et al.*, 1966, Perfect *et al.*, 1980). *In vitro*, the oxidative burst exerted by neutrophils effectively kills *C. neoformans* (Chaturvedi *et al.*, 1996, Mambula *et al.*, 2000, Miller *et al.*, 1991). However, despite rapid antimicrobial activity *in vivo*, cryptococci are only partially cleared from the infected site (Perfect *et al.*, 1980, Gadebusch *et al.*, 1966). Interestingly, induced neutropenia in mice increases survival after pulmonary challenge with *C. neoformans* (Mednick *et al.*, 2003), a counter-intuitive finding that may be due to the absence of neutrophils resulting in more interleukin (IL)-4 and IL-10 signaling which, in turn, modifies the inflammatory status and reduces tissue damage due to the aggressive oxidative burst (Mednick *et al.*, 2003). Together with data showing neutrophils being present in infected tissues only in low numbers and at early stages of infection (Feldmesser *et al.*, 2000) this might suggest a more immune-regulatory than antimicrobial role of neutrophils.

Besides killing of pathogens by means of respiratory burst, neutrophils also produce antimicrobial peptides and proteins as part of the antimicrobial response (Lehrer *et al.*, 1990). One such family of antimicrobial peptides – the defensins – is found in abundance in human, rat, rabbit and guinea pig neutrophils, however, expression is lacking in mouse neutrophils (Eisenhauer *et al.*, 1992). As mice are routinely used as system to model cryptococcal disease, this finding needs to be considered when assessing the role of neutrophils in the anticryptococcal immune defence. The lack of defensins might also be a reason for high susceptibly of mice towards challenge with the yeast.

1.2.1.2.4 MACROPHAGES

The importance of macrophages in cryptococcal infections has become more and more obvious in the last decade. Research has revealed an intriguing interaction between the phagocytic effectors and yeast cells that revealed *C. neoformans* as an intracellular parasite (Figure 6) (Feldmesser *et al.*, 2001b). After phagocytosis, *Cryptococcus* might be killed by but can also survive within the host cell. This can result in either a latent state or yeast proliferation within macrophages. Eventually, the host cell is exited by lysis or a non-lytic escape mechanism called expulsion to colonise different tissues. Furthermore, lateral transfer of yeast cells from one macrophage to another has been described (Ma *et al.*, 2007, Alvarez *et al.*, 2007, Del Poeta, 2004, Feldmesser *et al.*, 2000, Feldmesser *et al.*, 2001b, Tucker *et al.*, 2002). A detailed description of cryptococcal interactions with macrophages can be found in section three of this chapter.

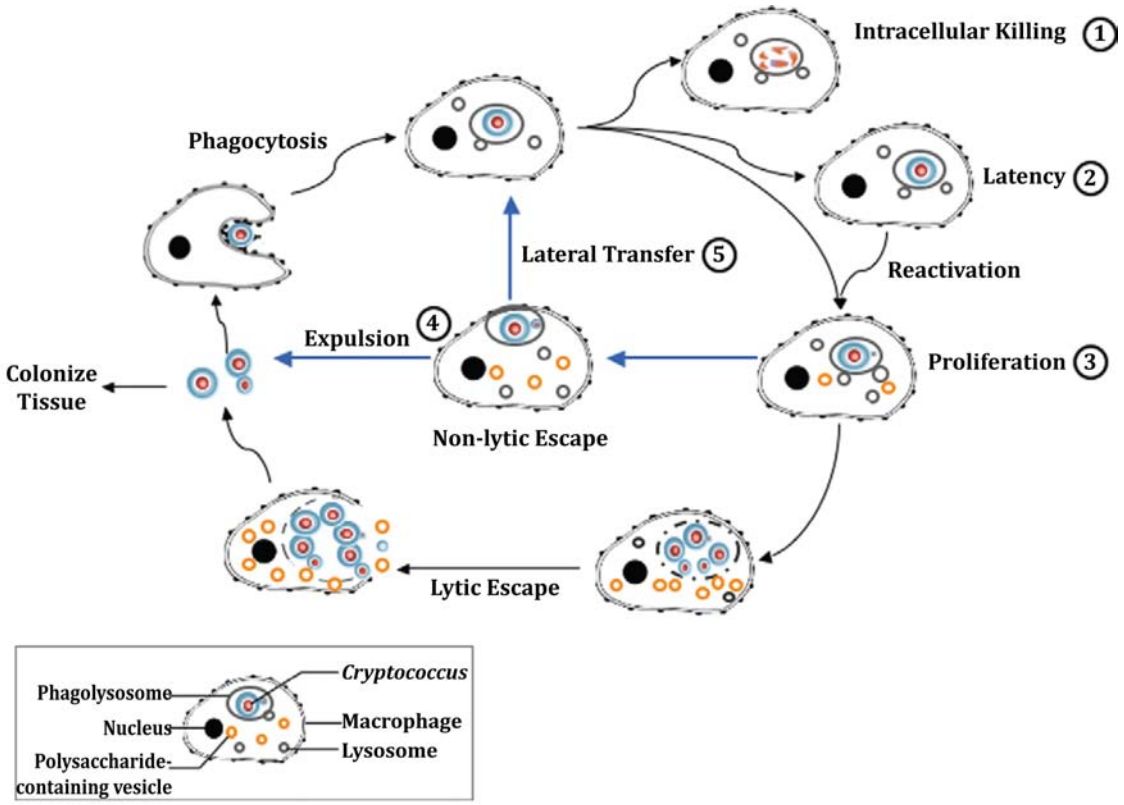

Figure 6: Schematic interaction between macrophages and *Cryptococcus*. After the yeast is ingested by macrophages it can be killed (1), go into a latent state (2) or start to proliferate within the phagocytes (3). Escape from within macrophages can occur by host cell lysis or non-lytic by expulsion (4) and result in colonization of other tissues. Furthermore, the yeast can be directly transferred from one macrophage to another (5). (Taken and modified from Ma and May 2009 (Ma *et al.*, 2009b)).

1.2.2 THE ADAPTIVE IMMUNE RESPONSE TO *CRYPTOCOCCUS*

The development of an adaptive immune response is essential to overcoming cryptococcal infection. This section will concentrate on the antibody and cell mediated immune response towards *Cryptococcus*.

1.2.2.1 ANTIBODY MEDIATED IMMUNE RESPONSE TO *CRYPTOCOCCUS*

With *Cryptococcus* being a facultative intracellular pathogen, there is some controversy about the importance of antibody-mediated immune mechanisms for effective microbial clearance. Several cases of cryptococcosis have been reported in patients with primary or acquired B cell, antibody or lymphoproliferative deficiencies (Casadevall *et al.*, 2005) and antibodies against cryptococcal proteins and capsular polysaccharides are routinely found in individuals without an apparent infection (Abadi *et al.*, 1999, Fleuridor *et al.*, 1999, Houpt *et al.*, 1994), indicating either latent or asymptomatic cleared infections. Passive administration of capsule binding antibody prolongs survival and/or reduces fungal burdens in experimental cryptococcosis (Mukherjee *et al.*, 1992, Fleuridor *et al.*, 1998). Anticryptococcal antibodies elicit their protective function by opsonising pathogens for Fc-receptor dependent phagocytosis and by activating the classical complement pathway. In addition, direct antibody opsonization of cryptococci leading to complement-independent (but complement receptor-dependent via CD18) uptake into macrophages has been described (Netski *et al.*, 2002, Taborda *et al.*, 2002). The specificity of antibodies seems to be of great importance for protective efficacy. Generally, it is thought that the two domains of antibodies fulfill two different functions: the variable region is responsible for antigen binding and the constant region for the effector functions. In studies with *C. neoformans* it has been shown that this classical view might have to be rethought, since antibodies identical in their variable region but differing in their constant region show diverse binding affinity and specificity to a univalent peptide antigen (Torres *et al.*, 2007, Dam *et al.*, 2008, Torres *et al.*, 2008). In addition, antibody subgroups developed from the same B-cell can be either protective or non-protective

according to their staining pattern (annular or punctuate). Although derived from the same B-cell, the two subtypes recognize spatially distinct areas of the cryptococcal capsule and only a punctuate opsonization pattern can induce a protective immune response in mice (Mukherjee *et al.*, 1995, Nussbaum *et al.*, 1997). The preponderance of protective compared to non-protective antibodies determines the efficacy of the antibody-mediated response to *C. neoformans* infection. It appears that small differences in antibody epitope specificities may have a large impact on the protective effect afforded by anticryptococcal antibodies. Those that are protective show a punctuate distribution within the capsule and those with an annular pattern of capsular distribution are non-protective (Mukherjee *et al.*, 1995). Furthermore, enhancement of cryptococcal disease has been described due to excess antibodies triggering immune-unresponsiveness (Savoy *et al.*, 1997, Kozel *et al.*, 1977). The concentration of antibody plays an important role for its protective functions. In mouse models, administration of antibody in higher concentrations can be less effective than in lower concentrations when subsequently challenged with *C. neoformans*. This so-called prozone-like activity suggests that antibodies during cryptococcosis can be protective, non-protective or even disease enhancing depending on the antibody isotype and dose (Taborda *et al.*, 2002, Taborda *et al.*, 2001).

Evidence from mouse models suggests that the protective effect of antibodies is at least partly due to an interaction with cell-mediated immunity. Mice defective in CD4, IFN-γ and Th1/Th2 associated cytokines cannot be protected by passive administration of IgG1 antibodies, whereas mice deficient in CD8, natural killer cells or complement factor C3 can (Shapiro *et al.*, 2002, Beenhouwer *et al.*, 2001, Yuan *et al.*, 1997). Thus, antibody-mediated immunity is a significant part in the host defense that integrates into a complex network of different elements of protective anticryptococcal immunity.

1.2.2.2 CELL MEDIATED IMMUNE RESPONSE TO *CRYPTOCOCCUS*

The number of cryptococcosis cases drastically increased with the onset of the AIDS pandemic and, to date, the highest incidence is still found in HIV-stricken sub-Saharan Africa (Park *et al.*, 2009). Besides HIV patients, individuals with extensive corticosteroid treatment, organ transplantation, leukemia or lymphoma and sarcoidosis belong to a high-risk group for cryptococcal infections (Mitchell *et al.*, 1995). The common feature of all of these predispositions is a defect in CMI. This part of the host defence contributes to cryptococcal killing either directly by cytotoxic effects or indirectly by regulatory functions of natural killer (NK) cells or T lymphocytes. NK, $CD4^+$ and $CD8^+$ cells all exhibit direct antimicrobial activity to *C. neoformans* (Levitz *et al.*, 1994, Zheng *et al.*, 2007) and secrete the proteins granulysin and perforin that are both able to induce cryptococcal permeabilization and lysis (Ernst *et al.*, 2000, Voskoboinik *et al.*, 2006). Although NK cells express both proteins, perforin is the main mediator of anticryptococcal killing via a PI3K-dependent ERK1/2 signaling pathway (Ma *et al.*, 2004, Marr *et al.*, 2009, Wiseman *et al.*, 2007). In contrast, $CD4^+$ and $CD8^+$ lymphocytes utilize the anticryptococcal function of granulysin that is expressed upon activation of STAT5 and PI3K in the presents of IL-2/IL-15 and IL-15, respectively (Ma *et al.*, 2002, Zheng *et al.*, 2008, Zheng *et al.*, 2007). In HIV patients, these two pathways are defective, resulting in inefficient killing of *C. neoformans* (Zheng *et al.*, 2007).

Alongside the ability to directly lyse cryptococci, the regulatory arm of CMI seems to be an even more important part of fungal clearance. The outcome of cryptococcosis depends on the immune status of the infected individual and the expression of host cytokines, regulatory immune signaling molecules, generated in response to the pathogen. Cytokines regulate the induction of the three main lines of immune response: Th1, Th2 and Th17. Th1 and Th17 immune profiles are proinflammatory and activate antimicrobial functions of effector cells upon infection with intracellular pathogens. A Th2 response is activated after infection with extracellular pathogens and results in an antibody-mediated immune response (Mosmann *et al.*, 1989). Both Th1 and Th2 cytokines are involved in protection against *C. neoformans*, but whereas Th1 associated cytokines are

essential for natural immunity, Th2 associated immunity is not protective in mice (Beenhouwer *et al.*, 2001, Hoag *et al.*, 1997, Huffnagle, 1996). Increased expression of Th1 cytokines, such as TNF-α and IFN-γ, results in improved fungal control (Flesch *et al.*, 1989, Kawakami *et al.*, 1995, Milam *et al.*, 2007, Wormley *et al.*, 2007) and supports pulmonary clearance (Zhang *et al.*, 2009) whilst IFN-γ knockout mice show increased fungal burden (Arora *et al.*, 2005). In addition, Müller *et al*. (2007) have recently demonstrated a significant role for IL-17 and the associated Th17 response in modulating survival of *C. neoformans*–infected mice (Muller *et al.*, 2007, Kleinschek *et al.*, 2006). In contrast, Th2 cytokines such as IL-4 and IL-13 reduce the host's ability to deal with *C. neoformans in vivo* (Blackstock *et al.*, 2004, Decken *et al.*, 1998, Muller *et al.*, 2007, Kawakami *et al.*, 1999). The incidence of cryptococcosis increases throughout the course of HIV infection and correlates with the loss of Th1 response in HIV-infected patients (Altfeld *et al.*, 2000) and with a Th2 cytokine profile in transplant patients (Singh *et al.*, 2008). Thus, the Th1-Th2-Th17 balance is essential for survival of cryptococcosis.

In addition to DCs and neutrophils, primary lymphocytes and NK cells as well as γδ T cells are involved in the maintenance of this cytokine balance during infection (Wozniak *et al.*, 2006, Mednick *et al.*, 2003, Nanno *et al.*, 2007, Uezu *et al.*, 2004). NK cells produce high concentrations of IFN-γ and IL-4 that trigger Th1 mediated immunity but not Th2 related immune responses (Kawakami *et al.*, 2001). This activation is opposed by the function of γδ T cells; depletion of γδ T cells in a mouse model leads to a decreased fungal burden and reduced IFN-γ levels (Uezu *et al.*, 2004). Since Th1 immunity is proinflammatory, exaggerated Th1 activation during infection might have negative consequences for individuals and thus γδ T cells might function as down-regulators of Th1 responses to sustain a healthy Th1-Th2 balance (Kawakami, 2004). However, *C. neoformans* is able to actively change the Th1/Th2 balance towards a Th2 profile by expressing eicosanoids (e.g. prostaglandins and leukotrienes), which are potent inhibitors of Th1-type immunity (Noverr *et al.*, 2003). In addition, expression of the virulence factor urease promotes a Th2 immune response within the lungs via an unknown mechanism (Cox *et al.*, 2000).

1.2.3 IMMUNOTHERAPY IN CRYPTOCOCCAL DISEASE

Current anti-fungal treatment regimes involve combination therapy of amphotericin B, flucytosine and fluconazole (Perfect *et al.*). However, all are associated with toxic side effects and low cost-efficiency (Centre for Disease Control and Prevention). In addition, the new generation of antifungals, echinocandins, are not active against *C. neoformans* and in consequence are not used in clinical practice, thus limiting the range of antifungals available to treat the disease (Maligie *et al.*, 2005). The introduction of highly active antiretroviral therapy (HAART) has reduced the incidence of cryptococcosis in developed countries, but not the short-term mortality and hence HAART has not improved the clinical outcome of cryptococcosis. Despite rapid clinical intervention, the three-month mortality of acute cryptococcal meningoencephalitis is as high as 20 % in HIV patients (Lortholary *et al.*, 2006, Dromer *et al.*, 2007). This poor prognosis has resulted in the need for exploration of alternative treatment regimes such as immunotherapy, passive immunization and cytokine-based treatment strategies. One promising approach might be the use of adjunctive passive immunotherapy with monoclonal antibodies. As the administration of anti-capsular antibodies is protective in infected mice (Dromer *et al.*, 1987, Graybill *et al.*, 1981) a phase I trial with the monoclonal antibody 18B7 was conducted in HIV patients recovered from cryptococcal meningitis (Larsen *et al.*, 2005). Therapy was well tolerated for antibody concentrations up to 1 mg/kg with higher doses showing pharmacological effects (Larsen *et al.*, 2005). A second antibody, 2G8, targeting the cell wall glucan has exerts remarkable anticryptococcal activity *in vitro* and *in vivo* and might be a good candidate as a new therapeutic agent (Rachini *et al.*, 2007). Thus, there is clear potential for anticryptococcal antibody-mediated therapy. However, it remains a significant challenge to design treatment strategies considering the complex pharmacodynamics of administrated antibodies and antigens within the host as well as drug-associated toxicity. Vaccination with GXM-tetanus toxoid conjugates in mouse model systems has shown promise (Devi *et al.*, 1991, Devi, 1996) but is not yet approved for clinical use.

Cytokine-based treatments have also been proposed for cryptococcosis treatment. IFN-γ levels at the site of infection correlate with fungal burden (Siddiqui *et al.*, 2005) and administration of IFN-γ has successfully improved the outcome of systemic cryptococcosis in mice model systems (Lutz *et al.*, 2000, Clemons *et al.*, 2001) and in one human patient (Netea *et al.*, 2004). However, although IFN-γ seems to have a protective role in mice (Hoag *et al.*, 1997, Arora *et al.*, 2005) and to increase fungicidal activity of murine macrophages (Flesch *et al.*, 1989), the same treatment reduces anticryptococcal activity in human macrophages (Reardon *et al.*, 1996, Levitz *et al.*, 1990), suggesting that this line of treatment may be less advantageous for human patients.

Recent approaches also tested radioimmunotherapy for treatment of high burden of *C. neoformans* in mice. Mortality was reduced and no evidence found for selection of radio-resistant cells. Although this strategy was more effective than antifungal treatment, residual yeast cells that were likely shielded by a biofilm, an abscess or within host cells, were able to survive and proliferate after treatment (Bryan *et al.*, 2009, Bryan *et al.*, 2010).

Since *C. neoformans* is a major pathogen of immunocompromised patients, new strategies need to consider targeted modification of the patient's immune system, for instance by the selective administration of pro-inflammatory cytokines, to encourage the expression of a protective immune profile. Intracellular localisation provides *Cryptococcus* with a niche to escape host immune mechanisms (e.g. complement and antibodies) and also reduces the exposure to antifungal agents. Future research will need to consider the ability to parasitise host cells in order to advance therapeutic schemes. Targeting intracellular survival and growth and/or cryptococcal virulence factors expressed during disease might offer new strategies to improve anticryptococcal treatment.

1.3 MACROPHAGE-*CRYPTOCOCCUS* INTERACTION: INTRACELLULAR PROLIFERATION AND EXIT STRATEGIES

Pathogens have evolved a great variety of strategies to achieve survival within the host environment. Intracellular parasitism, as one of these strategies, has a significant impact on pathogenesis and important implications for the effectiveness of both the host's immune response and therapeutic reagents. This section discusses the ability of the pathogenic cryptococci to proliferate intracellularly and examines the different strategies cryptococci use to exit host cells. It will also address the importance of these two traits in pathogenesis.

1.3.1 *CRYPTOCOCCUS* AS AN INTRACELLULAR PROLIFERATOR

In vitro, intracellular multiplication (Figure 7) of *C. neoformans* was first reported in isolated murine peritoneal macrophages (Mitchell *et al.*, 1972) and in macrophages derived from human peripheral blood monocytes (Diamond *et al.*, 1973a) and has since also been shown in human fetal microglia (Lee *et al.*, 1995), in murine alveolar macrophages (Tucker *et al.*, 2002) and in human endothelial cells (Coenjaerts *et al.*, 2006). Although an earlier study observed effective

intracellular killing of *C. neoformans* by human leukocytes during the first four hours of infection (Tacker *et al.*, 1972), a subsequent study demonstrated that *C. neoformans* first needs to adapt to the host cell environment before commencing replication (Diamond *et al.*, 1973a). Thus, experiments over a shorter time-frame might underestimate the intracellular proliferative potential.

In vivo, it remains difficult to demonstrate intracellular proliferation directly, relying instead on indirect evidence such as histological examinations, which provide data at fixed time points but do not allow direct observation of intracellular proliferation (Feldmesser *et al.*, 2001b). However, observations made in rat (Goldman *et al.*, 2000) and mouse model organisms (Feldmesser *et al.*, 2000) and also from histopathological studies in patients (Granier *et al.*, 1987) point towards intracellular replication of *Cryptococcus in vivo*. Feldmesser *et al*. (2001) (Feldmesser *et al.*, 2001b) summarized the following observations as evidence for intracellular replication *in vivo*: (1) the higher number of intracellularly budding yeast as compared with extracellularly budding yeast; (2) the fact that intracellular cryptococcal cells increase both in number and in the range of sizes they display (a sign of active budding) and (3) the observation of intracellular budding yeast cells at all stages of budding.

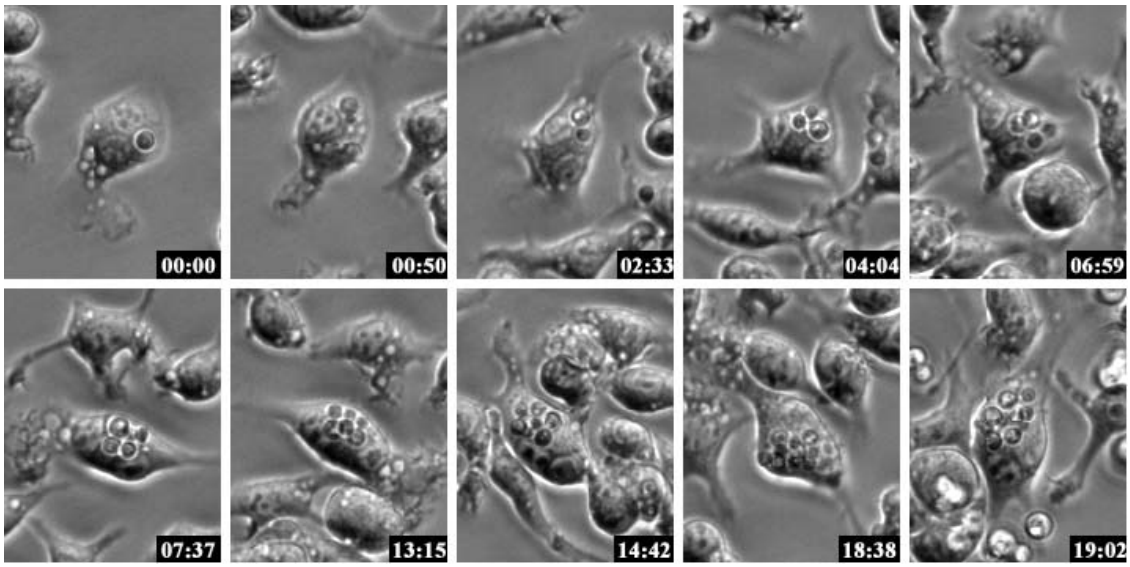

Figure 7: Intracellular proliferation of *Cryptococcus gattii.* Within a J774 murine macrophage, an intracellular yeast cell starts budding after 50 minutes and continues replication until the macrophage is filled with yeast cells after 19 hours. Times are shown in hours: minutes: seconds.

Nowadays, *Cryptococcus* is generally accepted as a facultative intracellular pathogen that can replicate inside host cells whilst retaining the ability to grow in an extracellular niche within the host and in the environment (Feldmesser *et al.*, 2001a). The intracellular location provides a dual benefit to *Cryptococcus*, both in avoiding extracellular host immune mechanisms, such as complement, and in reducing exposure to antifungal agents. Indeed, maintenance of *Cryptococcus* within phagocytic cells is important for progression of cryptococcosis (Kechichian *et al.*, 2007). The establishment of different *in vitro* systems that utilize cell lines (Mukherjee *et al.*, 1994, Lee *et al.*, 1995) and the application of techniques such as live cell imaging (Ma *et al.*, 2006, Alvarez *et al.*, 2006), have contributed to rapid advances in our understanding of the molecular mechanisms influencing *Cryptococcus*'s ability to parasitize macrophages.

1.3.1.1 THE ORIGIN AND EVOLUTION OF CRYPTOCOCCAL INTRACELLULAR PROLIFERATION

The question of how and why *Cryptococcus* has acquired and maintained virulence mechanisms that enable intracellular proliferation is still unanswered. However, the interactions between *C. neoformans* and environmentally widespread invertebrates and protists has led to the proposal that virulence towards mammalian cells might have arisen from protective mechanisms used by the yeast against environmental predators. Co-incubation of the free-living soil amoebae *Acanthamoeba castellanii* or *Dictyostelium discoideum* with *C. neoformans* results in intracellular budding and growth, eventually causing lysis of the host amoebae (Steenbergen *et al.*, 2003, Steenbergen *et al.*, 2001). Interestingly, mutations in known mammalian virulence factors significantly inhibited cryptococcal growth in this system. Interestingly, melanization protects acapsular, but not encapsulated, strains from amoeboid killing (Steenbergen *et al.*, 2001), suggesting that melanization is not a critical virulence factor in this host. Notably, *D. discoideum* mutants impaired in phagocytosis or exocytosis (Tuxworth *et al.*, 2001, Wood *et al.*, 1996, Brazill *et al.*, 2000), are both susceptible to the hypovirulent strain Cap67

(Steenbergen *et al.*, 2003). Thus, as in humans, the outcome of intracellular parasitism results from a complex interaction between host and pathogen factors. Intriguingly, repeated passage of *C. neoformans* through *D. discoideum* results in increased virulence in mice (Steenbergen *et al.*, 2003). This increase is correlated with phenotypic changes, such as increased capsule size and more rapid melanization (Steenbergen *et al.*, 2003), and is probably a microevolutionary process similar to that previously reported in HIV-infected patients with recurrent cryptococcocal meningitis (Sullivan *et al.*, 1996). Cryptococcal proliferation within amoebae is remarkably similar to replication within mammalian phagocytes. Therefore, the selective pressure to survive and replicate within amoebae may have driven evolution of adaptation mechanisms to mammalian hosts and may be critical for the maintenance of intracellular proliferation traits in this organism.

However, although these interactions offer explanations for mechanisms involved in virulence and in intracellular proliferation in the immunocompromised host, they do not explain the recent origin of certain hypervirulent *C. gattii* strains (Stephen *et al.*, 2002, Hoang *et al.*, 2004, Bartlett *et al.*, 2008, MacDougall *et al.*, 2007). Strikingly, data on the maximal intracellular proliferation rates (IPR) of different *C. gattii* strains show that an enhanced ability to replicate within macrophages might have enabled certain *C. gattii* strains to cause symptomatic infections in otherwise healthy individuals. A comparison of *C. gattii* strains of different genotypes revealed an increase in IPRs in genotype VGIIa strains (AFLP6A), the hypervirulent genotype responsible for the Vancouver Island Outbreak (VIO) (Kidd *et al.*, 2004). Since there is also a clear correlation between IPR and virulence in mice, the exceptional virulence of the Vancouver Island *Cryptococcus* population seems to be a direct result of an enhanced ability to multiply intracellularly in mammalian macrophages (Ma *et al.*, 2009a). Whole-genome microarray analysis has identified a large number of candidate genes that may influence proliferative capacity and revealed an unexpected role for mitochondrial genes in regulating cryptococcal hypervirulence in the Vancouver Island strains. Upon encounter of the intracellular niche, expression of mitochondrial genes is upregulated in these strains whilst the mitochondrial DNA

copy number remains unaffected (Ma *et al.*, 2009a). Moreover, Vancouver Island isolates show a distinctive mitochondrial phenotype. The mitochondrial network can appear diffuse, globular or tubular. Highly virulent strains VGIIa strains show a significant increase in mitochondria with tubular morphology after macrophage passage compared to low proliferative strains (Ma *et al.*, 2009a). Previous work in the related species *C. neoformans* has demonstrated that mitochondrial genotype does not influence virulence (Toffaletti *et al.*, 2004). Thus, mitochondrial regulation of virulence must have evolved after C. *gattii* and *C. neoformans* diverged and may potentially explain the very different behavior of these two pathogens.

Mitochondrial functions include oxidative respiration, resistance to oxidative stress (Grant *et al.*, 1997), certain heme synthesis reactions (Oh-hama, 1997) and sterol synthesis (Rossier, 2006). *C. neoformans* mutants with impaired mitochondrial functions show reduced oxidative respiration and higher sensitivity to reactive oxygen species under low oxygen conditions (Ingavale *et al.*, 2008). In this context, increased intracellular replication might be due to additional mitochondrial genes, polymorphisms or greater mitochondrial plasticity that allow for more rapid adaptation to environmental changes such as available oxygen and oxidative stress. Furthermore, a high percentage of tubular mitochondria will allow closer proximity of proteins involved in mitochondrial functions and might enable to compensate for proteins damaged by host cell stresses. Future research will hopefully reveal how mitochondria influence cryptococcal intracellular proliferation at the molecular level.

1.3.2 CRYPTOCOCCAL ESCAPE FROM THE HOST CELL

To cause the disease state observed in cryptococcosis, cryptococci must eventually escape the phagocyte in which they initially replicate. Different escape routes influence both secondary disease states and the role that the adaptive and innate immune system will play in subsequent pathology. More generally, host cell escape may be important both for the multi-tissue passage of *Cryptococcus* through the

body and for maintaining latency. At least three exit strategies for *Cryptococcus* are currently recognized: lysis, expulsion and lateral transfer. Each of these is addressed in turn below.

1.3.2.1 HOST CELL LYSIS

Host cell lysis is the most common escape route for intracellular pathogens (Figure 8). Microorganisms are often enclosed in at least two membranes (an endocytic or phagocytic one, as well as the host cell plasma membrane) and must disrupt these to escape. Many virulence factors, such as pore forming proteins (PFPs), phospholipases and proteases, are thought to function through lysing host cell membranes. The mechanisms of host cell membrane disruption are not well understood but are assumed to involve a combination of pore forming and phospholipase proteins. To date, no pore forming proteins that function to attack host membranes have been identified in the *Cryptococcus* genome, but phospholipase B (*plb1*) is an obvious candidate cell-lysis factor. Although cryptococcal parasitism of macrophages does not obviously require escape from the phagosome, three experimental observations suggest that *Cryptoccocus*-containing phagosomes may be permeabilised. Firstly, phagosomal membranes containing *Cryptococcus* appear to have holes when viewed by transmission electron microscopy (Feldmesser *et al.*, 2002, Tucker *et al.*, 2002). Secondly, fluorescent dextran that is phagocytosed along with cryptococci subsequently diffuses out of the phagosome into the cytoplasm (Tucker *et al.*, 2002, Johnston *et al.*, 2010). Finally, *Cryptococcus* containing phagosomes cannot maintain an acidic pH (Tucker *et al.*, 2002). This permeabilisation of the phagosome may be required to provide access to cytoplasmic nutrients to support proliferation, as the PLB1 mutant is growth-inhibited in macrophages (Noverr *et al.*, 2003). Nevertheless, the lysis of phagosomes or host cells by PLB has not been shown directly.

Mechanical burden alone, in the absence of permeabilising factors, is not well described as a mechanism for host cell lysis for intracellular pathogens. However, the concurrent expansion of the cryptococcal capsule and rapid proliferation of

many *Cryptococcus* strains within macrophages means that mechanical rupture of cell membranes may provide an alternative explanation for lysis (Alvarez *et al.*, 2006, Tucker *et al.*, 2002). Interestingly, the cryptococcal capsule component glucuronoxylomannan has been associated with induction of nitric oxide synthase and nitric oxide leading to rat macrophage apoptosis *in vitro* and release of yeast cells (Chiapello *et al.*, 2008), although this is morphologically different to the non-apoptotic lysis of *Cryptococcus*-infected cells.

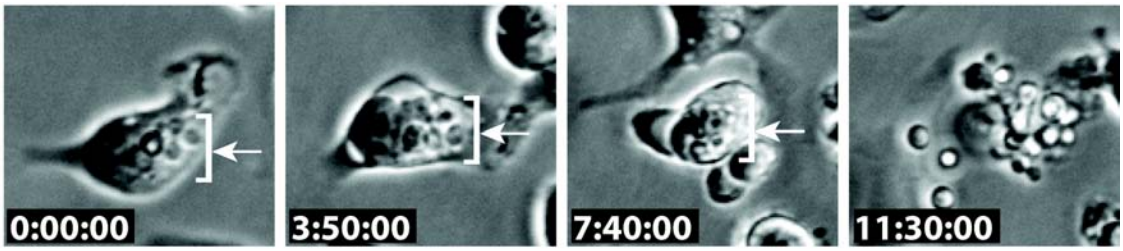

Figure 8: *Cryptococcus* can exit escaping macrophages by lysis. Time-lapse microscopy of J774 macrophages. Arrows indicate intracellular cryptococci. Times are shown in hours: minutes: seconds.

1.3.2.2 EXPULSION

Many intracellular pathogens have mechanisms for controlled expulsion from host cells. These generally fall into two types; actin-based protrusion and membrane extrusion. Actin-based protrusion has been described for *Listeria monocytogenes*, *Rickettsia sp.*, *Shigella flexneri* and *Burkholderia pseudomallei,* all of which hijack the host actin cytoskeleton to form plasma membrane projections that are endocytosed by neighbouring cells (Stevens *et al.*, 2006). In contrast, cryptococcal expulsion (Figure 9) occurs without any obvious reliance on the actin cytoskeleton (Alvarez *et al.*, 2006, Ma *et al.*, 2006). Two other superficially similar exit strategies have been reported, the triple membrane single cell budding of *Orientia tsutsugamushi* (Schaechter *et al.*, 1957) and the large vacuole multi-cell extrusion of *Chlamydia spp*. (Hybiske *et al.*, 2007).

Cryptococcal expulsion bears a striking resemblance to exocytosis, the process by which internal vesicles fuse with the plasma membrane and release their contents to the outside environment. The presentation of antigens also relies on the exocytic machinery, a process that is especially important in phagocytes. Exocytosis of large particles has been observed only once, though, in the social amoeba *Dictyostelium discoideum* (Clarke *et al.*, 2002).

Expulsion of *C. neoformans* and *C. gattii* occurs in macrophage cell lines (Alvarez *et al.*, 2008, Alvarez *et al.*, 2006, Ma *et al.*, 2006), primary murine macrophages (Alvarez *et al.*, 2006) and primary human macrophages (Alvarez *et al.*, 2006, Alvarez *et al.*, 2009). The rate of expulsion is increased 2.5 fold in primary human macrophages (Ma *et al.*, 2006), suggesting that it may be a frequent event in infected patients. After expulsion of cryptococci, macrophages are still motile and able to divide (Alvarez *et al.*, 2006, Ma *et al.*, 2006). Expelled cryptococci are also viable (Alvarez *et al.*, 2006, Ma *et al.*, 2006) and can be re-phagocytosed (Alvarez *et al.*, 2008). Expulsion appears to be a process triggered by the yeast, since heat killed cryptococci are not expelled (Alvarez *et al.*, 2006, Ma *et al.*, 2006), a finding that contrasts with the expulsion of dead yeast fragments by *Dictyostelium* (Clarke *et al.*, 2002). Expulsion events are rare during the first two hours of infection but,

after this initial lag phase, events are randomly distributed over the period of observation (Alvarez *et al.*, 2006, Ma *et al.*, 2006). The expulsion event itself takes approximately 60 seconds (Alvarez *et al.*, 2006, Ma *et al.*, 2006) but detailed data on the kinetics of expulsion is not currently available. Expulsion occurs with both *C. neoformans* (in both varieties) and with *C. gattii* (Alvarez *et al.*, 2006, Ma *et al.*, 2006) but there is significant inter-strain variation in the frequency of expulsion (Ma, Voelz, Johnston and May, unpublished data).

An interesting aspect of intracellular parasitism is the question what happens to the proliferating pathogen when the host cell divides. In the case of *Cryptococcus* it has been shown that yeast cells are unequally distributed after mitosis due to phagosomal fusion which in turn increases the occurrence of expulsion events (Luo *et al.*, 2008).

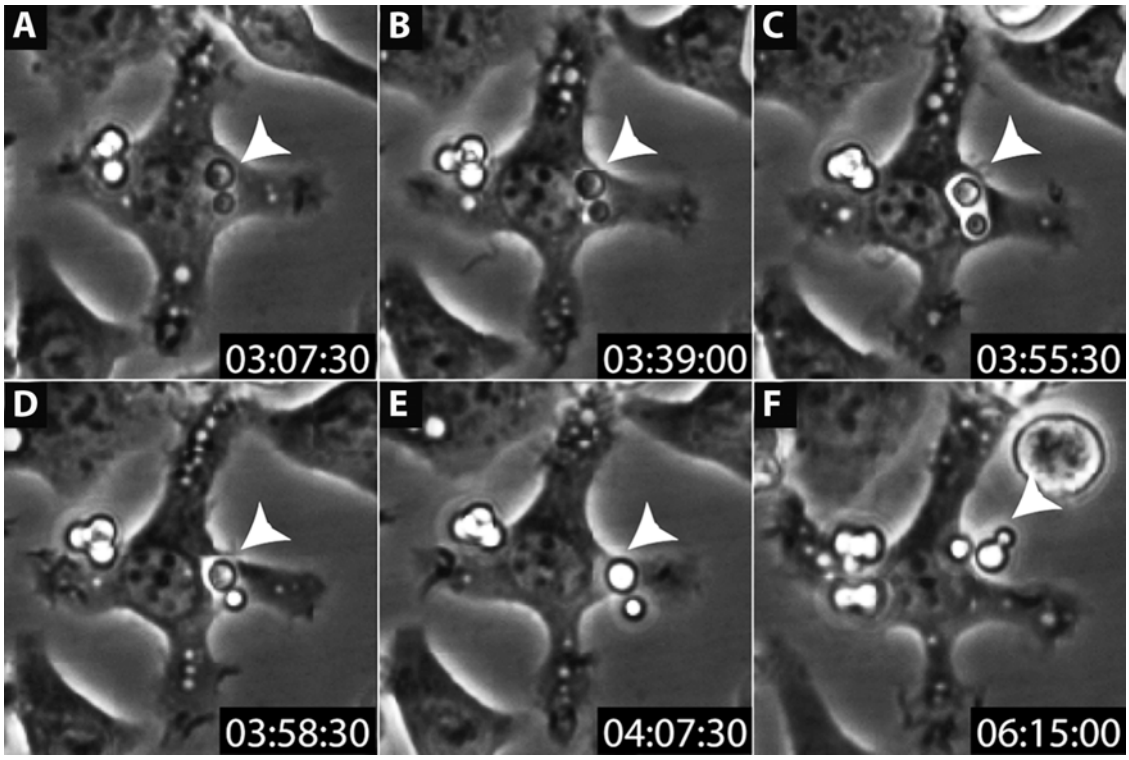

Figure 9: Cryptococcal expulsion from within a macrophage. *Cryptococcus* can exit macrophages in a novel non-lytic way that does not involve killing of the host cell or the yeast. Panels A-C show an intracellular yeast up to 3 hours 55 minutes 30 seconds. Three minutes later (panel D) the yeast is suddenly expelled. The macrophage and the yeast both stay alive as shown by continuing proliferation (panel E-F).

A key unanswered question in the field is the role played by different phagocytic uptake routes on subsequent cryptococcal behavior. The molecular processes that underlie phagocytosis vary extensively with different receptors as well as with size and shape of the engulfed particle (Champion *et al.*, 2006, Huynh *et al.*, 2007). Although the route of phagocytic uptake is not predictive of cryptococcal expulsion (Alvarez *et al.*, 2006, Ma *et al.*, 2006), frequency is reduced with complement opsonization (Alvarez *et al.*, 2006, Ma *et al.*, 2006). Since the phagocytosis of *Cryptococcus*, even when heavily opsonized, will likely include multiple types of receptors, the behavior of each engulfed cell is likely to be influenced by a complex interplay of multiple signaling pathways. Antibody-opsonized yeast cells exit the macrophages as biofilm like colonies aggregated by polysaccharides whereas complement-opsonized cryptococci are expelled individually (Alvarez *et al.*, 2008).

Prior to expulsion or proliferation, phagosomes containing *Cryptococcus* mature normally and fuse with lysosomes (Alvarez *et al.*, 2006, Ma *et al.*, 2006) and perturbation of this process modulates expulsion. Expulsion is reduced upon treatment with concanamycin A (Alvarez *et al.*, 2006, Ma *et al.*, 2006), an inhibitor of the V-type ATPase that is responsible for acidification of endosomes and lysosomes that fuse with the phagosome (Drose *et al.*, 1997). In contrast, chloroquine, a weak base that accumulates in acidic vesicles, buffering the pH, enhances the rate of expulsion (Alvarez *et al.*, 2006, Ma *et al.*, 2006). Since chloroquine and concanamycin A should produce similar effects on the phagosome, the difference in modulating expulsion may be due to a secondary activity of chloroquine, for example on the *Cryptococcus* vacuole (Harrison *et al.*, 2002). Chloroquine has been previously described to enhance anticryptococcal activity of bone marrow macrophages and is protective in murine infection (Levitz *et al.*, 1997a). The discovery that chloroquine increases expulsion therefore raises the possibility that the enhancement of anticryptococcal activity may be due to increased expulsion of *Cryptococcus* into the extracellular milieu where they are susceptible to killing by complement.

Expulsion does not require activation of macrophages with particular cytokines or other agonists (Alvarez *et al.*, 2006, Ma *et al.*, 2006). However, the rate of expulsion

is significantly higher in macrophages activated by so-called Type I cytokines (interferon gamma, or tumour necrosis factor alpha) than in those activated by Type II cytokines (e.g. interleukins 4 or 13) (Voelz *et al.*, 2009).

Phagosomes and other cellular vesicles, even very small ones, are relatively flat at the scale of the fusion of membrane bilayers. Thus, for fusion to occur, a significant charge barrier must be overcome by a local and transient high membrane curvature. Phagosomes containing even a single cryptococcal cell are relatively large and those in which substantial cryptococcal proliferation has occurred can represent a significant proportion of the host cell's volume. This, and other, energetic barriers make a purely mechanical explanation for cryptococcal expulsion highly unlikely. This is supported by experimental evidence that inert particles (heat-killed yeast or polystyrene beads) are never expelled by macrophages (Alvarez *et al.*, 2006, Ma *et al.*, 2006). Normally, macrophages function in the lung to clear indigestible particles and then travel up and out of the lungs before being swallowed (Brain, 1980). Were macrophages to freely expel indigestible material, lung clearance would be severely impaired.

The molecular mechanism of cryptococcal expulsion is unknown but, since exocytosis is regulated by a large number of protein complexes that are responsible for membrane fusion and specificity, it is extremely unlikely that *Cryptococcus* provides all these components itself. Instead, one possibility is that cryptococcal expulsion involves the hijacking of host cell factors in order to harness the host cell's exocytic machinery for expulsion. An analogous mechanism occurs in other intracellular pathogens, such as the Gram positive bacterium *Listeria monocytogenes*, which uses the bacterial protein ActA to 'hijack' the host Arp2/3 complex in order to stimulate the production of an actin tail for bacterial motility (May *et al.*, 1999). Such hijacking factors, however, are yet to be identified in *Cryptococcus*.

A recent publication has shown that actin might indeed play an important role during expulsion. The study revealed that phagosomes containing cryptococci undergo repeated cycles of actin polymerization; so-called actin flashes. These

flashes occur in form of a dynamic actin cage around the phagosome immediately after permeabilization of the phagolysosomal membrane. Interestingly, the occurrence of actin flashes and cryptococcal expulsion is inversely correlated indicating that the actin cage might act to inhibit expulsion (Johnston *et al.*, 2010).

1.3.2.3 LATERAL TRANSFER

A number of intracellular bacteria can be transferred laterally between host cell types (Bernardini *et al.*, 1989, Portnoy *et al.*, 2002, Stevens *et al.*, 2006) but the mechanism of transmission of bacteria that spread from cell to cell is not well understood even when the mechanism of escape is. *Listeria monocytogenes* polymerizes a tail of host actin that propels the bacterium into the plasma membrane (Dabiri *et al.*, 1990), whereupon the resulting membrane protrusion is engulfed by neighboring cells and the bacteria internalized. Internalization is an active process, since the force of the membrane protrusion alone is insufficient, but further details are unknown (Robbins *et al.*, 1999).

Similarly, *Cryptococcus* can be directly transferred from macrophage to macrophage in both macrophage cell lines (Figure 10) (Alvarez *et al.*, 2007, Ma *et al.*, 2007), and primary macrophages (Alvarez *et al.*, 2007, Ma *et al.*, 2007). Lateral transfer shares the same basic requirements as expulsion: it does not occur with heat-killed *Cryptococcus* or latex beads (Alvarez *et al.*, 2007) and is independent of both the phagocytic receptor type and the cryptococcal strain (Ma *et al.*, 2007). Unlike expulsion, however, lateral transfer is dependent on the actin cytoskeleton since treatment with the actin depolymerising drug cytochalasin D completely inhibits lateral transfer. The relationship between expulsion and lateral transfer is unclear, but it is easy to imagine that lateral transfer may occur when expulsion occurs in the close proximity of a suitable acceptor cell that can receive the ejected *Cryptococcus*. As cytochalasin D does not inhibit expulsion, it is therefore likely that it is the process of acceptance that is actin dependent, as with normal phagocytic processes. A second possibility is that a transient (actin-dependent) channel is opened between the two cells for transfer of *Cryptococcus*. Since macrophages

form frequent and intimate contacts with each other and with other cell types (for example, in order to form Langerhans or foreign body giant cells or to activate T cells) it is likely that lateral transfer represents an important route for prolonged intracellular persistence *in vivo*.

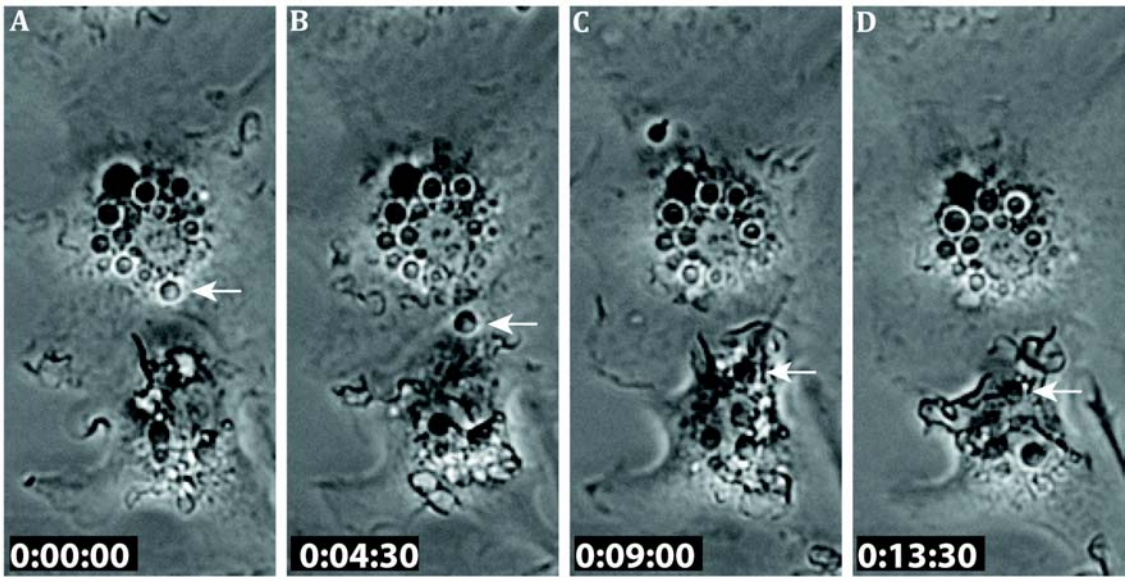

Figure 10: Lateral Transfer. *Cryptococcus* can be transferred from one macrophage to another. Time-lapse microscopy of lateral transfer in human primary macrophages. An intracellular yeast cell is first to be seen in the upper macrophage (A). This macrophage contacts a second macrophage and the yeast cell is transferred between them (B). Eventually, the yeast cell is detected intracellularly within the lower macrophage (C+D). Arrows indicate intracellular cryptococci. Times are shown in hours: minutes: seconds.

1.3.2.4 MACROPHAGES AND THE BLOOD-BRAIN-BARRIER

Cryptococcus predominantly infects the central nervous system after dissemination and hence has to cross the blood-brain-barrier (BBB). An understanding of the mechanism(s) by which the yeast invades the CNS is fundamental in deciphering disease pathogenesis during cryptococcosis.

Currently, three potential hypotheses have been proposed for cryptococcal entry into the brain, although little experimental evidence exists to date. Firstly, it has been suggested that the yeast can cross the endothelial cell layer transcellularly. *C. neoformans* can be mechanically trapped in small mouse brain capillaries (Shi *et al.*, 2010), adhere to and be internalized by endothelial cells *in vitro* (Ibrahim *et al.*, 1995) and by endothelial cells of the leptomeningeal capillaries *in vivo* (Chretien *et al.*, 2002). Secondly, the potential of a 'Trojan Horse'-like mechanism where *Cryptococcus* is transferred within macrophages across the BBB has been proposed. Evidence in support of this model has come from the observation of mononuclear cells containing intracellular yeast within meningeal capillaries (Chretien *et al.*, 2002) and also from a study in a mouse model where infection with macrophages containing cryptococci led to threefold increase in fungal burden within the brain compared to injection of free yeast cells (Charlier *et al.*, 2009). Thirdly, the potential for lateral transfer of cryptococcal cells from circulating leukocytes to the brain endothelium, as is known to occur from one macrophage to another, has been discussed as potential mechanism for invading the CNS.

It is now clear that cryptococci are adept intracellular pathogens, with complex mechanisms that allow them to proliferate within, and eventually exit from, host phagocytes. However, a vital and unanswered question is how the different facets of intracellular behaviour affect the progress of cryptococcal disease. There can be little doubt that intracellular proliferation ultimately benefits the pathogen, but the question of whether expulsion and/or lateral transfer slows or enhances disease progression remains unanswered. On the one hand, cryptococci expelled from

circulating monocytes will likely be exposed to a far greater immune attack than those that remain intracellular. However, if many monocytes are infected and there has been substantial intracellular proliferation then expulsion may lead to fungaemia as the extracellular fungi overwhelm the circulation. In addition, the 'Trojan Horse' hypothesis suggests that *Cryptococcus* crosses the blood brain barrier within parasitized macrophages (Charlier *et al.*, 2009, Luberto *et al.*, 2003), in which case the subsequent expulsion of the pathogen within the brain tissue is likely to be critical. Finally, it is also possible that cryptococci may be transferred directly from macrophages to endothelial cells via lateral transfer, followed by polar expulsion of *Cryptococcus* into the central nervous system. In the years ahead, the development of more effective therapeutic regimes is likely to rely heavily on the elucidation of both the molecular mechanisms that underlie the complexity of host manipulation by *Cryptococcus* and the impact that these mechanisms have on the progress of disease in infected patients.

1.4 CRYPTOCOCCAL VIRULENCE MECHANISMS IN THE INTERACTION WITH HOST CELLS

Pathogens have evolved a great variety of strategies to gain advantage within the host environment and to successfully undermine the host's defense mechanisms. Intracellular parasitism in particular is associated with a continuous struggle between the pathogen and its host cell. Within host cells, *Cryptococcus* encounters a harsh environment of reactive oxygen and nitrogen species; oxygen, nutrient and metal ion deprivation; low pH and high temperatures. Therefore, the yeast expresses multiple virulence factors including a capsule, melanin and a variety of secreted enzymes that can modify the host's defense mechanisms. This section will focus on strategies applied by *Cryptococcus* that counteract the host's responses in order to establish itself within the intracellular niche.

Interestingly, *Cryptococcus* does not seem to utilize manipulative strategies similar to those used by other intracellular pathogens. In fact, the yeast seems to be well adapted to the harsh environment within the host cell. In contrast to pathogens such as *Listeria monocytogenes* or *Shigella flexneri*, *C. neoformans* resides in and does not escape from the phagosome (Southwick *et al.*, 1996, Shoham *et al.*, 2005,

Levitz *et al.*, 1999). Moreover, *C. neoformans* does not inhibit phagosome-lysosome fusion in human macrophages (Levitz *et al.*, 1999) as has been shown for *Legionella pneumophila* (Horwitz, 1983) nor does the yeast interfere with phagosome maturation or acidification, as occurs during infections with *Histoplasma capsulatum* or *Mycobacterium avium* (Sturgill-Koszycki *et al.*, 1994, Strasser *et al.*, 1999, Shoham *et al.*, 2005, Levitz *et al.*, 1999). Instead the yeast survives and replicates in the acidic phagolysosome and, in fact, any increase in phagosomal pH (e.g. by experimental addition of chloroquine or ammonium chloride), leads to reduced intracellular proliferation (Levitz *et al.*, 1997a).

The cryptococcal polysaccharide capsule is the best-studied virulence factor (reviewed in (Zaragoza *et al.*, 2009)). It inhibits phagocytosis by macrophages (Levitz *et al.*, 1989, Granger *et al.*, 1985, Bolanos *et al.*, 1989), dendritic cells (Vecchiarelli *et al.*, 2003) and neutrophils (Kozel *et al.*, 1984, Dong *et al.*, 1997, Diamond *et al.*, 1972) and consequently non-encapsulated strains are phagocytosed three-times more effectively by human leukocytes (Bulmer *et al.*, 1967, Cross *et al.*, 1997). This effect seems to result from a masking mechanism of opsonins where the polysaccharides form a barrier between the opsonin and their receptor (McGaw *et al.*, 1979). Once infection is established, high concentrations of free glucuronoxylomannan (GXM), the major component of the cryptococcal capsule, are found in patient's bodily fluids making it likely that many antibodies form immune complexes before they can efficiently opsonise yeast cells (Powderly *et al.*, 1994). In addition, *C. neoformans* expresses the factor anti-phagocytic protein 1 (APP1) that inhibits uptake through a complement-mediated mechanism of binding to complement receptors 2 and 3 (Luberto *et al.*, 2003, Stano *et al.*, 2009).

Besides its anti-phagocytic properties, the cryptococcal capsule also provides protection against reactive oxygen (ROS) and nitrogen species within host cells. Part of the strategy by which phagocytic cells kill pathogens is the production of oxygen and nitrogen radicals (Diamond *et al.*, 1972, Alspaugh *et al.*, 1991, Hibbs *et al.*, 1987, Lovchik *et al.*, 1995, Murray *et al.*, 1983, Walker *et al.*, 1981). The cryptococcal polysaccharide capsule is an important factor in protecting against

oxidative stress by buffering reactive oxygen species (ROS). The capsule becomes enlarged upon interaction with phagocytic cells *in vivo* and *in vitro* (Feldmesser *et al.*, 2001a) and is important for the yeast's ability to multiply intracellularly, since encapsulated, but not acapsular, yeast cells can replicate inside macrophages (Feldmesser *et al.*, 2000). Cryptococcal susceptibility to ROS is directly correlated with capsule size; ROS kill cells with larger capsules less efficiently than cells with smaller capsules (Zaragoza *et al.*, 2008). The effect can be mimicked in cells with a small capsule by adding soluble capsular polysaccharide to the medium, thus demonstrating that resistance is directly mediated by the presence of capsular material (Zaragoza *et al.*, 2008). In fact, an earlier study showed that GXM reduces cryptococcal killing and production of superoxide in primary human neutrophils (Monari *et al.*, 2003). This effect may underlie the phenomenon of phenotypic switching, characterized by a switch in cryptococcal colony morphology between smooth and mucoid, with the latter showing increased survival in the murine macrophage cell line J774 (Fries *et al.*, 2001, Jain *et al.*, 2006, Guerrero *et al.*).

Furthermore, during intracellular growth a range of secreted enzymes are involved in detoxifying oxygen and nitrogen radicals: superoxide dismutase (SOD) (Cox *et al.*, 2003), an alternative oxidase (AOX1) (Akhter *et al.*, 2003), a flavinhemoglobin denitrosylase (FHB1) (de Jesus-Berrios *et al.*, 2003), urease (URA1) (Cox *et al.*, 2000), glutathione peroxidase (GLR1) (Missall *et al.*, 2004) and thiol peroxidase (TSA1) (Missall *et al.*, 2004). Superoxide dismutase (SOD) converts superoxide to hydrogen peroxide and oxygen (Fridovich, 1995) and a *C. neoformans sod1* mutant strain exhibits significantly attenuated growth inside primary human and murine macrophages (Cox *et al.*, 2003). Disruption of the alternative oxidase gene *aox1* also leads to significantly slower growth within murine alveolar macrophages (Akhter *et al.*, 2003). Similarly, FHB1, a flavohemoglobin denitrosylase, plays an important role in the response to nitrosative stress and knockout of *fbh1* leads to reduced proliferation in the murine macrophage cell line MH-S (de Jesus-Berrios *et al.*, 2003). In addition, the urease URE1 (Cox *et al.*, 2000) and the thiol peroxidase TSA1 (Missall *et al.*, 2004) have been shown to be involved in counteracting oxidative and nitrosative

stresses, although there are no direct data on the impact of these proteins on intracellular proliferation. The function of all these enzymes is dependent on the availability of NADPH. Two sources of NADPH are glucose-6-phosphate dehydrogenase (ZWF1) and NADP(+)-dependent isocitrate dehydrogenase (IDP1). Whilst deletion of *zwf1* does not change cryptococcal susceptibility to oxidative stress, mutation of *idp1* results in a sensitivity phenotype towards nitrosative stress (Brown *et al.*, 2010).

The pigment melanin, produced by the enzyme laccase, is thought to provide protection from both oxygen- and nitrogen reactive species in *Cryptococcus* by virtue of its antioxidant properties (Wang *et al.*, 1994, Wang *et al.*, 1995). The melanized *C. neoformans* strain 145 is more resistant to cell death caused by lymphocytes than the less melanized strain 52 (Huffnagle *et al.*, 1995). A model for the regulation of melanin production by the sphingolipid pathway in *Cryptococcus* proposes activation of protein kinase C1 (PKC1) via inositol-phosphoryl ceramide synthase (IPC1) through the regulation of diacylglycerol (DAG) and phytoceramide concentrations, resulting in subsequent PKC1-dependent laccase activation (Heung *et al.*, 2004). Deletion of *pkc1* shows that the gene is essential for the defense against oxidative and nitrosative stresses, however, as deletion of downstream targets in the signaling cascade does not show the same effect, PKC1 might also function independent of the MAP-kinase pathway (Gerik *et al.*, 2008). An *ipc1* mutant shows a decrease in melanin production (Luberto *et al.*, 2001) and significant down-regulation of intracellular growth in J774 macrophages. IPC1 consumes phytoceramide to produce complex sphingolipids and DAG. Thus, IPC1 probably increases cryptococcal survival via the activation of melanin production (Luberto *et al.*, 2001). Interestingly, DAG has been implicated in activation of PKC1, an activator of laccase (Heung *et al.*, 2004). The enzyme laccase is also involved in the synthesis of melanin by oxidizing catecholamine substrates (Williamson, 1997). However, Liu *et al.* (1999) (Liu *et al.*, 1999) reported a protective function of laccase that is independent of melanin synthesis. The *C. neoformans* strain 2E-TU, a laccase-deficient strain, is more sensitive towards killing by murine alveolar macrophages than the laccase-positive strain 2E-TUC. This laccase-mediated

protection from killing by macrophages also occurs in media lacking suitable catecholamine substrates and thus does not require melanin production. Further investigation revealed an iron oxidase function of laccase that may maintain iron in an oxidized form, thereby inhibiting production of hydroxyl radicals by the host cell (Liu *et al.*, 1999).

Glucosylceramide (GlcCer), a glycosphingolipid found at the surface of *C. neoformans* cells, has been identified as a regulator of fungal virulence in recent years (Rittershaus *et al.*, 2006). Knockout of the GlcCer synthase GCS1 results in a very interesting phenotype in mouse models where the mutant is rendered avirulent following nasal inhalation yet causes fatal disease when injected intravenously (Rittershaus *et al.*, 2006). The *Δgcs1* strain also shows a specific growth defect under high CO_2 and at neutral pH but still grows well within macrophages (Rittershaus *et al.*, 2006). Within tissues, the CO_2 concentration is relatively high at 5 % compared to 0.04 % in the atmosphere, suggesting that the sphingolipid might be involved in adaptation to the conditions within the host environment and that the mutant is impaired in traversing the lung tissue to reach the intracellular niche (Mitchell, 2006).

Within the intracellular environment, *Cryptococcus* is deprived of oxygen and nutrients. *Cryptococcus* grows very well under atmospheric oxygen condition (21 % O_2) but has to face low oxygen concentrations in the host ranging from approximately 12 % in the blood to only 3-6 % in tissues and the brain. In this context, Chun *et al.* (2007) (Chun *et al.*, 2007) and Chang *et al.* (2007) (Chang *et al.*, 2007) identified a mutant of the sterol regulatory element binding protein (SREBP) homolog Sre1p that is unable to grow under hypoxic conditions and shows reduced virulence in a mouse model. The Sre1p homolog is believed to be an oxygen-sensing component of the cholesterol biosynthesis regulatory pathway in mammals that is required for the induction of sterol synthesis genes under low oxygen concentrations (Lee *et al.*, 2007, Chang *et al.*, 2007). In mammals, SREBPs are localized in the ER-membrane and contain two transmembrane segments in a hairpin fashion with the N- and C-terminus pointing towards the cytoplasm. The N-terminal region functions as a basic helix-loop-helix-leucine zipper transcription

factor whereas the C-terminal region binds the cleavage activating protein SCAP (Figure 11) (Rawson, 2003). A similar pathway has been found in the fission yeast *Schizosaccharomyces pombe*. The SREBP homologs are called Sre1 and Sre2, the SCAP homolog Scp1. This pathway regulates adaptation to hypoxic conditions whereby low oxygen and decreased oxygen-dependent sterol synthesis lead to proteolytic cleavage of Sre1-Scp1 and activation of sterol synthesis gene transcription (Hughes *et al.*, 2005) and thus, might be a potential pathway for adaptation to the intracellular environment within phagocytes.

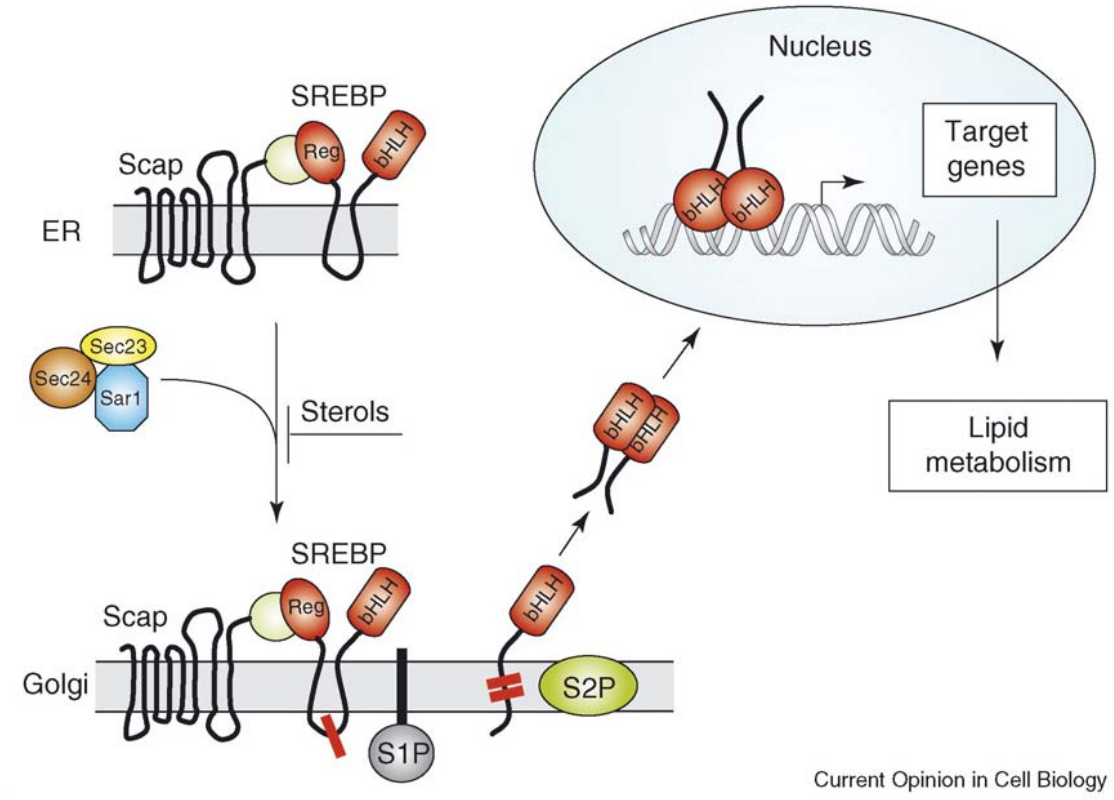

Figure 11: Schematic cholesterol biosynthesis regulatory pathway. The transmembrane protein SREBP is activated by proteolytic cleavage. The activated N-terminus acts as transcription factor and activates the transcription of targets genes involved in lipid metabolism. (Taken from Bengoechea-Alonso & Ericsson 2007 (Bengoechea-Alonso *et al.*, 2007)).

Under nutrient limitation, autophagy appears to be one way in which *Cryptococcus* acquires additional nutrients upon starvation. A cryptococcal strain lacking *vps34,* a component of the type I kinase sub-complex that is required for autophagy, is rapidly killed by murine macrophages (Kihara *et al.*, 2001). In addition, no autophagic bodies were detected in the mutant cells (Hu *et al.*, 2008). Strikingly, autophagy is normally a host response to control the replication of intracellular pathogens such as *Mycobacterium tuberculosis* (Gutierrez *et al.*, 2004) and *Legionella pneumophila* (Amer *et al.*, 2005). *Cryptococcus* therefore represents a rare example of a pathogen, rather than its host, utilizing autophagy during intracellular growth. There is also growing evidence that cryptococci increase nutrient flow into the phagolysosome via membrane disruption. Phospholipases hydrolyze ester linkages in glycerophospholipids, which can result in destabilization of membranes, cell lysis and release of second messengers (Ghannoum, 2000, Schmiel *et al.*, 1999). Phagocytosed *C. neoformans* cells, negative for phospholipase B (PLB) expression, display a defect in the onset of budding. This leads to a lag in intracellular proliferation relative to wild type cells (Cox *et al.*, 2001). As phospholipases can cause membrane damage and are also involved in lipid metabolism (Wright *et al.*, 2007), they may therefore be important for increasing nutrient availability to the pathogen.

Beside nutrient and oxygen starvation, intracellular cryptococci also experience low concentrations of metal ions. Many cryptococcal virulence enzymes such as laccase, SOD, catalase and urease, depend upon metal ions and thus cation-homeostasis is important for their functions. *C. neoformans* expresses two ferroxidases CFO1 and CFO2. CFO1 is required for the reductive iron uptake system and enables the utilization of transferrin as iron source during infection. Deletion of *cfo1* reduces cryptococcal virulence in mice (Jung *et al.*, 2009). To inhibit cryptococcal replication, macrophages actively try to reduce the concentration of metal ions in the phagolysosome. The macrophage-expressed protein NRAMP1 (natural resistance-associated-macrophage protein 1), which is homologous to the membrane transporters SFM1 and SFM2 in *Saccharomyces cerevisiae*, has been suggested to be involved in transport of divalent cations, such

as Mn^{2+}, Zn^{2+} or Fe^{2+}, across the phagosome membrane (Supek *et al.*, 1996). The *Nramp1*$^{-}$ bone marrow derived macrophage cell line 129.1 shows significantly reduced anticryptococcal activity in the first six hours after infection (Blasi *et al.*, 2001). This might reflect an altered intracellular environment with better cation availability for cryptococcal metal-dependent enzymes and therefore higher enzymatic activity and better protection from oxidative and nitrosative stress. Notably, many studies on *Cryptococcus*-host cell interactions use macrophage cell lines (e.g. RAW) derived from BALB/c mice (Barton *et al.*, 1995). However, it has been shown that these mice have defects in NRAMP1, and thus the intracellular proliferative potential might be overestimated in some cases.

Following uptake, the phagolysosome pH rapidly decreases to below pH 5.5 (Sturgill-Koszycki *et al.*, 1994) to improve antimicrobial activity. However, *Cryptococcus* actively prefers an acidic environment and phagosome alkalinization, by agents such as chloroquine, inhibits cryptococcal survival and intracellular proliferation (Levitz *et al.*, 1999). In addition, increased pH also reduces cation availability and might inhibit yeast enzyme functions. Nonetheless, *Cryptococcus* still needs to adapt to the low phagolysosomal pH. The enzyme inositol phosphosphingolipid-phospholipase C (ISC1), an enzyme generating phytoceramide, seems to be important in providing protection from the acidic milieu. In *S. cerevisiae*, phytoceramide plays an important role in regulating PMA1 (Ferreira *et al.*, 2001, Gaigg *et al.*, 2005), an ATPase that is involved in the regulation of intracellular pH (Holyoak *et al.*, 1996, Stadler *et al.*, 2001, Soteropoulos *et al.*, 2000) as well as oxidative (Sigler *et al.*, 1991) and nitrosative stress (Zhao *et al.*, 2004). In fact, intracellular survival in J774 macrophages of the *isc1* mutant strain was significantly reduced and the strain was more sensitive to oxidative, nitric and acidic stress (Shea *et al.*, 2006). The cryptococcal VSP41 homolog has also been implicated in regulating metal ion concentrations by copper loading of the iron transporter FET3 in yeast (Radisky *et al.*, 1997). Disruption of *vps41* in *C. neoformans* results in abolishment of intracellular growth in J774 macrophages as well as reduced cryptococcal growth on iron- and copper-deficient media (Liu *et al.*, 2006).

It is clear that the processes that allow the transition between extracellular and intracellular proliferation of *Cryptococcus* in host cells are controlled. However, very little is known about the signaling pathways regulating the expression of the virulence factors described above. The cryptococcal two-component stress regulator SKN7 has been shown to be involved in oxidative stress signaling in endothelial cells. Disruption of *skn7* results in significantly impaired growth in primary human umbilical-vein endothelial cells (Coenjaerts *et al.*, 2006). In addition, the Rho-type GTPases CDC42 and RAC have been implicated in the regulation of high temperature growth, mating and cell morphology in *C. neoformans* (Alspaugh *et al.*, 2000, Nichols *et al.*, 2007, Vallim *et al.*, 2005, Waugh *et al.*, 2003) whilst RDI1 (a Rho-GTPase dissociation inhibitor that regulates GTPase activity in fission yeast (Koch *et al.*, 1997, Nakano *et al.*, 2003)) is important for intracellular growth (Price *et al.*, 2008).

In addition to host cell and *Cryptococcus* factors, immune-signaling molecules such as cytokines regulate yeast survival. Cytokine signaling leads to downstream activation or inhibition of antimicrobial effects in other immune cells such as phagocytic effector cells; Th1 cytokines activate macrophages to create an oxidative and nitrosative burst as microbicidal mechanisms (classically activated macrophages) (Shoham *et al.*, 2005, Huffnagle, 1996) whereas Th2 polarized host responses lead to inhibition of phagocyte activity (alternatively activated macrophages) and enhanced susceptibility to *C. neoformans* (Koguchi *et al.*, 2002). This alternative activation is associated with up-regulated expression of genes involved in tissue repair such as arginase-1 and the mannose receptor (reviewed in (Gordon, 2003)). Arginase-1 competes with inducible nitric oxidase for the substrate L-arginine and so decreases synthesis of nitric oxide (Hesse *et al.*, 2001). Furthermore, a recent study has suggested that anti-inflammatory cytokines might enhance iron uptake and storage by macrophages by suppressing the activation of iron regulatory protein 1 and 2, leading to translational repression of the iron storage protein ferritin or translational activation of the membrane receptor for iron uptake (Osterholzer *et al.*, 2009b). This would result in increased metal ion availability and thus increased activity of virulence factors. In fact, intracellular

cryptococcal proliferation is significantly higher, and the occurrence of expulsion significantly lower, in macrophages activated by Th2 cytokines IL-4 or IL-13 than in cells stimulated by Th1 cytokines, such as IFN-γ and TNF-α (Figure 12) (Voelz *et al.*, 2009). Likewise, the number of intracellular cryptococci is increased in alveolar macrophages isolated from IFN-γ knockout mice (Arora *et al.*, 2005). It is therefore likely that a shift to a Th2 environment results in activation changes in phagocytic effector cells and hence to a change in the composition of phagolysosomes. However, IFN-γ treatment increases intracellular growth of *C. neoformans* in human macrophages (Levitz *et al.*, 1990, Reardon *et al.*, 1996), suggesting that aspects of this response may be host species specific. To counteract Th1-related cytokine activation, *C. neoformans* expresses eicosanoids (Noverr *et al.*, 2001), for example prostaglandins and leukotrienes, which are potent inhibitors of Th1-type immunity that shift the Th1-Th2 balance towards a Th2 immune response and thus more efficient intracellular proliferation (Noverr *et al.*, 2003).

Thus within the host the establishment of an intracellular niche by *Cryptococcus* results from the activity of a great variety of virulence factors that coordinate to undermine the host's defense response. Although much progress has been made in identifying these virulence factors, the molecular mechanisms by which adaptation to the intracellular environment is mediated and how these factors are regulated remains to be fully elucidated.

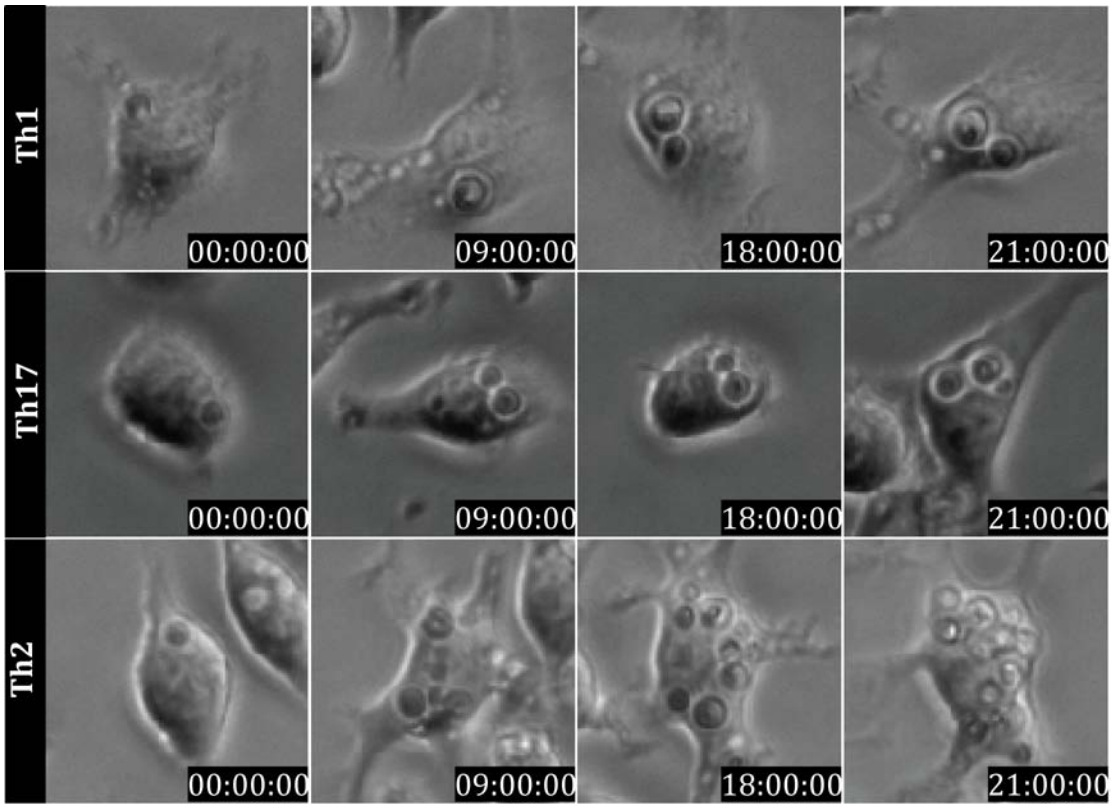

Figure 12: Th1/Th2/Th17 balance during cryptococcosis. The ability of macrophages to inhibit cryptococcal growth is strongly dependent on cytokine balance. A Th1 and/or Th17 cytokine profile leads to less intracellular *C. neoformans* and *C. gattii* proliferation whereas a dominant Th2 cytokine profile increases cryptococcal proliferative potential. The three panels show intracellular yeast proliferation at 0, 9, 18 and 21 hours after treatment with the Th1 cytokine TNF-α, the Th17 cytokine IL-17 and the Th2 cytokine IL-13.

1.5 AIMS AND STRATEGY

Cryptococcosis is a constant and increasing medical problem, due to both the HIV pandemic and to the emergence of highly virulent strains. In addition, currently applied antifungal treatment regimes are not satisfactory for a number of reasons. This has led to a substantially increased effort to understand the pathogenesis of the fungus in recent years. We now have an understanding of how the host immune system tries to clear the yeast during an infection and have also started to decipher the mechanisms by which *Cryptococcus* undermines the host immune system. Much of these recent data highlight the importance of the cryptococcal/macrophage interaction – not only as an intracellular niche but potentially also as trafficking vehicle for dissemination. This leaves us with a complex network that has to be considered in the development of more effective anticryptococcal therapies. Future research will not only have to focus on the molecular mechanisms of pathogenicity but also on the effect on cryptococcal disease within a treated host. The research presented in this thesis tries to deepen the understanding of the role macrophages play during cryptococcosis and concentrates on four aspects.

The first study focuses on the host, in particular on the effect of immune regulation on the interaction between macrophages and *Cryptococcus*. It is well established

that *C. neoformans* is a pathogen of the immunocompromised showing defects in CMI, and also that Th1 but not Th2 cytokine profiles are protective in cryptococcal disease. However, these facts rely on observations made in whole organisms. This part of the thesis analyses the effect of different cytokine profiles on the interaction with macrophages in an attempt to understand the importance of the Th1/Th2 balance during disease.

The second part of this thesis is a technical chapter. Current approaches for the investigation of macrophage-*Cryptococcus* interactions are very time-consuming and low throughput. This section reports the analysis of yeast uptake, intracellular replication and occurrence of expulsion via a flow cytometry approach by creating GFP-expressing cryptococcal type strains. The mutant phenotypes are analysed and strategies for automated analysis described.

The third study concentrates on the question of how certain *C. gattii* strains have acquired a hypervirulent phenotype that causes disease in immunocompetent individuals. This section examines the role of mitochondria in adaptation to the intracellular environment within macrophages and examines the effect of different host cell stresses on the morphology of yeast mitochondria and the behavior of cryptococcal mitochondria within host cells over time. In addition, available mitochondrial genomes are investigated and the first steps towards a comparative mitochondrial genome analysis undertaken.

The final chapter presents data on the involvement of the sterol response element binding protein 1 (Sre1p) in oxygen signaling during interaction between macrophages and *Cryptococcus*.

CHAPTER 2

MATERIAL AND METHODS

Major parts of this chapter have been published or have been submitted for publication:

Voelz, K., S. A. Johnston, J. C. Rutherford and R. C. May. 2010. Automated analysis of cryptococcal macrophage parasitism using GFP-tagged cryptococci: a tool for the research community. PLoS One (Submitted)

Byrnes, E. J. 3rd, W. Li, Y. Lewit, H. Ma, K. Voelz, P. Ren, D. A. Carter, V. Chaturvedi, R. J. Bildfell, R. C. May and J. Heitman. 2010. Emergence and pathogenicity of highly virulent Cryptococcus gattii genotypes in the northwest United States. PLoS Pathog. **6:** e1000850. (Byrnes *et al.*, 2010)

Voelz, K. and R. C. May. 2009. Cytokine signaling regulates the outcome of intracellular macrophage parasitism by *Cryptococcus neoformans*. Infect Immun. **77: 3450**-3457 (Voelz *et al.*, 2009)

2.1 MICROBIAL CULTURE TECHNIQUES

2.1.1 *CRYPTOCOCCUS* STRAINS AND CULTIVATION

Cryptococcus strains (Table 2) were cultured in media (YPD) containing 1 % peptone, 1 % yeast extract and 2 % D-(+)-glucose either on plates or in liquid culture at 25°C with shaking at 240 revolutions per minute (rpm) or rotating at 20 rpm. For molecular manipulations (Voelz *et al.*, 2009, Ma *et al.*, 2006), yeast were grown on plates or in liquid culture at 30°C with shaking at 180 rpm. Stocks were frozen down in 20 % glycerol at -80°C.

Table 2: *Cryptococcus* strains used for experimental work. Serotype and additional information are presented if available.

Species **Strain**	**Sero-type**	**Geno-type (AFLP)**	**IPR in PMA activated J774 macrophages (Ma *et al.*, 2009a)**	**Additional Information**
C. neoformans H99	A	1	1.42	Clinical isolate, USA
C. neoformans ATCC90112	A	1	2.85	Clinical isolate from cerebrospinal fluid, USA
C. neoformans JEC21	D	2	2.12	Clinical isolate, AIDS case, USA
C. gattii R265	B	6	1.74	Clinical isolate from Vancouver Island outbreak, Canada
C. gattii A1M-R271	B	6	2.04	Clinical isolated from immunocompetent male, British Columbia, Canada
C. gattii A1M-F2932	B	6	2.98	Clinical isolated from immunocompetent male, British Columbia, Canada
C. gattii ENV152	B	6	2.28	Alder tree, Vancouver Island, Canada
C. gattii CBS7229^{T}	B	4	0.56	Meningitis, China
C. gattii CBS8684	B	6	0.90	Wasp nest, Uruguay
C. gattii CBS7750	B	6	0.93	*E. camaldulensis*, USA
C. gattii CBS1930	B	6	1.14	Sick goat, Aruba

2.1.2 *SACCHAROMYCES CEREVISIAE* STRAIN AND CULTIVIAITON

The uracil negative *Saccharomyces cerevisiae* MLY40 (Lorenz *et al.*, 1997) was used for homologous recombination in this study. The yeast was cultured either on YPD plates or in liquid media at 30°C with shaking at 180 rpm. Stocks were frozen down in 15 % glycerol at -80°C.

2.1.3 *ESCHERICHIA COLI* STRAIN AND CULTIVIATION

The *Escherichia coli* strain DH5α was cultured on LB broth media either on plates or in liquid media at 37°C with shaking at 220 rpm. Stocks were frozen down in 40 % glycerol at -80°C.

2.2 CELL CUTLURE TECHNIQUES

2.2.1 MAMMALIAN CELLS AND GROWTH CONDITIONS

The semi-adherent macrophage-like cell line J774 and human primary monocyte-derived macrophages were used for experimental work. The cell line is derived from a reticulum sarcoma that arose in a female BALB/c/NIH mouse (Ralph *et al.*, 1975). The cells were used between passage 5 and 20 after thawing and cultured in Dulbecco's Modified Eagle Medium (DMEM) supplemented with 10 % heat-inactivated fetal bovine serum (FBS), 2 mM glutamine, 100 units/ml streptomycin and 100 units/ml penicillin (culture media) at 37°C and 5 % CO_2 (Voelz *et al.*, 2009, Ma *et al.*, 2006). Human primary peripheral blood monocytes were isolated from Buffy coats from eight independent healthy volunteers supplied by the local blood transfusion unit. To separate and collect mononuclear cells, the sample was diluted two-fold and 30 ml was centrifuged over a 20 ml Ficoll-Paque PLUS cushion at 400 relative centrifugal force (rcf) for 30 min. The mononuclear layer was collected and washed multiple times with phosphate-buffered saline (PBS, pH 7.2) to remove platelets. Monocytes were isolated by adherence to plastic at a concentration of 4-6 x 10^6 cells/ml in RPMI 1640 media supplemented with 2 % FBS, 2 mM glutamine, 100 units/ml streptomycin and 100 units/ml penicillin

at 37°C and 5 % CO_2 for 1 hr. Non-adherent lymphocytes were removed with warm PBS and adherent cells differentiated into macrophages in RPMI 1640 media supplemented with 10 % FBS, 2 mM glutamine, 100 units/ml streptomycin and 100 units/ml penicillin at 37°C and 5 % CO_2 (culture media) containing 100 units/ml GM-CSF. After incubation overnight, the cells were washed with warm PBS and detached with ice-cold PBS on ice for 30 min. The macrophages were collected, resuspended and plated into 24 well plates at a concentration of 5 x 10^5 cells/well in RPMI 1640 culture media containing 100 units/ml GM-CSF. The next day, the media was replaced by GM-CSF free RPMI 1640 culture media and the cells cultured for another 4 days at 37°C and 5 % CO_2 before assays were commenced (Voelz *et al.*, 2009).

2.2.2 FREEZING DOWN STOCKS OF J774 MACROPHAGES

To freeze down J774 macrophage stocks, cells were grown until 90 % confluent, mechanically detached from the tissue culture flask using a cell scraper and transferred into centrifuge tubes. Cells were collected by centrifugation for 10 min at 1000 rcf and 20°C. The supernatant was discarded and the macrophages resuspended in filter sterilized freezing media containing 50 % FBS, 40 % DMEM and 10 % Dimethyl sulfoxide (DMSO). Aliquots were frozen down for 3 hr at -20°C and 24 hr at -80°C before being transferred to -80°C. Quick handling was required to avoid cell damage caused by DMSO.

2.2.3 DEFROSTING J774 CELLS FROM LIQUID NITROGEN

Aliquots of J774 cells were defrosted from liquid nitrogen storage and 10 ml of DMEM culture media was added immediately to avoid cell damage caused by DMSO. The cells were collected for 10 min at 1000 rcf and 20°C. The supernatant was removed, fresh pre-warmed culture media added and transferred into tissue culture flasks for cell culture.

2.2.4 SUBCULTURE OF J774 MACROPHAGES

To subculture J774 macrophages, the media was removed and replaced with fresh pre-warmed DMEM culture media. Cells were mechanically detached from the tissue culture flask, diluted to the desired concentration and cultured in fresh culture media in tissue culture flasks.

2.3 ANALYSIS OF MACROPHAGE PARASITISM BY *CRYPTOCOCCUS*

2.3.1 CONDITIONS USED FOR INFECTION OF MACROPHAGES WITH *CRYPTOCOCCUS* SP., PHAGOCYTOSIS ASSAYS, PROLIFERATION ASSAYS AND LIVE CELL IMAGING

For the analysis of cytokine influence, macrophages were treated with the cytokines IFN-γ, TNF-α, IL-17, IL-4 or IL-13. As a negative control and for experiments under hypoxic conditions, macrophages were activated with PMA for 1 hr only. Cobalt chloride ($CoCl_2$) was used to mimic hypoxic conditions (Table 3) (Lee *et al.*, 2007).

Table 3: Treatments and concentration used for infection of macrophages.

Condition	Concentration
PMA	150 ng/ml
IFN- γ	10 U/ml
TNF-α	1 ng/ml
IL-17	10 ng/ml
IL-4	10 ng/ml
IL-13	10 ng/ml
Cobalt Chloride	0.1 mM
Hypoxia	3 % O_2

2.3.2 INFECTION OF MACROPHAGES WITH *CRYPTOCOCCUS*

Cryptococcus strains were cultured in liquid YPD media (1 % peptone, 1 % yeast extract, 2 % D-(+)-glucose) for 24 hr at 25°C with shaking at 240 rpm or rotating at 20 rpm prior to experimental use (Voelz *et al.*, 2009, Ma *et al.*, 2006). One ml of J774 cells (10^5 cells/ml) in culture media were plated into each well of a 24-well tissue-culture-treated plate 24 hr prior to infection and kept at 37°C and 5 % CO_2. One hr before infection, J774 cells were switched to serum-free DMEM (as culture media but without FBS) with, if applicable, the culture condition to be tested (see section 2.3.1). The human primary macrophages were pre-incubated in the conditions to be tested 24 hr prior to the experiment in RPMI 1640 culture media and 1 hr in serum-free RPMI 1640 culture media before infection. At the same time, *Cryptococcus* cells from 24-hr-old liquid cultures were washed 3 x with PBS, counted in a haemocytometer and opsonized with 10 μg/ml of the monoclonal antibody 18B7 (a kind gift from Arturo Casadevall) or 10 % human serum at 37°C for 1 hr. Human serum was obtained from blood drawn from healthy volunteers, which was allowed to clot for 3 hr at 37°C before the serum fraction was drawn off and used immediately. After pre-incubation, the opsonized yeast cells were directly added to J774 cells or peripheral blood macrophages at a ratio of ten yeast cells per macrophage and phagocytosis was allowed to proceed for 2 hr at 37°C in a 5 % CO_2 atmosphere. Afterwards, non-internalized yeast cells were removed by extensive washes with pre-warmed PBS and effectiveness of washing was controlled under a microscope (Voelz *et al.*, 2009, Ma *et al.*, 2006).

2.3.3 PHAGOCYTOSIS ASSAY

To assess the extent of *Cryptococcus* phagocytosis, J774 cells or human primary macrophages were grown on 13 mm glass coverslips and infected as described above. Coverslips for cell culture were prepared by acid-wash to remove any dirt or detergent and to enhance cell adhesion. The coverslips were covered with 1 M hydrochloride acid and swirled for five minutes. Afterwards, the acid was rinsed with copious amounts of distilled water followed by several washes with

100 % ethanol. The coverslips were kept in 100 % ethanol until further use. Cells were fixed on the coverslips with 4 % formaldehyde for 20 min at 4°C. The coverslips were washed three times in PBS and twice in distilled water before being mounted in Mowiol mounting media (100 mM Tris-HCl pH 8.5, 9 % Mowiol, 25 % glycerol) on microscope glass slides. Mowiol mounting media is a polyvinyl alcohol solution with hardening properties. Due to its optical properties – non-absorbent and not light scattering when used with immersion oil - it prepares sample cover slips for microscopy. A total of at least 1000 cells were observed per sample coverslip and scored for cells with internalized yeast cells. The extent of *Cryptococcus* phagocytosis was calculated as the percentage of cells with internalized *Cryptococcus* (percentage phagocytosis) (Voelz *et al.*, 2009).

2.3.4 PROLIFERATION ASSAY

The ability of *Cryptococcus* to proliferate within J774 cells and human primary macrophages was analyzed in proliferation assays. Following infection, fresh serum-free culture media was added to the wells and further cultured at 37°C in a 5 % CO_2 atmosphere. When pre-treated, the cultures were maintained at the concentrations mentioned above. Samples were taken after infection and removal of non-internalized yeast cells at 0, 18, 24, 48 and 72 hr. Intra- and extracellular yeast cells were counted separately after Trypan blue staining with a haemocytometer. For extracellular yeast numbers, the extracellular media was collected in a reaction tube and the well washed with 200 µl PBS and collected in the same tube to collect any remaining extracellular yeast. Cells with intracellular *Cryptococcus* cells remain attached to the bottom of the dish. To count the intracellular yeast cell number, cells were lysed in 200 µl distilled H_2O at 37°C for 30 min. The cells were scraped off and collected, and an additional 200 µl PBS was used to wash the well and added to the same collection tube. The intracellular yeast cell number was then counted and calculated relative to time point T=0. The maximal Intracellular Proliferation Rate (IPR) was used as a measure of intracellular proliferative capacity and is calculated as the highest intracellular

yeast count (typically at 18 or 24hrs) divided by the initial intracellular yeast count at T=0. The IPR was calculated separately for each individual experiment and for each condition (relative to cells incubated with the same condition to control for differential uptake) (Voelz *et al.*, 2009).

2.3.5 LIVE CELL IMAGING

Following infection of J774 cells and human primary macrophages with *Cryptococcus* as described above, fresh serum-free culture media and the corresponding condition used for pre-treatment were added to the wells before further culture at 37°C and 5 % CO_2 in a controlled chamber (OKOLAB). Cells were imaged on a Nikon Eclipse TE2000-U microscope with 20 x phase contrast objective and 1 x optivar. Images were captured every 90 seconds for 20 hr on a Nikon Digital Sight DS-Qi1MC camera and compiled into time lapse movies using the software NIS-Elements AR 3.0. The number of expulsion events in three independent experiments for each cytokine was counted by eye (Voelz *et al.*, 2009).

2.3.6 ACCUTASE TREATMENT

J774 macrophages were detached and separated by Accutase (PAA) treatment. The cells were incubated with the undiluted proteolytic and collagenolytic enzyme mix for 15 min at 37°C and then gently dissociated by pipetting to ensure a single cell suspension; cell separation was checked by eye under a microscope.

2.3.7 FLOW CYTOMETRY

Samples were fixed by adding an equal volume of 2 % formaldehyde and 2 % FBS in PBS. Flow cytometry parameters were measured using a FACSCaliber instrument (BD Biosciences) and analysed with CellQuestPro (BD Biosciences). To

enable comparison of different samples/time points, the number of flow cytometry events over a fixed time period was assessed. Intracellular proliferation was calculated by measuring the geometric mean of GFP fluorescence of macrophages containing cryptococci, normalising this value to the geometric mean of extracellular cryptococci and multiplying by the number of macrophages containing cryptococci. These values for each time point was normalised to time point zero and the maximum ratio taken as the maximum proliferation rate. Flow cytometry measurements and analysis of data was carried out together with Dr. S. A. Johnston (School of Biosciences, University of Birmingham).

2.4 ANALYSIS OF CRYPTOCOCCAL STRAINS

2.4.1 SUSCEPTIBILITY TREATMENT OF *CRYPTOCOCCUS* STRAINS

To test *C. gattii* strains for their susceptibility towards different stress conditions, different settings were created to mimic different degrees of hypoxia (0, 0.025, 0.05, 0.075, 0.1, 0.15, 0.3 and 0.6 mM $CoCl_2$), oxidative (0, 0.125, 0.25, 0.5, 1, 3, 6 and 14 mM H_2O_2), nitrosative (0, 0.25, 0.5, 2.5, 5, 10, 15 and 20 mM $NaNO_2$), cell wall (0, 0.005, 0.01, 0.025, 0.05, 0.1, 0.25 and 0.5 % sodium dodecyl sulphate (SDS) and 0.0001, 0.001, 0.01, 0.025, 0.05, 0.1 and 0.3 mM NaCl) and radiation (UV 254nm; 0, 0.005, 0.01, 0.02, 0.03, 0.04, 0.06, 0.08 and 0.1 J/cm^2) stress. *Cryptococcus* strains were cultured in liquid YPD media (1 % peptone, 1 % yeast extract, 2 % D-(+)-glucose) for 24 hr at 25°C with shaking at 240 rpm prior to experimental use (Ma *et al.*, 2006). *Cryptococcus* cells from 24-hr-old liquid cultures were washed three times with PBS, counted in a haemocytometer and adjusted to 10^5 cells per ml in serum-free DMEM. One ml of the yeast solution was added into each well of a 48-well plate and the stress factor was transferred accordingly. The yeast was then incubated at 37°C and 5 % CO_2. To assess the influence of the stresses on cryptococcal growth, serial dilutions were plated and colony-forming units (CFUs) counted after 0 and 24 hr. For UV treatments, yeast

was allowed to recover for 30 min at 37°C before plating. CFUs relative to time point 0 and relative to an untreated control were calculated to enable comparison between several *Cryptococcus* strains with different growth rate.

$$\text{Relative CFU} = \frac{\frac{\text{CFU}_{\text{T=24 treated}}}{\text{CFU}_{\text{T=0}}}}{\frac{\text{CFU}_{\text{T=24 untreated}}}{\text{CFU}_{\text{T=0}}}}$$

GFP expressing strains were tested for their susceptibility towards cellular stresses with the following conditions: hypoxia (3 % oxygen or treatment with 0.05, 0.1 and 0.3 mM $CoCl_2$ (Lee *et al.*, 2007)), oxidative (0.25, 0.5 and 1 mM H_2O_2) or nitrosative (1, 5 and 20 mM $NaNO_2$) stress, or exposure to cell wall damage (0.005, 0.01 and 0.05 % SDS or 0.05, 0.1 and 0.3 mM NaCl) in serum-free DMEM, the medium routinely used in macrophage assays. Cryptococcal cells from 24 hr old cultures were washed three times with PBS, counted in a haemocytometer and adjusted to 10^5 cells/ml in serum-free DMEM. One ml of yeast solution was incubated with the appropriate stress in 48-well plates and left at 37°C and 5 % CO_2 for 24 hr without shaking. To assess the influence of stress conditions on cryptococcal growth, serial dilutions were plated and CFUs counted after 0 and 24 hr. CFUs relative to time point 0 were calculated.

2.4.2 MITOCHONDRIAL MORPHOLOGY ASSAY

The mitochondrial morphology assays were conducted in a similar way to those in previous studies, with modifications (Ma *et al.*, 2009a). *C. gattii* cells were grown overnight at 37°C in DMEM untreated or under a stress condition (1 mM H_2O_2, 5 mM $NaNO_2$, 0.1 mM $CoCl_2$, 3 % O_2, 0.005 % SDS, 0.05 mM NaCl) in a 5 % CO_2

incubator without shaking for 24 hr, or isolated from macrophages 24 hr after infection. After UV treatment, yeast were allowed to recover for 30 min at 37°C. Growth in YPD media at 25°C was also included as control. For time course experiments, cells were recovered from macrophages and stained after 0, 2, 6, 12, 18 and 24 hr. The cells were harvested, washed with PBS twice and re-suspended in PBS containing the Mito-Tracker Red CMXRos (Invitrogen) at a final concentration of 20 nM. Cells were incubated for 15 min at 37°C. After staining, cells were washed in triplicate and re-suspended in PBS. For each condition, more than 100 yeast cells per replicate for each of the tested strains were chosen randomly and analyzed. For quantifying different mitochondrial morphologies, images were collected using a Zeiss Axiovert 135 TV microscope with a 100 x oil immersion Plan-Neofluar objective. Both fluorescence images and phase contrast images were collected simultaneously. Images were captured with identical settings on a QIcam Fast 1394 camera using the QCapture Pro51 version 5.1.1 software. All images were processed identically in ImageJ and mitochondrial morphologies were analyzed and counted blindly (Byrnes *et al.*, 2010).

2.5 MOLECULAR METHODS

2.5.1 BIOLISTIC TRANSFORMATION

Different systems have been applied to transform *Cryptococcus* including electroporation, biolistic and *Agrobacterium*-mediated transformation. Problems have been encountered due to the polysaccharide capsule, different transformation efficiencies for different serotypes and ectopic or extrachromosomal insertion of DNA (Toffaletti *et al.*, 1993, McClelland *et al.*, 2005, Idnurm *et al.*, 2004, Davidson *et al.*, 2000, Varma *et al.*, 1992a, Edman *et al.*, 1990).

The first successful transformation of *C. neoformans* was described in the early 1990's. DNA was introduced into yeast cells using an electric field. Short electric pulses of high voltage lead to short-term increase in plasma membrane permeability and allow the entry of macromolecules such as DNA into the cell. The analysis of the transformants showed a very low efficiency of only 12 % stable transformation with linear DNA. Attempts to transform *Cryptococcus* with circular DNA resulted in even lower efficiencies. Furthermore, the DNA was ectopically integrated or maintained extrachromosomal in most of the cases. At this stage, only overexpression and complementation of genes was possible. To allow gene

knockout or replacement studies improved transformation techniques were required (Edman *et al.*, 1990, Varma *et al.*, 1992a).

June Kwon-Chung's group applied *Agrobacterium*-mediated transformation to further increase transformation efficiencies. *Agrobacterium tumefaciens* is a gram-negative soil bacterium that can cause crown galls in infected plants. During infection, a part of the so-called bacterial T_i plasmid, the T-DNA, can be transferred into and expressed in the host. High transformation efficiencies for all different serotypes were achieved using this method. More important, almost 100 % of these transformants were reported to be stable and 50 – 80 % showed only one T-DNA insertion. Unfortunately, homologous recombination was not observed with this method (McClelland *et al.*, 2005, Idnurm *et al.*, 2004).

Shortly after the first successful electroporation of *Cryptococcus*, biolistic transformation was tested to improve transformation efficiency. Particles coated with DNA were shot into cells using a so-called gene gun. Transformation efficiencies were increased to 15 – 24 % with homologous recombination frequencies of up to 50 % in serotype A and 1 – 4 % in serotype D. Biolistic transformation also enabled transformation with circular DNA. However, this DNA delivery system did not result in sufficient stable transformation efficiencies and showed a high percentage of ectopic and extrachromosomal DNA integration (Davidson *et al.*, 2000, Toffaletti *et al.*, 1993).

2.5.1.1 CLONING STRATEGY

Two slightly different strategies were applied for the knockout of the gene *sre1* and the knock in of a GFP cassette. The former comprised the creation of a knockout cassette by homologous recombination of overlapping PCR fragments in *S. cerevisiae,* followed by biolistic bombardment and homologous recombination in the target genome (Figure 13) whereas the latter randomly integrates a GFP-expression cassette ligated into a plasmid in the target genome. For construction of GFP-tagged cryptococcal strains, *C. neoformans* serotype A strain H99 and *C. gattii*

serotype B strain R265 were transformed with a GFP construct by biolistic bombardment (Toffaletti *et al.*, 1993). The insertion cassette was constructed by PCR amplification with overlapping primers of the *C. neoformans* JEC21 *act1* promoter (AY483215), the GFP coding sequence and the *C. neoformans* JEC21 *trp1* terminator (AY483215) followed by lithium acetate transformation in the uracil negative *Saccharomyces cerevisiae* strain MLY40 (Lorenz *et al.*, 1997) to achieve homologous recombination of overlapping DNA fragments into the plasmid pRS426 (Christianson *et al.*, 1992). The plasmid was recovered from *S. cerevisiae,* electroporated into *Escherichia coli* DH5α and the GFP construct isolated by PCR. After digestion with XhoI and BamHI the promoter/GFP/terminator cassette was ligated into the shuttle vector pAG32 (Goldstein *et al.*, 1999) for biolistic DNA delivery. The GFP construct containing shuttle vector pAG32 was directly used for biolistic transformation.

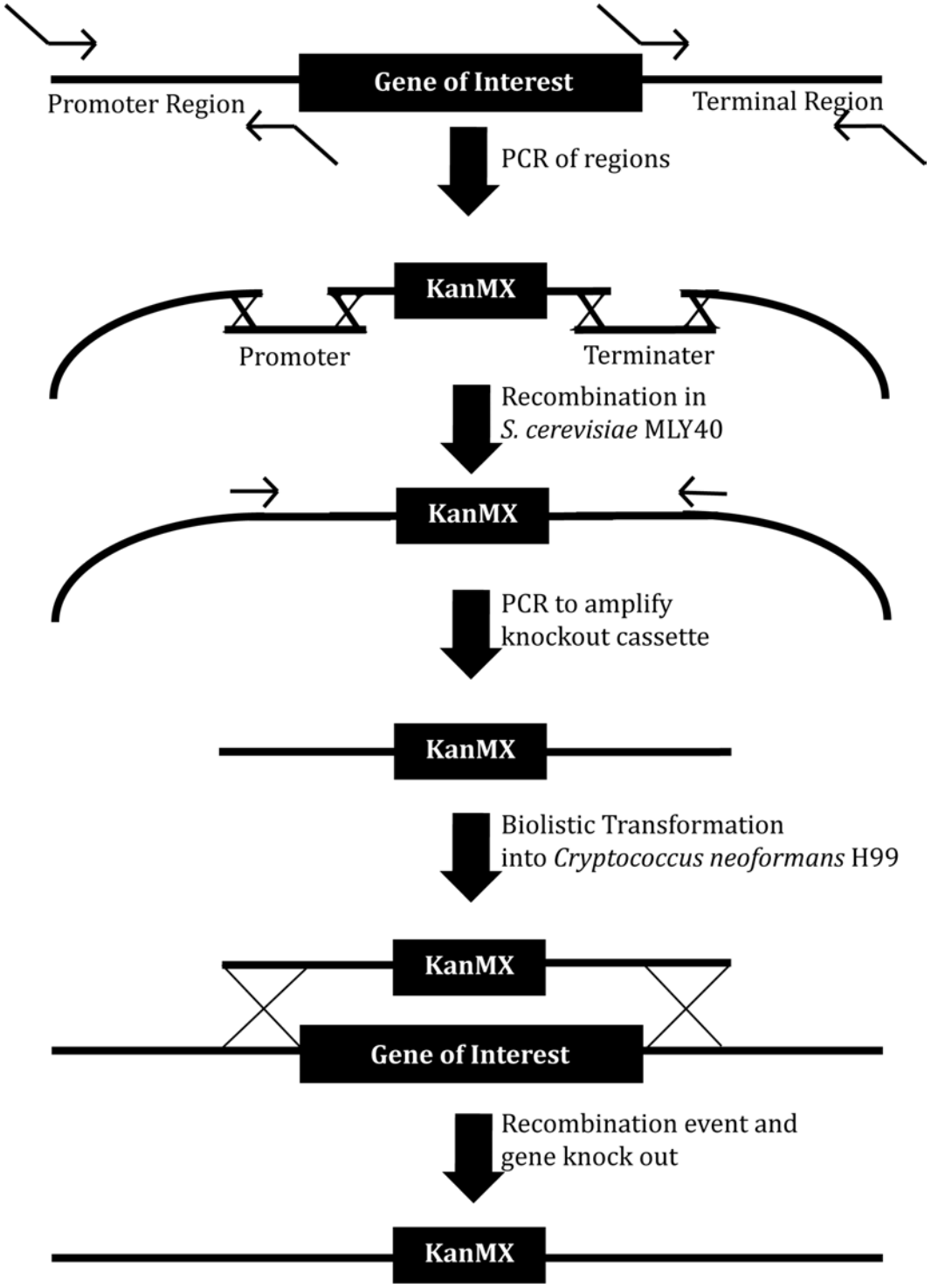

Figure 13: Cloning strategy for the knockout of the target gene *sre1*. Overlapping fragments are combined with help of the DNA repair machinery of *S. cerevisiae* to create a knockout cassette containing a selection marker. The knockout cassette is amplified by PCR and introduced in the *C. neoformans* H99 genome by biolistic bombardment. A recombination event between the flanking ends of the knockout cassette and genomic DNA leads to the knockout of the desired gene.

2.5.1.2 DNA ISOLATION FROM *CRYPTOCOCCUS*

DNA from *Cryptococcus* for subsequent polymerase chain reactions was isolated using a method developed by Bolano *et al.* 2001 (Bolano *et al.*, 2001). The yeast were cultured on YPD plates containing 0.5 M NaCl for two days at 25°C to reduce the capsule size. A loopful of the yeast culture was added to an urea buffer containing 10.7 M urea, 5.0 M NaCl, 1.0 M TRIS pH 8.0, 1.0 M Na_2EDTA pH 8.0 and 20 % SDS and 150 µl sterile sand and incubated for 3 hr at room temperature to further break down the capsule. The cells were pelleted by centrifugation at 4000 rcf for 2 min and the supernatant was removed. The pellet was resuspended in an equal volume of lysis buffer containing 0.5 % SDS, 0.5 % sarkosyl, 10 mM TRIS and 1 mM EDTA pH 7.5 and phenol-chloroform (1:1) and homogenized at 30 rounds per second for 5 min to lyse the cells. Cell debris was removed by centrifugation at 13,500 rcf for 15 minutes at 4°C. The supernatant with the DNA was collected in a fresh tube, an equal volume of 96 % ethanol and 0.13 volume of 3.0 M ice-cold sodium acetate were added and the mixture was gently mixed. DNA was precipitated for 60 min at -20°C. The DNA was collected by centrifugation at 13.500 rcf for 15 min at 4°C, the supernatant removed and the DNA pellet air dried before being resuspended in 10 mM TRIS and 1 mM EDTA pH 7.5 (TE buffer). DNA was stored at 4°C.

DNA from *Cryptococcus* for subsequent southern hybridization was isolated by an alternative protocol. 50 ml YPD media were inoculated with *Cryptococcus* and incubated at 30°C and shaking at 180 rpm. The cells were collected by centrifugation at 900 rcf for 10 min and the pellet lyophilized at -80°C overnight. The pellet was pulverized with 3-5 ml of 3 mm glass beads and vigorous vortexing. The powder was resuspended in 10 ml of CTAB buffer (2 % CTAB, 1.4 M NaCl, 20 mM EDTA and 100 mM TRIS-HCl pH 8.8) and the suspension incubated at 65°C for 30 min. The sample was cooled before an equal volume of chloroform was added and mixed gently. The supernatant was collected by centrifugation at 900 rcf for 10 min, transferred to a fresh tube and an equal volume of isopropanol added. The DNA was pelleted at 900 rcf for 10 min and washed with ice-cold 70 % ethanol. The pellet was then dried and resuspended in TE or water with 20 µg/ml

RNase. The DNA was then recovered by phenol:chloroform extraction and ethanol precipitation.

2.5.1.3 DNA EXTRACTION WITH PHENOL:CHLOROFORM

Phenol:Chloroform extraction was conducted to remove proteins from extracted DNA. An equal volume of phenol:chloroform was added to the sample and mixed until an emulsion formed. The mixture was centrifuged for 1 min at maximum speed in a tabletop centrifuge and the aqueous phase transferred to a fresh tube. The process was repeated until no protein was visible in the interphase anymore and then phenol residues removed with an equal volume of chloroform. The DNA in the aqueous phase after centrifugation was recovered by ethanol precipitation.

2.5.1.4 DNA ETHANOL PRECIPITATION

Ethanol precipitation was carried out to recover DNA after phenol:chloroform extraction. 1/10 sample volume of 3 M sodium acetate and 4 volumes of ice-cold 100 % ethanol were added to the DNA solution and incubated at -20°C overnight. The DNA was collected by centrifugation for 30 min at maximum speed in a tabletop centrifuge. The supernatant was discarded and the pellet washed with a full volume of ice-cold 80 % ethanol. Several washing steps were performed until traces of salts were removed fro the sample before the pellet was dried and resuspended in TE buffer.

2.5.1.5 POLYMERASE CHAIN REACTION

Target DNA sequences were amplified using specific primers (Table 4) and polymerase produced by the hyperthermophilic archaebacterium *Pyrococcus furiosus* or a thermostable DNA polymerase named after the thermophilic bacterium *Thermus aquaticus* in a polymerase chain reaction (PCR).

The DNA was first denatured for 10 min at 100°C. The PCR reactions for amplification of the products for the transformation cassette were conducted with the Expand High Fidelity PCR System (Roche) in a reaction mix containing 1 x Expand HIFI reaction buffer, 0.2 mM dNTPs, 0.2 µM specific forward primer, 0.2 µM specific reverse primer and 2.5 U of Expand High Fidelity polymerase. After initial denaturation at 95°C for 10 min, 5 cycles of denaturation at 95°C for 1 min, annealing at primer specific temperature for 3 min and extension at 72°C for 3 min were followed by 25 cycles of denaturation at 95°C for 1 min, annealing at primer specific temperature for 1 min and extension at 72°C for 3 min and a final extension at 72°C for 10 min were conducted to amplify the DNA.

PCR reactions for amplification of the transformation cassette for biolistic transformation were performed with 1.25 U Taq polymerase (GoTaq, Promega), in a reaction mix containing 1 x GoTaq reaction buffer, 0.2 mM dNTPs, 0.2 µM specific forward primer, 0.2 µM specific reverse primer. After initial denaturation at 95°C for 5 min, 30 cycles of denaturation at 95°C for 30 sec, annealing at primer specific temperature for 30 sec and extension at 72°C for 5 min followed by a final extension at 72°C for 10 min were conducted to amplify the DNA. A negative control without DNA was used to check for contaminations. Fragments were separated in an agarose gel electrophoresis.

Table 4: Primers used for construction of the *sre1*KO and GFP expression cassette. F – forward, R – reverse.

Primer Sequence 5' 3'	**Anneal. Temp.**
***Sre1* part 1**	61°C
F:TTTGGTACCGGGCCCCCCCTCGAGGTCGACGGTATCGATAATGAGAAGGAGTTGACGAGGA	
R:CATGGTCATAGCTGTTTCCTGACTCATCACCCATTCCATTGA	
***Sre1* part 2**	61°C
F:CCCTATAGTGAGTCGTATTACGCTTCAACAACAGTCTCAGCA	
R:AGAACTAGTGGATCCCCCGGGCTGCAGGAATTCGATATCACTTTATCGGTTGTCAGAGCTT	
***Sre1*/KanMX cassette from plasmid pJAF1**	61°C
F:TCAATGGAATGGGTGATGAGTCAGGAAACAGCTATGACCATG	
R:TGCTGAGACTGTTGTTGAAGCGTAATACGACTCACTATAGGG	
***Sre1* KO cassette**	61°C
F:ATGAGAAGGAGTTGACGAGGA	
R:CTTTATCGGTTGTCAGAGCTT	
***Sre1* southern**	55 °C
F:AGGATATGCTCGCTGAGATGAG	
R:GTACGATCCATCACAGCCACAT	
KanMX southern	55 °C
F:ATGTTTCGCTTGGTGGTCGAA	
R:GGATGTGCGTTGAACAGAGCT	
***Actin act1* from *C. neoformans* JEC21 promoter for GFP cassette**	61°C
F:TTGGGTACCGGGCCCCCCCTCGAGGTCGACGGTATCGATAAGGCTGCGGGAGGTGAGCTGG	
R:CTCCTCGCCCTTGCTCACCATAGACATGTTGGGCGAGTTTTAC	
***GFP* coding sequence for GFP cassette**	61°C
F:GTAAAACTCGCCCAACATGTCTATGGTGAGCAAGGGCGAGGAG	
R:CCTTACGGCCTTCACAATTACTTGTACAGCTCGTCCATGCCG	
***Tryptophan trp1* terminator from *C. neoformans* JEC21 for GFP cassette**	61°C
F:CGGCATGGACGAGCTGTACAAGTAATTGTGAAGGCCGTAAGG	
R:AGAACTAGTGGATCCCCCGGGCTGCAGGAATTCGATATCAGAAGAGATGTAGAAACGAGTTTCG	
***GFP* cassette**	55 °C
F:GTAGGATCCAGGCTGCGGGAGGTGAGCTGG	
R:GTAGGATCCGAAGAGATGTAGAAACGAGTTTCG	

2.5.1.6 PLASMIDS

Different plasmids were used for the process of biolistic transformation of *Cryptococcus*. The plasmid pJAF1 (Figure 14 A) contains an ampicillin resistance gene and the KanMX cassette, a neomycin resistance gene under the control of the *C. neoformans* H99 *act* promoter and *trp* terminator, used as marker for positive transformation events. The plasmid pRS426 (Figure 14 B) (Christianson *et al.*, 1992) was used for creation of the *sre1* knockout cassette and the GFP expression construct by homologous recombination in *S. cerevisiae*. The plasmid contains an ampicillin resistance and the *ura3* gene. The GFP cassette was ligated into the plasmid pAG32 (Figure 14 C) (Goldstein *et al.*, 1999) containing the hygromycin B resistance and ampicillin resistance gene that was then randomly integrated into the *C. neoformans* H99 genome.

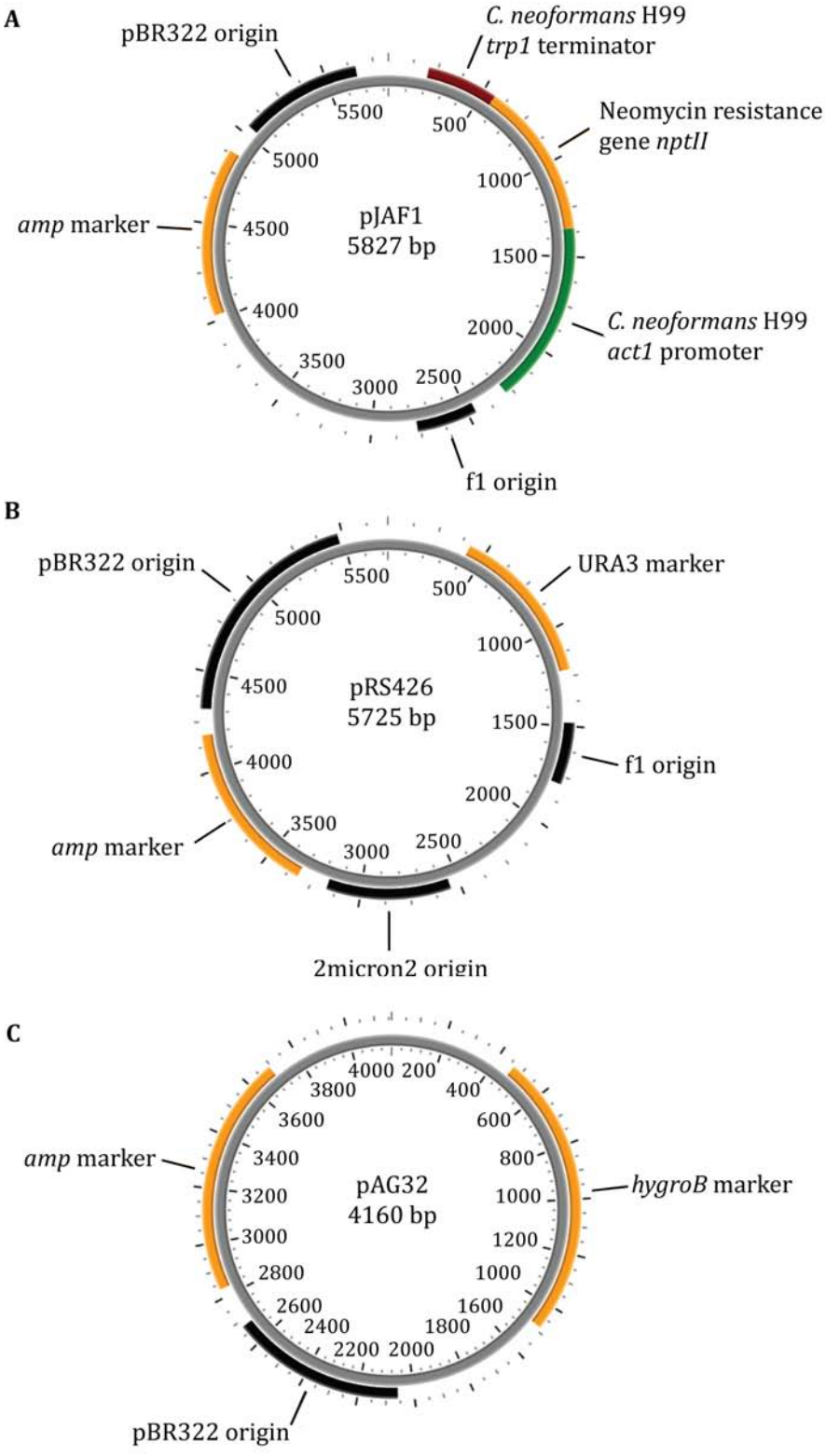

Figure 14: Plasmids used in this study. (A) The selection marker KanMX for *sre1* knockout was isolated from the plasmid pJAF1 (B) The plasmid pRS426 was used for homologous recombination of overlapping PCR fragments in *S. cerevisiae*. (C) The GFP cassette for expression in *Cryptococcus* was ligated into the plasmid pAG32 and then randomly integrated into the yeast genome by biolistic transformation.

2.5.1.7 PLASMIDS DNA PREPARATION

Plasmid DNA from bacteria was isolated with the FastPlasmid™ kit (Eppendorf). A bacterial colony was grown over night in LB media with the appropriate selection marker, the cells collected by centrifugation at 12,000 rcf for 1 min and the supernatant discarded. The pellet was resuspended in 400 µl of ice-cold lysis solution on a vortex and then incubated at room temperature for 3 min. The lysate was transferred to a spin column assembly and centrifuged for 60 sec at maximum speed in a tabletop centrifuge. The plasmid DNA, bound to the column, was washed with 400 µl of washing buffer, centrifuged and dried by another centrifugation step. To elute the plasmid DNA 50 µl of elution buffer was added to the spin column and centrifuged for 60 sec at maximum speed in a table top centrifuge.

2.5.1.8 RESTRICTION DIGEST OF DNA FRAGMENTS AND PLASMIDS

Restriction enzymes recognize specific DNA sequences and cut DNA into smaller fragments. The genomic DNA or plasmid DNA was incubated with 5 U/µg DNA of the appropriate restriction enzyme in 1 x buffer at the relevant temperature and 0.5 mg/ml bovine serum albumin (BSA) for 1 hr. Table 5 shows the restriction enzymes used in this study with their specific recognition sites and incubation temperature. The digested DNA was then check on an agarose gel and purified for further use.

Table 5: Restriction enzymes used in this study. Enzymes are presented with their specific recognition site and incubation temperature

Restriction Enzyme	**Recognition Site**	**Temp. in °C**	**Use**
HindIII	5' AAGCTT 3' 3' TTCGAA 5'	37	Restriction of pRS426 for homologous recombination in *S. cerevisiae*
BamHI	5' GGATCC 3' 3' CCTAGG 3'	37	Restriction of pRS426 to check for *sre1*ko cassette Restriction of pAG32 for ligation of GFP-cassette
XhoI	5' CTCGAG 3' 3' GAGCTC 5'	37	Restriction of pAG32 for ligation of GFP-cassette Restriction of GFP cassette out of pRS426
AgeI	5' ACCGGT 3' 3' TGGCCA 5'	37	Restriction of cryptococcal genomic DNA for southern analysis of *sre1* mutants
SpeI	5' ACTAGT 3' 3' TGATCA 5'	37	Restriction of cryptococcal genomic DNA for southern analysis of *sre1* mutants

2.5.1.9 ALKALINE PHOSPHATASE TREATMENT OF RESTRICTED PLASMID DNA

To keep restricted plasmids in a linear form and to avoid undesirable ligation, the 5' end phosphate groups of DNA can be removed with alkaline phosphatase. One unit of alkaline phosphatase (CIAP, Promega) and reaction buffer with a final concentration of 1 x was directly added in the restriction mix and incubated for 1 hr at 37°C. Then, another unit of the enzyme was added for 30 min at 37°C. Fragments was analysed on an agarose gel and extracted for further use.

2.5.1.10 LIGATION OF PURIFIED DNA FRAGMENTS INTO A PLASMID

To create a GFP-containing plasmid for biolistic transformation, the GFP cassette was obtained from the plasmid pRS426 by restriction digest with *BamHI* and *XhoI*. The target plasmid pAG32 was prepared by restriction with the same enzymes and following alkaline phosphatase treatment. The fragments were analysed on an agarose gel and extracted. The concentrations of plasmid and insert were determined with a NanoDrop ND-1000 spectrometer. Integration of the GFP cassette into the target vector pAG32 was performed at a plasmid:vector ratio of 1:3 with 1 U T4 DNA ligase (Promega) in 1 x ligase buffer overnight at 4°C. The optimal amount of insert was calculated with the following equation.

$$\text{ng insert} = \frac{\text{ng vector x kb insert}}{\text{kb vector}} \times \frac{3}{1}$$

The ligation mix was then transformed into *E. coli* and plated on selective media containing 200 µg/ml Carbenicillin. Potentially positive transformants were analysed by restriction and PCR analysis.

2.5.1.11 AGAROSE GEL ELECTROPHORESIS

Nucleic acids can be separated according to the molecular weight by agarose gel electrophoresis and detected with the intercalating and fluorescent agent ethidium bromide. For that purpose, 1 % agarose gels were prepared in 1 x TBE buffer (10 mM TRIS, 150 mM NaCl pH 7.6) or 1 x TBA buffer (89 mM TRIS, 89mM boric acid, 2 mM EDTA) and 0.5 µg/ml ethidium bromide. DNA samples were mixed with DNA loading buffer (Promega), loaded onto the gel and separated at 2.3 V/cm with 1 x TBE or TAE as running buffer. A 1 kb or 100 bp DNA ladder was also separated to estimate the fragment size. Fragments were detected by UV-transillumination.

2.5.1.12 DNA PURIFICATION AND GEL EXTRACTION

DNA extraction and gel purification was performed using the GenElute™ gel extraction kit (Sigma). To recover DNA from agarose gels, the gel slices were solubilized in 3 volumes (100 mg gel equates to 300 µl) of gel solubilization solution by incubation at 55°C for 10 min and vortexing every 3 min. To adjust the pH of the mixture, 3 M NaAc was added. The sample was mixed with 1 gel volume of 100 % isopropanol and loaded onto a prepared binding column and centrifuged for 1 min at maximum speed in a table top centrifuge. The binding column was prepared by adding 500 µl of column preparation solution and centrifugation for 1 min at maximum speed in a tabletop centrifuge. After binding of the DNA to the column, the column was washed with 700 µl of wash solution and then 50 µl elution solution was added, incubated for 1 min and centrifuged for 1 min at maximum speed in a table top centrifuge to elute the DNA.

2.5.1.13 PREPARATION OF CHEMICALLY *ESCHERICHIA COLI*

A single colony of *Escherichia coli* DH5α was grown in 5 ml liquid LB media overnight at 37°C and shaking at 220 rpm. The next day the culture was diluted in 500 ml fresh LB media and further cultured at 30°C and shaking at 180 rpm. At an

optical density (OD) of OD_{595} = 0.2, sterile MgCl was added to a final concentration of 20 mM and then the culture further incubated. At OD_{595} = 0.5 the culture was incubated for 2 hr in an ice-water bath. The cells were pelleted by centrifugation at 900 rcf for 5 min at 4°C, the supernatant removed and the cells resuspended in half of the original volume of ice cold Ca/Mn medium (100 mM $CaCl_2$, 70 mM $MnCl_2$, 40 mM $C_2H_3O_2Na$ pH 5.5). The cells were incubated on ice for a further 2 hr, pelleted by centrifugation at 900 rcf for 5 min at 4°C, the supernatant removed and the cells resuspended in 1/20 of the original volume of Ca/Mn medium with 15 % glycerol. Aliquots were frozen in liquid nitrogen and stored at -80°C.

2.5.1.14 TRANSFORMATION OF DNA INTO *E. COLI*

Chemically competent *E. coli* DH5α from -80°C were thawed on ice. The DNA to be transformed was added, the sample was mixed and incubated for 30 min on ice. Afterwards, the cells were subjected to a heat shock at 42 °C for 1 min and 30 sec. The sample was cooled on ice before 1 ml of LB media was added and the cells recovered for 40 min at 37 °C. The cells were collected by centrifugation at 2,500 rcf for 5 min in a table top centrifuge, washed with 500 µl of ddH_2O, resuspended in 100 µl of ddH_2O and plated on selective media.

2.5.1.15 LITHIUM ACETATE TRANSFORMATION OF YEAST

The uracil negative strain of *Saccharomyces cerevisiae* MLY40 (Lorenz *et al.*, 1997) was transformed by lithium acetate transformation to achieve homologous recombination of overlapping DNA fragments into the HindIII cut plasmid pRS426. A 5 ml overnight culture in YPD was diluted into 50 ml of YPD and further incubated. At an OD_{595} = 0.7, the cells were harvested for 5 min at 300 rcf, washed twice with ddH_2O before being resuspended in 300 µl of 100 mM LiAc. Transformations were conducted with 50 µl of the prepared yeast cells, 40 % PEG 4000, 1.5 mg/ml sonicated salmon sperm DNA to enhance the DNA uptake. The mixture was mixed, LiAc pH 7.5 added to a final concentration of 96 mM and the

mixture was vortexed again. The transformation mixture was incubated at 30°C for 20 min and then heat shocked at 42°C for 15 min. The cells were collected for 1 min at 3,000 rcf and resuspended in ddH_2O. Serial dilutions were plated on SD media (0.17 % yeast nitrogen base without amino acids, 0.5 % ammonium sulphate, 2 % glucose and 2 % agar) plates and incubated at 30°C for 5 days.

2.5.1.16 PLASMID RECOVERY FROM *S. CEREVISIAE*

After homologous recombination in *S. cerevisiae*, the plasmid has to be recovered and transformed into *E. coli* for further amplification for biolistic transformation. Colonies were grown in 5 ml of liquid SD medium at 30°C and 180 rpm overnight. The cells were collected for 30 sec at maximum speed in a tabletop centrifuge, the supernatant discarded. The cells were resuspended in 100 µl STET breaking buffer (8 % sucrose, 50 mM TRIS-HCl pH 8.0, 50 mM EDTA, 5 % Triton X-100), 0.3 g of 0.5 mm glass beads added and the cells ribolysed for 5 x 20 sec. Another 100 µl of STET buffer was added; the mixture was vortexed and then incubated at 100°C for 3 minutes. The sample was cooled on ice and centrifuged for 10 min at 4°C at maximum speed in a tabletop centrifuge. The top 100 µl were transferred to 50 µl 7.5 M ammonium acetate and the plasmid DNA freeze precipitated for 1 hr at -20°C. Impurities were removed by centrifugation for 10 min at 4°C and maximum speed in a tabletop centrifuge. The top 100 µl were transferred to 200 µl 70 % ethanol and centrifuged for 10 min at maximum speed in a tabletop centrifuge. The pellet was washed in 70 % ethanol and resuspended in ddH_2O before being transformed into *E. coli.*

2.5.1.17 BIOLISTIC TRANSFORMATION

The process of biolistic transformation is divided into three steps: yeast preparation, DNA preparation and biolistic bombardment.

For preparation of the parental strains H99 and R265, the strains were grown overnight in 50 ml YPD media at 30°C and shaking at 180 rpm. Cells were collected by centrifugation for 5 min at 900 rcf and washed with dH_2O. Cells were then resuspended in ¼ of the original volume and aliquots of 300 µl were plated on YPD plates containing 1 M sorbitol and left to dry.

For preparation of the DNA, 0.6 µm gold micro carriers (BioRad) were subjected to subsequent washing steps in dH_2O and 1 ml of 100 % ethanol. The sample was then aliquoted into 250 µl portions; another 750 µl of 100 % ethanol was added to each aliquot. Prepared gold micro carriers were stored at 4°C. An aliquot of 10 µl gold micro carriers was mixed with 10 µl of 1 µg/µl DNA, 10 µl 2.5 M $CaCl_2$ and 2 µl of 1 M spermidine – free base and incubated for 5 minutes at room temperature to allow binding of the DNA to the gold particles. The gold micro carriers were then pelleted by centrifugation for 1 minute at 800 rcf, washed in 500 µl 100 % ethanol and afterwards resuspended in 12 µl 100 % ethanol. The 2.5 cm micro carrier biolistic discs (BioRad) were washed in 100 % ethanol and dried before the sample was applied to the centre of a prepared micro carrier biolistic disc.

For biolistic bombardment, the gold micro carriers were accelerated in a helium-generated vacuum (1350 psi rupture discs, BioRad) and shot onto the prepared YPD plates with *Cryptococcus* in a BioRad PDS-1000/He biolistic particle delivery system. After transformation, yeast cells on plates were recovered for 5 hr at 30°C and then washed of with 1 ml of YPD media and plated on selection media containing 250 µg/ml hygromycin B for GFP mutants and containing 300 µg/ml G418 for selection of *sre1*ko mutants. The plates were incubated for 5 days at 30°C. Potential GFP transformants were analysed phenotypically; *sre1* knockout was confirmed by southern analysis.

2.5.1.18 SOUTHERN HYBRIDIZATION

Southern analysis is used to identify specific DNA regions by hybridization with a labeled complementary DNA probe. In the context of this study, probes were designed and restrictions enzymes were chosen in a way that results in specific hybridization signals that allow for analysis of potential *Cryptococcus* transformants for knockout of *sre1* and control for potential undesired genomic rearrangements or random integration events. DNA was isolated from randomly selected colonies and DNA concentration measured with a NanoDrop ND-1000 spectrometer. Thirty μg of DNA subjected to restriction with the enzymes *AgeI* and *SpeI* before the restricted DNA fragments were slowly separated on a 1 % agarose gel. The DNA was depurinated by gentle agitation in 0.25 M HCl for 10 min and denatured in 0.4 M NaOH for 30 min. The nitrocellulose membrane (GeneScreen hybridization membranes, NEN® Life Science Products) was wet with dH_2O and eliquibrated in 0.4 M NaOH for 10 min. Alkaline capillary transfer with 0.4 M NaOH overnight transferred the DNA onto the membrane. The membrane was rinsed in 2xSSC (0.03 M sodium citrate, 0.3 NaCl, pH 7.2) and partially dried before the DNA was cross-linked to the membrane with ultraviolet light in a UV stratalinker at 120,000 μJoules/cm^2. The membrane was pre-hybridized in 10 ml of modified Church buffer (0.36 M Na_2HPO_4, 0.14 M NaH_2PO_4, 1mM EDTA and 7 % SDS) for 30 min at 65°C. Hybridization probes were amplified with specific primers, the product separated on an agarose gel and extracted. The DNA probe was then labeled with the Prime-a-Gene labeling kit (Promega). The probe was denatured for 2 min at 100°C and chilled on ice. 6 ng of DNA were labeled in a reaction in 1 x buffer, with 20 μM of each unlabeled dNTP, 400 μg/ml nuclease-free BSA, 333 nM [α-^{32}P]dCTP (50μCi) and 5 U DNA polymerase I large Klenow fragment for 1 hr at room temperature. The reaction was then stopped at 100°C for 2 min, chilled on ice and 2 μl of 0.5 M EDTA was added. The probe was added directly into the pre-hybridization buffer and hybridization was allowed over night at 65°C. To remove unspecific bound probe, the membrane was washed twice for 15 min with pre-warmed wash buffer 1 (0.1 % SDS, 2xSSC), twice for 15 min with pre-warmed wash buffer 2 (0.1 % SDS, 0.5xSSC) and twice for 15 min with pre-warmed wash

buffer 3 (0.1 % SDS, 0.1xSSC). DNA bound probe was detected by autoradiography overnight at -80°C on a Fuji medical X-ray film 100 NF.

2.5.1.19 IDENTIFICATION OF GFP INTEGRATION SITE

The GFP construct together with the unlinearised shuttle vector was randomly integrated in the cryptococcal genome. To identify the integration site, a single primer PCR approach followed by sequencing with a second specific sequencing primer was applied (Karlyshev *et al.*, 2000).

DNA was isolated from GFP-tagged strains with the MasterPure™ Yeast DNA Purification Kit (Epicentre). Briefly, yeast cells from 2 ml YPD overnight cultures were collected and resuspended in 300 µl of Yeast Cell Lysis Solution. Cells were lysed by vortexing with glass beads for 5 min followed by incubation at 65°C for 15 min. The samples were cooled down on ice for 5 min, 150 µl of MPC Protein Precipitation Reagent added and vortexed for 10 sec. Cellular debris was removed by centrifugation for 10 min at 13,000 rcf, the supernatant containing the DNA transferred to a fresh sample tube and 500 µl of isopropanol added to precipitate DNA. DNA was recovered by centrifugation for 10 min at 13,000 rcf, the pellet washed with 500 µl 70 % ethanol before being resuspended in 50 µl TE buffer. Subsequently, the RNA was degraded by RNase A treatment (1 µl of 5µg/µl RNase A) for 30 min at 37°C and DNA extracted with phenol: chloroform followed by ethanol precipitation (Section 5.1.3 and 5.1.4).

The PCR strategy involved three rounds of amplification with a single specific primer for the integrated DNA fragment (Karlyshev *et al.*, 2000). Firstly, integration-specific templates were linearly amplified at an annealing temperature of 50°C. This step was followed by a round of amplification at low annealing temperature (30°C) allowing for non-specific primer binding on the opposite strand in regions adjacent to the integration site. Lastly, amplification at 50°C annealing temperature allowed for further amplification of fragments. PCR was carried out with 1.25 U GoTaq Flexi DNA polymerase (Promega) in 1 x colorless

GoTaq Flexi Buffer with 4 mM $MgCl_2$, 0.2 mM of each dNTP, 0.4 µM primer and 0.5 µg DNA and the following cycle: 1 min at 94°C; 20 cycles of 30 sec 94°C, 30 sec 50°C, 3 min 72°C; 30 cycles of 30 sec 94°C, 30 sec 30°C, 2 min 72°C; 30 cycles of 30 sec 94°C, 30 sec 50°C, 2 min 72°C and a final extension of 7 min at 72°C. PCR products were purified to remove excess enzyme, nucleotides and primer with the Wizard SV Gel and PCR Clean-Up System (Promega). An equal volume of Membrane Binding Solution was added to prepare PCR samples for DNA affinity columns. The samples were applied to SV minicolumns, incubated for 1 min and then transferred to the column membrane by centrifugation for 1 min at 16,000 rcf. DNA was washed in subsequent steps with 700 µl and 500 µl of Membrane Wash Solution with alternating centrifugation steps of 1, 5 and 1 min at 16,000 rcf. DNA was eluted with 50 µl of nuclease-free water by centrifugation for 1 min at 16,000 rcf. A small amount of product was visualized by agarose gel electrophoresis (Section 5.1.11).

Afterwards, the PCR products were sequenced with 3.2 pmol of a second primer specific for the integrated DNA fragment, designed closely downstream of the primer used for PCR amplification, in a ABI 3730 capillary sequencer. Sequencing was conducted by the Genomics facility, University of Birmingham.

2.6 BIOINFORMATICS AND STATISTICAL ANALYSIS

2.6.1 BIOINFORMATICS ANALYSIS

Cryptococcal mitochondrial genome information was annotated using the open reading frame finder from the National Centre for Biotechnology Information (NCBI) and the basic local alignment search tools (Blast) available from the Broad Institute of MIT and Harvard and NCBI. Multiple alignments were created with the software Mauve 2.0 (Darling *et al.*, 2010). Information from sequencing reactions was analysed using the sequence Mac Sequence View software and blast search engines.

2.6.2 STATISTICAL ANALYSIS

At least three individual experiments were performed for each assay. Data were tested for normality using the Kolmogorov-Smirnov test and for homogeneity of variances using the Levene statistic. If data were normally distributed and showed homogeneity of variance, statistically significant differences among the mean data were analysed using a One-Way ANOVA. Multi-comparisons (Tukey Honestly

Significant Differences (HSD) tests) were performed to identify statistically significant differences between pairs. A p-value of $p < 0.05$ after controlling for multiplicity was considered to be statistically significant.

Different cryptococcal genotypes were compared for their median IPR values using the non-parametric Mann-Whitney U-test and values of $p<0.025$, after controlling for multiplicity, were accepted as statistically significant (http://elegans.swmed.edu/~leon/stats/utest.cgi).

For assessment of data from expulsion assays and from mitochondrial staining, results from at least three individual assays were tested for statistically significant differences using a χ^2- test. P-values of < 0.05 were considered to be statistically significant. Furthermore, Pearson correlation was used to measure the correlation between tubular mitochondrial morphology and IPR values; an F-value of $P<0.05$ was considered to be a significant correlation

CHAPTER 3

CYTOKINE SIGNALING REGULATES THE OUTCOME OF MACROPHAGE PARASITISM BY *CRYPTOCOCCUS NEOFORMANS*

Major parts of this chapter have been published:

Voelz, K. and R. C. May. 2009. Cytokine signaling regulates the outcome of intracellular macrophage parasitism by *Cryptococcus neoformans*. Infect Immun. **77: 3450**-3457 (Voelz *et al.*, 2009)

In healthy hosts, cryptococcal infection is usually self-limiting, suggesting effective clearance or maintenance in a latent state by phagocytic cells. The outcome of cryptococcosis depends on the immune status of the infected individual and the cytokine pattern generated in response to the pathogen. Although it is well established that the host's cytokine profile dramatically affects the outcome of cryptococcal disease, the molecular basis for this effect is unclear. Both Th1 and Th2 cytokines are involved in protection against *C. neoformans*, but whereas Th1 associated cytokines are essential for natural immunity, Th2 associated immunity is not protective in mice (Beenhouwer *et al.*, 2001, Hoag *et al.*, 1997, Huffnagle, 1996). Increased expression of Th1 cytokines, such as TNF-α and IFN-γ, result in improved fungal control (Flesch *et al.*, 1989, Kawakami *et al.*, 1995, Milam *et al.*, 2007, Wormley *et al.*, 2007) whilst IFN-γ knockout mice show increased fungal burden (Arora *et al.*, 2005). Recently, Müller *et al*. (2007) showed a significant role for Th17 response and the pro-inflammatory cytokine IL-17 in modulating survival of *Cryptococcus*–infected mice. In contrast, Th2 cytokines such as IL-4 and IL-13 reduce the host's ability to deal with *C. neoformans in vivo* (Blackstock *et al.*, 2004, Decken *et al.*, 1998, Muller *et al.*, 2007, Kawakami *et al.*, 1999).

Despite these observations from animal models, little work has been done on the *in vitro* effect of Th1, Th17 and Th2 cytokines on the interaction between macrophages and *Cryptococcus*. This section reports a systematic study of cytokine

influence on macrophage-*Cryptococcus* interactions in a representative selection of *Cryptococcus* strains. The results demonstrate that Th1 and Th17-stimulated macrophages are significantly better at phagocytosing cryptococci and at controlling intracellular proliferation of this pathogen than Th2-stimulated cells. In contrast, Th2-activated macrophages show a significantly lower rate of cryptococcal expulsion than Th1 or Th17-activated cells. Together, these data help explain the susceptibility phenotype associated with Th2 cytokine profiles *in vivo*.

3.1 MACROPHAGE ACTIVATION

Macrophages were treated with different cytokines to mimic Th1, Th17 and Th2 activation. It was chosen to investigate the Th1 cytokines IFN-γ, TNF-α, the Th17 cytokine IL-17 and the Th2 cytokines IL-4 and IL-13 as there is already considerable *in vivo* information available describing the influence of these cytokines on cryptococcosis. To avoid artifacts due to over-stimulation, the lowest cytokine concentrations previously demonstrated to induce Th1, Th2 or Th17 phenotypes were used, as follows: 10 units/ml IFN-γ (Murray *et al.*, 1985), 1 ng/ml TNF-α (Roilides *et al.*, 1998), 10 ng/ml IL-17 (Higgins *et al.*, 2006), 10 ng/ml IL-4 (Weiss *et al.*, 1997) and 10 ng/ml IL-13 (Weiss *et al.*, 1997). To confirm that the cytokines were nonetheless functional at these concentrations, macrophage morphology and phagocytic capacity after cytokine exposure was monitored.

Untreated J774 and primary macrophages appeared mainly round or occasionally slightly spread. However, following exposure of J774 cells to mouse or primary macrophages to human recombinant cytokines, most cells were extensively elongated and spread, demonstrating that cells are effectively activated by cytokines at these concentrations (Figure 15 A). To detect any cytokine-evoked cytotoxic effects on macrophages, growth was monitored over 72 hours. Neither J774 (Figure 15 B) nor human monocyte-derive macrophages (Figure 15 B) exhibited any cytokine-induced cytotoxicity.

Given the well-established role of pro-inflammatory cytokines in enhancing

phagocytosis (Kawakami *et al.*, 1995) the ability of macrophage-like cells and human primary macrophages to phagocytose *Cryptococcus* when treated with Th1, Th17 and Th2 cytokines was used as a second parameter to show the efficacy of cytokine treatment. Untreated or cytokine treated macrophages were infected with *C. neoformans* strain ATCC90112, H99 or *C. gattii* strain R265 and analyzed for uptake rates (percentage phagocytosis). Whilst Th1/Th17 cytokines induced an increase in cryptococcal phagocytosis, neither IL-4 nor IL-13 treatment significantly altered uptake rates (Figure 16 A). Similar results were obtained for all three cryptococcal strains in both mouse and human macrophages (Figure 16 A & B), suggesting that Th1/Th17-dependent enhancement of phagocytosis is not strain-specific. It is noted that most of the increases are not statistically significant, most likely because of experimental error and variation. However, given that the results agree with those previously published (Kawakami *et al.*, 1995, Kozel, 1993b, Mucci *et al.*, 2003, Collins *et al.*, 1992) and due to the high costs of cytokines, it was felt that the observed trends are sufficient to show efficacy of cytokine treatment and subsequent analysis was instead focused on the cytokine influence on intracellular proliferation and expulsion.

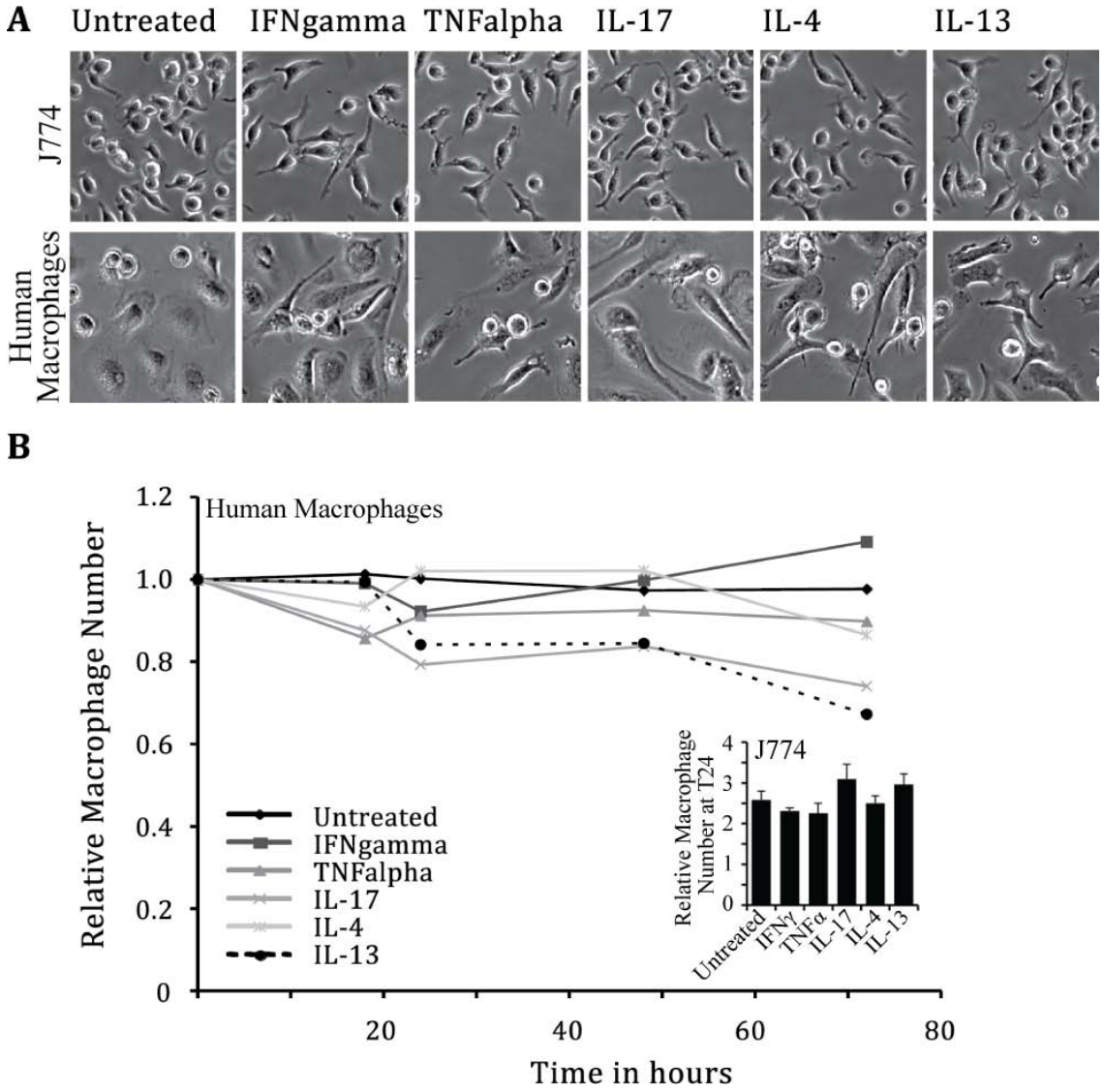

Figure 15: Assessment of cytokine efficacy. Treatment with cytokines at the chosen concentrations results in morphological changes in both J774 and human primary monocyte-derived macrophages but does not influence macrophage survival. J774 and human primary monocyte-derived macrophages were treated with Th1 (10 units/ml IFN-γ, 1 ng/ml TNF-α), Th17 (10 ng/ml IL-17) or Th2 (10 ng/ml IL-4 or 10 ng/ml IL-13) cytokines and then monitored to assess cytokine efficacy at the chosen cytokine concentrations. (A) Representative images of cytokine-treated J774 and human primary macrophage cells. Note the polarized and spread morphology of activated, but not control, cells (B) Cytokine treatment does not significantly influence human primary or J774 macrophage survival. The data are presented as the mean of at least three individual experiments ± 2 x standard error of the mean.

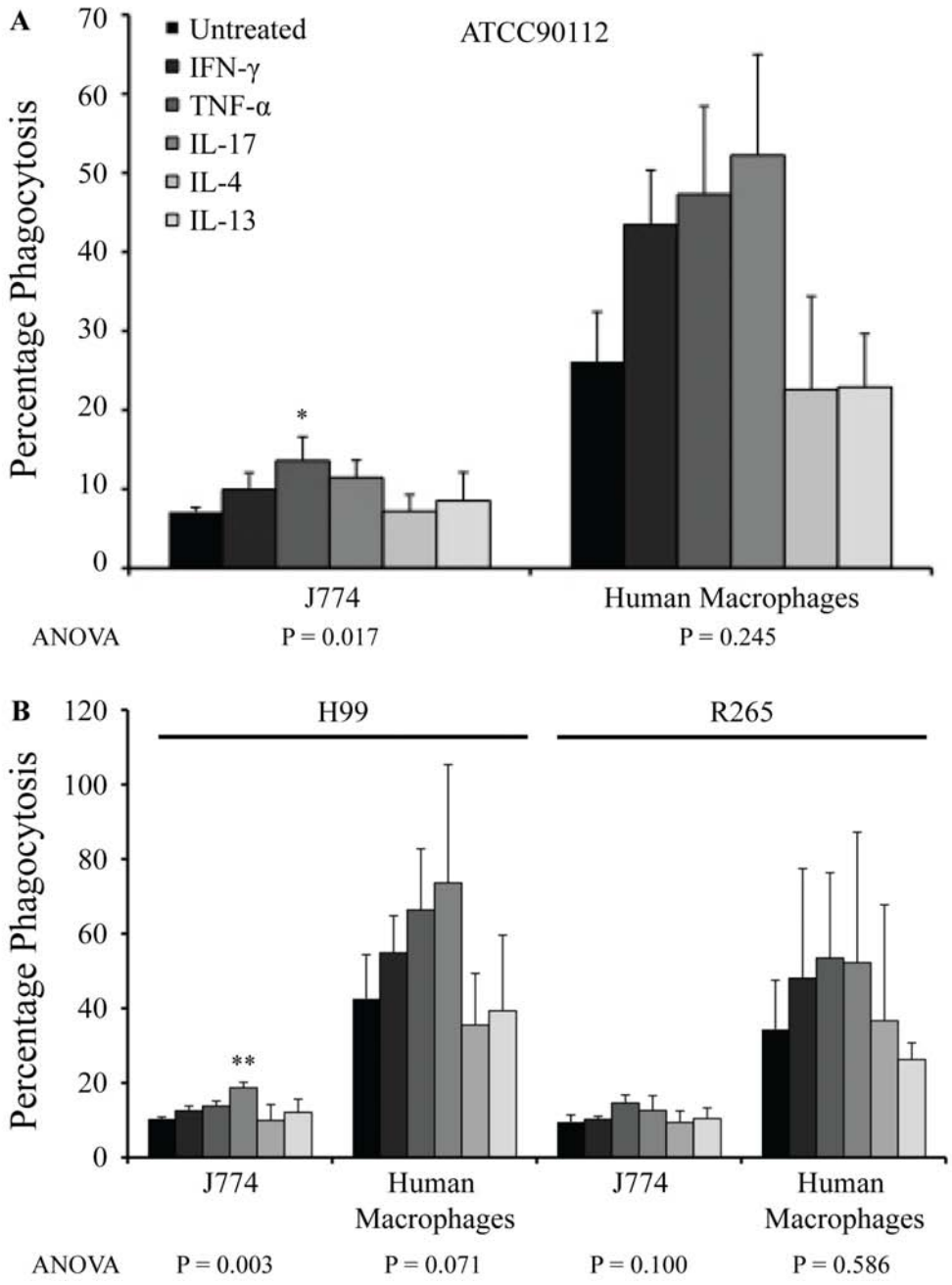

Figure 16: *Cryptococcus* uptake after cytokine treatment. *Cryptococcus* uptake is increased in a Th1 and Th17 cytokine, but not altered in Th2 cytokine, treated J774 cells and human macrophages. Untreated and Th1 (10 units/ml IFN-γ, 1 ng/ml TNF-α), Th17 (10 ng/ml IL-17) or Th2 (10 ng/ml IL-4 or 10 ng/ml IL-13) cytokine treated J774 cells were infected with *C. neoformans* strains ATCC90112 and H99 or *C. gattii* strain R265 and then assessed for cryptococcal uptake. (A) Percentage phagocytosis of *C. neoformans* ATCC90112. There is a trend for increased uptake after Th1/Th17 cytokine treatment but no influence on yeast uptake after treatment with Th2 cytokines. (B) Similar trends can be found in all three selected *Cryptococcus* strains. The data are presented as the mean of at least three individual experiments ± 2 x standard error of the mean. The means were tested for statistical significance using Tukey HSD test assuming equal variances. Statistically significant differences compared to the control are indicated by asterisks (* $P < 0.05$, ** $P \leq 0.01$).

3.2 INTRACELLULAR PROLIFERATION IN J774 MACROPHAGES

Cryptococcus is known to survive and proliferate within macrophages. A method to monitor intracellular *Cryptococcus* proliferation in cell culture systems that has recently been developed was used (Ma *et al.*, 2009a). *In vitro*, the intracellular yeast cell number increases steadily for the first 18 to 24 hours before the number starts to decline due to host cell lysis. Maximal Intracellular Proliferation Rate (IPR) was used as a measure of proliferative capacity that enables easy comparison of intracellular proliferation between different conditions (Figure 17 A).

To analyze if Th1, Th17 or Th2 cytokines influence intracellular cryptococcal proliferation, untreated or cytokine pre-treated J774 macrophages were infected with the *C. neoformans* strains ATCC90112 or H99 or the *C. gattii* strain R265 and monitored for intracellular proliferation over 72 hours. In all three strains, treatment with the Th1 cytokine IFN-γ did not alter IPR whereas IPR was significantly increased in macrophages treated with the Th2 cytokine IL-4 (Figure 17 B). To confirm that these findings were not specific to these two cytokines, IPR following J774 macrophage pre-treatment with TNF-α (Th1 cytokine), IL-17 (Th17 cytokine) or IL-13 (Th2 cytokine) was measured. All three cryptococcal strains showed similar trends in this experimental analysis and so, for simplicity, representative data for only one strain is presented. In all cases, Th1/Th17 cytokines did not alter IPR whilst Th2 activation increased it (Figure 17 C). None of the cytokine treatments altered the timing of the maximal IPR, which always occurred at either 18 or 24 hours post infection.

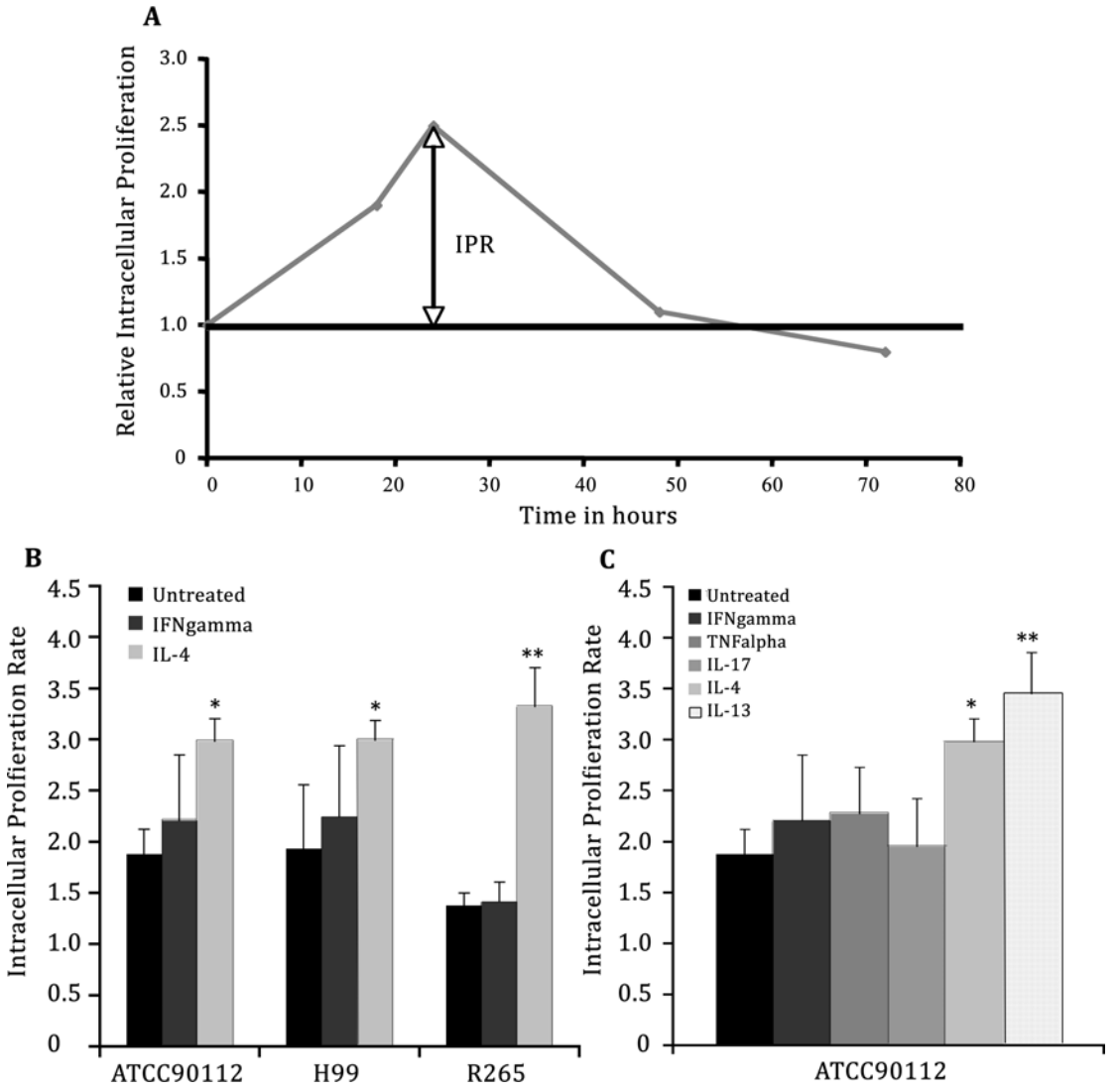

Figure 17: Intracellular *Cryptococcus* proliferation in J774 macrophages after cytokine treatment. Intracellular *Cryptococcus* proliferation is increased in Th2 cytokine, but not altered in Th1/Th17 cytokine, treated J774 cells. Untreated and Th1 (10 units/ml IFN-γ, 1 ng/ml TNF-α), Th17 (10 ng/ml IL-17) or Th2 (10 ng/ml IL-4 or 10 ng/ml IL-13) cytokine treated J774 cells were infected with *C. neoformans* strains ATCC90112 and H99 or *C. gattii* strain R265 and then further incubated under the same conditions to monitor intracellular yeast proliferation. (A) Schematic graph illustrating how IPR was derived. (B) IPR is not altered under the influence of the Th1 cytokine IFN-γ but increases under the influence of the Th2 cytokine IL-4 for all three selected strains. (C) IPR of ATCC90112 is unaltered following treatment with the Th1 cytokines IFN-γ, TNF-α and the Th17 cytokine IL-17 but increases significantly following treatment with the Th2 cytokines IL-4 or IL-13. The data are presented as the mean of at least three individual experiments ± 2 x standard error of the mean. The means were tested for statistical significance using Tukey HSD test assuming equal variances. Statistically significant differences compared to the control are indicated by asterisks (* $P < 0.05$, ** $P \leq 0.01$).

3.3 INTRACELLULAR PROLFERATION IN PRIMARY HUMAN MACROPHAGES

To rule out any cell line specific effects and to test the clinical relevance of this study, intracellular proliferation assays were conducted in primary human monocyte-derived macrophages. As with J774 macrophages, IPR was much lower in human macrophages activated with the Th1 cytokine TNF-α or the Th17 cytokine IL-17 than in cells treated with the Th2 cytokines IL-4 or IL-13. It is interesting to note that, in contrast to J774 cells, human primary macrophages that were untreated or treated with IFN-γ tend to have IPR values higher than those following TNF-α and IL-17 cytokine activation (Figure 18), although future investigation of this phenomenon would require a larger donor pool in order to overcome significant donor-to-donor variability. Thus, the enhancement of IPR that occurs following Th2 stimulation is conserved between mouse and human cells.

The possibility that mammalian cytokines may directly affect yeast growth was considered. However, none of the recombinant mouse or human cytokines used in this study caused significant differences in growth rate relative to untreated controls after 24 hours (peak time for IPR), either in the presence or absence of macrophages (Figure 19). Thus, cytokine signaling alters the capacity of macrophages to control intracellular cryptococci, rather than impacting on extracellular killing or the yeast directly.

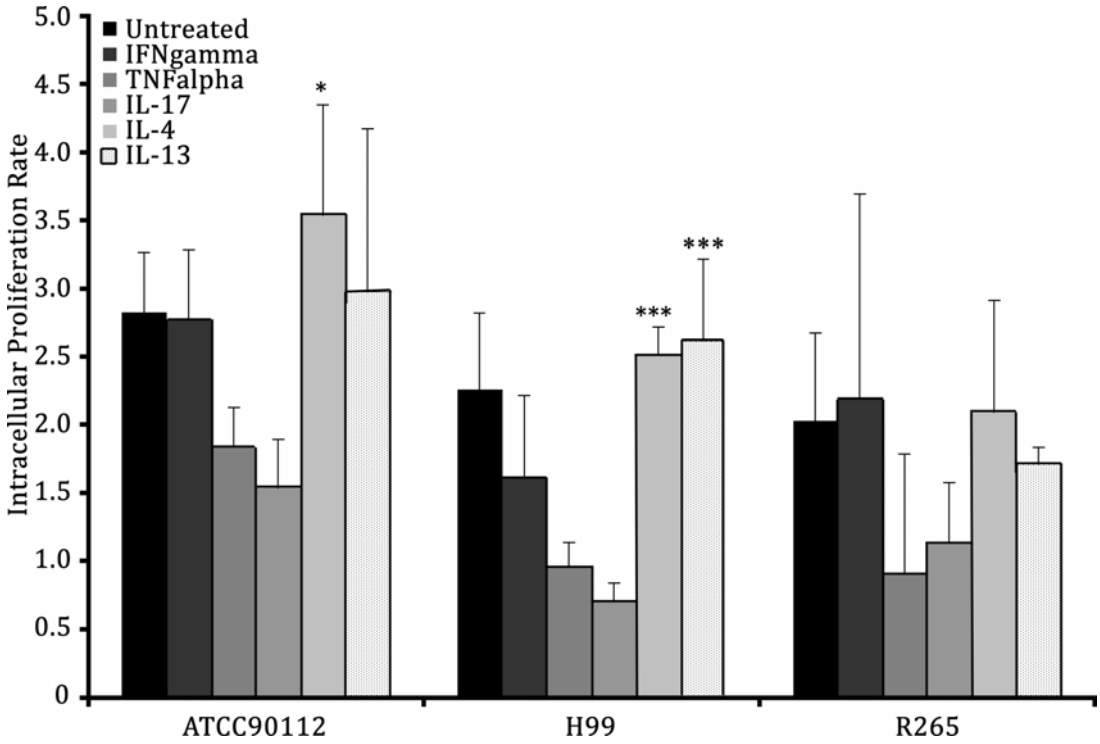

Figure 18: Intracellular *Cryptococcus* proliferation in human macrophages after cytokine treatment. Intracellular *Cryptococcus* proliferation is increased in Th2 cytokine but not altered in TNF-α and IL-17 cytokine treated human primary macrophages. Untreated and Th1 (10 units/ml IFN-γ, 1 ng/ml TNF-α), Th17 (10 ng/ml IL-17) or Th2 (10 ng/ml IL-4 or 10 ng/ml IL-13) cytokine treated human primary macrophages were infected with *C. neoformans* strains ATCC90112 and H99 or *C. gattii* strain R265 and then further incubated under the same conditions to monitor intracellular yeast proliferation. IPR is low following treatment with the Th1 cytokine TNF-α and the Th17 cytokine IL-17 but higher following treatment with the Th2 cytokines IL-4 or IL-13, although due to high donor variability and multiplicity of testing, not all comparisons are significant at the 5 % level. The data are presented as the mean of at least three individual experiments ± 2 x standard error of the mean. Statistically significant differences compared to TNF-α and IL-17 are indicated by asterisks (* $P < 0.05$, ** $P \leq 0.01$, *** $P \leq 0.001$).

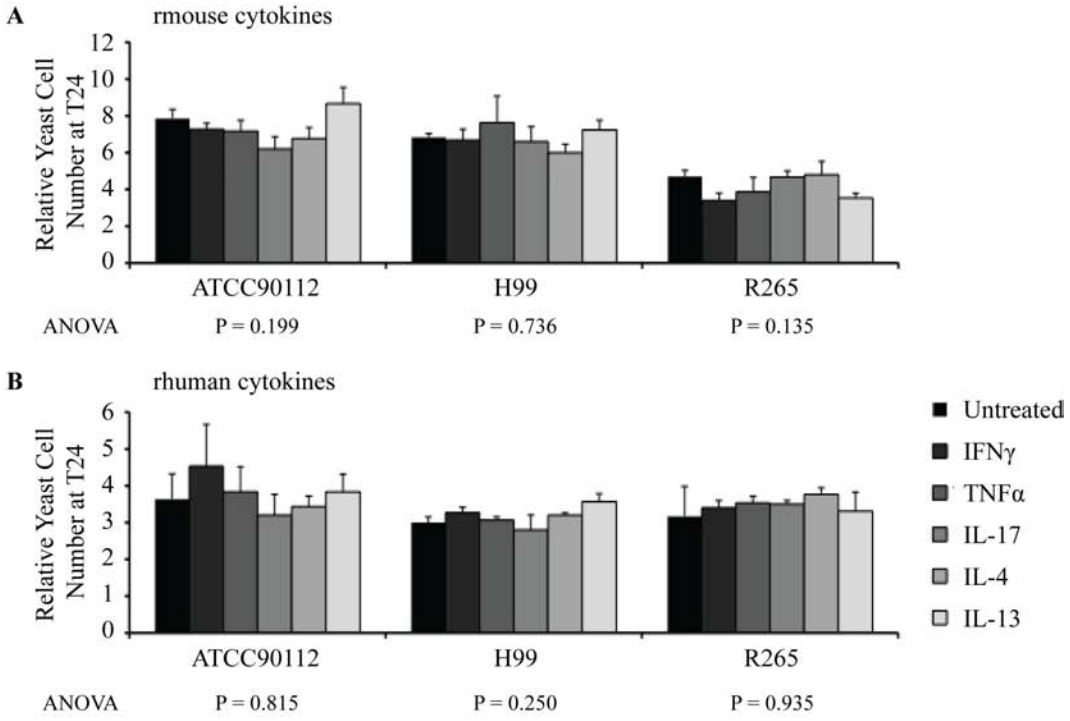

Figure 19: Direct effect of cytokines on *Cryptococcus* growth. Untreated and Th1 (10 units/ml IFN-γ, 1 ng/ml TNF-α), Th17 (10 ng/ml IL-17) or Th2 (10 ng/ml IL-4 or 10 ng/ml IL-13) cytokine treated yeast cells were monitored for growth. Recombinant mouse (A) or human (B) cytokines do not significantly alter growth after 24 hr treatment. The data are presented as the mean of at least three individual experiments ± 2 x standard error of the mean.

3.4 THE INFLUENCE OF CYTOKINE SIGNALING ON EXPULSION EVENTS IN J774 MACROPHAGES

Expulsion is believed to be a possible trafficking mechanism by which *Cryptococcus* disseminates within the infected individual without triggering local inflammation (Ma *et al.*, 2006, Alvarez *et al.*, 2006). Thus, the influence of the selected Th1, Th17 and Th2 cytokines on the occurrence of cryptococcal expulsion was analysed using live cell imaging. A total of 10,031 J774 macrophages (of which 1208 showed internalized yeast cells) and 115 expulsion events were observed. All three *Cryptococcus* strains showed similar results (Figure 20). However, expulsion is a very rare event (Ma *et al.*, 2006) and to enable statistical analysis of the results for the different treatments, the data for all three strains were pooled and analysed using χ^2-test. No statistically significant differences were found between untreated macrophages and cells activated with the Th1 cytokines IFN-γ ($P > 0.5$), TNF-α ($P > 0.2$) or Th17 cytokine IL-17 ($P > 0.2$). Strikingly, however, the occurrence of expulsion was significantly reduced (more than three-fold) in cultures treated with the Th2 cytokines IL-4 ($P = 0.0001$) or IL-13 ($P = 0.0001$). Furthermore, a pairwise comparison of expulsion rates between Th1/Th17 and Th2 cytokine treatments showed that the expulsion rate is significantly higher in each of the pro-inflammatory cytokine environments compared to each Th2 cytokine environment ($P < 0.01$ for all combinations).

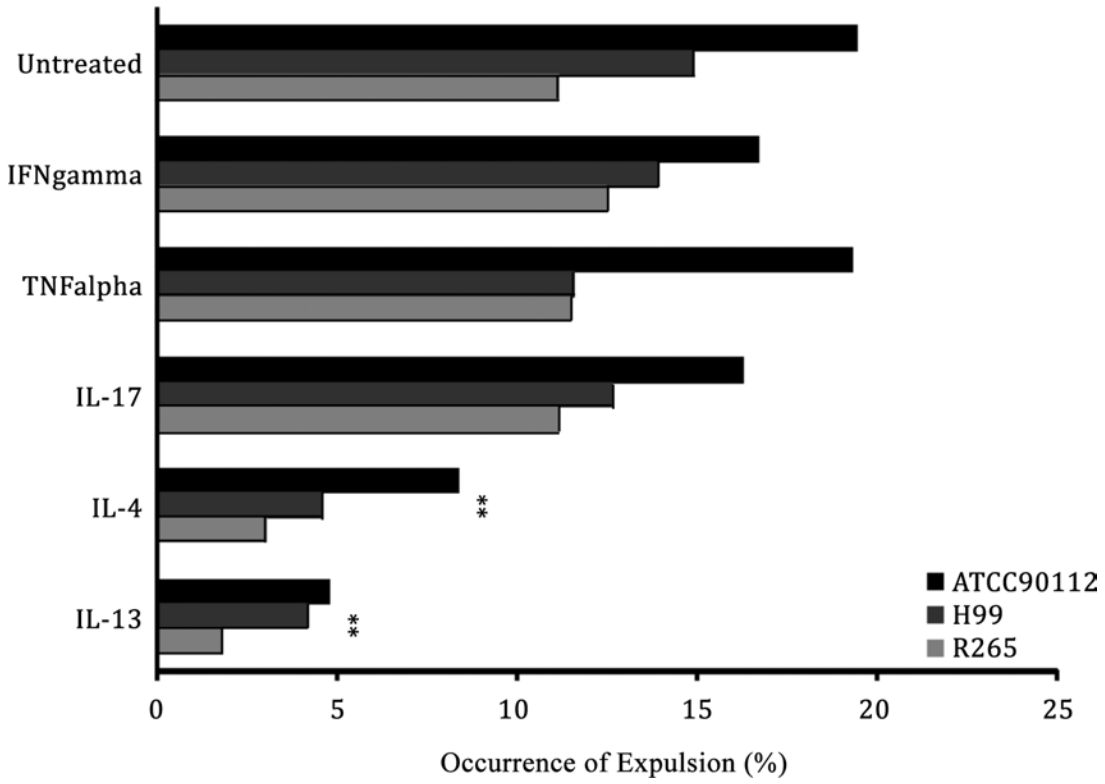

Figure 20: Occurrence of cryptococcal expulsion in J774 macrophages after cytokine treatment. Occurrence of cryptococcal expulsion is reduced in Th2 cytokine but not altered in TNF-α and IL-17 cytokine treated J774 macrophages. Untreated and Th1 (10 units/ml IFN-γ, 1 ng/ml TNF-α), Th17 (10 ng/ml IL-17) or Th2 (10 ng/ml IL-4 or 10 ng/ml IL-13) cytokine treated J774 cells were infected with *C. neoformans* strains ATCC90112 and H99 or *C. gattii* strain R265, then further incubated under the same conditions whilst monitoring for cryptococcal expulsion. Occurrence of expulsion is significantly reduced following treatment with Th2 cytokines IL-4 or IL-13 compared to untreated or Th1/Th17 treated cells. The presented data were obtained from at least three individual experiments and analysed for statistical significance using χ^2 tests. Statistically significant differences are indicated by asterisks (** $P \leq 0.01$).

3.5 THE INFLUENCE OF CYTOKINE SIGNALING ON EXPULSION EVENTS IN HUMAN PRIMARY MONOCYTE-DERIVED MACROPHAGES

To test whether the reduction of expulsion in response to Th2 cytokines is an artifact of the J774 cell line, human primary macrophages were activated with the Th1 cytokines IFN-γ, TNF-α, the Th17 cytokine IL-17 or the Th2 cytokines IL-4 and IL-13, infected with cryptococci and then imaged and analysed for the occurrence of expulsion. As with J774 macrophages, all three cryptococcal strains showed similar trends (Figure 21) and data was therefore pooled for all three strains to permit statistical analysis. As with J774 macrophages, expulsion rates did not differ significantly between untreated macrophages and cells activated with the Th1 cytokines IFN-γ ($P > 0.12$) or Th17 cytokine IL-17 ($P > 0.68$), although expulsion events were slightly ($P = 0.03$) more common in TNF-α treated cells. In contrast, however, the occurrence of expulsion was significantly reduced in cultures treated with the Th2 cytokines IL-4 and IL-13 compared to untreated samples ($P = 0.0001$ and $P = 0.04$ respectively). Thus Th2 cytokines reduce expulsion rates in both J774 and human primary macrophages.

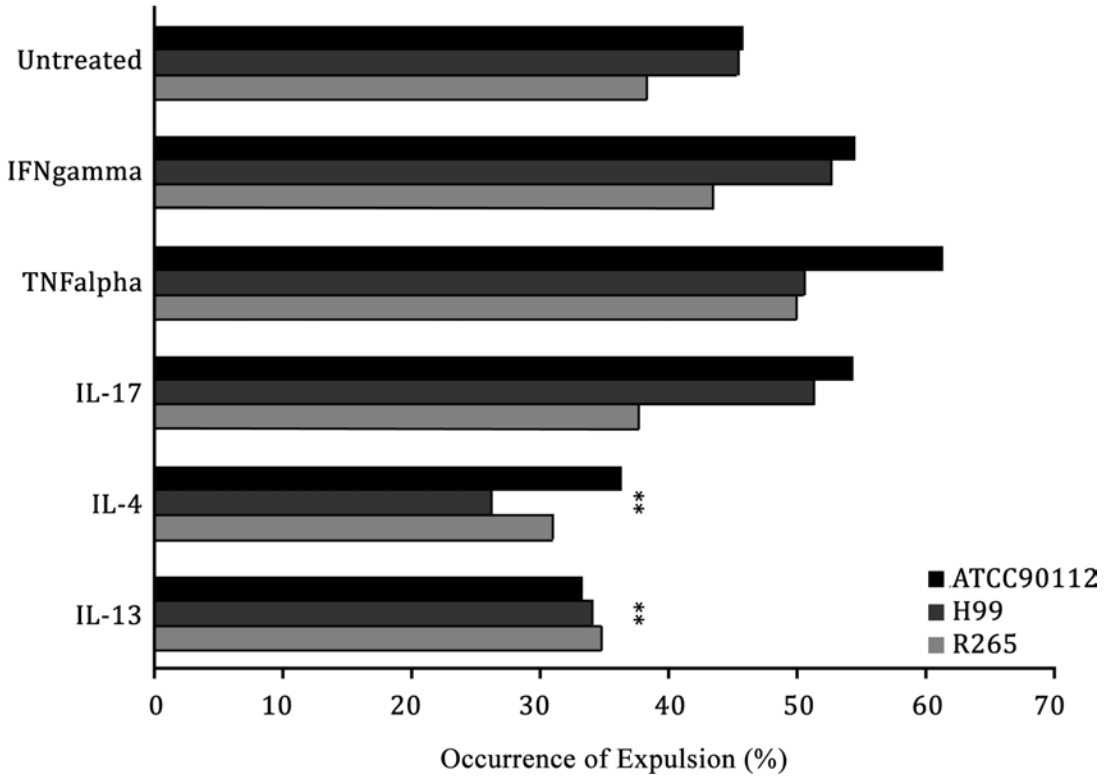

Figure 21: Occurrence of cryptococcal expulsion in human macrophages after cytokine treatment. Occurrence of cryptococcal expulsion is reduced in Th2 cytokine but not altered in TNF-α and IL-17 cytokine treated human primary macrophages. Untreated and Th1 (10 units/ml IFN-γ, 1 ng/ml TNF-α), Th17 (10 ng/ml IL-17) or Th2 (10 ng/ml IL-4 or 10 ng/ml IL-13) cytokine treated human primary macrophages were infected with *C. neoformans* strains ATCC90112 and H99 or *C. gattii* strain R265, then further incubated under the same conditions whilst monitoring for cryptococcal expulsion by live cell imaging. Occurrence of expulsion is significantly reduced following treatment with Th2 cytokines IL-4 or IL-13 compared to untreated or Th1/Th17 treated cells. The presented data were obtained from at least three individual experiments and analysed for statistical significance using χ^2 tests. Statistically significant differences are indicated by asterisks (** $P \leq 0.01$).

3.6 INTRACELLULAR PROLIFERATION RATE AND EXPULSION OF COMPLEMENT OPSONIZED *CRYPTOCOCCUS* IN CYTOKINE TREATED J774 MACROPHAGES

While opsonising antibodies to *Cryptococcus* may or may not be present during an infection, complement opsonization should occur in all healthy individuals. To determine the effect of Th1, Th17 and Th2 cytokines on complement-opsonized yeast, intracellular proliferation and occurrence of expulsion were assessed in cytokine treated J774 cells infected with serum-opsonized *C. neoformans* strain ATCC90112 cells. As with antibody-opsonized yeast, complement-opsonized yeast proliferated more readily in, but was expelled less frequently from, Th2-stimulated macrophages than from Th1 or Th17 stimulated macrophages (Figure 22). Thus the effects of cytokine activation appear to be largely independent of the opsonin present on the cryptococcal surface.

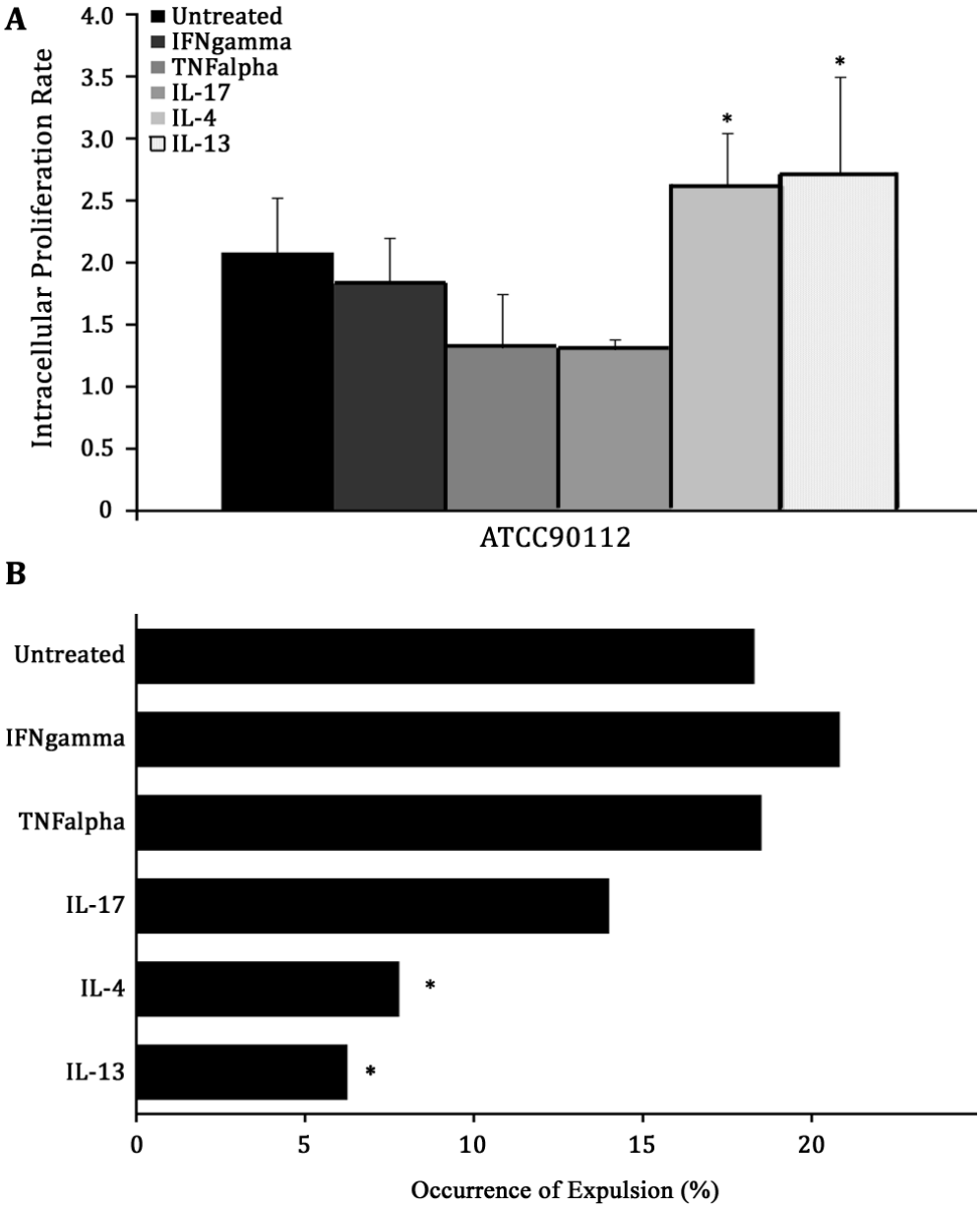

Figure 22: Effect of cytokine treatment after complement-mediated opsonisation. Complement-mediated opsonization does not change the effect of cytokine stimulation on cryptococcal behaviour. Untreated and Th1 (10 units/ml IFN-γ, 1 ng/ml TNF-α), Th17 (10 ng/ml IL-17) or Th2 (10 ng/ml IL-4 or 10 ng/ml IL-13) cytokine treated human primary macrophages were infected with *C. neoformans* strain ATCC90112, opsonized in fresh human serum, and then further incubated under the same conditions to monitor intracellular yeast proliferation or to monitor cryptococcal expulsion by live cell imaging. (A) IPR is significantly lower following treatment with the Th1 cytokine TNF-α and the Th17 cytokine IL-17 in comparison with both of the Th2 cytokines. The data are presented as the mean of at least three individual experiments ± 2 x standard error of the mean. (B) Occurrence of expulsion is reduced following treatment with Th2 cytokines IL-4 or IL-13 compared to untreated cells or cells treated with IFN-γ. Data were obtained from at least three individual experiments. Statistically significant differences are indicated by asterisks (* $P < 0.05$).

3.7 DISCUSSION

The importance of a Th1 immune response for controlling cryptococcal burden is evident from the high incidence of severe *Cryptococcus neoformans* infections in HIV patients (Wadhwa *et al.*, 2008) and from data obtained in numerous mouse models (Flesch *et al.*, 1989, Kawakami *et al.*, 1995, Milam *et al.*, 2007, Wormley *et al.*, 2007). Here, a molecular explanation for these *in vivo* observations is provided. The results strongly suggest inhibition of anticryptococcal macrophage functions, such as phagocytosis and intracellular clearance, by Th2 cytokines, which would be likely to lead to a higher fungal burden in hosts showing a Th2-dominated response, as previously reported (Blackstock *et al.*, 2004, Decken *et al.*, 1998, Muller *et al.*, 2007).

Three different *Cryptococcus* strains were selected to represent the two most important serotypes. The *C. neoformans* serotype A strains ATCC90112 and H99, both clinical isolates from patient cerebrospinal fluid, represent the serotype most commonly isolated from immunocompromised patients and which is responsible for 95 % of all *C. neoformans* infections (Hull *et al.*, 2002). The *C. gattii* serotype B strain R265 is a clinical isolate from the ongoing cryptococcosis outbreak in immunocompetent individuals in British Columbia, Canada, an outbreak that highlights the potential of *Cryptococcus* as an emerging pathogen (Fraser *et al.*, 2003, MacDougall *et al.*, 2007). Trends were similar for all three strains throughout the study and thus the influence of cytokine signaling on cryptococcal pathogenesis is likely to be common to both *Cryptococcus* species, despite the different disease etiology between them.

The lowest possible cytokine concentrations were deliberately selected for this study in order to minimize the risk of artifacts. Given this, it needs to be recognized that there might be more dramatic effects on cryptococcal behavior at higher concentrations and thus that Th1/Th17/Th2 balance may profoundly affect the path of disease progression in infected patients.

The data demonstrates that intracellular yeast proliferation is increased after Th2

activation of macrophages. These findings provide a molecular explanation for the protective effect of Th1 cytokines such as IFN-γ and TNF-α (Kawakami *et al.*, 1995, Milam *et al.*, 2007, Wormley *et al.*, 2007) and Th17 cytokines such as IL-17 (Muller *et al.*, 2007), and the non-protective effect of Th2 cytokines such as IL-4 and IL-13 (Blackstock *et al.*, 2004, Decken *et al.*, 1998, Muller *et al.*, 2007), in mouse model systems.

Two additional interesting observations can be made from the IPR dataset. Firstly, it is intriguing that IFN-γ suppresses cryptococcal IPR far more effectively in J774 cells than in human primary macrophages. This observation is in agreement with previous reports demonstrating a reduction in the inhibition of cryptococcal growth in human alveolar and monocyte-derived macrophages after IFN-γ treatment (Levitz *et al.*, 1990, Reardon *et al.*, 1996). Such findings may indicate differences in IFN-γ related regulation of anticryptococcal functions in mouse and human macrophages. Secondly, in J774 cells treatment with pro-inflammatory cytokines did not alter cryptococcal proliferation as compared with untreated controls. This is suggestive of the fact that J774 macrophages may already be partially activated by the presence of opsonized cryptococci and/or the tissue culture environment.

It is also demonstrated for the first time that Th2, but not Th1 or Th17, cytokine treatment leads to a significant reduction in the occurrence of cryptococcal expulsion, a recently-described phenomenon that appears to be unique to this pathogen (Alvarez *et al.*, 2006, Ma *et al.*, 2006). The relevance of expulsion for disease progression is, as yet, unclear. However, cryptococci expelled from circulating monocytes will likely be exposed to a far greater immune attack than those that remain intracellular. In addition, reduced expulsion might favor the dissemination of *Cryptococcus* to the central nervous system in parasitized macrophages via a 'Trojan Horse' mechanism (Charlier *et al.*, 2009, Luberto *et al.*, 2003). Thus, suppression of cryptococcal expulsion by a dominant Th2 cytokine profile may benefit the pathogen and reduce the host's likelihood of surviving an infection. It is important to note that reduced expulsion alone is insufficient to account for the increased IPR observed in Th2-stimulated macrophages; even in

Th1-stimulated cells, expulsion is a very rare effect (Ma *et al.*, 2006) that cannot account for the differences observed in IPR. Thus, cytokine signaling operates in at least two ways; firstly, to modify intracellular proliferation and secondly to influence the likelihood of expulsion.

How might cytokine-signaling impact on intracellular cryptococcal behavior? The most likely scenario is that cytokine activation triggers changes in the composition of the phagosome that favor either expulsion (Th1/Th17) or proliferation (Th2). Recent data suggest that one such change may be the availability of metal ions. Many cryptococcal virulence factors such as laccase, SOD, catalase and urease depend upon metal ions and thus cation homeostasis. Interestingly, the anti-inflammatory cytokines IL-4 and IL-13 have been suggested to enhance iron uptake and storage by macrophages by suppression of activation of iron regulatory protein-1 and -2, leading to translational repression of the iron storage protein ferritin or transcriptional activation of the membrane receptor for iron uptake (Weiss *et al.*, 1997). Thus, higher metal ion availability might increase the activity of cryptococcal virulence factors and could lead to increased intracellular proliferation in Th2-stimulated cells. In this regard, it is intriguing that urease, a cryptococcal virulence factor (Cox *et al.*, 2000), promotes a non-protective Th2 immune response within the lung (Osterholzer *et al.*, 2009b), suggesting that *Cryptococcus* may actively bias the host's cytokine profile to its own advantage.

Cryptococcosis incidence increases throughout the course of AIDS and correlates with the loss of Th1 response in AIDS patients (Altfeld *et al.*, 2000) and with a Th2-type cytokine profile in transplant recipients (Singh *et al.*, 2008). The presented data indicate that the loss of Th1 cytokines significantly reduces the ability of macrophages to deal with *Cryptococcus* and prevents efficient cryptococcal clearance in HIV patients and, therefore, that pro-inflammatory cytokines may be a useful therapeutic agent for the treatment of this disease. IFN-γ has been successfully applied to enhance chemotherapy of systemic cryptococcosis in BALB/c mice (Lutz *et al.*, 2000) and in immunocompromised SCID mice (Clemons *et al.*, 2001) and thus, has been suggested as a potential therapeutic regime in humans. However, there seem to be differences in IFN-γ related signaling in mice

and humans. IFN-γ has clearly been demonstrated to have a protective role in mouse model systems of cryptococcosis (Hoag *et al.*, 1997, Bava *et al.*, 1995) and to increase fungicidal activity of murine macrophages (Flesch *et al.*, 1989). However, in human cells, IFN-γ treatment reduces the capacity of human alveolar macrophages (Reardon *et al.*, 1996) and human monocyte-derived macrophages (Levitz *et al.*, 1990) to inhibit cryptococcal growth, a finding that is supported by the presented data. Although IFN-γ levels at the site of infection have been negatively correlated with cryptococcal CFU (Siddiqui *et al.*, 2005) and IFN-γ therapy has proved successful in one patient (Netea *et al.*, 2004), these *in vitro* data suggest that IFN-γ treatment may not always be an appropriate therapeutic approach.

Taken together, these data suggest that the poor prognosis of Th2-cytokine profiles in cryptococcal infection may in part result from a combination of increased intracellular proliferation and reduced expulsion of the pathogen. These effects are independent of cryptococcal strain or phagocytic opsonin and may therefore represent a general phenomenon associated with intracellular pathogens.

CHAPTER 4

AUTOMATED ANALYSIS OF CRYPTOCOCCAL MACROPHAGE PARASITISM USING GFP-TAGGED CRYPTOCOCCI

Major parts of this chapter have been submitted for publication:

Voelz, K., S. A. Johnston, J. C. Rutherford and R. C. May. 2010. Automated analysis of cryptococcal macrophage parasitism using GFP-tagged cryptococci. PLoS One (Submitted)

Research into the interaction between *Cryptococcus* and macrophages in recent years has established this as a model system for investigation of cryptococcal virulence, since intracellular yeast proliferation in macrophages correlates well with virulence data from mice (Ma *et al.*, 2009a, Byrnes *et al.*, 2010). However, experimental approaches to quantify macrophage parasitism rely on time-lapse imaging and/or manual colony counts of isolated yeast, both of which are low throughput, time-consuming methods. To facilitate faster analysis of cryptococcal intracellular parasitism, the use of fluorescently tagged yeast together with flow cytometry was investigated. This section reports the production of two cryptococcal strains that show strong, stable GFP expression: a GFP-positive *C. neoformans* serotype A type strain H99 and a GFP-positive *C. gattii* serotype B type strain R265 (an isolate from the ongoing Vancouver Island Outbreak (Kidd *et al.*, 2004)). Both strains were extensively characterised and their responses to environmental and host stress conditions and their virulence in the macrophage model system remain unaltered. Using these strains, a flow cytometry-based approach for accurate, high throughput quantification of macrophage parasitism was developed. Taken together, these findings represent a powerful resource for the cryptococcosis research community and should facilitate rapid advances in our understanding of cryptococcal virulence.

4.1 RANDOM GENOMIC INTEGRATION AND EXPRESSION OF A GFP CONSTRUCT IN *C. NEOFORMANS* H99 AND *C. GATTII* R265

To achieve constitutive GFP expression, a construct where GFP is under the control of the actin promoter and tryptophan terminator was created. Both sequences, obtained from NCBI for the *C. neoformans* strain JEC21 (AY483215), were used for the design of overlapping primers. The three overlapping PCR products were combined into the vector pRS426 (Christianson *et al.*, 1992) to create a GFP construct using the homologous recombination machinery of *S. cerevisiae*. Afterwards, the construct was recovered by PCR and ligated into the vector pAG32 (Goldstein *et al.*, 1999), which was used as shuttle vector for biolistic bombardment (Figure 23 A). Three individual biolistic transformations yielded a range of hygromycin resistant and GFP expressing *C. gattii* R265 colonies but only two transformant *C. neoformans* H99 colonies. All positive colonies were re-streaked onto selective YPD plates. Eight *C. gattii* R265 strains (R265_GFP6, R265_GFP13, R265_GFP14, R265_GFP15, R265_GFP17, R265_GFP18, R265_GFP20, R265_GFP21) stably expressing GFP were randomly selected for further analysis. Of the two transformed H99 colonies, one showed unstable GFP expression that was lost after being re-streaked and hence only a single GFP-expressing H99 strain was used for further analysis. As a first step to analyse these GFP-strains, growth in YPD media at 25°C was assessed. Strains R265_GFP20 and R265_GFP21 showed a statistically significant reduction in growth rate in YPD compared to the parental R265 strain and these two strains were therefore excluded from further analysis. However, none of the remaining mutants were altered in their ability to growth in YPD media (Figure 23 B).

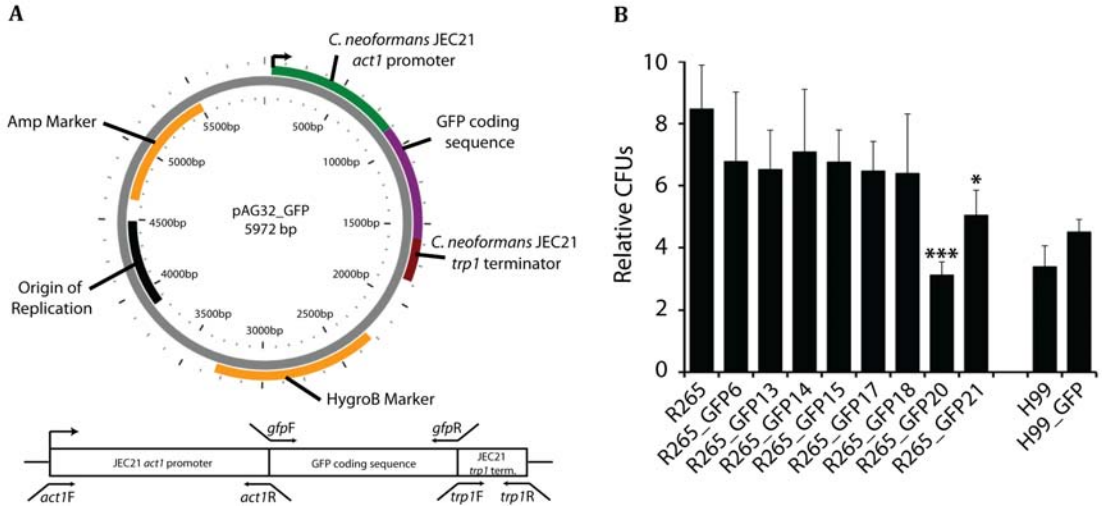

Figure 23: GFP expressing mutants. (A) Plasmid map of pAG32 containing GFP construct and GFP-construct with primer localisation below. (B) Growth rate analysis of the GFP-positive strains. Yeast were grown in YPD media at 25°C with rotation (20 rpm). Colony forming units were counted at time point 0 and 24 hr and relative strain growth calculated. Plasmid map was created using the PlasMapper 2.0 (Dong *et al.*, 2004). (* P-Value < 0.05, *** P-Value < 0.001).

4.2 IDENTIFICATION OF GFP INTERGATION SITE

The GFP construct together with the unlinearised shuttle vector was randomly integrated in the cryptococcal genome. However, for applications such as random mutagenesis it would be important to be able to identify the integration site. Hence, it was attempted to identify the integration site by a single primer PCR approach followed by sequencing with a second specific sequencing primer (Karlyshev *et al.*, 2000). PCR-primer were designed approximately every 500 bp to cover the whole plasmid (Table 6).

Table 6: Primer used for Single PCR procedure and following sequencing.

Name	Sequence (5'-3')	Tm in °C
GFP Sequ.	GGC ATG GAC GAG CTG TAC AAG	56
GFP PCR	TCC TGC TGG AGT TCG TGA C	53
pAG32-1Sequ.	CAT GAT GTG ACT GTC GCC CGT AC	59
pAG32-1PCR	CTC CTT GAC AGT CTT GAC GTG	54
pAG32-2Sequ.	GTG TCA CGT TGC AAG ACC TG	54
pAG32-2PCR	CGA GAG CCT GAC CTA TTG C	53
pAG32-3Sequ.	CTT GTA TGG AGC AGC AGA CG	54
pAG32-3PCR	CAA TAC GAG GTC GCC AAC ATC	54
pAG32-4Sequ.	GCT GTC GAT TCG ATA CTA ACG	52
pAG32-4PCR	TGT GAA TGC TGG TCG CTA TAC	52
pAG32-5Sequ.	GAT ACC TGT CCG CCT TTC TC	54
pAG32-5PCR	CTA TAA AGA TAC CAG GCG TTT CC	53
pAG32-6Sequ.	CTC AGT GGA ACG AAA ACT CAC G	55
pAG32-6PCR	CTT TTC TAC GGG GTC TGA CG	54
pAG32-7Sequ.	CTC GTC GTT TGG TAT GGC TTC	54
pAG32-7PCR	TAC AGG CAT CGT GGT GTC AC	54
pAG32-8Sequ.	CAG GGT TAT TGT CTC ATG AGC	52
pAG32-8PCR	CGA CAC GGA AAT GTT GAA TAC TC	53
pAG32-9Sequ.	CAG AGC AGA TTG TAC TGA GAG TG	55
pAG32-9PCR	GCT GGC TTA ACT ATG CGG CAT	54

The initial PCR products contained mixtures of different fragments – integration specific fragments and random fragments from other genomic regions (Figure 24 A). The mixtures were subjected to sequencing with an integration site specific primer located downstream of the original PCR primer and sequences were then analysed with the basic local alignment search tools (Blast) available from the Broad Institute of MIT and Harvard and NCBI. Analysis was concentrated on the GFP-positive strain R265_GFP6. Sequences from reactions using the primer sets pAG32-1 to pAG32-7 did not return any significant matches within the R265 genome. However, a 129 bp long fragment within the sequence data from reactions with the primer sets GFP, pAG32-8 and pAG32-9 could be identified within the genome and aligns with the locus for anthranilate synthase component 2 (Figure 24 B). A literature search suggested that this component is part of the tryptophan operon in *Salmonella typhimurium* and *E. coli* (Horowitz *et al.*, 1982, La Scolea *et al.*, 1972). With *trp1* supplying the terminator in the GFP construct, this observation prompted further analysis of the 129 bp fragment. Closer examination of the matches with the R265 genome revealed that all three localize within the same area of the R265 genome (228852-228980) and an alignment of the 129 bp section with the *trp1* terminator sequence from *C. neoformans* JEC21 (AY483215) showed 88 % sequence identity (Figure 24 C). This indicates that the 129 bp match the terminator region of the GFP construct and/or terminator regions of genes involved in tryptophan synthesis within the R265 genome. Furthermore, the chromatogram of the region downstream of the 129 bp fragment seems to show more than one sequence being overlaid (Figure 24 D). Taken together, no definite statement about the integration site can be made. However, an observation made after DNA microinjection into nuclei of mammalian cultured cells might help to explain this phenomenon. Multiple copies of the transforming gene were, dependent on the DNA concentration, integrated as concatemer at one or few sites in the host genome (Folger *et al.*, 1982). Thus, adjustment of plasmid DNA concentration for biolistic transformation might reduce or prevent the formation of concatemer and enable identification of the DNA integration site in the future.

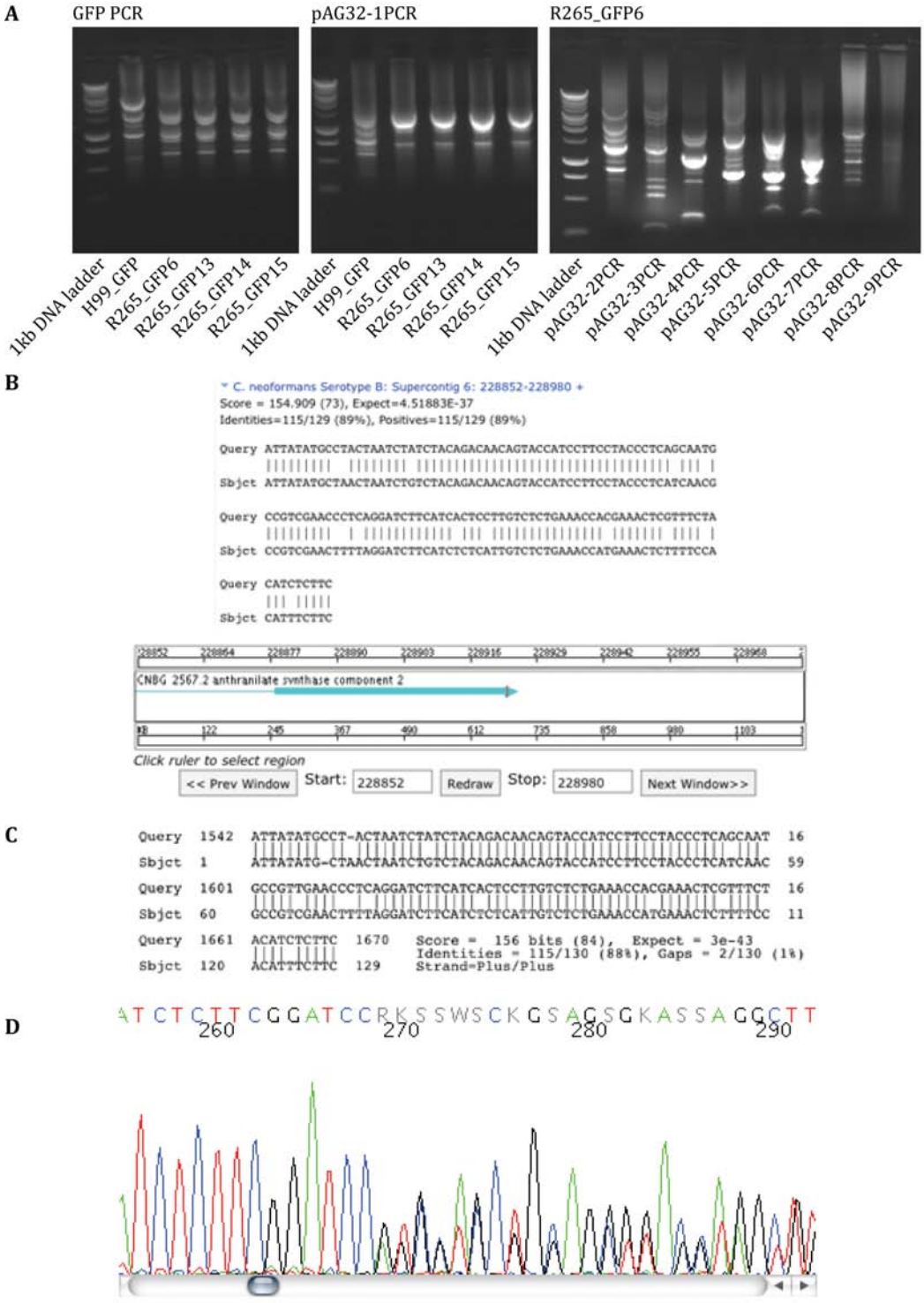

Figure 24: Identification of GFP integration site. (A) The single primer PCR approach resulted in a mixture of PCR products. (B) Analysis of sequence data from primer sets GFP, pAG32-8 and pAG32-9 resulted in matches within the anthranilate synthase component 2 within the R265 genome (alignment shown for GFP sequence data). (C) Closer examination revealed that this match is against the *trp1* terminator of either the GFP a construct or terminator region of genes involved in tryptophan synthesis in R265. (D) Furthermore, the chromatogram downstream of the 129 bp match shows the clear sequence trace of the fragment turning into multiple overlapping traces.

4.3 GFP EXPRESSING STRAINS SHOW NO ALTERED RESPONSE TO STRESS CONDITIONS

Within the host environment *Cryptococcus* encounters a variety of stresses. The five selected GFP-positive strains were tested in an *in vitro* system for their ability to cope with different stress conditions in comparison with their parental strains (Figure 25 & Table 7). Growth rates of all five GFP-expressing strains were indistinguishable from their respective parental strains at two different temperatures (25°C and 37°C). In addition, none of the strains were altered in their response to hypoxia (3 % oxygen or treatment with 0.05, 0.1 and 0.3 mM $CoCl_2$ (Lee *et al.*, 2007)), oxidative (0.25, 0.5 and 1 mM H_2O_2) or nitrosative (1, 5 and 20 mM $NaNO_2$) stress, or exposure to cell wall damage (0.005, 0.01 and 0.05 % SDS or 0.05, 0.1 and 0.3 mM NaCl). Thus, none of the GFP-expressing strains show any significant changes in their response to stress conditions.

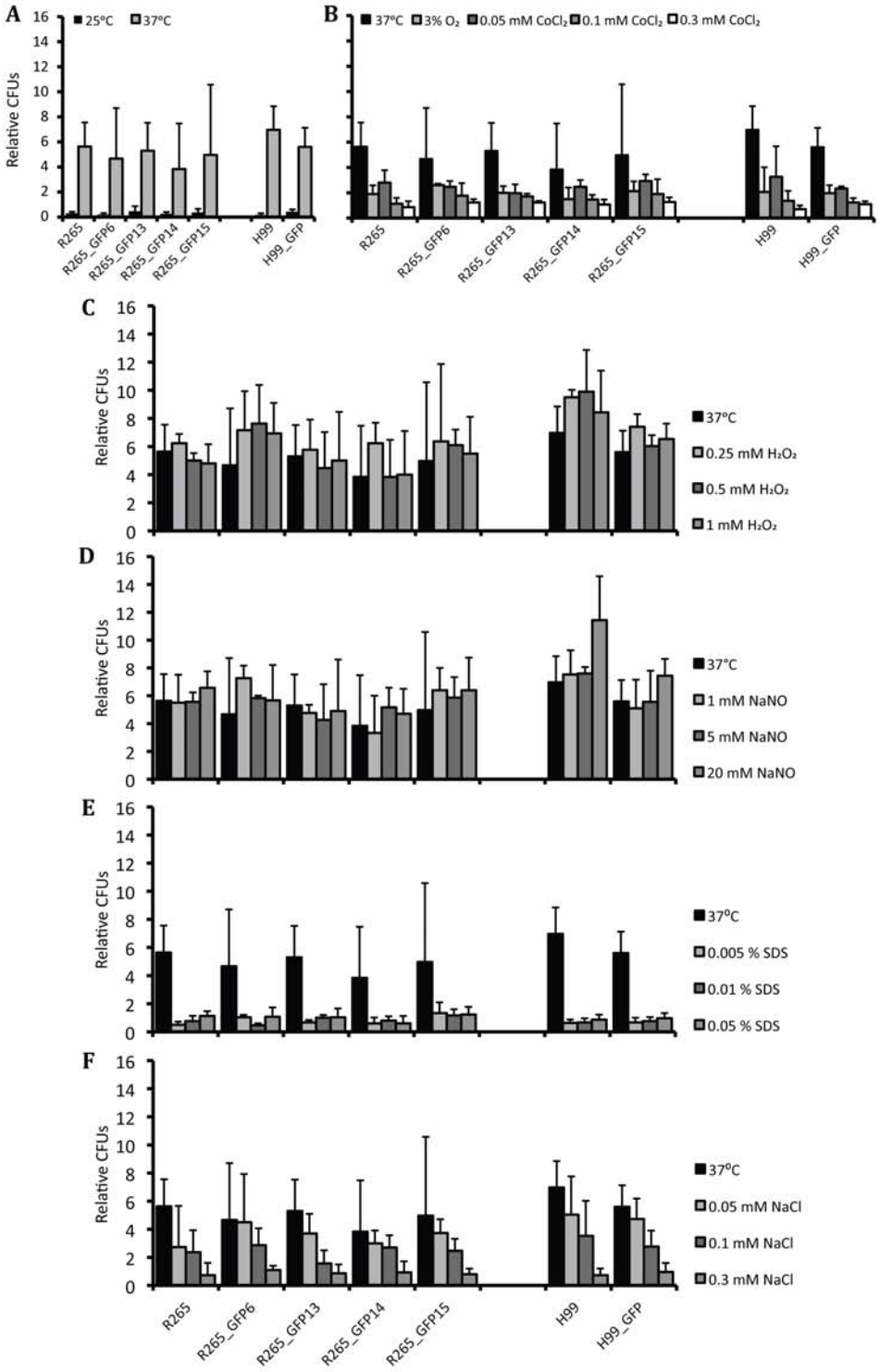

Figure 25: Response of GFP expressing strains to stress. The stress tolerance of the GFP-expressing isolates was tested by incubation under stress conditions for 24 hours followed by relative CFU analysis. Neither high temperature (A), hypoxia (B), oxidative stress (C), nitrosative stress (D), SDS exposure (E) or high salt (F) resulted in any significant differences in survival relative to non-GFP expressing parental strains (Table 7). Data are presented as means of at least three independent repeats with 2 x standard error.

Table 7: P-values of statistical analysis. Results from CFU counts from stress treatments and intracellular virulence assays of GFP-positive strains were compared to parental strains.

Condition \ Strain		R265				H99
		GFP6	GFP13	GFP14	GFP15	GFP
	25°C	0.975	0.861	1.000	0.994	0.623
	37°C	0.999	1.000	0.984	1.000	0.996
	3 % O_2	0.937	1.000	0.996	1.000	1.000
$CoCl_2$	**0.05 mM**	0.999	0.919	0.999	1.000	0.871
	0.1 mM	0.857	0.908	0.993	0.724	1.000
	0.3 mM	0.697	0.697	0.973	0.614	0.614
H_2O_2	**0.25 mM**	0.988	1.000	1.000	1.000	0.899
	0.5 mM	0.602	1.000	0.984	0.988	0.211
	1 mM	0.887	1.000	0.999	1.000	0.930
$NaNO_2$	**1 mM**	0.790	0.996	0.613	0.989	0.490
	5 mM	1.000	0.883	1.000	1.000	0.523
	20 mM	0.998	0.954	0.924	1.000	0.301
SDS	**0.005 %**	0.484	0.995	1.000	0.095	1.000
	0.01 %	0.797	0.923	1.000	0.535	0.999
	0.05 %	1.000	1.000	0.748	1.000	1.000
NaCl	**0.05 mM**	1.000	1.000	0.970	1.000	1.000
	0.1 mM	0.998	0.980	1.000	1.000	0.984
	0.3 mM	0.976	1.000	0.999	1.000	0.998
Percentage Phagocytosis		0.877	0.969	0.794	0.918	0.851
IPR		0.972	0.916	1.000	0.989	0.989
Occurrence of Expulsion		0.934	0.718	0.904	0.433	0.264

4.4 GFP EXPRESSING STRAINS SHOW NO ALTERATION IN VIRULENCE IN MACROPHAGES

Since macrophage/cryptococcal interactions are critical for disease progression (Kechichian *et al.*, 2007, Shao *et al.*, 2005), it was tested whether the expression of GFP altered cryptococcal behaviour within phagocytic effector cells. Using the J774 macrophage-like cell line, each of the GFP positive strains was tested for a) phagocytic uptake (Figure 26 A), b) intracellular proliferation (Figure 26 B) and c) the occurrence of expulsion (Figure 26 C). All of the GFP-expressing strains were indistinguishable from their parental strains in each parameter tested (Table 7). Thus expression of GFP in these strains does not alter their ability to parasitise macrophages.

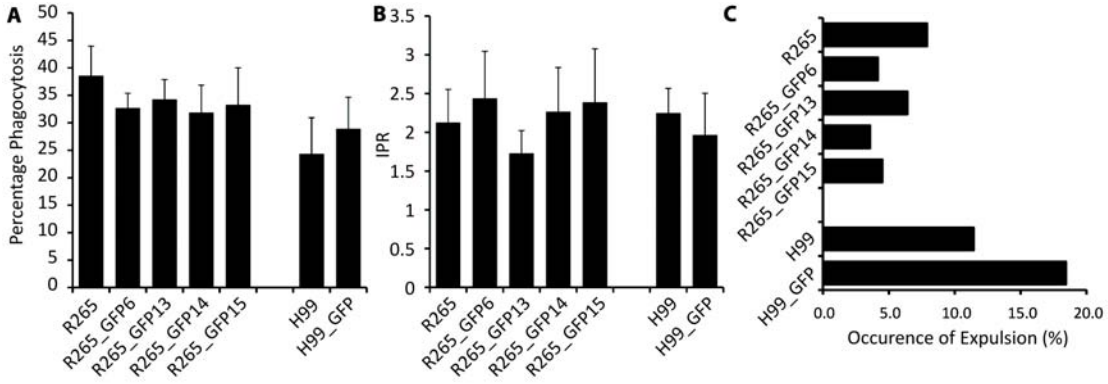

Figure 26: Analysis of intracellular virulence parameters. J774 macrophages were infected with GFP-positive isolates or their parental strains and analysed for yeast uptake (A), maximal intracellular yeast cell proliferation (IPR) (B) and occurrence of cryptococcal expulsion (C). No statistically significant differences were found between the GFP-expressing strains and their parental counterpart (Supplementary table 1). Data are presented as mean ($n \geq 3$) with 2 x standard error (A & B) or accumulated data from three independent repeats (C).

4.5 GFP EXPRESSING STRAINS CAN BE USED FOR AUTOMATED ANALYSIS OF CRYPTOCOCCAL INTERACTION WITH MACROPHAGES

To date, analysis of cryptococcal interactions with macrophages has required elaborate and time-consuming experimental approaches. Potentially, flow cytometry-based systems offer an accurate but high-throughput alternative strategy for analysing intracellular proliferation. Since the GFP-positive strains described above are unaltered in their behaviour in macrophages, these strains were used to develop a flow cytometry-based methodology for quantifying intracellular proliferation of cryptococci in collaboration with Dr. S. A. Johnston. By microscopy, all five GFP positive strains showed evenly distributed GFP expression within the cytoplasm (Figure 27 A). Furthermore, analysis of fluorescence and forward scatter by flow cytometry showed all five GFP expressing strains were clearly distinct from both the non-GFP expressing parental strains and from uninfected macrophages (Figure 27 B). The previously published method for assaying proliferation within macrophages requires lysis of macrophages followed by manual counting of numerous replicate samples using either a haemocytometer or by plating on YPD plates and counting colony forming units (CFU) (Voelz et al., 2009; Ma et al., 2009). To validate the flow cytometry based method, replicate samples were taken from macrophage infections with the same GFP-expressing strain and compared proliferation quantification by flow cytometry, CFU and haemocytometer count. Comparison of *Cryptococcus* proliferation from all three counting methods showed no significant differences. Thus, flow cytometry offers a reliable and rapid alternative to manual count-based methods of analysis (Figure 27 C).

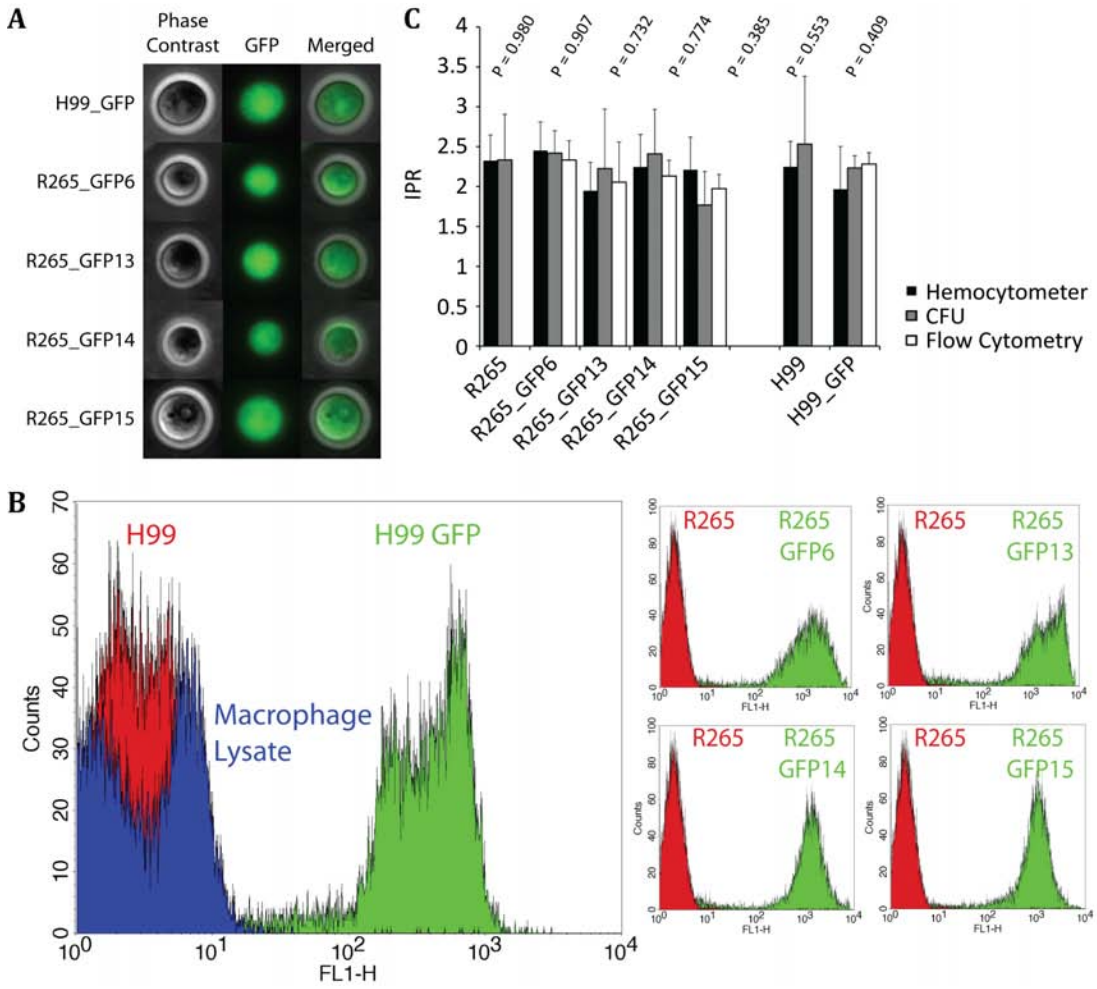

Figure 27: Automated counting of intracellular *Cryptococcus* proliferation within macrophages. (A) GFP expression in GFP-positive strains selected for analysis in this study. (B) GFP-tagged strains were first analysed for their expression profile. All GFP-expressing strains are clearly discernable from GFP-negative cryptococci or cell debris. (C) Replicate samples were used for quantifying intracellular yeast cell numbers after macrophage infection via haemocytometer (black bars), CFU count (grey bars) or flow cytometry (white bars). For all of the strains, there was no statistically significant difference between any of the three counting methods. Data are presented as means with 2 x standard error from at least three independent repeats.

4.6 A NON-LYTIC METHOD OF QUANTIFIYNG MACROPHAGE-*CRYPTOCOCCUS* INTERACTION BY FLOW CYTOMETRY

To date, all methods for quantifying intracellular cryptococcal proliferation involve a lysis step to free any intracellular yeast cells for counting. Lysis is methodologically undesirable since it increases processing time, increases the risk of sample loss and may potentially damage intracellular cryptococci. Accutase, a proteolytic and collagenolytic enzyme mix, allows detachment and dissociation of mammalian cells without significantly influencing viability (Bajpai *et al.*, 2008), potentially enabling quantification of fungal burden within infected macrophages without lysis. J774 macrophage cultures were infected with H99_GFP, incubated according to the protocol for IPR assays and then treated with the enzyme mix instead of being lysed. Flow cytometry demonstrated that extracellular yeast cells, macrophages and macrophages with intracellular yeast cells formed three distinct regions based upon their size (forward scatter, FSC) and GFP fluorescence intensity (Figure 28 A). By comparing events counted for macrophages versus events counted for macrophages with intracellular cryptococci percentage phagocytosis could by accurately quantified (Figure 28 B). In addition, by calculating fluorescence intensity, intracellular cryptococcal proliferation could be quantified without the need to lyse the macrophage culture (Figure 28 C).

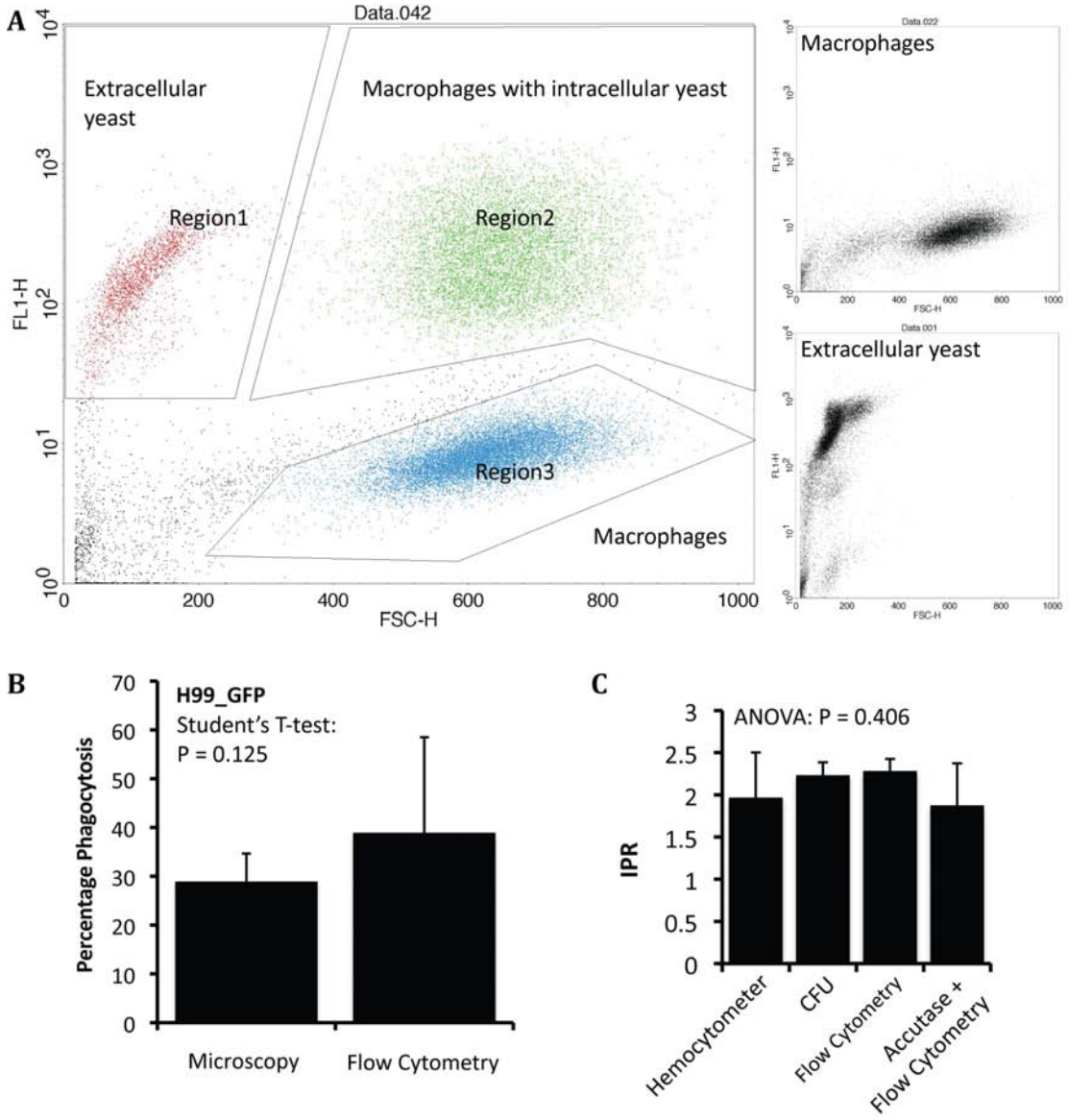

Figure 28: Assessment of virulence parameters in the macrophage model system after treatment with Accutase. Macrophages were infected with the GFP-positive H99 strain H99_GFP and cultured in the same way as for a normal infection assay. Samples were taken at standard time points but instead of cell lysis, the cultures were treated with Accutase to detach and dissociate cells. (A) Extracellular yeast, uninfected macrophages and macrophages with intracellular yeast cells show three distinct populations in a scatter plot. (B) Phagocytic uptake can be quantified by comparing the proportions of infected and uninfected macrophages using flow cytometry. Results are not statistically different between the two approaches. (C) Intracellular proliferation can also be determined with this approach by calculating fluorescence intensity. Results are not statistically different from IPR measurements with a hemocytometer, by CFU counts or flow cytometry counting after macrophage lysis. Data are presented as means with 2 x standard error from at least three independent repeats.

4.7 DISCUSSION

The generation of *Cryptococcus* type strains expressing GFP; *C. gattii* GFP-positive serotype B R265 strains and a *C. neoformans* GFP-positive serotype A H99 strain was described.

Transformation of *Cryptococcus* with plasmid DNA can result in non-homologous integration into the genome or extrachromosomal integration of the target sequence; the former being mitotically stable, the latter unstable (Varma *et al.*, 1992a). All mutants analysed in this study show stable GFP expression indicating stable ectopic integration within the genome. The one H99 transformant with unstable GFP expression is thus very likely a mutant that harboured the GFP containing plasmid extrachromosomal (Varma *et al.*, 1992a, Toffaletti *et al.*, 1993). Unfortunately, it was not possible to identify the GFP integration site following PCR and sequencing. Analysis of the sequence chromatograms revealed the presence of overlaying sequences indicating potential multiple integration events within the *Cryptococcus* genome and/or the integration of transgene concatemer. An observation made after DNA microinjection into nuclei of mammalian cultured cells might help to explain this phenomenon. Multiple copies of the transforming gene were, depending on the DNA concentration, integrated as concatemer at one or few sites in the host genome (Folger *et al.*, 1982). Thus, adjustment of plasmid DNA concentration for biolistic transformation might reduce or prevent the formation of concatemer and enable identification of the DNA integration site in the future.

However, all characterised strains show strong and stable GFP expression and are indistinguishable from non-fluorescent parental isolates in terms of growth rate, stress tolerance or their ability to parasitize macrophages. These strains were then used to develop and validate a flow cytometry based assay for quantifying intracellular cryptococcal proliferation.

Endogenous GFP expression has substantial advantages over exogenous fluorescent labels since it does not require any secondary manipulations such as

staining or treatment with a probe and thus can be directly used for analysis. Although GFP is generally regarded as a protein that does not influence cellular processes, it is known that in *Salmonella enterica* expression of GFP alters establishment of the intracellular niche in epithelial cells and macrophages (Knodler *et al.*, 2005). However, careful analysis indicates that the GFP expressing cryptococci reported here show no significant differences in their stress responses or behaviour within macrophages.

GFP and its molecular cousins (Shaner *et al.*, 2005) offer many advantages over dye labelling previously used to track *Cryptococcus in vivo* and *in vitro* (Charlier *et al.*, 2009, Chretien *et al.*, 2002, Santangelo *et al.*, 2004, Shi *et al.*). Such dyes (for example fluorescein isothiocyanate) are significantly phototoxic in comparison to GFP, a major impediment to live imaging. GFP is stably expressed and is not diluted by proliferation, making long term study *in vivo* a possibility. In addition, multi-colour expression systems have been established that could be easily adapted to allow the tracking of many members of an infective population simultaneously (Livet *et al.*, 2007).

The interaction with macrophages plays a key role in the outcome of cryptococcal infections. After phagocytosis, *Cryptococcus* manipulates host macrophages to establish itself as an intracellular parasite that can survive and proliferate within the macrophage phagolysosome (Feldmesser *et al.*, 2000). This intracellular niche might help to explain how *Cryptococcus* stays latent within infected individuals and also how the yeast disseminates within the host. Phagocytosis, intracellular proliferation and the ability to exit macrophages in a non-lytic manner (expulsion) are important parameters in understanding *Cryptococcus*-macrophage interactions (Ma *et al.*, 2006, Ma *et al.*, 2009a, Voelz *et al.*, 2009, Goldman *et al.*, 2001, Idnurm *et al.*, 2005, Hu *et al.,* Alvarez *et al.*, 2009, Alvarez *et al.*, 2006, Alvarez *et al.*, 2007, Alvarez *et al.*, 2008, Geunes-Boyer *et al.*, 2009, Oliveira *et al.,* Goldman *et al.*, 2000, Bobak *et al.*, 1988, Bolanos *et al.*, 1989, Brummer *et al.*, 1994, Bulmer *et al.*, 1967, Bulmer *et al.*, 1975, Cross *et al.*, 1997, Del Poeta, 2004, Diamond *et al.*, 1973a, Griffin, 1981, Kozel *et al.*, 1988, Levitz *et al.*, 1997a, Luberto *et al.*, 2003, Miller *et al.*, 1991, Mitchell *et al.*, 1972, Monari *et al.*, 2003). In particular, the ability to

proliferate within these host cells is an important pathogenesis feature as it correlates with *in vivo* virulence data from mice (Ma *et al.*, 2009a). However, to date the analysis of intracellular proliferation and yeast uptake by phagocytes has required time consuming methods, thus preventing high throughput screening or related experimental approaches. The data presented here describe GFP-positive derivatives of widely used *Cryptococcus* strains coupled with a flow cytometry approach that enables efficient and high-throughput analysis of virulence parameters in the macrophage model system. Flow cytometry allows the absolute analytical separation of infected macrophages and therefore this population can be separately assessed for immune regulatory changes. Furthermore this methodology potentially permits high throughput examination of drugs and antifungal components from both new and existing libraries, and, critically, the ability to analyse within the host macrophage environment.

Furthermore, it will also allow for assessment of cryptococcal interaction with other model systems. Some cell lines such as HD11 chicken macrophages show only very low cryptococcal uptake (S.A. Johnston, personal communication). However, as pigeons have been described as a carrier of *Cryptococcus* and pigeon guano as an infection source (Ellis *et al.*, 1990a, Emmons, 1960), a deeper understanding of how the yeast acts within this environment might help to develop prophylactic measures to prevent infections. The 'Trojan Horse' model for dissemination implicates macrophages as vehicle for cryptococcal crossing of the epithelial layer of the blood-brain barrier. GFP expressing *Cryptococcus* in combination with a secondary stain (e.g. red fluorescent tagged macrophages) might be an easy tool to trace yeast cells within the host and during passage of the blood-brain barrier. Similarly, the GFP-positive yeast could easily be followed in transparent model systems such as the zebra fish or amoeba.

In summary, a reliable tool for rapid and simple quantification of cryptococcal macrophage parasitism is reported, which can easily be transferred to other *in vivo* and *in vitro* model systems.

CHAPTER 5

THE VANCOUVER ISLAND OUTBREAK (VIO) AND MITOCHONDRIAL INVOLVEMENT IN MACROPHAGE PARASITISM

Parts of this chapter have been published:

Byrnes, E. J. 3rd, W. Li, Y. Lewit, H. Ma, K. Voelz, P. Ren, D. A. Carter, V. Chaturvedi, R. J. Bildfell, R. C. May and J. Heitman. 2010. Emergence and pathogenicity of highly virulent Cryptococcus gattii genotypes in the northwest United States. PLoS Pathog. **6:** e1000850. (Byrnes *et al.*, 2010)

In 1999, an ongoing and spreading outbreak of cryptococcosis in healthy individuals caused by unusual *C. gattii* strains of the genotype VGIIa started on Vancouver Island, Canada (Kidd *et al.*, 2004). To date, deciphering the molecular mechanisms underlying this hypervirulence has still proven to be a scientific challenge. Recent advances correlated an enhanced ability of Vancouver Island Outbreak (VIO) isolates to proliferate within macrophages with virulence in mice (Ma *et al.*, 2009a), suggesting that the increased virulence of the VIO population might result from a greater capability to parasite macrophages. The search for candidate genes influencing this proliferative capacity by whole-genome microarray analysis identified an unexpected role of mitochondrial genes and tubular mitochondrial morphology in regulating macrophage parasitism by VIO isolates (Ma *et al.*, 2009a).

The following sections try to further understand how these VIO *C. gattii* strains have acquired a hypervirulent phenotype that causes disease in immunocompetent individuals. It focuses on the role of mitochondria in adaptation to the intracellular environment within macrophages and examines the effect of different host cell stresses on the morphology of yeast mitochondria and the behavior of cryptococcal mitochondria within host cells over time. In addition, available mitochondrial genomes are studied and the first steps towards a comparative mitochondrial genome analysis undertaken.

5.1 INCREASED IPR AND TUBULAR MITOCHONDRIAL MORPHOLOGY AS GENERAL CHARACTERISTICS OF HYPERVIRULENCE IN VGII SUBGROUPS

The original outbreak on Vancouver Island has predominantly been caused by *C. gattii* strains of the VGII subtype a (Kidd *et al.*, 2004). However, the genotype VGIIc has recently emerged as another hypervirulent cluster causing an outbreak in Oregon, USA (Byrnes *et al.*, 2009c). The outbreak lineages VGIIa and VGIIc were evaluated against the non-outbreak subgroup VGIIb in regard to their proliferative potential in macrophages and mitochondrial morphology after passage through macrophages. IPR data for eight VGIIc, 20 VGIIa and three VGIIb isolates were obtained from a previous study (Ma, 2009, Ma *et al.*, 2009a) and median values for each genotype compared. The median IPR value of VGIIc is statistically similar to the median VGIIa IPR value (P = 0.862), however, significantly different from the median IPR value of VGIIb (P = 0.024) (Figure 29 A). High IPR values in VGIIa isolates correlate with the ability to form highly tubular mitochondria after encounter of the intracellular conditions in macrophages (Ma *et al.*, 2009a). Four VGIIc isolates (EJB12, EJB18, EJB52 and A6M-R38) and two environmental control isolates (CBS8684 and CBS7750) were explored in regard to their mitochondrial morphology after macrophage exposure in this context. Three of the VGIIc isolates showed significantly higher percentages of tubular mitochondria after passage through macrophages than the environmental control strains whilst maintaining low level of tubular mitochondria after incubation in macrophage-free culture medium (DMEM) (Figure 29 B). EJB52 seemed to be an exception and did not follow the trend of increased tubular mitochondria morphology. However, inspection of the IPR value revealed this isolate as an outlier with a low IPR value of 0.97. A subsequent regression analysis of IPR versus percentage of cells with tubular mitochondria showed a significant correlation between the two parameters with an R^2-value of 0.85 and F-value of 22.686 (P = 0.009) (Figure 29 C).

Previous research has shown high IPR values and high percentages of tubular mitochondria after macrophage passage as characteristics of the VGIIa genotype (Ma *et al.*, 2009a). A similar pattern has now been described for a second hypervirulent VGII subgroup VGIIc. Similar to the VGIIa genotype, the VGIIc subgroup shows a significantly enhanced ability to proliferate within macrophages and an increased proportion of tubular mitochondria after exposure to macrophages. Taken together, both outbreak genotypes VGIIa and VGIIc seem to be phenotypically alike and potentially share common virulence attributes that enable more efficient adaptation to the intracellular niche within macrophages. Furthermore, this indicates that similar molecular mechanisms regulate the virulence phenotype. Mitochondria seem to play an important role in this context; however, the exact role remains to be determined.

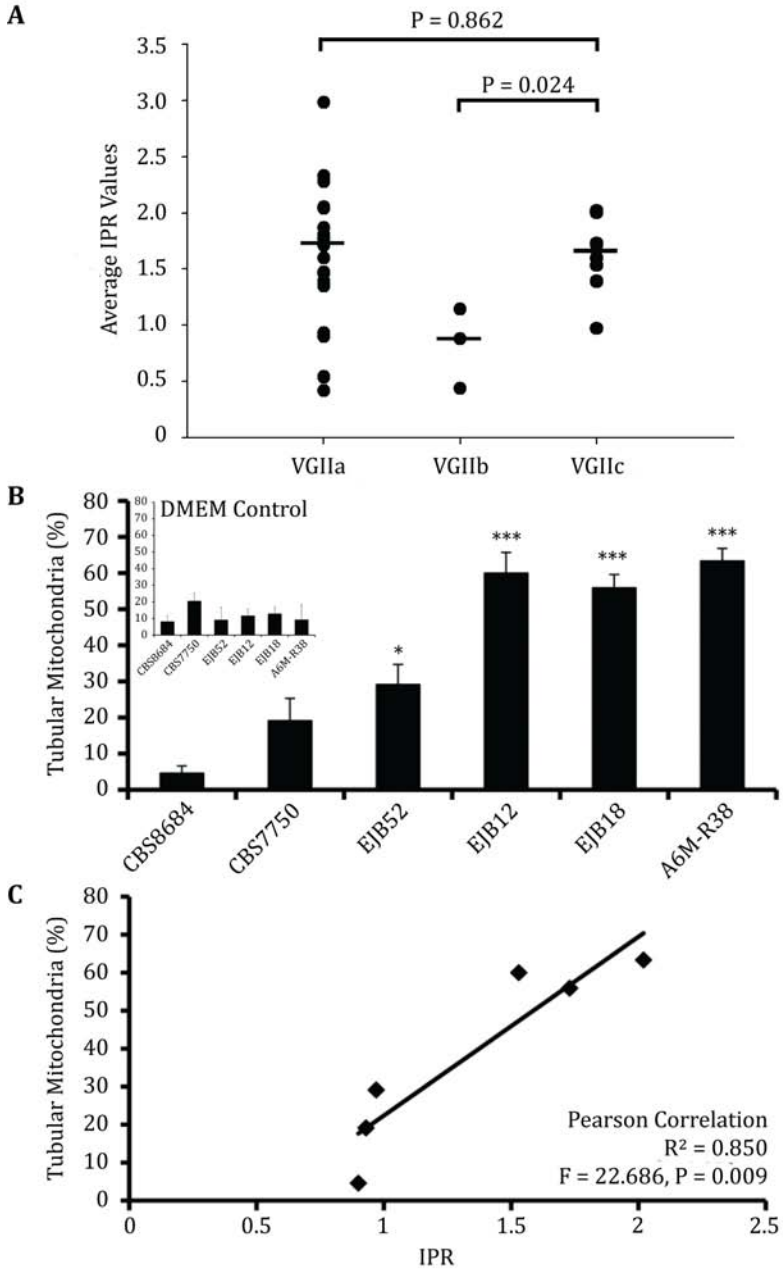

Figure 29: Increased IPR and tubular mitochondria morphology as general characteristics of hypervirulence in VGII subgroups. (A) Median IPR values of each population were compared with the non-parametric Mann-Whitney U-test and values of $p < 0.025$, after controlling for multiplicity, and were accepted as statistically significant (http://elegans.swmed.edu/~leon/stats/utest.cgi). IPR rates for VGII are similar to VGIIa IPR data, however, statistically significantly different from VGIIb IPR rates. (B) Similar to VGIIa isolates, VGIIc isolates form highly tubular mitochondria following encounter of the intracellular niche within macrophages. The data are presented as the mean of at least three individual experiments ± 2 x standard error of the mean. The means were tested for statistical significance using Student's T-test assuming equal variances. Statistically significant differences compared to the control are indicated by asterisks (* $P < 0.05$, ** $P \leq 0.01$, *** $P \leq 0.001$). (C) As shown before for the VGIIa subgroup, VGIIc IPR values correlate with the percentage of tubular mitochondria due to macrophage exposure.

5.2 TEMPORAL MITOCHONDRIAL MORPHOLOGY IN VIO AND NON-VIO STRAINS UPON EXPOSURE TO THE INTRACELLULAR NICHE

The ability to proliferate within macrophages correlates in *C. gattii* isolates with the formation of tubular mitochondria: isolates with high IPR values show a high percentage, isolates with low IPR a low proportion of tubular mitochondrial after exposure to macrophages (Ma *et al.*, 2009a, Byrnes *et al.*, 2010). However, assessment of mitochondrial morphology has only been performed at 24 hours post infection, usually the time point of maximal intracellular yeast cell number. This approach, however, does not offer insight into whether mitochondria in strains with high proliferative capacity tubularise faster than mitochondria in strains with low IPR or if the latter generally lacks the ability for formation of tubular mitochondria. To address this question, the VIO strain CDCF2932 and the environmental isolate CBS8684 were chosen as high and low proliferators, respectively, and mitochondrial morphology within macrophages monitored after 0, 2, 6, 12, 18 and 24 hours post infection. The VIO strain CDCF2932 shows the first signs of tubularisation after two hours within the intracellular environment and continues to increase the percentage of tubular mitochondria up to 24 hours. In contrast, the proportion of tubular mitochondria stays consistently low over time in the environmental isolate (Figure 30 A). It seems likely that globular morphology is the precursor for formation of tubular mitochondria. Interestingly, the amount of mitochondria with globular morphology also seems to follow a certain pattern: whereas the VIO strain already shows a high percentage after two hours of infection that drops with onset of tubularisation, the control strain initially shows low levels of globular mitochondria that slowly increase over time but don't fully tubularise in the non-VIO strain (Figure 30 B).

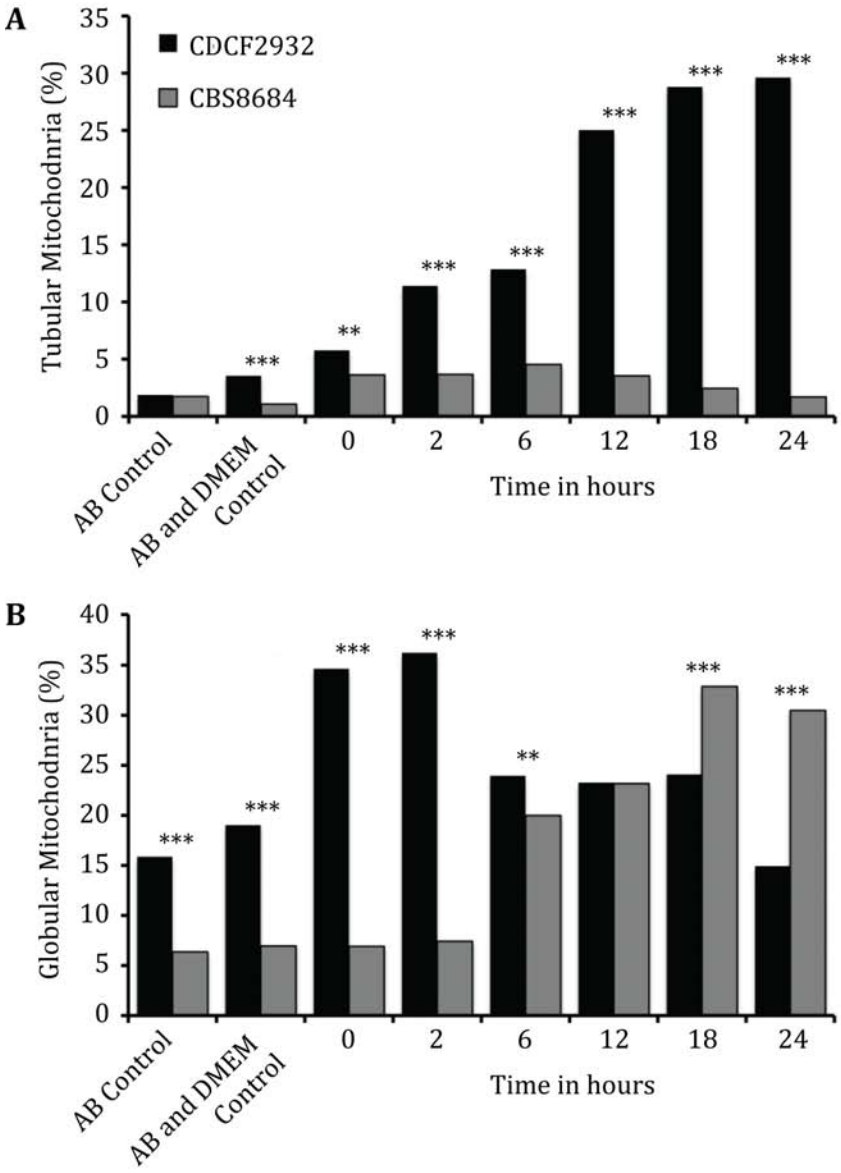

Figure 30: Temporal pattern of yeast mitochondrial morphology. Mitochondrial morphologies were analysed at different time points after exposure to the intracellular environment of macrophages. J774 macrophages were infected with either *C. gattii* strain CDCF2932 or CBS8684 for 2 hr and then further incubated. Samples were taken at 0, 2, 6, 12, 18 and 24 hr, mitochondria stained and cells analysed for the proportions of tubular and globular mitochondria. (A) The VIO strain CDCF2932 shows first signs of tubularisation after two hours within the intracellular environment and continues to increase the percentage of tubular mitochondria up to 24 hours. In contrast, the proportion of tubular mitochondria stays consistently low over time in the environmental isolate CBS8684. (B) The amount of mitochondria with globular morphology also seems to follow a certain pattern: whereas the VIO strain already shows a high percentage after two hours of infection that drops with onset of tubularisation, the control strain initially shows low levels of globular mitochondria that slowly increase over time. Data were obtained from at least three individual experimental repeats and analysed for statistically significant differences using χ^2 tests. Statistically significant differences are indicated by asterisks (** $P \leq 0.01$, *** $P \leq 0.001$). AB – antibody.

5.3 MITOCHONDRIAL FUNCTIONS AND THE SEARCH FOR THE MOLECULAR MECHANISM UNDERLYING HYPERVIRULENCE

Mitochondria seem to be the key to understanding the enhanced ability of VGIIa and VGIIc strains to parasitise macrophages and in the long run to understand the hypervirulence phenotypes of these subgroups. Mitochondria fulfill a variety of essential cell functions: oxidative respiration, resistance to oxidative stress (Grant *et al.*, 1997), certain heme synthesis reactions (Oh-hama, 1997) and sterol synthesis (Rossier, 2006). To assess potential mechanisms underlying hypervirulence it is necessary to understand the influence of these features in the adaptation to the intracellular environment. The following section therefore investigates the influence of hypoxic conditions on macrophage-*Cryptococcus* interaction and tests the stress susceptibility of VIO strains.

5.3.1 MACROPHAGE-*CRYPTOCOCCUS* INTERACTION UNDER HYPOXIC CONDITIONS

Most tissue culture is done at atmospheric oxygen concentration. However, the oxygen concentrations within the human body differ significantly, ranging from 21 % in the lungs, 12 % in the blood stream and down to 3-6 % in tissues and the brain. *Cryptococcus* encounters all these different oxygen concentrations within a host and has to adapt to them in order to colonize successfully. The research presented so far indicates that mitochondria play an important role in enabling infections. Hence, the interaction between macrophages and the yeast was analysed under hypoxic conditions (3 % O_2 or following treatment with the hypoxia mimicking agent cobalt chloride (Lee *et al.*, 2007)). The macrophage ability to internalize *Cryptococcus* was not significantly changed when cultured at 3 % O_2 but significantly increased upon treatment with 0.1 mM $CoCl_2$ (Figure 31 A). *Cryptococcus* was not able to proliferate in macrophages when cultured at 3 % oxygen or treated with 0.1 mM $CoCl_2$ (Figure 31 B). Extracellular proliferation and yeast control growth under hypoxic conditions were also reduced. However, *Cryptococcus* was still able to proliferate at low oxygen

concentrations when grown in the absence of macrophages (Figure 31 C & D). Macrophage growth was similar to the control in the first 24 hours but the relative macrophage number was reduced afterwards (Figure 31 E). Thus, there seems to be a clear inhibitory effect of hypoxia on intracellular yeast proliferation and, in fact, *Cryptococcus* does not establish within the intracellular niche. However, this effect might be slightly overestimated due to generally reduced yeast cell growth within hypoxic conditions. Furthermore, *Cryptococcus* leaves the intracellular niche significantly more often, as shown by an increased number of expulsion events under hypoxic conditions (Figure 31 F).

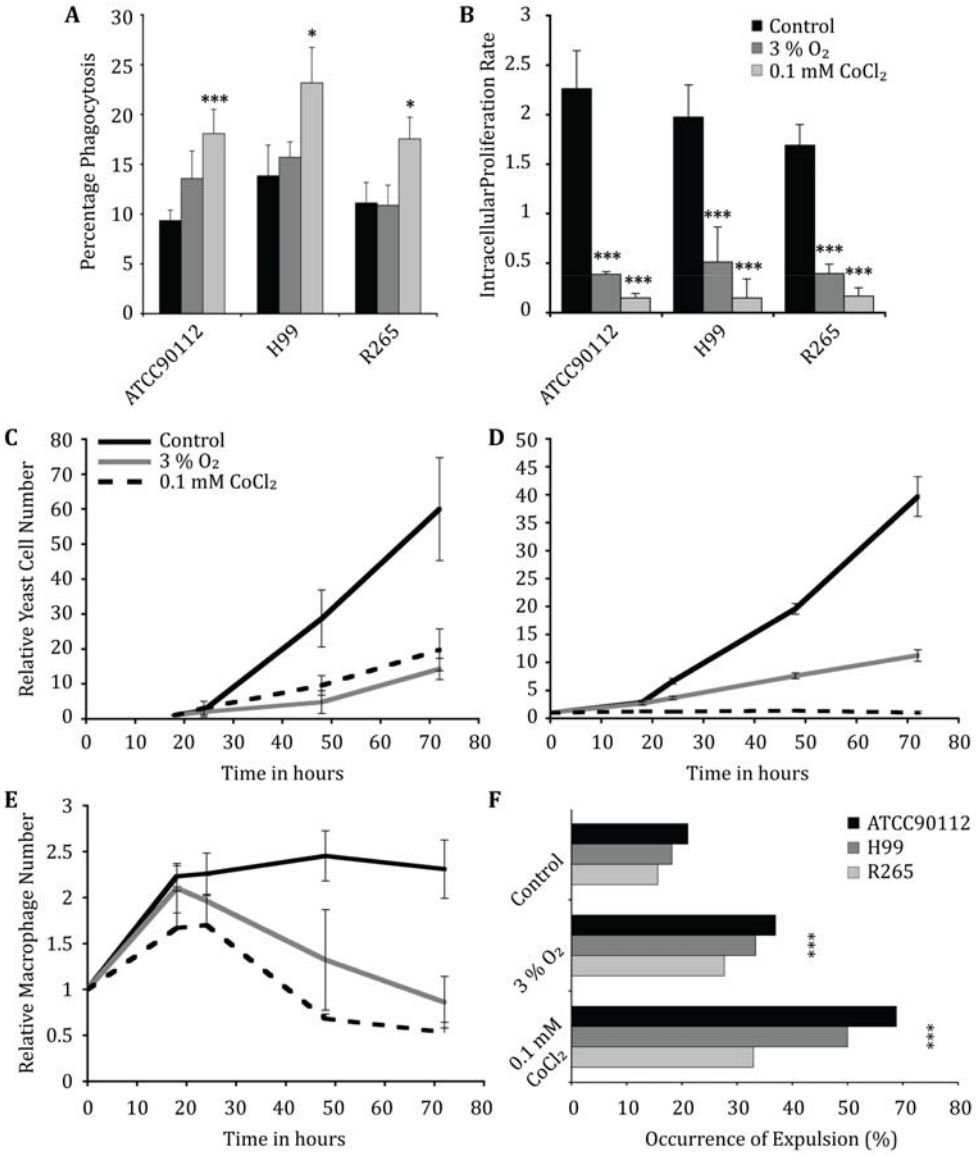

Figure 31: Macrophage-*Cryptococcus* interaction under hypoxic conditions. The effect of hypoxia on yeast uptake, intracellular and extracellular proliferation, yeast growth, macrophage growth and yeast expulsion was analysed. J774 macrophages infected with C. neoformans strains ATCC90112 or H99 or C. gattii strain R265, yeast control and macrophages alone were incubated at atmospheric O2 (control), 3 % O2 or 0.1 mM CoCl2. Phagocytosis was analysed after 2 hr infection as proportion of macrophages with internalized cryptococci. The number of intra- and extracellular, yeast control and macrophages were counted at 0, 18, 24, 48 and 72 hr and is expressed relative to the number at T=0. Expulsion events were monitored over 20 hr by live-cell imaging. (A) Phagocytosis of *Cryptococcus* is not altered by culture in 3 % O2 but is significantly enhanced by treatment with 0.1 mM CoCl2. (B) *Cryptococcus* fails to proliferate within macrophages under hypoxic conditions. (C) Extracellular proliferation rate is decrease (ATCC90112 shown as example). (D) The yeast control also shows reduced growth (ATCC90112 shown as example). (E) Macrophage growth was not altered in the first 24 hr, macrophages died quicker afterwards. (F) Occurrence of expulsion is significantly increased under hypoxic conditions. Data were obtained from at least three individual experiments and are presented as means with 2 x standard error of the mean. Statistically significant differences are indicated by asterisks (* $p < 0.05$, *** $p < 0.001$).

5.3.2 SUSCEPTIBILITY PHENOTYPES OF *C. GATTII* IN VIO AND NON-VIO STRAINS

Important features of mitochondria are resistance mechanisms to withstand damage caused by the host attack with oxidative and nitrosative stress, stresses that may otherwise severely limit cryptococcal growth within the macrophage phagosome. To explore the possibility that mitochondrial tubularisation provides cryptococci with an improved ability to handle different stress conditions, four *C. gattii* strains with high IPR and four *C. gattii* strains with low IPR (Table 8) (Ma *et al.*, 2009a) were selected and analysed for growth under hypoxia ($CoCl_2$) (Figure 33 A), oxidative stress (H_2O_2) (Figure 33 B), nitrosative stress ($NaNO_2$) (Figure 32 C) und UV stress (Figure 32 G) as well as cell wall stress (SDS and NaCl) (Figure 32 E & F). The number of colony forming units negatively correlated with the severity of stress applied for all conditions except $NaNO_2$. Nitrosative stress did not seem to influence yeast growth although the same conditions dramatically inhibit growth of a control organism, the *E. coli* strain DH5α (Figure 32 D). However, although all of the stresses tested represent potential growth-limiting conditions during an intracellular infection, no trend towards an increased resistance of high IPR strains to any of the stress conditions was observed. Statistical analysis by ANOVA detected significant differences in the data sets for SDS and UV treatment. However, closer examination showed that this was due to only one strain acting as outlier. This indicates that an increased stress tolerance with enhanced ability to growth is not underlying the hypervirulence in highly proliferative *C. gattii* strains.

Table 8: *C. gattii* strains chosen for phenotypic analysis. Analysis included different host and environmental stress conditions. The selection was made to cover a range of IPR values.

Strain	IPR	Source/Feature
CBS7229	0.56	Meningitis, China
CBS8684	0.90	Wasp nest. Uruguay
CBS7750	0.93	*E. camaldulensis*, USA
CBS1930	1.14	Sick goat, Aruba
R265	1.74	Clinical isolate, British Columbia
CDCR271	2.04	Clinical isolate, British Columbia
ENV152	2.28	Alder tree, Vancouver Island
CDCF2932	2.98	Clinical isolate, British Columbia

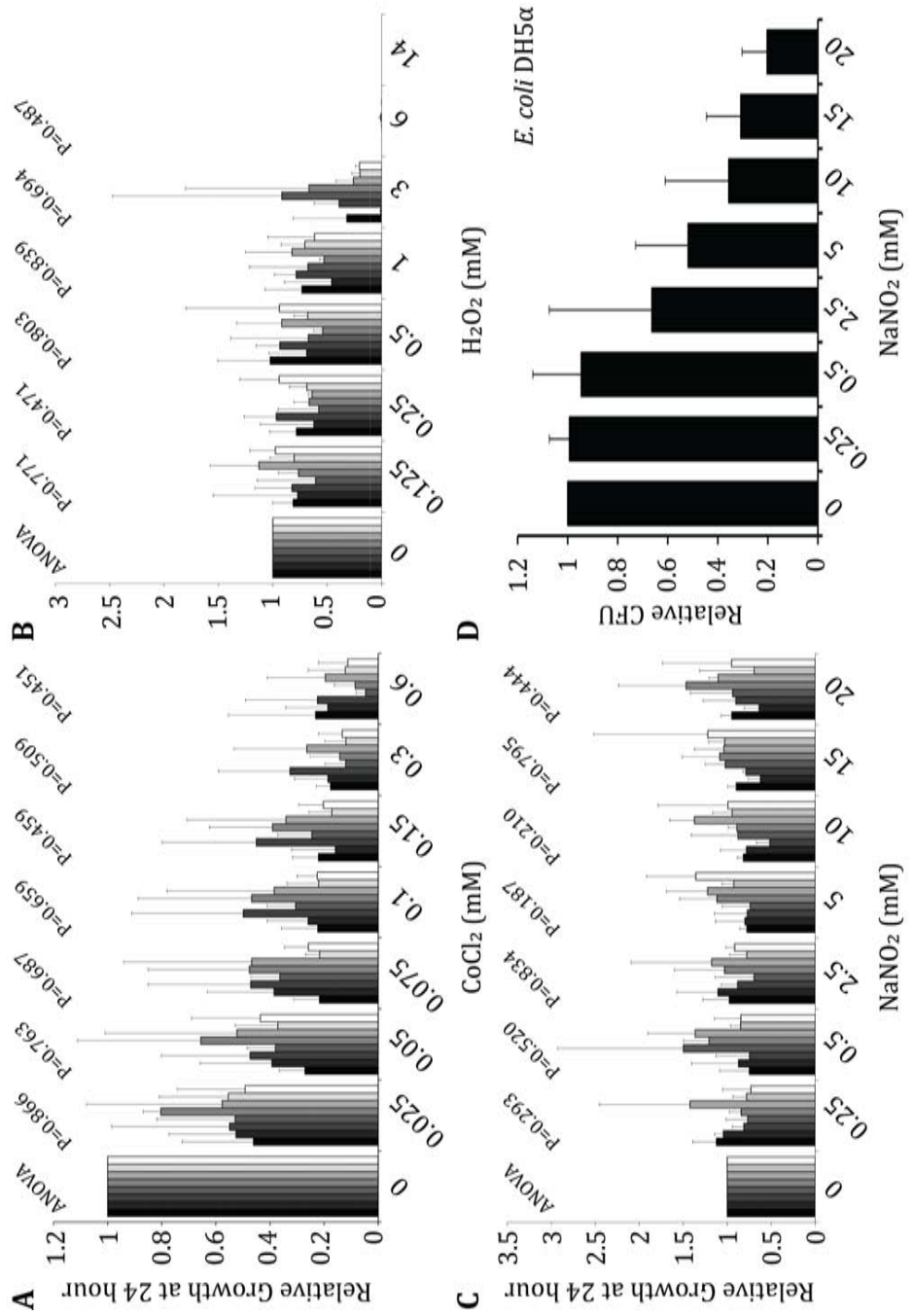
A
Relative Growth at 24 hour
ANOVA
p=0.866
p=0.763
p=0.687
p=0.659
p=0.459
p=0.509
p=0.451
0
0.025
0.05
0.075
0.1
0.15
0.3
0.6
CoCl2 (mM)
B
ANOVA
p=0.771
p=0.471
p=0.803
p=0.839
p=0.694
p=0.487
0
0.125
0.25
0.5
1
3
6
14
C
Relative Growth at 24 hour
ANOVA
p=0.293
p=0.520
p=0.834
p=0.187
p=0.210
p=0.795
p=0.444
0
0.25
0.5
2.5
5
10
15
20
NaNO2 (mM)
D
E. coli DH5α
Relative CFU
0
0.25
0.5
2.5
5
10
15
20
NaNO2 (mM)
H2O2 (mM)

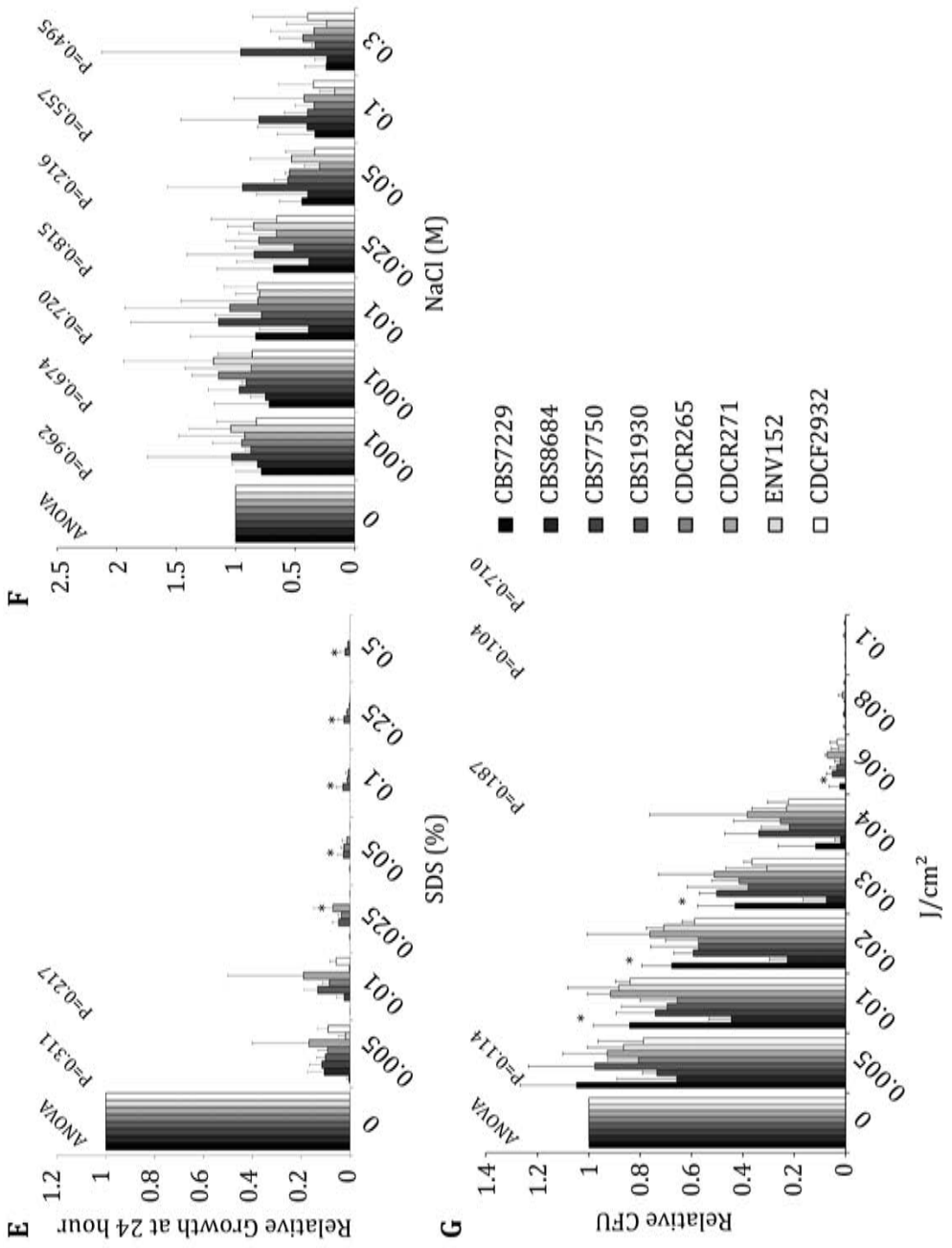

Figure 32: Stress susceptibility of *C. gattii* strains. Four strains with low (columns 1-4) and four strains with high (column 5-8) IPR values were assessed for growth after 24 hours after exposure to different stress conditions: (A) hypoxia mimicking agent $CoCl_2$, (B) H_2O_2 as oxidative stress, (C) $NaNO_2$ as nitrosative stress inducer with (D) a *E. coli* DH5α control, (E) SDS and (F) NaCl as cell wall stresses and (G) UV stress. CFU were counted after 0 and 24 hours treatment and the numbers analysed relative to time point 0 and untreated control. Data are obtained from at least three individual experimental repeats and presented as mean with 2 x standard error of the mean. The means were tested for statistical significant differences using Tukey HSD test assuming equal variances. Statistically significant differences are indicated by asterisks (* $p < 0.05$).

5.4 MITOCHONDRIAL MORPHOLOGY IN THE RESPONSE TO HOST AND ENVIRONMENTAL STRESS CONDITIONS

The analysis of mitochondrial functions in *Cryptococcus* and stress susceptibly phenotypes in *C. gattii* VIO and non-VIO strains did not show any significant trends for either subgroup that might have helped to explain the increased ability to grow intracellularly in hypervirulent genotypes. However, as earlier data indicated an involvement of tubular mitochondria in hypervirulence (Byrnes *et al.*, 2010, Ma *et al.*, 2009a), the response of cryptococcal mitochondria towards individual host and environmental stress conditions was analysed in an attempt to narrow down potential triggers responsible for tubularisation. Data from the stress treatments was used to determine stress doses of 50 % growth inhibition. These doses were then used to treat the selected cryptococcal strains and yeast were isolated for assessment of mitochondrial morphology. Interestingly, the formation of tubular mitochondria correlated positively with IPR values under several 'host' stress situations (1 mM H_2O_2, 5 mM $NaNO_2$, 3 % O_2 and 0.1 mM $CoCl_2$) and during exposure to UV. In contrast, however, IPR values correlate negatively with mitochondrial tubularisation following cell wall or osmotic stresses (0.005 % SDS, 0.05 M NaCl) (Figure 33 A). To compare VIO strains with non-VIO strains, the data for each subgroup were pooled and statistically analysed using a χ^2-test. This approach revealed a significantly higher percentage of tubular mitochondria in VIO strains after macrophage passage and under oxidative, nitrosative, hypoxic and UV stress. On the contrary, mitochondria of non-VIO strains tubularised more frequently than mitochondria of VIO strains under cell wall stress (Figure 33 B).

Taken together, VIO strains appear to respond better to certain stresses. However, this advantage seems to be at the cost to form tubular mitochondria under cell wall stress. This adaptation is somehow connected with mitochondria and in particular with the formation of tubular mitochondria.

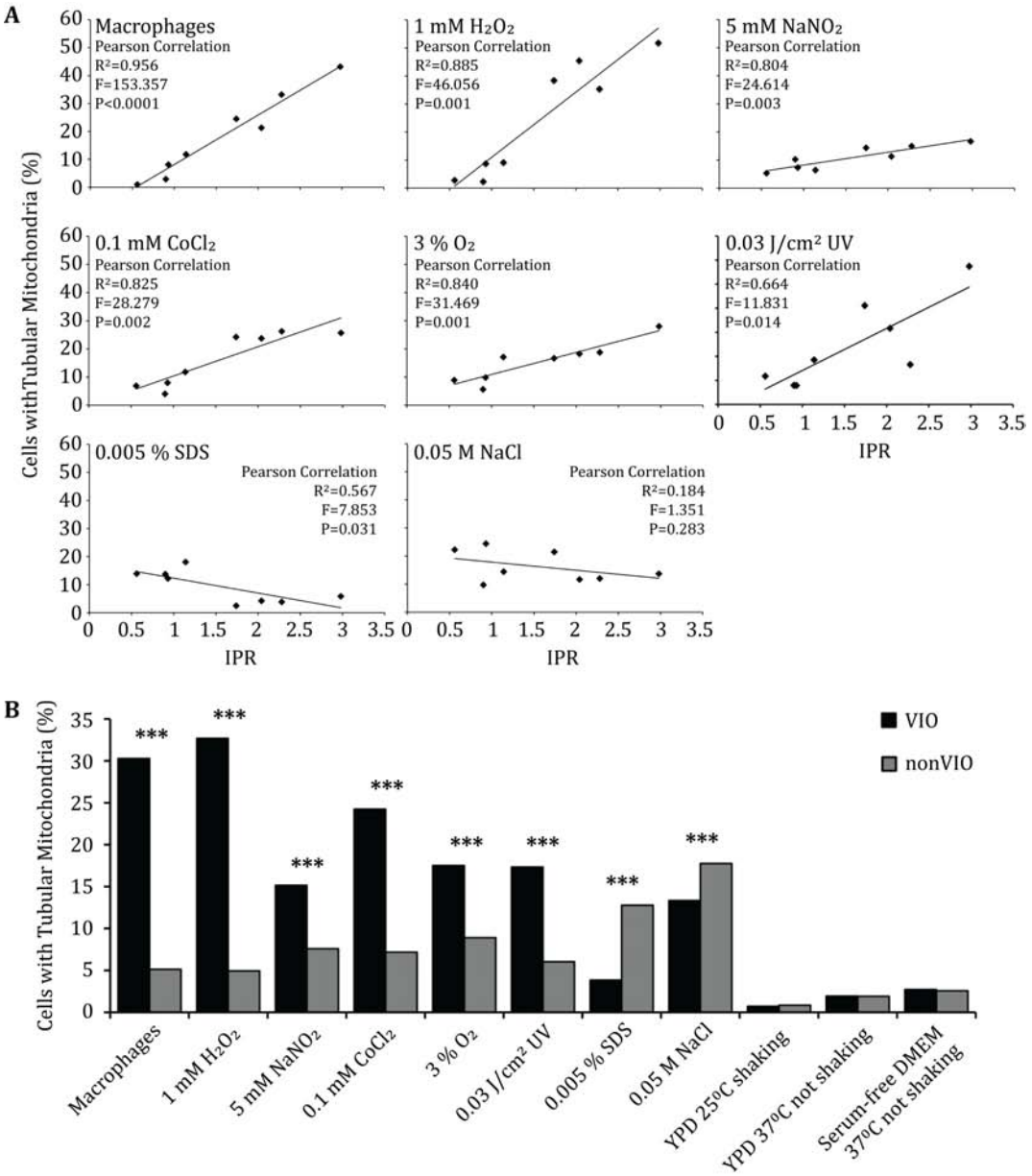

Figure 33: Cryptococcal mitochondria morphology after stress treatment. To analyse the effect of host and environmental stresses on the morphology of cryptococcal mitochondria in VIO and non-VIO strains, yeast were passaged through macrophages or incubated with 1 mM H_2O_2, 5mM $NaNO_2$, 0.1 mM $CoCl_2$, 3 % O_2, 0.03 J/cm² UV, 0.005 % SDS or 0.05 M NaCl for 24 hours and cells then counted for the number of yeast with tubular mitochondria. (A) Formation of tubular mitochondria correlated positively with IPR values under host stress situations and UV stress but correlated negatively with IPR values under cell wall stresses. (B) To compare VIO strains versus non-VIO strains, the data for each subgroup were combined and statistically analysed using a χ^2-test. This approach revealed a significantly higher percentage of tubular mitochondria in VIO strains after macrophage passage and under oxidative, nitrosative, hypoxic and UV stress. On the contrary, mitochondria of non-VIO strains tubularised more frequently than mitochondria of VIO strains under cell wall stress. Data were obtained from at least three individual experiments and are presented as accumulated data. Statistically significance was tested using χ^2 tests and significant differences are indicated by arrows (*** $p < 0.0001$).

5.5 GENETIC UNCOUPLING OF TUBULAR MITOCHONDRIAL MORPHOLOGY AND IPR

A previous study analysed the mitochondrial contribution to the hypervirulent phenotype of VIO strains (Ma, 2009). Due to the uniparental inheritance of mitochondria from MATa mating type (Xu *et al.*, 2000), it is possible to explore the role of mitochondrially-encoded control of virulence by replacing mitochondria from a 'good' proliferator (high IPR strain) with mitochondria from a poor (low IPR) proliferator. In this case, good proliferating MATa and α VGII strains were mated with poorly proliferating MATα and a VGIII strains, respectively, to create progenies containing only mitochondria from a good or poor proliferator (Figure 34 A). Both parental strains, and randomly selected F1 progeny, were then analysed for their IPR values (Ma, 2009). Interestingly, possession of mitochondria from a high IPR parent did not result in high IRP values in all offspring suggesting that both the nuclear and the mitochondrial genome are involved in regulating the hypervirulence phenotype. Conversely, however, all offspring containing mitochondria from a parental strain with low IPR subsequently showed low potential to proliferate within macrophages. Thus, a 'high IPR' mitochondrion is necessary, but not sufficient, for enhanced intracellular proliferation (Ma, 2009).

To establish whether the mechanism of virulence in progeny strains was also conserved, offspring from both crosses were tested for their ability to form tubular mitochondria upon exposure to macrophages. In cross 1, in which progeny share a 'low IPR' mitochondrial type, F1 strains showed a significantly lower percentage of tubular mitochondria after macrophage passage than the high proliferating MATα parent R265 (Figure 34 B). Thus, the mitochondrial genetic background from high proliferative strains is essential for increased tubularisation upon encounter of the intracellular niche. The second cross, in which all progeny share a 'high IPR' mitochondrial type, results in a range of IPR values in the F1 strains, from 0.57 to 1.78 (Ma, 2009). However, in the progeny of this cross, the link between IPR and mitochondrial tubularisation appears to have been broken. There is no correlation between these two parameters for the strains tested, and most F1 strains show an

increased proportion of tubular mitochondria after macrophage passage but also when grown in DMEM (Figure 34 C & D). Taken together, this indicates that the mitochondrial genomic make up is essential for the formation of tubular mitochondria specifically within macrophages but that its interaction with the nuclear genomic background also plays an important role. Thus, in the second cross it appears as if the mitochondrial morphology has been uncoupled from intracellular proliferation, suggesting that the formation of tubular mitochondria might be negatively regulated by nuclear encoded genes and this link was lost following the change into a non-hypervirulent VGIII background and hence from the inhibitory function of a nuclear regulated pathway normally preventing tubularisation.

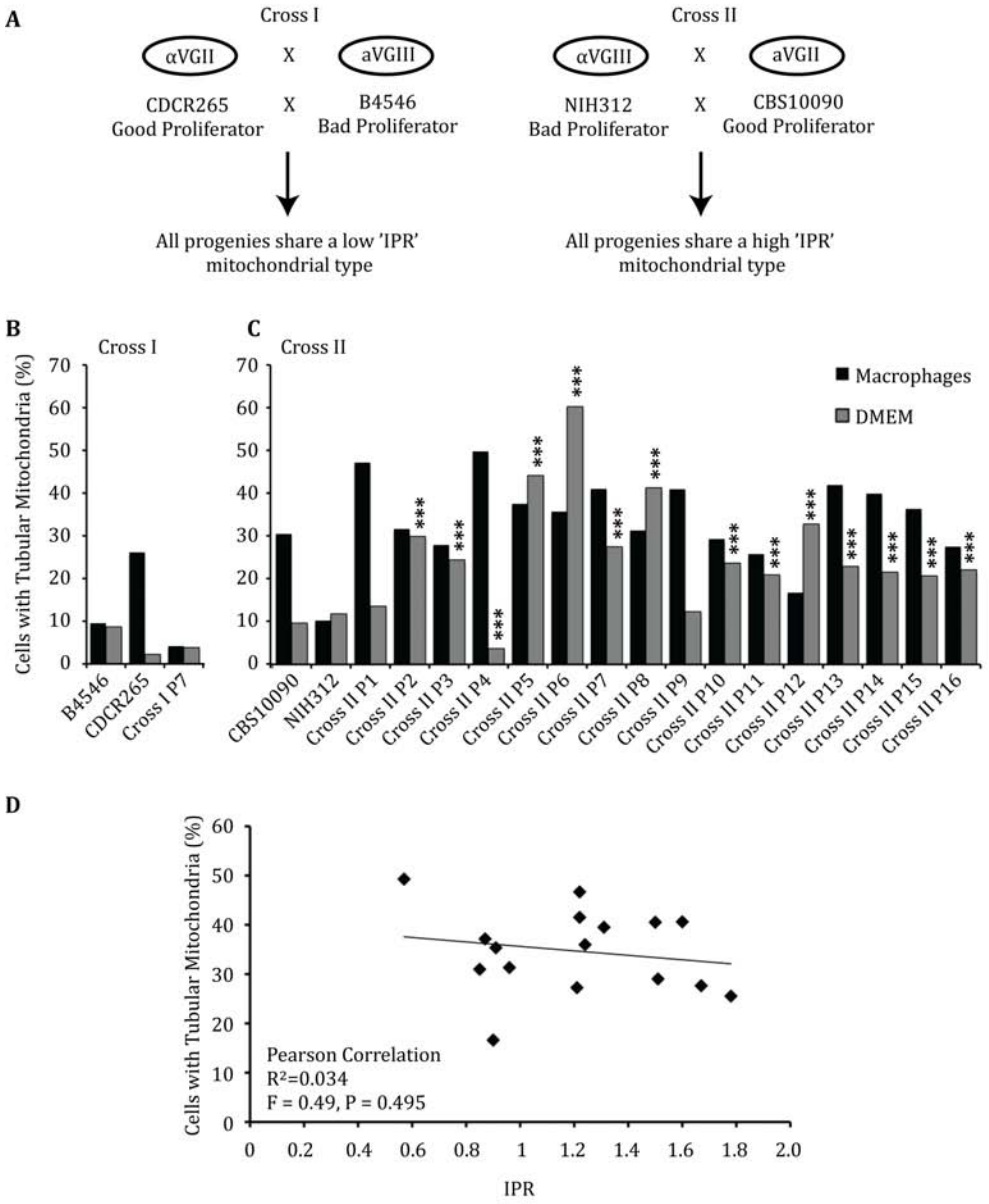

Figure 34: Genetic uncoupling of tubular mitochondria morphology and IPR. (A) Offspring from crosses that replaced mitochondria from a good proliferator into a poor proliferator nuclear background and vice versa were obtained (Ma, 2009). Yeast were either grown in serum-free DMEM (macrophage growth media) or used to infect macrophages. After 24 hours, yeast cells were harvested and stained for mitochondria and the percentage of cells with tubular mitochondria counted. (B) Formation of tubular mitochondria in offspring from both crosses. Offspring from cross I show low tubularisation both after macrophage passage and after growth in DMEM. However, most offspring from cross II show an increased proportion of tubular mitochondria in the DMEM control condition, indicating uncoupling from a nuclear regulated pathway normally inhibiting tubularisation. Data were obtained from at least three individual experiments and are presented as accumulated data. Statistical significance was tested using χ^2 tests and significant differences in tubularisation after macrophage passage and in DMEM are indicated by arrows (*** $p < 0.0001$). (C) This results in IPR not being correlated with the percentage of tubular mitochondria after macrophage exposure anymore.

5.6 ANALYSIS OF MITOCHONDRIAL GENOMIC FEATURES IN THE SEARCH FOR THE MOLECULAR MECHANISM UNDERLYING HYPERVIRULENCE

Data presented earlier in this thesis provides evidence that mitochondria and, in particular, the ability to form tubular mitochondria upon entry into the intracellular niche are important players in the regulation of hypervirulence in VIO strains. Research described in the next paragraphs will turn the focus to methods to uncover the underlying mechanisms by genomic approaches. It will analyse a set of microarray data and also describe the first steps towards a parallel sequencing strategy for comparative analysis of mitochondrial genomes.

5.6.1 COMPARATIVE ANALYSIS OF MITOCHONDRIAL GENOMES

Currently, seven cryptococcal isolates have been sequenced and the mitochondrial genome sequence of five strains could be obtained from online sources (Broad Institute of MIT and Harvard) or were kindly provided by collaborators (Prof. J. Heitman (Department of Molecular Genetics and Microbiology, Duke University), Prof. T. Boekhout (CBS Fungal Biodiversity Centre, The Netherlands) and Prof. J. Kronstad (Michael Smith Laboratories, The University of British Columbia)). The size of the mitochondrial genomes ranges from 24,919 bp in the *C. neoformans* strain H99 up to 34,790 bp in the *C. gattii* strain R265. The other three isolates *C. neoformans* JEC21, *C. gattii* CDCR272 and *C. gattii* WM276 have mitochondrial genomes of 33,199 bp, 34,642 bp and 34,342 bp size, respectively. Due to large gaps in the sequence, the data for CDCR272 was excluded from further analysis; however, the other four strains were compared for open reading frames and the distribution of introns. With the help of Dr. A. Haines (School of Biosciences, University of Birmingham), the mitochondrial DNA sequences were rotated to enable alignment with the genome alignment visualization software Mauve 2.3.1 (Darling *et al.*, 2010). Using the NCBI's open reading frame (ORF) finder (http://www.ncbi.nlm.nih.gov. /gorf/gorf.html), ORFs encoding 15 different

genes in a conserved order were identified in all four strains (Figure 35 A). A striking difference between strains was found in the number of introns. Introns within the mitochondrial genomes were identified with the online tool RNAweasel (http://megasun.bch.umontreal.ca/RNAweasel). Within the H99 mitochondrial genome, the smallest of the four, only two introns were identified, whereas in the larger mitochondrial genomes up to 16 introns could be detected, all belonging to intron group I (Figure 35 B). Group I introns are self-catalytic introns with maturase and homing endonucleases functions that are particularly abundant in fungal mitochondrial genes (Lang *et al.*, 2007, Saldanha *et al.*, 1993). Within the intronic regions of ORFs encoding cytochrome oxidase subunit 1 and apocytochrome B genes, several internal ORFs potentially encoding so-called homing endonucleases containing a LAGLIDADG motif (Lang *et al.*, 2007, Saldanha *et al.*, 1993) were found. This is particularly interesting, as homing endonuclease have been connected with intron mobility and integration of group I introns relies on precise cleavage of intron-free regions by homing endonucleases and subsequent activation of DNA repair machinery (Lang *et al.*, 2007).

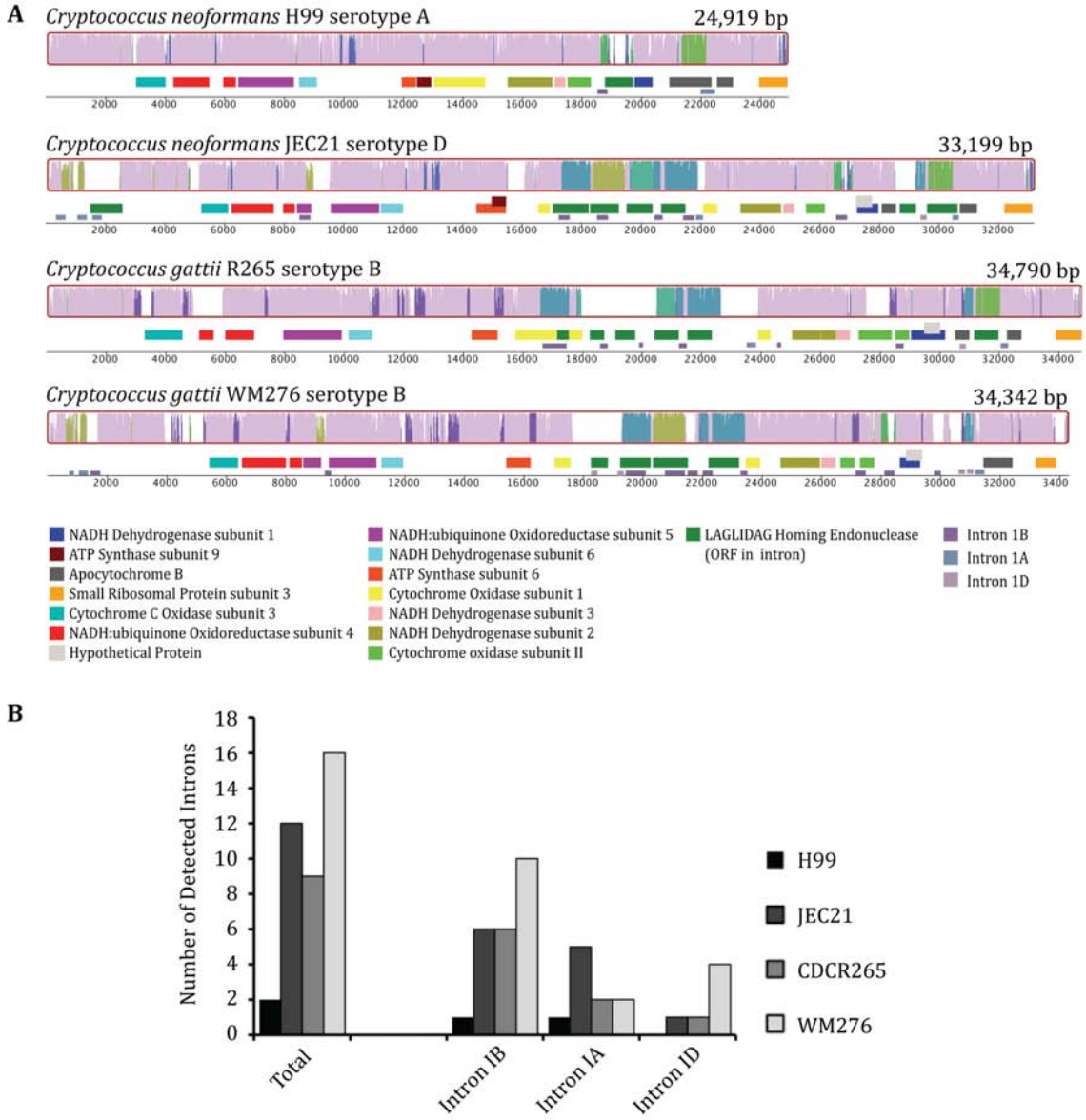

Figure 35: Comparative alignment of cryptococcal mitochondrial genome sequences. (A) Four cryptococcal mitochondrial genome sequences from *C. neoformans* strains H99 and JEC21 and *C. gattii* strains R265 and WN276 were aligned using the alignment visualization software Mauve 2.3.1 and annotated using the NCBI's ORF finder. All four strains showed the same gene order. Similar colours in the alignment represent sequence similarity between strains. (B) Mitochondrial genomes were also analysed for introns using the intron search tool RNAweasel. Only a small number of introns were found in H99 mitochondrial DNA, the smallest of the mitochondrial genomes, whereas the bigger genomes contain significantly more introns. All introns belong to group I.

5.6.2 MITOCHONDRIAL GENE EXPRESSION

Phenotypic analysis of VIO strains has repeatedly shown an important role of mitochondria and tubular mitochondrial morphology in enhanced intracellular proliferation. However, the underlying mechanisms are still unknown. In a recent comparative whole-genome microarray study RNA from *C. gattii* strains with IPR values from 0.44 and 2.33 was isolated after macrophage passage and then individually hybridized against a pooled RNA sample from all strains (Ma, 2009). This analysis identified 1,367 probes with significantly correlation between expression and IPR values. These target loci were evenly distributed across the *C. gattii* R265 nuclear genome; however, the mitochondrial genome was significantly overrepresented despite no increase in DNA copy number (Ma *et al.*, 2009a, Ma, 2009). This prompted a closer examination of the microarray results from mitochondrial probes. The expression data from the mitochondrial probes seem to follow a trend where strains with low IPR values show generally negative expression levels of mitochondrial genes compared to the pooled sample and the expression levels increase with increasing IPR values (Figure 36 A). In fact, when the sum of expression data from all mitochondrial probes were plotted against IPR values, a statistically significant positive correlation was observed (Figure 36 B). However, no specific loci could be established that might regulate hypervirulence.

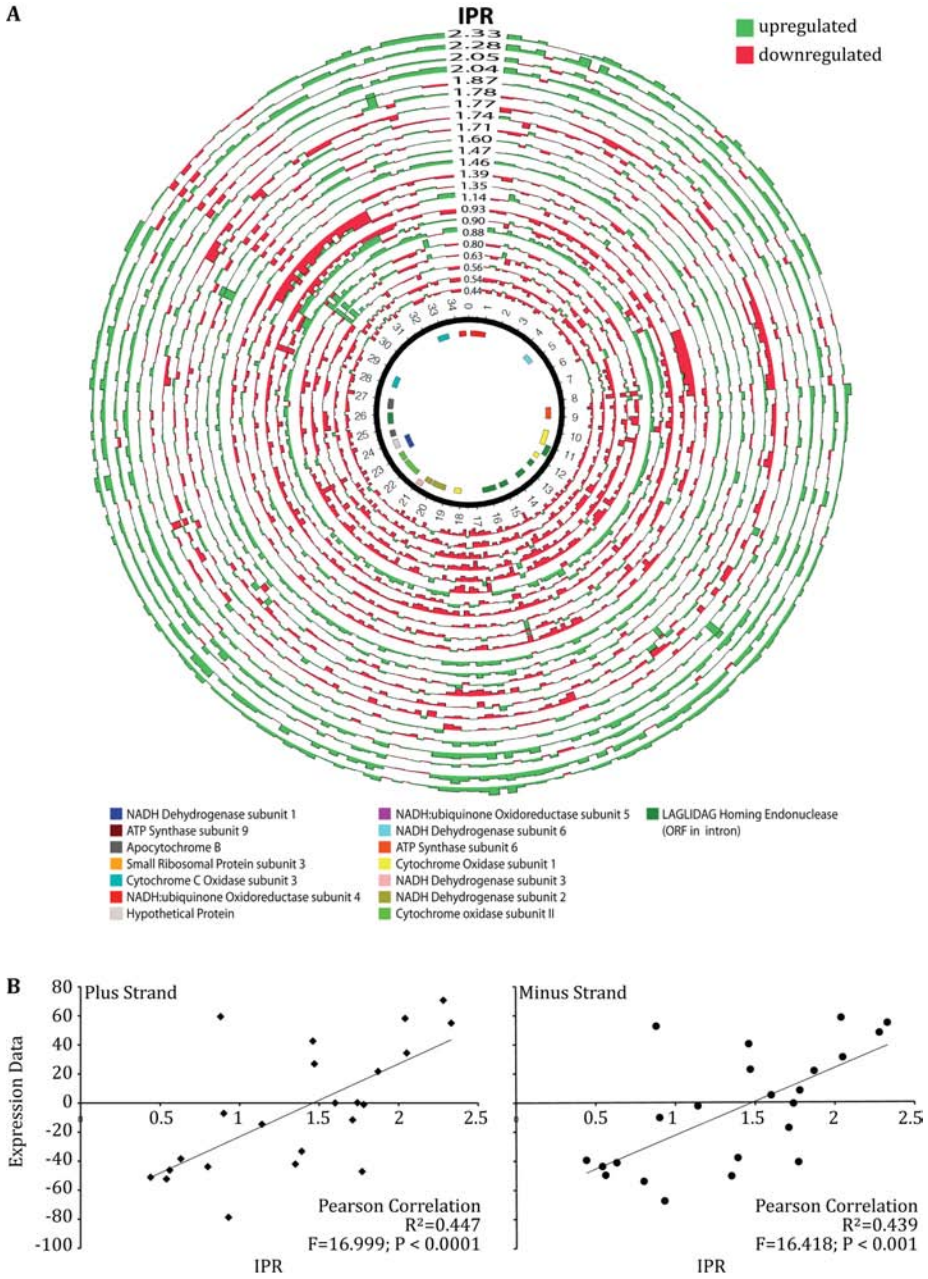

Figure 36: Mitochondrial expression data across a spectrum of IPR values. Microarray data from *C. gattii* strains with IPR values from 0.44 up to 2.33 where analysed. (A) The data of minus and plus DNA strand showed negative expression of mitochondrial genes in low IPR strains and expression levels increase with increase of ability to proliferate intracellularly. Green peaks represent positive expression, red peaks negative expression levels relative to expression level from a pooled RNA sample of all strains. The centre circle represents the annotated R265 genome. The annotation legend can be found underneath the expression diagram. Figure 30 A was created with the program Circos (Krzywinski *et al.*, 2009) and help from Dr. Anthony Haines. (B) When accumulated expression data of each DNA strand from all loci for each strain was plotted versus IPR values, a significant correlation between proliferative potential and overall gene expression was detected.

5.6.3 COMPARATIVE ANALYSIS OF MITOCHODNRIAL *C. GATTII* GENOMES

It is very likely that changes in the genetic make up are directly or indirectly accountable for the increased ability to grow intracellularly in macrophages. Different potential scenarios are imaginable: Firstly, single nucleotide polymorphisms might have enabled the yeast to withstand the harsh environment caused by oxidative and nitrosative stress within macrophages and/or enhanced the functionality of virulence factors. Furthermore, it might be possible that strains from the outbreak lineage have gained additional coding regions and/or that gene duplications have occurred leading to increased virulence. Finally, nucleotide changes within regulatory regions could have increased or decreased expression levels of virulence-related genes resulting in hypervirulence. Genomic comparison of strains from the outbreak lineage and phylogenetic reconstruction of sequences will enable the identification of possible genetic differences that are responsible for changes in mitochondrial functions and thus might be the genetic foundation of hypervirulence

In cooperation with F. Hagen (CBS Fungal Biodiversity Centre, The Netherlands), existing nuclear and mitochondrial MLST datasets, phenotypic and virulence analyses, as well as intracellular proliferation assays, were used to create phylogenetic relationships between strains (Figure 37 A & B). The virulence assays had been performed in two different systems, an intranasal infection model using Balb/c mice (Ma *et al.*, 2009a) and the intracellular proliferation rates (IPR) of *Cryptococcus* cells in a J774 macrophage cell line (Ma *et al.*, 2009a). The three well-known virulence factors of melanin, phospholipase and proteinase production, as well as 19 pathogenicity related enzymes had been tested at 25ºC and 37ºC, as described before (Ma et al., 2009). Neighbour-Joining phylogenetic trees according to the four mitochondrial loci *ATP6*, mtlrRNA, *NAD2* and *NAD4* (3203nt) and the seven nuclear loci *GPD1,* IGS1*, LAC1, MPD1, PLB1, SOD1 and URA5* (4607nt) were reconstructed by F. Hagen using the Pearson correlation coefficient in Bionumerics version 4.61 (Applied Maths, St. Martems-Latem, Belgium) (Meyer *et al.*, 2009, Bovers *et al.*, 2008, Xu *et al.*, 2009, Bovers *et al.*, 2009). No major differences in the phylogenetic clustering were found when the mitochondrial (Figure 37 A) and

nuclear MLST (Figure 37 B) results were compared. Phenotypic data was mapped on the phylogenetic trees to observe correlations between a specific *C. gattii* AFLP genotype and the tested array of virulence factors (F. Hagen). With this information 19 *C. gattii* strains were selected that represent a range of isolates within the species for subsequent comparative genome analysis (Table 9). To confirm strain identity, all 19 selected strains were analysed by AFLP (Figure 38).

A


Mitochondrial Loci
Virulence
Melanin
Phospholipase
20
40
60
80
100
IPR values
Mouse pathogenicity
Melanin 25°C - Day 1
Melanin 25°C - Day 2
Melanin 25°C - Day 3
Melanin 25°C - Day 4
Melanin 25°C - Day 5
Melanin 25°C - Day 6
Melanin 25°C - Day 7
Melanin 25°C - Day 8
Melanin 25°C - Day 9
Melanin 25°C - Day 10
Melanin 37°C - Day 1
Melanin 37°C - Day 2
Melanin 37°C - Day 3
Melanin 37°C - Day 4
Melanin 37°C - Day 5
Melanin 37°C - Day 6
Melanin 37°C - Day 7
Melanin 37°C - Day 8
Melanin 37°C - Day 9
Melanin 37°C - Day 10
Phospholipase 25°C
Phospholipase 37°C

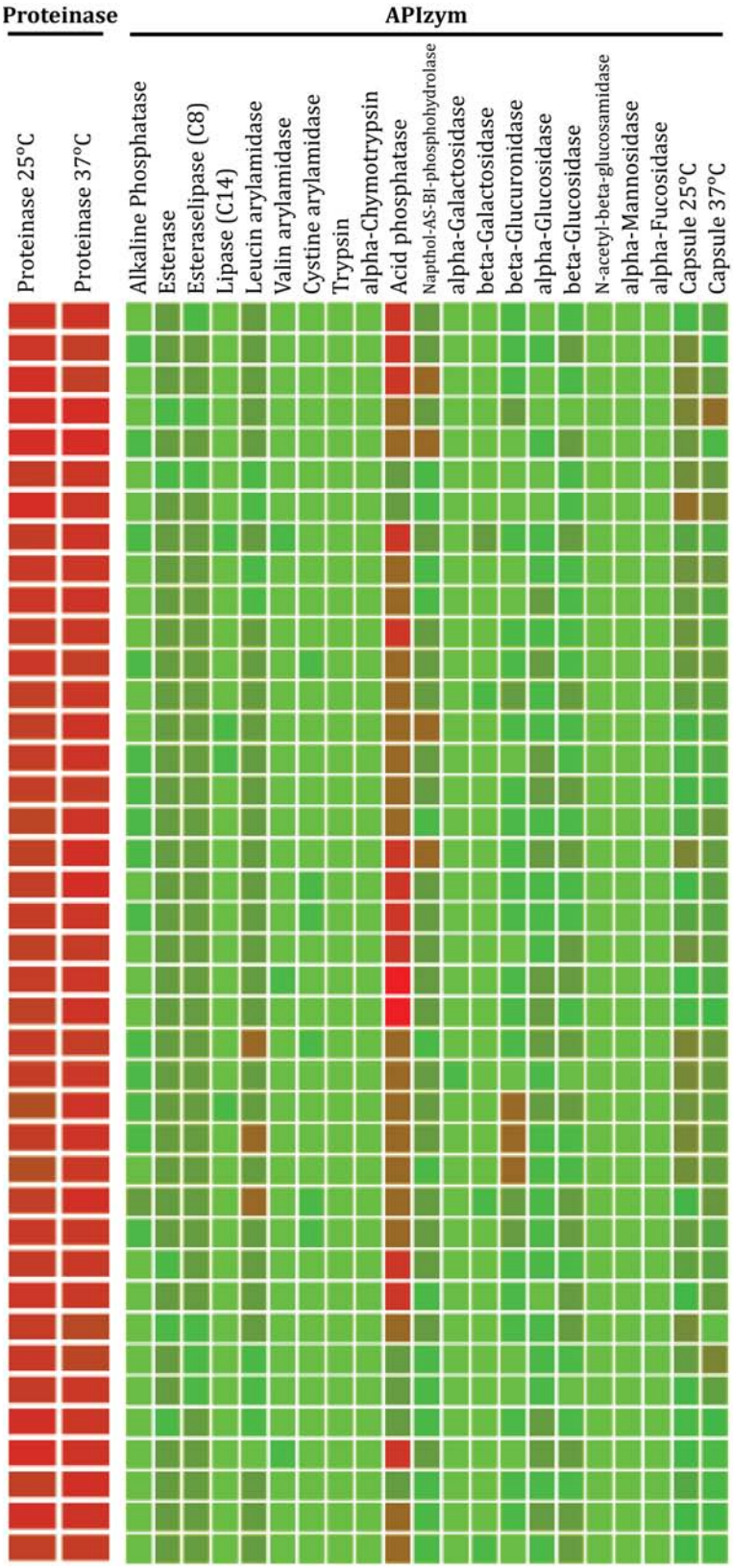
Proteinase
APIzym
Proteinase 25°C
Proteinase 37°C
Alkaline Phosphatase
Esterase
Esteraselipase (C8)
Lipase (C14)
Leucin arylamidase
Valin arylamidase
Cystine arylamidase
Trypsin
alpha-Chymotrypsin
Acid phosphatase
Napthol-AS-BI-phosphohydrolase
alpha-Galactosidase
beta-Galactosidase
beta-Glucuronidase
alpha-Glucosidase
beta-Glucosidase
N-acetyl-beta-glucosamidase
alpha-Mannosidase
alpha-Fucosidase
Capsule 25°C
Capsule 37°C
CBS7229 4 a
WM276 4 alpha
WM179 4 alpha
CBS919 4 alpha
CBS6992 4 alpha
56A 4 alpha
CBS6290 4 alpha
CDCR265 6A alpha
CBS6956 6A alpha
CBS7750 6A alpha
CDCF2866 6A alpha
CDCF2932 6A alpha
CDCF3016 6A alpha
CDCR271 6A alpha
CDCR376 6A alpha
CDCR406 6A alpha
CBS10485 6A alpha
ENV131 6A alpha
ENV152 6A alpha
RB14 6A alpha
RB50 6A alpha
RB59FH 6A alpha
RB59JF 6A alpha/alpha
CBS1930 6B a
MTW4 6B alpha
CBS8684 6A alpha
MTPi2 6B alpha
CBS10089 6B alpha
CDCR272 6B alpha
CBS10090 6A a
WM0483 6B alpha
M27055 7 alpha
CBS10101 7 alpha
B5742 7 alpha
B5748 7 alpha
CBS6993 5 alpha
CBS8755 5 alpha
CN043 5 alpha
384C 5 alpha
WM278 5 alpha

B

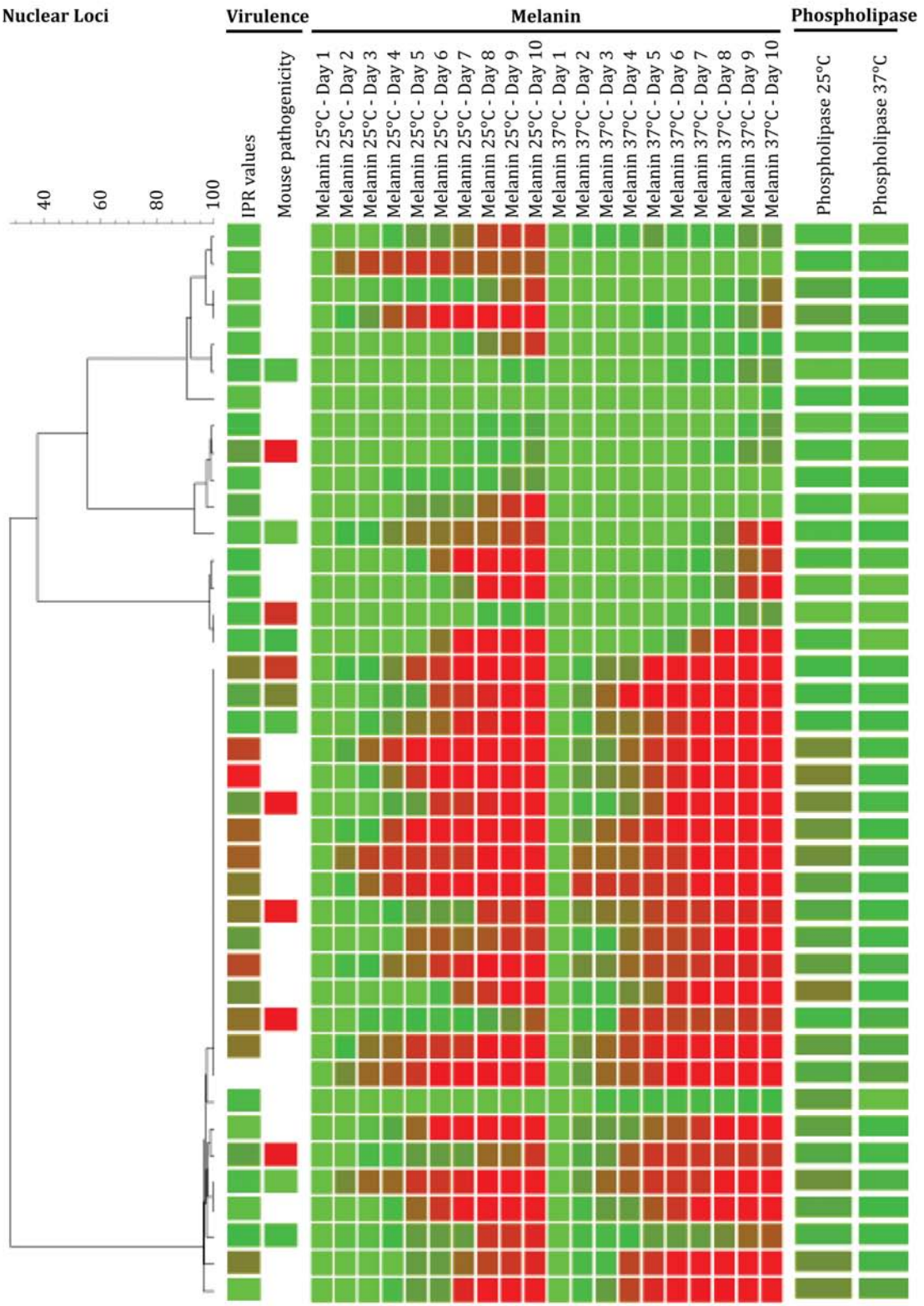
Nuclear Loci
Virulence
Melanin
Phospholipase
40
60
80
100
IPR values
Mouse pathogenicity
Melanin 25°C - Day 1
Melanin 25°C - Day 2
Melanin 25°C - Day 3
Melanin 25°C - Day 4
Melanin 25°C - Day 5
Melanin 25°C - Day 6
Melanin 25°C - Day 7
Melanin 25°C - Day 8
Melanin 25°C - Day 9
Melanin 25°C - Day 10
Melanin 37°C - Day 1
Melanin 37°C - Day 2
Melanin 37°C - Day 3
Melanin 37°C - Day 4
Melanin 37°C - Day 5
Melanin 37°C - Day 6
Melanin 37°C - Day 7
Melanin 37°C - Day 8
Melanin 37°C - Day 9
Melanin 37°C - Day 10
Phospholipase 25°C
Phospholipase 37°C

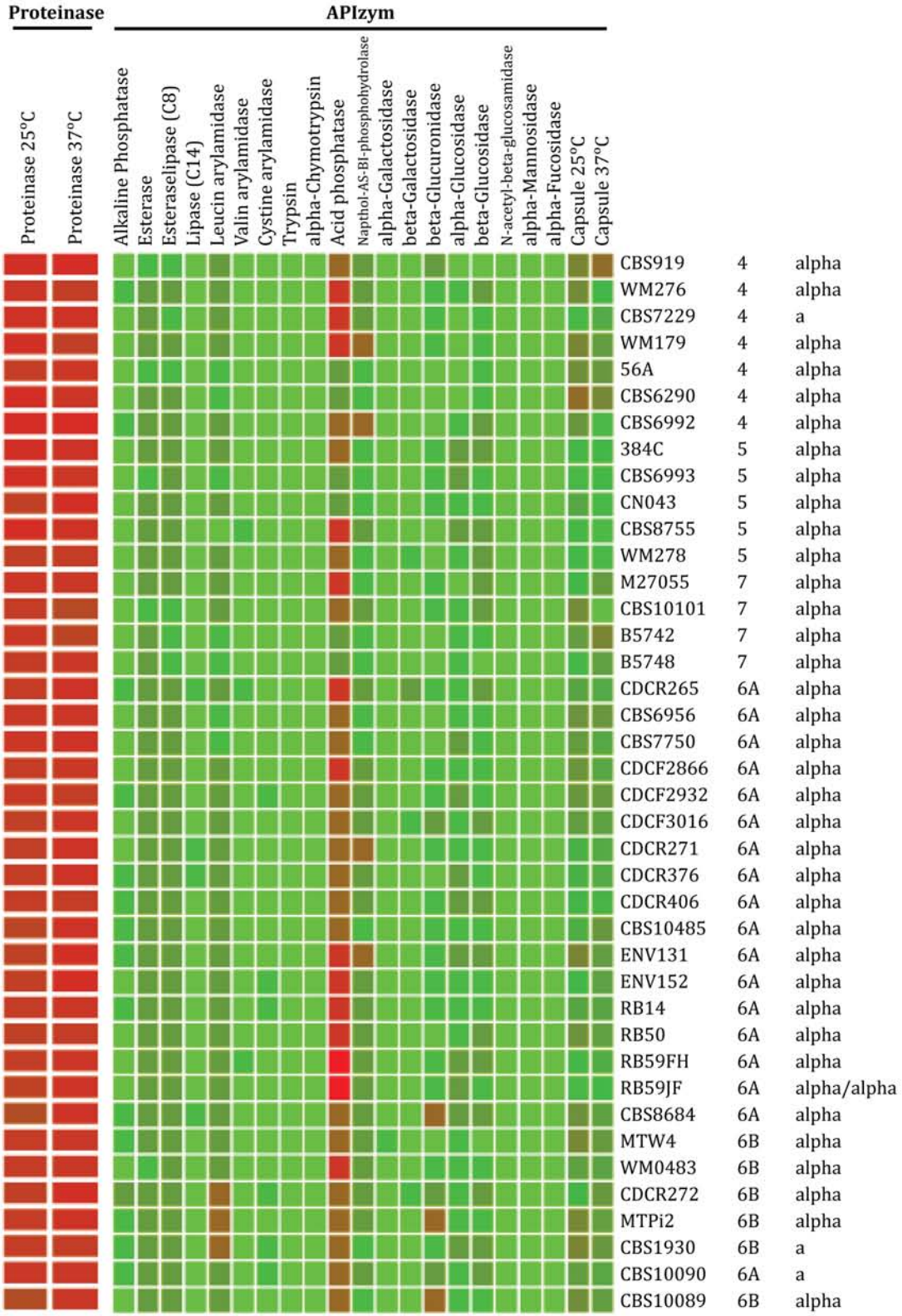

Figure 37: Phylogenetic constructions of *C. gattii* strains. MLST data, data from phenotypic analysis and virulence data were used to model the evolutionary relationship between *C. gattii* strains. The reconstructions were then used to select a wide range of *C. gattii* strains for DNA isolation. Colour code: green low to red high.

Table 9: *C. gattii* strains selected for comparative analysis of mitochondrial genomes.

Strain	Genotype	IPR	Strain details
CBS7229	AFLP4	0.56	China, meningitis isolate
CBS6955	AFLP5		Clinical isolate, USA
CBS6993	AFLP5	1.45	USA, California, CSF human
CBS10485	AFLP6A	1.78	Danish tourist visited Vancouver Island, Canada
ENV152	AFLP6A	2.28	Canada, Vancouver Island, Alder tree
CBS10090	AFLP6A	1.71	Greece, clinical
A1M-R271	AFLP6A	2.04	Canada, British Columbia, clinical, immunocompetent male
A1M-F3016	AFLP6A	1.47	Canada, dead wild Dall's porpoise
CBS8684	AFLP6A	0.90	Uruguay, wasp nest
A1M-F2932	AFLP6A	2.98	Canada, British Columbia, clinical, immunocompetent patient
LA362	AFLP6B	1.36	Brazil, parrot liver
ICB180	AFLP6B	0.42	Brazil, *Eucalyptus* sp. tree
ICB184	AFLP6B	0.54	Brazil, tree
CBS1930	AFLP6B	1.14	Aruba, sick goat
CBS10089	AFLP6B	0.44	Greece, clinical
CCA242	AFLP6B		Spain
LMM265	AFLP6B		Brazil
EJB18	AFLP6c	1.73	USA, Oregon, clinical
CBS10101	AFLP7	1.00	S.-Africa, reference strain of *Cryptococcus gattii*

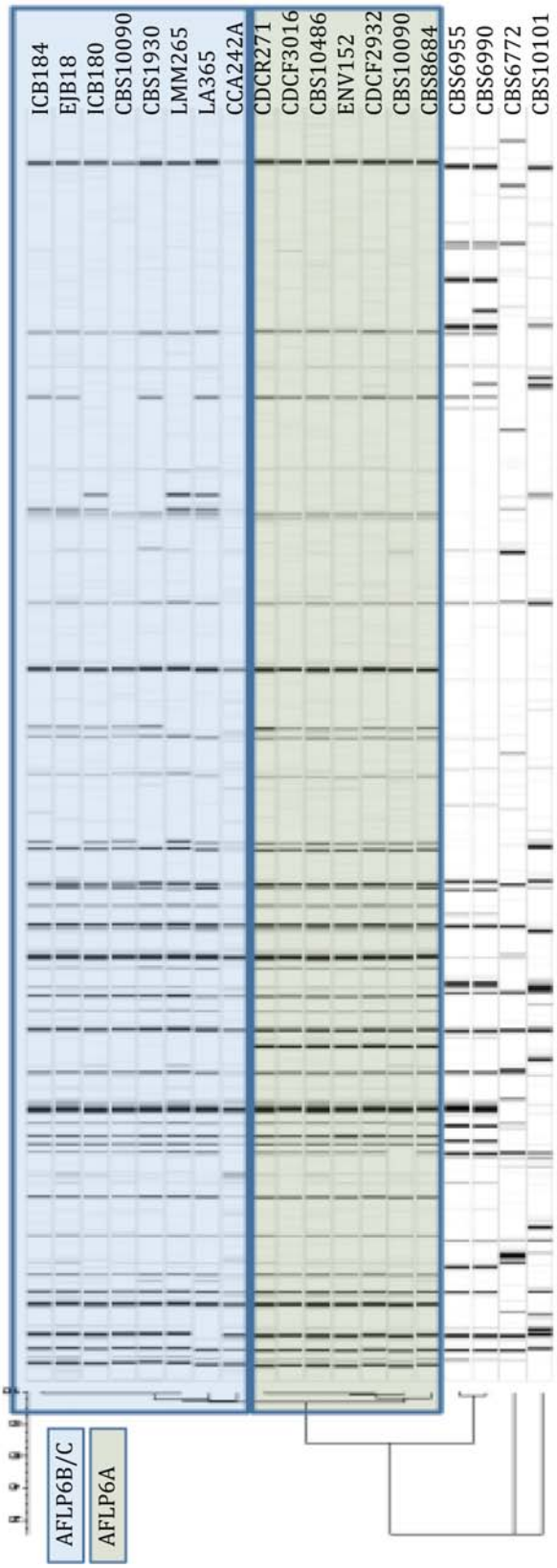

Figure 38: AFLP phylogenetic tree for selected *C. gattii* strains. Strains were selected for comparative mitochondrial genome sequencing and AFLP analysis was carried out to ensure strain identity. All strains tested here show the expected AFLP pattern (personal communication F. Hagen).

Following the selection of *C. gattii* strains and confirmation of strain identity, we isolated high quality total DNA from each strain. To amplify mitochondrial DNA for parallel sequencing it was opted for a long-range PCR approach (Hu *et al.*, 2007, Jex *et al.*, 2008). Together with Dr. A. Jex (Department of Vetenary Science, The University of Melbourne), PCR primers were designed to amplify the whole mitochondrial genome. With help of the previously described alignment of mitochondrial genomes, eight primers were created that localised in conserved regions of the genes encoding the large ribosomal subunit (*rnl*), NADH dehydrogenase subunit 5 (*nad5*), cytochrome oxidase subunit 1 (*cox1*) and NADH dehydrogenase subunit 1 (*nad1*) (Table 10 A). Primers were paired to produce four overlapping amplicons: three fragments of about 6 kb and one slightly larger fragment of ~ 8 kb (Table 10 B) and PCR reactions were performed with the Kapa HiFi HotStart DNA Polymerase kit for long-range PCR (KapaBiosystems) according to the manufacturer's instructions and an initial thermocycling profile of initial denaturation 98°C for 5 minutes followed by 30 cycles of 1 minute denaturation at 98°C, 1 minute annealing at 53°C and 10 minutes extension at 72°C together with a final extension of 10 minutes at 72°C. This resulted in successful amplification of all four amplicons from the test strain CBS1930. However, the PCR product was contaminated by unspecific fragments (Figure 39 A). To improve specificity of the PCR reaction, the annealing temperature was increased to 55°C and the cycle number reduced to 25. This eliminated unspecific PCR products, however, at the cost of reduced yield for the three smaller amplicons and no product was obtained for the larger 8 kb amplicon (Figure 39 B). The optimization of this long-range PCR protocol to achieve a specific PCR product for the 8 kb amplicon is currently in progress. In the next step, the cycle number will be increased to 30 and the annealing temperature reduced to 54°C. Successfully amplified mitochondrial genomes will then be parallel sequenced with a 454-sequencer (Roche). Sequence data will be analysed for cryptic open reading frames present only in hypervirulent strains, for genomic rearrangements and single nucleotide polymorphisms. These data will then be compared with existing data on virulence and the ability to proliferate intracellularly/form tubular mitochondria to clarify the changes that have occurred and let to the increased virulence of strains in the Vancouver Island Outbreak.

Table 10: Primer designed for amplification of the whole mitochondrial genome. (A) Primer sequence and additional information. (B) Primer pairs used in this study and their predicted amplicon size.

A

Primer	Sequence 5' 3'	Length (bases)	T_m (°C)
Rnl F	CCATATAGCACTAGCGGATCA	21	52
Rnl R	CCAATAAAGTATCGGAGGACC	21	52
Nad5 F	ATGCTACTACCTGTACTTATTGTA	24	51
Nad5 R	CCTTCCCAACCTACAAACATAATA	24	52
Cox1 F	CGACGAATTCCTGACTATCCT	21	52
Cox1 R	CCATTCTAGAGATGTACTGTATC	23	52
Nad1 F	CCAGAAGCAGAATCAGAACTAGT	23	53
Nad1 R	CCACCTAGAAATAGGATTGCTG	22	53

B

Forward Primer	Reverse Primer	Fragment Size (kb)
Rnl F	*Nad5* R	~ 6
Nad5 F	*Cox1* R	~ 8
Cox1 F	*Nad1* R	~ 6
Nad1 F	*Rnl* R	~ 5.5

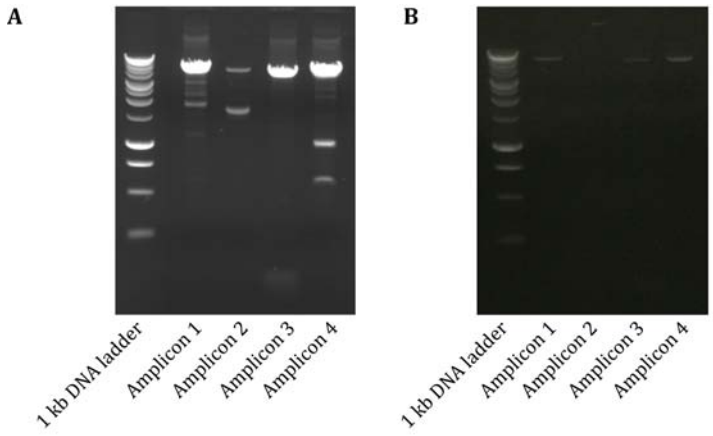

Figure 39: Optimization of long-range PCR to amplify the mitochondrial genomes of selected *C. gattii* strains. (A) Initial PCR reaction with a thermocycling profile of initial denaturation 98°C for 5 minutes followed by 30 cycles of 1 minute denaturation at 98°C, 1 minute annealing at 53°C and 10 minutes extension at 72°C with together with a final 10 minutes extension at 72°C resulted in unspecific PCR products. (B) Specificity was improved by increasing the annealing temperature to 55°C and reducing the cycle number to 25. However, this was at a cost of lower yield and no product was obtained for the larger 8 kb amplicon.

5.7 DISCUSSION

Isolates involved in the VIO outbreak have been shown to belong primarily to a single, hypervirulent *C. gattii* genotype (Kidd *et al.*, 2004). Interestingly, VIO isolates show a dramatically increased ability to replicate within macrophages (Ma, 2009, Ma *et al.*, 2009a). This intracellular proliferative ability correlates with virulence data obtained from mouse model systems and thus indicates that the hyper-proliferative phenotype might be the cause of the outbreak. Furthermore, subsequent microarray analysis revealed a large number of up-regulated genes in the highly proliferative strains, many of which are encoded by the mitochondrial genome or code for mitochondrial functions, and a correlation between increased intracellular proliferation and an unusual tubular mitochondria morphology of the outbreak strains after macrophage passage has been reported (Ma, 2009, Ma *et al.*, 2009a). However, the underlying molecular reasons for the hypervirulence of this particular lineage are not fully understood.

The data presented in this study further strengthens the evidence that mitochondria or mitochondrial functions may regulate hypervirulence in *C. gattii*. The data show that enhanced intracellular proliferative capacity is a common characteristic of the VGIIa VIO lineage and the related VGIIc lineage that has been causing a cryptococcosis outbreak in healthy individuals in Oregon (Byrnes *et al.*, 2010, Byrnes *et al.*, 2009c). The increase in proliferation is connected with increased formation of tubular mitochondria after exposure to macrophages. Interestingly, this difference seems to be due to a difference in temporal formation of tubular mitochondria: a VIO strain starts to form tubules shortly after entry into the intracellular niche whereas a non-VIO strain appears to fail to initiate tubularisation. This pattern is paralleled by the percentage of globular mitochondria; the VIO strain shows a high percentage of globular mitochondria before switching to the tubular morphology that drops after initiation of tubularisation. In contrast, the non-VIO strain only slowly builds up the proportion of globular mitochondria. It almost seems as if a certain threshold of globular mitochondria has to be crossed before tubular mitochondria can be formed.

To further investigate this behaviour, progeny from crosses between 'good' and 'poor' proliferators were analysed for their mitochondrial morphology. As the mitochondrial genome is inherited uniparentally from the MATa parent (Xu *et al.*, 2000), a cross between a good proliferating VGIIa MATa parent and a poorly proliferating VGIII MATα parent should result in all progeny inheriting a 'good proliferator' mitochondrial type and thus generating a high proportion of tubular mitochondria and high proliferation rate after macrophage exposure. In contrast, the opposite cross should produce progeny with the 'poor' mitochondrial type, low mitochondrial tubularisation and poor intracellular growth. Indeed the latter case turns out to be true, with progeny that inherit a 'poor' mitochondrial type all showing low IPR values (Ma, 2009) and a low percentage of tubular mitochondria after macrophage exposure. However, in a cross in which all progeny inherited a 'good' mitochondrial type, IPR values varied from 0.57 to 1.78 (Ma, 2009). In addition, an assessment of mitochondrial morphology revealed that most of the isolates have an increased proportion of tubular mitochondria even in the control situation. This data suggests that a hypervirulent mitochondrial background is necessary for increased virulence, but that a compatible nuclear genome is also required for enhanced ability to parasitise phagocytes (Ma, 2009). In addition, the constitutive production of tubular mitochondria in the progeny of this cross suggests the possible existence of a negative regulator of tubularisation that has been 'uncoupled' in the progeny during the recombination of the nuclear VGII and VGIII genomes. Recently, incompatibility between nuclear and mitochondrial genomes has been described for the two closely related species *S. bayanus* and *S. cerevisiae*. In particular one hybrid line with substitution of chromosome thirteen was completely sterile due to an inability of the *S. bayanus* nuclear encoded mitochondrial protein Aep2 to regulate translation of the *S. cerevisiae* mitochondrial OLI1 mRNA encoding a subunit of the ATP synthase complex (Lee *et al.*, 2008).

Mitochondrial morphology is regulated by opposing pathways – fusion and fission (Sesaki *et al.*, 1999, Bleazard *et al.*, 1999). Fusion events in *S. cerevisiae* are controlled by a protein complex consisting of Fzo1p, Mgm1p and Ugo1p dependent

on pH, GTP concentration and electrical membrane potential (Sesaki *et al.*, 1999, Meeusen *et al.*, 2003, Sesaki *et al.*, 2003, Wong *et al.*, 2000). Fzo1p in turn is regulated by the F-box protein Mdm30p whose mutation blocks fission (Fritz *et al.*, 2003). Furthermore, steady state levels of Fzo1p are increased in an *mdm30* mutant and decreased when *mdm30* is overexpressed (Fritz *et al.*, 2003). As F-box proteins are components of the E3 ubiquitin ligase complex which catalyses 26S proteasome-mediated degradation, it has been proposed that Mdm30p might negatively regulate Fzo1p by labeling the protein as substrate for protein degradation (Patton *et al.*, 1998). This hypothesis has been supported by observation of Fzo1p ubiquitination (Hitchcock *et al.*, 2003) and increased mitochondrial fragmentation and aggregation after knockout of the two E2 encoding enzymes *UBC4* and *UCB5* (Fisk *et al.*, 1999). Hence, the Mdm30p homologue in *C. gattii* potentially might be a negative regulator of initiation of tubularisation and explain the 'uncoupling' of tubularisation discussed above. Furthermore, maintenance of tubular morphology is controlled by a second set of proteins, Mmm1p, Mdm10p and Mdm12p, forming the MMM complex (Boldogh *et al.*, 2001) that connects mitochondrial tubules to other cellular structures or organizes scaffolding-like proteins to maintain tubular shape (Okamoto *et al.*, 2005). Weaker mitochondrial connection to this scaffold, or rearrangements within the backbone, might reduce stability of tubular morphology and thus result in failure to tubularise sufficiently. Understanding the molecular mechanisms regulating tubularisation in *C. gattii* might provide new targets for therapeutic approaches.

One hypothesis for the involvement of mitochondria in increased virulence is an enhancement of mitochondrial function during stress resistance. Mitochondrial functions include oxidative respiration and these organelles are important for handling low oxygen concentrations and oxidative or nitrosative stress. *C. neoformans* mutants with impaired mitochondrial function show reduced oxidative respiration and higher sensitivity to reactive oxygen species under hypoxic condition (Ingavale *et al.*, 2008). To address how mitochondria might regulate cryptococcal virulence, the influence of hypoxia and a signaling pathway

involved in oxygen signaling on the interaction with macrophages was evaluated. Most cell and tissue culture treatments are done at atmospheric oxygen concentrations. *Cryptococcus* grows very well under atmospheric oxygen condition (21 % O_2) but has to face low oxygen concentrations in the host ranging from approximately 21 % in the lungs, 12 % in the blood to only 3-6 % in tissues and the brain. Therefore, macrophage-*Cryptococcus* interactions were analysed under hypoxic conditions. The occurrence of expulsion was significantly increased under hypoxic conditions. When macrophages were infected with *Cryptococcus* under 3 % O_2, the macrophage's ability to internalize yeast was not altered whereas treatment with 0.1 mM $CoCl_2$ significantly increases yeast uptake. The chosen $CoCl_2$ concentration is very likely to cause more severe hypoxia than 3 % O_2 and thus indicates that *Cryptococcus* can adapt to low oxygen until a certain threshold. Once this threshold is passed, the anti-phagocytic properties of the yeast are restricted, allowing rapid uptake. Cryptococci were not able to proliferate in macrophages when kept in hypoxic conditions after infection. *Cryptococcus* is rarely found in solid tissues and, since the oxygen concentration can fall as low as 3 % in tissues, macrophages might be more effective in killing the yeast and thus in eliminating them from these locations.

One possible explanation for the hypervirulence of the VIO lineage is that the mitochondria of the *C. gattii* VIO strains have polymorphisms that produce an advantage under oxidative and nitrosative stress or low oxygen conditions. To test this possibility, four *C. gattii* strains with high IPR and four strains with low intracellular proliferative potential were tested under different stress conditions. However, no trend towards enhanced proliferative capacity of the strains with increased intracellular proliferation was detected under any of the stresses. Although there was no direct influence of stress conditions on the growth rate between high and low proliferators, there might be an enhanced ability to adapt to the intracellular environment due to mitochondrial functions that are only activated upon entry into the intracellular niche. One possibility would be greater mitochondrial plasticity in number or morphology that changes rapidly in response to the intracellular niche. Indeed, VIO strains appear to have an enhanced

ability to deal with certain stresses such as hypoxia, oxidative, nitrosative and UV stress by adapting a tubular mitochondrial morphology. Most of these conditions are encountered within the mature phagosome and might enable these strains to withstand the innate immune attack. Many mitochondrial functions are performed by reactions involving regulatory and enzymatic protein complexes or a cascade of different proteins. Damage to one of these proteins by host immune attack mechanisms could result in disruption of successive activation reactions and inhibition of mitochondrial functions ultimately leading to cell death. In mitochondria with tubular morphology, it is likely that multiple copies of the same protein are in close proximity and thus can replace damaged units; in essence, resulting in 'cross-complementation'. This would result in an increased tolerance to host stresses and an advantage in establishing within the intracellular niche.

It is very likely that changes in the genetic make up are directly or indirectly accountable for the increased ability to grow intracellularly in macrophages. Different potential scenarios are imaginable: Firstly, single nucleotide polymorphisms might have enabled the yeast to withstand the harsh environment caused by oxidative and nitrosative stress within infected phagocytes and/or enhanced the functionality of virulence factors. Furthermore, it might be possible that strains from the outbreak lineage have gained additional coding regions and/or that gene duplications have occurred leading to increased virulence. Finally, nucleotide changes within regulatory regions could have increased or decreased expression levels of virulence-related genes resulting in hypervirulence.

Available cryptococcal genomes were aligned and analysed for their gene synteny. Similar to an earlier study showing no differences in the gene order of *C. neoformans* strains IFO410 (var. *grubii*) and IFM5944 (var. *neoformans*), it was found that the mitochondrial gene arrangement is also conserved in *C. neoformans* strains H99 and JEC21 as well as in *C. gattii* strains R265 and WM276. Generally, there seems to be high sequence similarity between the genomes. However, there are several intronic regions, especially within the ORFs coding for cytochrome oxidase c subunit 1 (*cox1*), present in the *C. gattii* strains. Indeed, the number of detected introns in the *C. gattii* strains is much higher than in the H99 genome.

Many of these intronic regions encode putative endonucleases containing a LAGLIDADG motif (Saldanha *et al.*, 1993, Lang *et al.*, 2007). LAGLIDADG endonucleases have been implicated as maturases in splicing and as homing endonucleases facilitating group I intron mobility and activation of the DNA repair machinery (Burke, 1988, Lambowitz *et al.*, 1990, Perlman *et al.*, 1989, Lang *et al.*, 2007). The high abundance of ORFs potentially coding for these endonucleases raises the potential of greater mitochondrial genome plasticity by enabling rearrangements and additional integration of mobile introns that might affect regulatory regions. Activation of the DNA repair machinery by homing endonucleases might be an advantage during attack by oxidative and nitrosative stresses in mending DNA damage. In addition, the expression of maturases might accelerate the splicing process and facilitate increased levels of mitochondrial proteins. Interestingly, it has been described that the mitochondrial gene expression profile of *cox1* can be altered by temperature changes or encounter with the host environment in *C. neoformans* (Toffaletti *et al.*, 2003), whilst a subsequent study ruled out mitochondrial involvement in virulence in *C neoformans* A and D strains (Toffaletti *et al.*, 2004). In this context, data analysis from microarrays with a range of *C. gattii* strains revealed a positive correlation between mitochondrial expression level and IPR value.

Indications that mitochondria regulate pathogen virulence have previously been noted in the plant pathogen *Heterobasidion annosum* (Olson *et al.*, 2001). In this context, a comparative analysis of mitochondrial genomes of a range of *C. gattii* strains that have been selected based on data obtained from MLST, phenotypic analysis and IPR values and phylogenetic reconstruction of sequences will hopefully be the next step to the identification of the genetic basis of hypervirulence. Fortunately, much experimental progress has already been made to prepare mitochondrial DNA for a parallel sequencing approach and hopefully further insight will be obtained in the near future. With the current knowledge a particular focus will also be given to genes involved in regulating mitochondrial morphology. Directed knockout of these genes will help to understand how the

formation of tubular mitochondria is regulated in *C. gattii* and potential polymorphisms in VIO and non-VIO genes might reveal regulatory aspects.

In summary, striking results regarding the involvement of mitochondria in *C. gattii* hypervirulence are presented in this thesis. Mitochondrial plasticity seems to be the key in understanding the molecular mechanisms underlying the VIO outbreak. The next challenge will be to determine the genetic basis for this plasticity, based both on the mitochondrial and nuclear genomes.

CHAPTER 6

ADDITIONAL WORK

6.1 INVOLVEMENT OF THE STEROL RESPONSE ELEMENT BINDING PROTEIN IN MACROPHAGE PARASITISM

Under low oxygen conditions, *Cryptococcus* cannot proliferate intracellularly and shows an increase in the number of expulsion events. However, within the human body, the yeast has to adapt to different oxygen conditions. The sterol response element binding protein 1 (Sre1p) is involved in oxygen signaling in *Cryptococcus*. Low oxygen leads to reduced sterol synthesis followed by Sre1p activation. Knockout mutants of *sre1*, obtained by *Agrobacterium*-mediated transformation, fail to grow under low oxygen conditions and these mutants show decreased virulence in a mice model (Lee *et al.*, 2007, Chun *et al.*, 2007, Chang *et al.*, 2007).

The role of Sre1p in macrophage parasitism by *Cryptococcus* was examined. As *Agrobacterium*-mediated transformation does not allow for directed knockout, *sre1* was disrupted by homologous recombination following biolistic bombardment. After transformation, potential *sre1* knockout colonies were screened for their ability to grow on media containing 0.6 mM $CoCl_2$ and growth-negative colonies checked for correct integration of the knockout cassette by southern hybridization (Figure 40 A). Two individual mutants (5.52 and 6.15) were selected for further analysis of their behavior within macrophages. At

21 % O_2, neither *sre1* mutant could proliferate within J774 macrophages (Figure 40 B). However, when the mutants were analysed for growth and under oxidative and nitrosative stress, it became obvious that the mutants have a general growth defect compared to the parental strain (Figure 40 C). Interestingly, both knockout strains behaved similarly to the parental strain when subjected to cell wall stress, with mutant 6.15 even showing improved resistance to 0.5 % SDS (Figure 40 C). However, given the pleiotropic phenotypes of these mutants, we did not pursue the involvement of Sre1p in macrophage parasitism further.

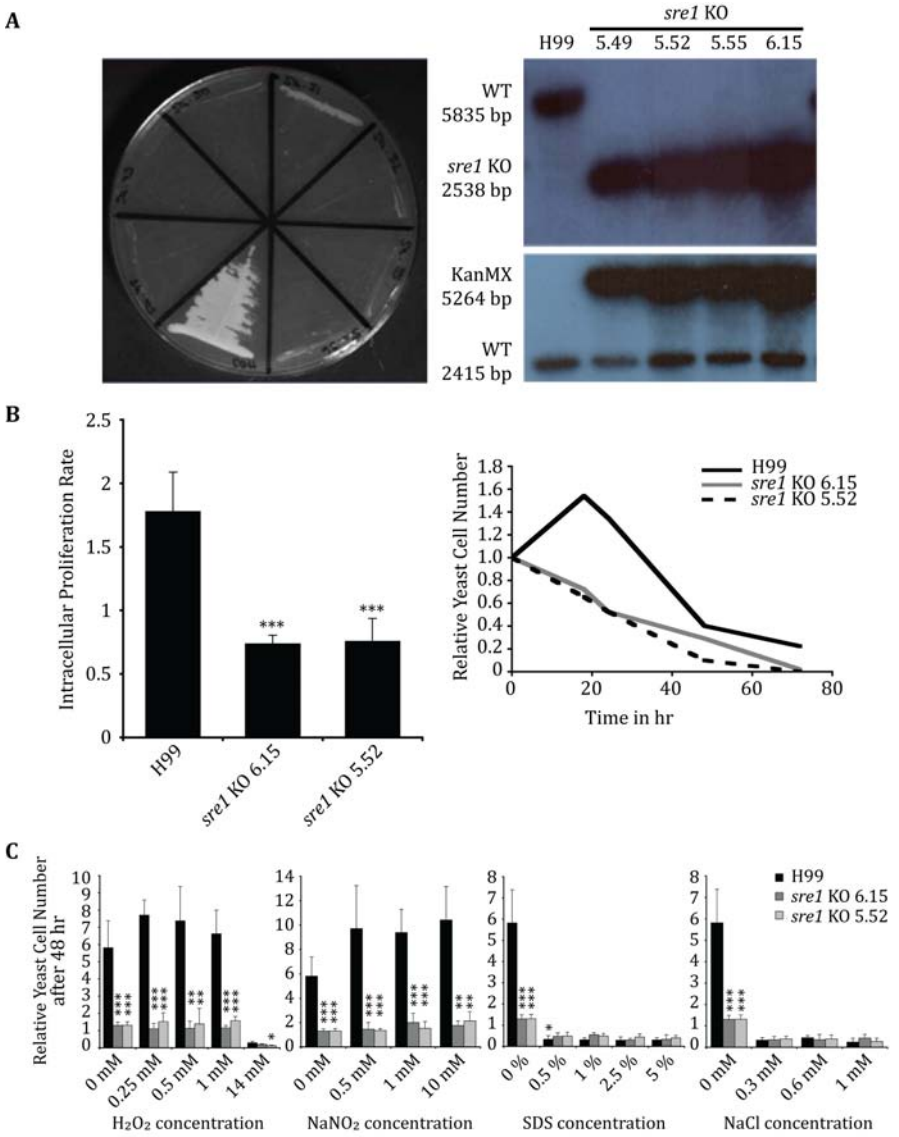

Figure 40: Analysis of *sre1* KO mutants. (A) Potential *sre1* KO colonies were screened for loss of ability to grow on 0.6 mM $CoCl_2$ containing YPD agar plates. A selection of four colonies was then subjected to Southern analysis to control for single integration of the knockout cassette and potential genomic rearrangements. (B) J774 cells were infected with *C. neoformans* strains H99 and the two independent *sre1* KO strains 6.15 and 5.52 at atmospheric oxygen levels and then further incubated under the same conditions whilst being monitored for intracellular proliferation. IPR was significantly reduced in both of the KO strains compared to the parental H99 strain. (C) The *sre1* KO strains and the parental *C. neoformans* H99 strain were subjected to oxidative (H_2O_2), nitrosative ($NaNO_2$) and cell wall stress (SDS and NaCl) in DMEM assay medium and growth assessed by hemocytometer countings after 48 hr incubation at 37°C. Both mutant strains showed a general growth defect revealed by significantly reduced yeast cell number after 48 hr incubation in the untreated control as well as under stress conditions. Data presented were obtained from at least three individual experiments and are shown as mean with 2 x standard error of the mean. The means were tested for statistical significant differences using Tukey HSD test assuming equal variances. Statistically significant differences are indicated by asterisks (*** $p < 0.001$).

6.1.1 DISCUSSION

Cryptococcus often invades the central nervous system where it faces O_2 concentrations of around 3 % thus indicating a mechanism that enables *Cryptococcus* to adapt to low oxygen conditions. In fact, there have been reports on *Cryptococcus* mutants defective in the *sre1* gene, that are unable to grow at low oxygen concentrations and show reduced virulence in mice models (Chang *et al.*, 2007, Chun *et al.*, 2007). In mammals, Sre1p functions as oxygen-sensing component of the cholesterol biosynthesis pathway that is required for the induction of sterol synthesis genes under low oxygen concentrations (Lee *et al.*, 2007, Chang *et al.*, 2007). Hughes *et al*. (2005) (Hughes *et al.*, 2005) identified a similar mechanism in *Schizosaccharomyces pombe*. Thus, an analogous pathway might also be involved in sensing low oxygen concentrations and be required for adaptation of *Cryptococcus* to the hypoxic environment in the brain to maintain sterols, a major component of the fungal cell membrane. To address the importance of this oxygen-signaling pathway in adaptation to hypoxic conditions, a *sre1* knockout mutant was created and tested during macrophage infection. The *sre1* mutant is not able to proliferate within macrophages at atmospheric oxygen levels. However, an analysis of the mutant showed a general growth defect compared to the parental strain. Thus, it is likely that Sre1p is involved in other essential pathways and no conclusions can be made on the involvement of Sre1p in the adaptation to the intracellular environment.

SUMMARY

The research presented in this thesis provides insight into several aspects of the interaction of *Cryptococcus* with phagocytic effector cells. It offers a potential explanation for the susceptibility phenotype of immunocompromised individuals that hopefully in the future will be applied in research and the design of novel anticryptococcal therapies. It also introduces an automatic approach using GFP-tagged strains that simplifies and accelerates the so far time-consuming analysis of parameters describing macrophage-*Cryptococcus* interaction. Finally, it proposes concepts to explain the increased virulence in *C. gattii* strains that have been causing outbreaks on Vancouver Island, Canada and in Oregon, USA. These ideas are a starting point for the design of exciting experimental approaches. Together, these findings will hopefully help to widen our understanding of this pathogen and how it causes disease to ultimately improve therapy and/or preventative measures.

REFERENCES

Abadi, J. and Pirofski, L. (1999). Antibodies reactive with the cryptococcal capsular polysaccharide glucuronoxylomannan are present in sera from children with and without human immunodeficiency virus infection. *J Infect Dis* **180,** 915-919.

Akhter, S., McDade, H.C., Gorlach, J.M., Heinrich, G., Cox, G.M. and Perfect, J.R. (2003). Role of alternative oxidase gene in pathogenesis of Cryptococcus neoformans. *Infect Immun* **71,** 5794-5802.

Aller, A.I., Martin-Mazuelos, E., Lozano, F., Gomez-Mateos, J., Steele-Moore, L., Holloway, W.J.*, et al.* (2000). Correlation of fluconazole MICs with clinical outcome in cryptococcal infection. *Antimicrob Agents Chemother* **44,** 1544-1548.

Alspaugh, J.A., Cavallo, L.M., Perfect, J.R. and Heitman, J. (2000). RAS1 regulates filamentation, mating and growth at high temperature of Cryptococcus neoformans. *Mol Microbiol* **36,** 352-365.

Alspaugh, J.A. and Granger, D.L. (1991). Inhibition of Cryptococcus neoformans replication by nitrogen oxides supports the role of these molecules as effectors of macrophage-mediated cytostasis. *Infect Immun* **59,** 2291-2296.

Altfeld, M., Addo, M.M., Kreuzer, K.A., Rockstroh, J.K., Dumoulin, F.L., Schliefer, K.*, et al.* (2000). T(H)1 to T(H)2 shift of cytokines in peripheral blood of HIV-infected patients is detectable by reverse transcriptase polymerase chain reaction but not by enzyme-linked immunosorbent assay under nonstimulated conditions. *J Acquir Immune Defic Syndr* **23,** 287-294.

Alvarez, M., Burn, T., Luo, Y., Pirofski, L.A. and Casadevall, A. (2009). The outcome of Cryptococcus neoformans intracellular pathogenesis in human monocytes. *BMC Microbiol* **9,** 51.

Alvarez, M. and Casadevall, A. (2006). Phagosome extrusion and host-cell survival after Cryptococcus neoformans phagocytosis by macrophages. *Curr Biol* **16,** 2161-2165.

Alvarez, M. and Casadevall, A. (2007). Cell-to-cell spread and massive vacuole formation after Cryptococcus neoformans infection of murine macrophages. *BMC Immunol* **8,** 16.

Alvarez, M., Saylor, C. and Casadevall, A. (2008). Antibody action after phagocytosis promotes Cryptococcus neoformans and Cryptococcus gattii macrophage exocytosis with biofilm-like microcolony formation. *Cell Microbiol* **10,** 1622-1633.

Amer, A.O. and Swanson, M.S. (2005). Autophagy is an immediate macrophage response to Legionella pneumophila. *Cell Microbiol* **7,** 765-778.

Arora, S., Hernandez, Y., Erb-Downward, J.R., McDonald, R.A., Toews, G.B. and Huffnagle, G.B. (2005). Role of IFN-gamma in regulating T2 immunity and the development of alternatively activated macrophages during allergic bronchopulmonary mycosis. *J Immunol* **174,** 6346-6356.

Bajpai, R., Lesperance, J., Kim, M. and Terskikh, A.V. (2008). Efficient propagation of single cells Accutase-dissociated human embryonic stem cells. *Mol Reprod Dev* **75,** 818-827.

Bartlett, K.H., Kidd, S.E. and Kronstad, J.W. (2008). The Emergence of Cryptococcus gattii in British Columbia and the Pacific Northwest. *Curr Infect Dis Rep* **10,** 58-65.

Barton, C.H., Whitehead, S.H. and Blackwell, J.M. (1995). Nramp transfection transfers Ity/Lsh/Bcg-related pleiotropic effects on macrophage activation: influence on oxidative burst and nitric oxide pathways. *Mol Med* **1,** 267-279.

Baum, G.L. and Artis, D. (1961a). Fungistatic effects of cell free human serum. *Am J Med Sci* **242,** 761-770.

Baum, G.L. and Artis, D. (1961b). Growth inhibition of Cryptococcus neoformans by cell free human serum. *Am J Med Sci* **241,** 613-616.

Baum, G.L. and Artis, D. (1963). Characterization of the Growth Inhibition Factor for Cryptococcus Neoformans (Gifc) in Human Serum. *Am J Med Sci* **246,** 53-57.

Bauman, S.K., Nichols, K.L. and Murphy, J.W. (2000). Dendritic cells in the induction of protective and nonprotective anticryptococcal cell-mediated immune responses. *J Immunol* **165,** 158-167.

Bava, A.J., Afeltra, J., Negroni, R. and Diez, R.A. (1995). Interferon gamma increases survival in murine experimental cryptococcosis. *Rev Inst Med Trop Sao Paulo* **37,** 391-396.

Beenhouwer, D.O., Shapiro, S., Feldmesser, M., Casadevall, A. and Scharff, M.D. (2001). Both Th1 and Th2 cytokines affect the ability of monoclonal antibodies to protect mice against Cryptococcus neoformans. *Infect Immun* **69,** 6445-6455.

Bengoechea-Alonso, M.T. and Ericsson, J. (2007). SREBP in signal transduction: cholesterol metabolism and beyond. *Curr Opin Cell Biol* **19,** 215-222.

Bernardini, M.L., Mounier, J., d'Hauteville, H., Coquis-Rondon, M. and Sansonetti, P.J. (1989). Identification of icsA, a plasmid locus of Shigella flexneri that governs bacterial intra- and intercellular spread through interaction with F-actin. *Proc Natl Acad Sci U S A* **86,** 3867-3871.

Bicanic, T., Harrison, T., Niepieklo, A., Dyakopu, N. and Meintjes, G. (2006). Symptomatic relapse of HIV-associated cryptococcal meningitis after initial fluconazole monotherapy: the role of fluconazole resistance and immune reconstitution. *Clin Infect Dis* **43,** 1069-1073.

Blackstock, R. and Murphy, J.W. (2004). Role of interleukin-4 in resistance to Cryptococcus neoformans infection. *Am J Respir Cell Mol Biol* **30,** 109-117.

Blasi, E., Colombari, B., Mucci, A., Cossarizza, A., Radzioch, D., Boelaert, J.R. and Neglia, R. (2001). Nramp1 gene affects selective early steps in macrophage-mediated anti-cryptococcal defense. *Med Microbiol Immunol* **189,** 209-216.

Bleazard, W., McCaffery, J.M., King, E.J., Bale, S., Mozdy, A., Tieu, Q*., et al.* (1999). The dynamin-related GTPase Dnm1 regulates mitochondrial fission in yeast. *Nat Cell Biol* **1,** 298-304.

Bobak, D.A., Washburn, R.G. and Frank, M.M. (1988). C1q enhances the phagocytosis of Cryptococcus neoformans blastospores by human monocytes. *J Immunol* **141,** 592-597.

Boekhout, T., Theelen, B., Diaz, M., Fell, J.W., Hop, W.C., Abeln, E.C*., et al.* (2001). Hybrid genotypes in the pathogenic yeast Cryptococcus neoformans. *Microbiology* **147,** 891-907.

Boekhout, T., van Belkum, A., Leenders, A.C., Verbrugh, H.A., Mukamurangwa, P., Swinne, D. and Scheffers, W.A. (1997). Molecular typing of Cryptococcus

neoformans: taxonomic and epidemiological aspects. *Int J Syst Bacteriol* **47,** 432-442.

Bolano, A., Stinchi, S., Preziosi, R., Bistoni, F., Allegrucci, M., Baldelli, F.*, et al.* (2001). Rapid methods to extract DNA and RNA from Cryptococcus neoformans. *FEMS Yeast Res* **1,** 221-224.

Bolanos, B. and Mitchell, T.G. (1989). Phagocytosis of Cryptococcus neoformans by rat alveolar macrophages. *J Med Vet Mycol* **27,** 203-217.

Boldogh, I.R., Yang, H.C. and Pon, L.A. (2001). Mitochondrial inheritance in budding yeast. *Traffic* **2,** 368-374.

Bovers, M., Hagen, F., Kuramae, E.E. and Boekhout, T. (2008). Six monophyletic lineages identified within Cryptococcus neoformans and Cryptococcus gattii by multi-locus sequence typing. *Fungal Genet Biol* **45,** 400-421.

Bovers, M., Hagen, F., Kuramae, E.E. and Boekhout, T. (2009). Promiscuous mitochondria in Cryptococcus gattii. *FEMS Yeast Res* **9,** 489-503.

Bozzette, S.A., Larsen, R.A., Chiu, J., Leal, M.A., Tilles, J.G., Richman, D.D.*, et al.* (1991). Fluconazole treatment of persistent Cryptococcus neoformans prostatic infection in AIDS. *Ann Intern Med* **115,** 285-286.

Brain, J.D. (1980). Macrophage damage in relation to the pathogenesis of lung diseases. *Environ Health Perspect* **35,** 21-28.

Brajtburg, J., Powderly, W.G., Kobayashi, G.S. and Medoff, G. (1990). Amphotericin B: current understanding of mechanisms of action. *Antimicrob Agents Chemother* **34,** 183-188.

Brandt, M.E., Hutwagner, L.C., Kuykendall, R.J. and Pinner, R.W. (1995). Comparison of multilocus enzyme electrophoresis and random amplified polymorphic DNA analysis for molecular subtyping of Cryptococcus neoformans. The Cryplococcal Disease Active Surveillance Group. *J Clin Microbiol* **33,** 1890-1895.

Brazill, D.T., Caprette, D.R., Myler, H.A., Hatton, R.D., Ammann, R.R., Lindsey, D.F.*, et al.* (2000). A protein containing a serine-rich domain with vesicle fusing properties mediates cell cycle-dependent cytosolic pH regulation. *J Biol Chem* **275,** 19231-19240.

Brown, S.M., Upadhya, R., Shoemaker, J.D. and Lodge, J.K. (2010). Isocitrate dehydrogenase is important for nitrosative stress resistance in Cryptococcus neoformans, but oxidative stress resistance is not dependent on glucose-6-phosphate dehydrogenase. *Eukaryot Cell* **9,** 971-980.

Brummer, E. and Stevens, D.A. (1994). Anticryptococcal activity of macrophages: role of mouse strain, C5, contact, phagocytosis, and L-arginine. *Cell Immunol* **157,** 1-10.

Bryan, R.A., Jiang, Z., Howell, R.C., Morgenstern, A., Bruchertseifer, F., Casadevall, A. and Dadachova, E. (2010). Radioimmunotherapy Is More Effective than Antifungal Treatment in Experimental Cryptococcal Infection. *J Infect Dis*.

Bryan, R.A., Jiang, Z., Huang, X., Morgenstern, A., Bruchertseifer, F., Sellers, R.*, et al.* (2009). Radioimmunotherapy is effective against high-inoculum Cryptococcus neoformans infection in mice and does not select for radiation-resistant cryptococcal cells. *Antimicrob Agents Chemother* **53,** 1679-1682.

Bulmer, G.S. and Sans, M.D. (1967). Cryptococcus neoformans. II. Phagocytosis by human leukocytes. *J Bacteriol* **94,** 1480-1483.

Bulmer, G.S. and Tacker, J.R. (1975). Phagocytosis of Cryptococcus neoformans by alveolar macrophages. *Infect Immun* **11,** 73-79.

Burke, J.M. (1988). Molecular genetics of group I introns: RNA structures and protein factors required for splicing--a review. *Gene* **73,** 273-294.

Buschke, A. (1895). Über eine durch coccidien hervorgerufene Krankheit des Menschen. *Deutsche Medizinische Wochenschrift* **21**.

Busse, O. (1894). Über parasitäre Einschlüsse und ihre Züchtung. *Zentralblatt Bakteriologie* **16,** 175-180.

Byrnes, E.J., 3rd, Bildfell, R.J., Frank, S.A., Mitchell, T.G., Marr, K.A. and Heitman, J. (2009a). Molecular evidence that the range of the Vancouver Island outbreak of Cryptococcus gattii infection has expanded into the Pacific Northwest in the United States. *J Infect Dis* **199,** 1081-1086.

Byrnes, E.J., 3rd, Li, W., Lewit, Y., Ma, H., Voelz, K., Ren, P.*, et al.* (2010). Emergence and pathogenicity of highly virulent Cryptococcus gattii genotypes in the northwest United States. *PLoS Pathog* **6,** e1000850.

Byrnes, E.J., 3rd, Li, W., Lewit, Y., Perfect, J.R., Carter, D.A., Cox, G.M. and Heitman, J. (2009b). First reported case of Cryptococcus gattii in the Southeastern USA: implications for travel-associated acquisition of an emerging pathogen. *PLoS ONE* **4,** e5851.

Byrnes, E.J. and Heitman, J. (2009c). Cryptococcus gattii outbreak expands into the Northwestern United States with fatal consequences. *F1000 Biol Reports* **1,** 62.

Campbell, G.D. (1966). Primary pulmonary cryptococcosis. *Am Rev Respir Dis* **94,** 236-243.

Casadevall, A. and Perfect, J.R. (1998) Cryptococcus neoformans Washington DC, American Society for Microbiology.

Casadevall, A. and Pirofski, L. (2005). Insights into mechanisms of antibody-mediated immunity from studies with Cryptococcus neoformans. *Curr Mol Med* **5,** 421-433.

Champion, J.A. and Mitragotri, S. (2006). Role of target geometry in phagocytosis. *Proc Natl Acad Sci U S A* **103,** 4930-4934.

Chang, Y.C., Bien, C.M., Lee, H., Espenshade, P.J. and Kwon-Chung, K.J. (2007). Sre1p, a regulator of oxygen sensing and sterol homeostasis, is required for virulence in Cryptococcus neoformans. *Mol Microbiol* **64,** 614-629.

Chang, Y.C. and Kwon-Chung, K.J. (1994). Complementation of a capsule-deficient mutation of Cryptococcus neoformans restores its virulence. *Mol Cell Biol* **14,** 4912-4919.

Chang, Y.C., Stins, M.F., McCaffery, M.J., Miller, G.F., Pare, D.R., Dam, T.*, et al.* (2004). Cryptococcal yeast cells invade the central nervous system via transcellular penetration of the blood-brain barrier. *Infect Immun* **72,** 4985-4995.

Charlier, C., Nielsen, K., Daou, S., Brigitte, M., Chretien, F. and Dromer, F. (2009). Evidence of a role for monocytes in dissemination and brain invasion by Cryptococcus neoformans. *Infect Immun* **77,** 120-127.

Chaturvedi, V., Wong, B. and Newman, S.L. (1996). Oxidative killing of Cryptococcus neoformans by human neutrophils. Evidence that fungal

mannitol protects by scavenging reactive oxygen intermediates. *J Immunol* **156,** 3836-3840.

Chen, S., Sorrell, T., Nimmo, G., Speed, B., Currie, B., Ellis, D.*, et al.* (2000). Epidemiology and host- and variety-dependent characteristics of infection due to Cryptococcus neoformans in Australia and New Zealand. Australasian Cryptococcal Study Group. *Clin Infect Dis* **31,** 499-508.

Chiapello, L.S., Baronetti, J.L., Garro, A.P., Spesso, M.F. and Masih, D.T. (2008). Cryptococcus neoformans glucuronoxylomannan induces macrophage apoptosis mediated by nitric oxide in a caspase-independent pathway. *Int Immunol* **20,** 1527-1541.

Chretien, F., Lortholary, O., Kansau, I., Neuville, S., Gray, F. and Dromer, F. (2002). Pathogenesis of cerebral Cryptococcus neoformans infection after fungemia. *J Infect Dis* **186,** 522-530.

Christianson, T.W., Sikorski, R.S., Dante, M., Shero, J.H. and Hieter, P. (1992). Multifunctional yeast high-copy-number shuttle vectors. *Gene* **110,** 119-122.

Chun, C.D., Liu, O.W. and Madhani, H.D. (2007). A link between virulence and homeostatic responses to hypoxia during infection by the human fungal pathogen Cryptococcus neoformans. *PLoS Pathog* **3,** e22.

Clarke, M., Kohler, J., Arana, Q., Liu, T., Heuser, J. and Gerisch, G. (2002). Dynamics of the vacuolar H(+)-ATPase in the contractile vacuole complex and the endosomal pathway of Dictyostelium cells. *J Cell Sci* **115,** 2893-2905.

Clemons, K.V., Lutz, J.E. and Stevens, D.A. (2001). Efficacy of recombinant gamma interferon for treatment of systemic cryptococcosis in SCID mice. *Antimicrob Agents Chemother* **45,** 686-689.

Coenjaerts, F.E., Hoepelman, A.I., Scharringa, J., Aarts, M., Ellerbroek, P.M., Bevaart, L.*, et al.* (2006). The Skn7 response regulator of Cryptococcus neoformans is involved in oxidative stress signalling and augments intracellular survival in endothelium. *FEMS Yeast Res* **6,** 652-661.

Collins, H.L. and Bancroft, G.J. (1992). Cytokine enhancement of complement-dependent phagocytosis by macrophages: synergy of tumor necrosis factor-alpha and granulocyte-macrophage colony-stimulating factor for phagocytosis of Cryptococcus neoformans. *Eur J Immunol* **22,** 1447-1454.

Cox, G.M., Harrison, T.S., McDade, H.C., Taborda, C.P., Heinrich, G., Casadevall, A. and Perfect, J.R. (2003). Superoxide dismutase influences the virulence of Cryptococcus neoformans by affecting growth within macrophages. *Infect Immun* **71,** 173-180.

Cox, G.M., McDade, H.C., Chen, S.C., Tucker, S.C., Gottfredsson, M., Wright, L.C.*, et al.* (2001). Extracellular phospholipase activity is a virulence factor for Cryptococcus neoformans. *Mol Microbiol* **39,** 166-175.

Cox, G.M., Mukherjee, J., Cole, G.T., Casadevall, A. and Perfect, J.R. (2000). Urease as a virulence factor in experimental cryptococcosis. *Infect Immun* **68,** 443-448.

Cross, C.E., Collins, H.L. and Bancroft, G.J. (1997). CR3-dependent phagocytosis by murine macrophages: different cytokines regulate ingestion of a defined CR3 ligand and complement-opsonized Cryptococcus neoformans. *Immunology* **91,** 289-296.

Crowley, M., Inaba, K. and Steinman, R.M. (1990). Dendritic cells are the principal cells in mouse spleen bearing immunogenic fragments of foreign proteins. *J Exp Med* **172,** 383-386.

Currie, B.P., Freundlich, L.F. and Casadevall, A. (1994). Restriction fragment length polymorphism analysis of Cryptococcus neoformans isolates from environmental (pigeon excreta) and clinical sources in New York City. *J Clin Microbiol* **32,** 1188-1192.

Dabiri, G.A., Sanger, J.M., Portnoy, D.A. and Southwick, F.S. (1990). Listeria monocytogenes moves rapidly through the host-cell cytoplasm by inducing directional actin assembly. *Proc Natl Acad Sci U S A* **87,** 6068-6072.

Dam, T.K., Torres, M., Brewer, C.F. and Casadevall, A. (2008). Isothermal titration calorimetry reveals differential binding thermodynamics of variable region-identical antibodies differing in constant region for a univalent ligand. *J Biol Chem* **283,** 31366-31370.

Darling, A.E., Mau, B. and Perna, N.T. (2010). progressiveMauve: multiple genome alignment with gene gain, loss and rearrangement. *PLoS ONE* **5,** e11147.

Datta, K., Bartlett, K.H., Baer, R., Byrnes, E., Galanis, E., Heitman, J.*, et al.* (2009). Spread of Cryptococcus gattii into Pacific Northwest region of the United States. *Emerg Infect Dis* **15,** 1185-1191.

Davidson, R.C., Cruz, M.C., Sia, R.A., Allen, B., Alspaugh, J.A. and Heitman, J. (2000). Gene disruption by biolistic transformation in serotype D strains of Cryptococcus neoformans. *Fungal Genet Biol* **29,** 38-48.

Davies, S.F., Clifford, D.P., Hoidal, J.R. and Repine, J.E. (1982). Opsonic requirements for the uptake of Cryptococcus neoformans by human polymorphonuclear leukocytes and monocytes. *J Infect Dis* **145,** 870-874.

de Jesus-Berrios, M., Liu, L., Nussbaum, J.C., Cox, G.M., Stamler, J.S. and Heitman, J. (2003). Enzymes that counteract nitrosative stress promote fungal virulence. *Curr Biol* **13,** 1963-1968.

Decken, K., Kohler, G., Palmer-Lehmann, K., Wunderlin, A., Mattner, F., Magram, J.*, et al.* (1998). Interleukin-12 is essential for a protective Th1 response in mice infected with Cryptococcus neoformans. *Infect Immun* **66,** 4994-5000.

Del Poeta, M. (2004). Role of phagocytosis in the virulence of Cryptococcus neoformans. *Eukaryot Cell* **3,** 1067-1075.

Devi, S.J. (1996). Preclinical efficacy of a glucuronoxylomannan-tetanus toxoid conjugate vaccine of Cryptococcus neoformans in a murine model. *Vaccine* **14,** 841-844.

Devi, S.J., Schneerson, R., Egan, W., Ulrich, T.J., Bryla, D., Robbins, J.B. and Bennett, J.E. (1991). Cryptococcus neoformans serotype A glucuronoxylomannan-protein conjugate vaccines: synthesis, characterization, and immunogenicity. *Infect Immun* **59,** 3700-3707.

Diamond, R.D. and Bennett, J.E. (1973a). Growth of Cryptococcus neoformans within human macrophages in vitro. *Infect Immun* **7,** 231-236.

Diamond, R.D. and Erickson, N.F., 3rd (1982). Chemotaxis of human neutrophils and monocytes induced by Cryptococcus neoformans. *Infect Immun* **38,** 380-382.

Diamond, R.D., May, J.E., Kane, M., Frank, M.M. and Bennett, J.E. (1973b). The role of late complement components and the alternate complement pathway in experimental cryptococcosis. *Proc Soc Exp Biol Med* **144,** 312-315.

Diamond, R.D., May, J.E., Kane, M.A., Frank, M.M. and Bennett, J.E. (1974). The role of the classical and alternate complement pathways in host defenses against Cryptococcus neoformans infection. *J Immunol* **112,** 2260-2270.

Diamond, R.D., Root, R.K. and Bennett, J.E. (1972). Factors influencing killing of Cryptococcus neoformans by human leukocytes in vitro. *J Infect Dis* **125,** 367-376.

Dong, X., Stothard, P., Forsythe, I.J. and Wishart, D.S. (2004). PlasMapper: a web server for drawing and auto-annotating plasmid maps. *Nucleic Acids Res* **32,** W660-664.

Dong, Z.M. and Murphy, J.W. (1997). Cryptococcal polysaccharides bind to CD18 on human neutrophils. *Infect Immun* **65,** 557-563.

Dromer, F., Charreire, J., Contrepois, A., Carbon, C. and Yeni, P. (1987). Protection of mice against experimental cryptococcosis by anti-Cryptococcus neoformans monoclonal antibody. *Infect Immun* **55,** 749-752.

Dromer, F., Mathoulin-Pelissier, S., Launay, O. and Lortholary, O. (2007). Determinants of disease presentation and outcome during cryptococcosis: the CryptoA/D study. *PLoS Med* **4,** e21.

Drose, S. and Altendorf, K. (1997). Bafilomycins and concanamycins as inhibitors of V-ATPases and P-ATPases. *J Exp Biol* **200,** 1-8.

Edman, J.C. and Kwon-Chung, K.J. (1990). Isolation of the URA5 gene from Cryptococcus neoformans var. neoformans and its use as a selective marker for transformation. *Mol Cell Biol* **10,** 4538-4544.

Eisenhauer, P.B. and Lehrer, R.I. (1992). Mouse neutrophils lack defensins. *Infect Immun* **60,** 3446-3447.

Ellis, D.H. and Pfeiffer, T.J. (1990a). Ecology, life cycle, and infectious propagule of Cryptococcus neoformans. *Lancet* **336,** 923-925.

Ellis, D.H. and Pfeiffer, T.J. (1990b). Natural habitat of Cryptococcus neoformans var. gattii. *J Clin Microbiol* **28,** 1642-1644.

Emmons, C.W. (1960). Prevalence of Cryptococcus neoformans in pigeon habitats. *Public Health Rep* **75,** 362-364.

Ernst, W.A., Thoma-Uszynski, S., Teitelbaum, R., Ko, C., Hanson, D.A., Clayberger, C., *et al.* (2000). Granulysin, a T cell product, kills bacteria by altering membrane permeability. *J Immunol* **165,** 7102-7108.

Fan, W., Kraus, P.R., Boily, M.J. and Heitman, J. (2005). Cryptococcus neoformans gene expression during murine macrophage infection. *Eukaryot Cell* **4,** 1420-1433.

Feldmesser, M., Kress, Y. and Casadevall, A. (2001a). Dynamic changes in the morphology of Cryptococcus neoformans during murine pulmonary infection. *Microbiology* **147,** 2355-2365.

Feldmesser, M., Kress, Y., Novikoff, P. and Casadevall, A. (2000). Cryptococcus neoformans is a facultative intracellular pathogen in murine pulmonary infection. *Infect Immun* **68,** 4225-4237.

Feldmesser, M., Mednick, A. and Casadevall, A. (2002). Antibody-mediated protection in murine Cryptococcus neoformans infection is associated with

pleotrophic effects on cytokine and leukocyte responses. *Infect Immun* **70,** 1571-1580.

Feldmesser, M., Tucker, S. and Casadevall, A. (2001b). Intracellular parasitism of macrophages by Cryptococcus neoformans. *Trends Microbiol* **9,** 273-278.

Ferreira, T., Mason, A.B. and Slayman, C.W. (2001). The yeast Pma1 proton pump: a model for understanding the biogenesis of plasma membrane proteins. *J Biol Chem* **276,** 29613-29616.

Findley, K., Rodriguez-Carres, M., Metin, B., Kroiss, J., Fonseca, A., Vilgalys, R. and Heitman, J. (2009). Phylogeny and phenotypic characterization of pathogenic Cryptococcus species and closely related saprobic taxa in the Tremellales. *Eukaryot Cell* **8,** 353-361.

Fisk, H.A. and Yaffe, M.P. (1999). A role for ubiquitination in mitochondrial inheritance in Saccharomyces cerevisiae. *J Cell Biol* **145,** 1199-1208.

Flesch, I.E., Schwamberger, G. and Kaufmann, S.H. (1989). Fungicidal activity of IFN-gamma-activated macrophages. Extracellular killing of Cryptococcus neoformans. *J Immunol* **142,** 3219-3224.

Fleuridor, R., Lyles, R.H. and Pirofski, L. (1999). Quantitative and qualitative differences in the serum antibody profiles of human immunodeficiency virus-infected persons with and without Cryptococcus neoformans meningitis. *J Infect Dis* **180,** 1526-1535.

Fleuridor, R., Zhong, Z. and Pirofski, L. (1998). A human IgM monoclonal antibody prolongs survival of mice with lethal cryptococcosis. *J Infect Dis* **178,** 1213-1216.

Folger, K.R., Wong, E.A., Wahl, G. and Capecchi, M.R. (1982). Patterns of integration of DNA microinjected into cultured mammalian cells: evidence for homologous recombination between injected plasmid DNA molecules. *Mol Cell Biol* **2,** 1372-1387.

Franzot, S.P., Salkin, I.F. and Casadevall, A. (1999). Cryptococcus neoformans var. grubii: separate varietal status for Cryptococcus neoformans serotype A isolates. *J Clin Microbiol* **37,** 838-840.

Fraser, J.A., Subaran, R.L., Nichols, C.B. and Heitman, J. (2003). Recapitulation of the sexual cycle of the primary fungal pathogen Cryptococcus neoformans var. gattii: implications for an outbreak on Vancouver Island, Canada. *Eukaryot Cell* **2,** 1036-1045.

Fridovich, I. (1995). Superoxide radical and superoxide dismutases. *Annu Rev Biochem* **64,** 97-112.

Fries, B.C., Taborda, C.P., Serfass, E. and Casadevall, A. (2001). Phenotypic switching of Cryptococcus neoformans occurs in vivo and influences the outcome of infection. *J Clin Invest* **108,** 1639-1648.

Fritz, S., Weinbach, N. and Westermann, B. (2003). Mdm30 is an F-box protein required for maintenance of fusion-competent mitochondria in yeast. *Mol Biol Cell* **14,** 2303-2313.

Gadebusch, H.H. and Johnson, A.G. (1966). Natural host resistance to infection with Cryptococcus neoformans. IV. The effect of some cationic proteins on the experimental disease. *J Infect Dis* **116,** 551-565.

Gaigg, B., Timischl, B., Corbino, L. and Schneiter, R. (2005). Synthesis of sphingolipids with very long chain fatty acids but not ergosterol is required

for routing of newly synthesized plasma membrane ATPase to the cell surface of yeast. *J Biol Chem* **280,** 22515-22522.

Garcia-Hermoso, D., Janbon, G. and Dromer, F. (1999). Epidemiological evidence for dormant Cryptococcus neoformans infection. *J Clin Microbiol* **37,** 3204-3209.

Gates, M.A. and Kozel, T.R. (2006). Differential localization of complement component 3 within the capsular matrix of Cryptococcus neoformans. *Infect Immun* **74,** 3096-3106.

Gerik, K.J., Bhimireddy, S.R., Ryerse, J.S., Specht, C.A. and Lodge, J.K. (2008). PKC1 is essential for protection against both oxidative and nitrosative stresses, cell integrity, and normal manifestation of virulence factors in the pathogenic fungus Cryptococcus neoformans. *Eukaryot Cell* **7,** 1685-1698.

Geunes-Boyer, S., Oliver, T.N., Janbon, G., Lodge, J.K., Heitman, J., Perfect, J.R. and Wright, J.R. (2009). Surfactant protein D increases phagocytosis of hypocapsular Cryptococcus neoformans by murine macrophages and enhances fungal survival. *Infect Immun* **77,** 2783-2794.

Ghannoum, M.A. (2000). Potential role of phospholipases in virulence and fungal pathogenesis. *Clin Microbiol Rev* **13,** 122-143, table of contents.

Goldman, D.L., Khine, H., Abadi, J., Lindenberg, D.J., Pirofski, L., Niang, R. and Casadevall, A. (2001). Serologic evidence for Cryptococcus neoformans infection in early childhood. *Pediatrics* **107,** E66.

Goldman, D.L., Lee, S.C., Mednick, A.J., Montella, L. and Casadevall, A. (2000). Persistent Cryptococcus neoformans pulmonary infection in the rat is associated with intracellular parasitism, decreased inducible nitric oxide synthase expression, and altered antibody responsiveness to cryptococcal polysaccharide. *Infect Immun* **68,** 832-838.

Goldstein, A.L. and McCusker, J.H. (1999). Three new dominant drug resistance cassettes for gene disruption in Saccharomyces cerevisiae. *Yeast* **15,** 1541-1553.

Gordon, S. (2003). Alternative activation of macrophages. *Nat Rev Immunol* **3,** 23-35.

Granger, D.L., Perfect, J.R. and Durack, D.T. (1985). Virulence of Cryptococcus neoformans. Regulation of capsule synthesis by carbon dioxide. *J Clin Invest* **76,** 508-516.

Granier, F., Kanitakis, J., Hermier, C., Zhu, Y.Y. and Thivolet, J. (1987). Localized cutaneous cryptococcosis successfully treated with ketoconazole. *J Am Acad Dermatol* **16,** 243-249.

Grant, C.M., MacIver, F.H. and Dawes, I.W. (1997). Mitochondrial function is required for resistance to oxidative stress in the yeast Saccharomyces cerevisiae. *FEBS Lett* **410,** 219-222.

Graybill, J.R., Hague, M. and Drutz, D.J. (1981). Passive immunization in murine cryptococcosis. *Sabouraudia* **19,** 237-244.

Griffin, F.M., Jr. (1981). Roles of macrophage Fc and C3b receptors in phagocytosis of immunologically coated Cryptococcus neoformans. *Proc Natl Acad Sci U S A* **78,** 3853-3857.

Guerrero, A., Jain, N., Wang, X. and Fries, B.C. (2010). Cryptococcus neoformans variants generated by phenotypic switching differ in virulence through effects on macrophage activation. *Infect Immun*.

Gutierrez, M.G., Master, S.S., Singh, S.B., Taylor, G.A., Colombo, M.I. and Deretic, V. (2004). Autophagy is a defense mechanism inhibiting BCG and Mycobacterium tuberculosis survival in infected macrophages. *Cell* **119,** 753-766.

Harrison, T.S. (2000). Cryptococcus neoformans and cryptococcosis. *J Infect* **41,** 12-17.

Harrison, T.S., Chen, J., Simons, E. and Levitz, S.M. (2002). Determination of the pH of the Cryptococcus neoformans vacuole. *Med Mycol* **40,** 329-332.

Hendry, A.T. and Bakerspigel, A. (1969). Factors affecting serum inhibited growth of Candida albicans and Cryptococcus neoformans. *Sabouraudia* **7,** 219-229.

Hesse, M., Modolell, M., La Flamme, A.C., Schito, M., Fuentes, J.M., Cheever, A.W.*, et al.* (2001). Differential regulation of nitric oxide synthase-2 and arginase-1 by type 1/type 2 cytokines in vivo: granulomatous pathology is shaped by the pattern of L-arginine metabolism. *J Immunol* **167,** 6533-6544.

Heung, L.J., Luberto, C., Plowden, A., Hannun, Y.A. and Del Poeta, M. (2004). The sphingolipid pathway regulates Pkc1 through the formation of diacylglycerol in Cryptococcus neoformans. *J Biol Chem* **279,** 21144-21153.

Hibbs, J.B., Jr., Taintor, R.R. and Vavrin, Z. (1987). Macrophage cytotoxicity: role for L-arginine deiminase and imino nitrogen oxidation to nitrite. *Science* **235,** 473-476.

Higgins, S.C., Jarnicki, A.G., Lavelle, E.C. and Mills, K.H. (2006). TLR4 mediates vaccine-induced protective cellular immunity to Bordetella pertussis: role of IL-17-producing T cells. *J Immunol* **177,** 7980-7989.

Hitchcock, A.L., Auld, K., Gygi, S.P. and Silver, P.A. (2003). A subset of membrane-associated proteins is ubiquitinated in response to mutations in the endoplasmic reticulum degradation machinery. *Proc Natl Acad Sci U S A* **100,** 12735-12740.

Hoag, K.A., Lipscomb, M.F., Izzo, A.A. and Street, N.E. (1997). IL-12 and IFN-gamma are required for initiating the protective Th1 response to pulmonary cryptococcosis in resistant C.B-17 mice. *Am J Respir Cell Mol Biol* **17,** 733-739.

Hoang, L.M., Maguire, J.A., Doyle, P., Fyfe, M. and Roscoe, D.L. (2004). Cryptococcus neoformans infections at Vancouver Hospital and Health Sciences Centre (1997-2002): epidemiology, microbiology and histopathology. *J Med Microbiol* **53,** 935-940.

Holyoak, C.D., Stratford, M., McMullin, Z., Cole, M.B., Crimmins, K., Brown, A.J. and Coote, P.J. (1996). Activity of the plasma membrane H(+)-ATPase and optimal glycolytic flux are required for rapid adaptation and growth of Saccharomyces cerevisiae in the presence of the weak-acid preservative sorbic acid. *Appl Environ Microbiol* **62,** 3158-3164.

Horowitz, H., Christie, G.E. and Platt, T. (1982). Nucleotide sequence of the trpD gene, encoding anthranilate synthetase component II of Escherichia coli. *J Mol Biol* **156,** 245-256.

Horwitz, M.A. (1983). The Legionnaires' disease bacterium (Legionella pneumophila) inhibits phagosome-lysosome fusion in human monocytes. *J Exp Med* **158,** 2108-2126.

Houpt, D.C., Pfrommer, G.S., Young, B.J., Larson, T.A. and Kozel, T.R. (1994). Occurrences, immunoglobulin classes, and biological activities of antibodies in normal human serum that are reactive with Cryptococcus neoformans glucuronoxylomannan. *Infect Immun* **62,** 2857-2864.

Hu, G., Hacham, M., Waterman, S.R., Panepinto, J., Shin, S., Liu, X*., et al.* (2008). PI3K signaling of autophagy is required for starvation tolerance and virulenceof Cryptococcus neoformans. *J Clin Invest* **118,** 1186-1197.

Hu, G. and Kronstad, J.W. (2010). A putative P-type ATPase, Apt1, is involved in stress tolerance and virulence in Cryptococcus neoformans. *Eukaryot Cell* **9,** 74-83.

Hu, M., Jex, A.R., Campbell, B.E. and Gasser, R.B. (2007). Long PCR amplification of the entire mitochondrial genome from individual helminths for direct sequencing. *Nat Protoc* **2,** 2339-2344.

Huffnagle, G.B. (1996). Role of cytokines in T cell immunity to a pulmonary Cryptococcus neoformans infection. *Biol Signals* **5,** 215-222.

Huffnagle, G.B., Chen, G.H., Curtis, J.L., McDonald, R.A., Strieter, R.M. and Toews, G.B. (1995). Down-regulation of the afferent phase of T cell-mediated pulmonary inflammation and immunity by a high melanin-producing strain of Cryptococcus neoformans. *J Immunol* **155,** 3507-3516.

Hughes, A.L., Todd, B.L. and Espenshade, P.J. (2005). SREBP pathway responds to sterols and functions as an oxygen sensor in fission yeast. *Cell* **120,** 831-842.

Hull, C.M. and Heitman, J. (2002). Genetics of Cryptococcus neoformans. *Annu Rev Genet* **36,** 557-615.

Huynh, K.K., Kay, J.G., Stow, J.L. and Grinstein, S. (2007). Fusion, fission, and secretion during phagocytosis. *Physiology (Bethesda)* **22,** 366-372.

Hybiske, K. and Stephens, R.S. (2007). Mechanisms of host cell exit by the intracellular bacterium Chlamydia. *Proc Natl Acad Sci U S A* **104,** 11430-11435.

Ibrahim, A.S., Filler, S.G., Alcouloumre, M.S., Kozel, T.R., Edwards, J.E., Jr. and Ghannoum, M.A. (1995). Adherence to and damage of endothelial cells by Cryptococcus neoformans in vitro: role of the capsule. *Infect Immun* **63,** 4368-4374.

Idnurm, A., Bahn, Y.S., Nielsen, K., Lin, X., Fraser, J.A. and Heitman, J. (2005). Deciphering the model pathogenic fungus Cryptococcus neoformans. *Nat Rev Microbiol* **3,** 753-764.

Idnurm, A., Reedy, J.L., Nussbaum, J.C. and Heitman, J. (2004). Cryptococcus neoformans virulence gene discovery through insertional mutagenesis. *Eukaryot Cell* **3,** 420-429.

Igel, H.J. and Bolande, R.P. (1966). Humoral defense mechanisms in cryptococcosis: substances in normal human serum, saliva, and cerebrospinal fluid affecting the growth of Cryptococcus neoformans. *J Infect Dis* **116,** 75-83.

Ingavale, S.S., Chang, Y.C., Lee, H., McClelland, C.M., Leong, M.L. and Kwon-Chung, K.J. (2008). Importance of mitochondria in survival of Cryptococcus

neoformans under low oxygen conditions and tolerance to cobalt chloride. *PLoS Pathog* **4,** e1000155.

Jain, N., Li, L., McFadden, D.C., Banarjee, U., Wang, X., Cook, E. and Fries, B.C. (2006). Phenotypic switching in a Cryptococcus neoformans variety gattii strain is associated with changes in virulence and promotes dissemination to the central nervous system. *Infect Immun* **74,** 896-903.

Janeway, C.A., Travers, P., Walport, M. and Shlomchik, M. (2001) Immunobiology. The immune system in health and disease. 5th edition., Garland Science.

Jarvis, J.N. and Harrison, T.S. (2007). HIV-associated cryptococcal meningitis. *AIDS* **21,** 2119-2129.

Jex, A.R., Hu, M., Littlewood, D.T., Waeschenbach, A. and Gasser, R.B. (2008). Using 454 technology for long-PCR based sequencing of the complete mitochondrial genome from single Haemonchus contortus (Nematoda). *BMC Genomics* **9,** 11.

Johnston, S.A. and May, R.C. (2010). The Human Fungal Pathogen Cryptococcus neoformans Escapes Macrophages by a Phagosome Emptying Mechanism That Is Inhibited by Arp2/3 Complex-Mediated Actin Polymerisation. *PLoS Pathog* **6**.

Jung, W.H., Hu, G., Kuo, W. and Kronstad, J.W. (2009). Role of ferroxidases in iron uptake and virulence of Cryptococcus neoformans. *Eukaryot Cell* **8,** 1511-1520.

Karlyshev, A.V., Pallen, M.J. and Wren, B.W. (2000). Single-primer PCR procedure for rapid identification of transposon insertion sites. *Biotechniques* **28,** 1078, 1080, 1082.

Kawakami, K. (2004). Regulation by innate immune T lymphocytes in the host defense against pulmonary infection with Cryptococcus neoformans. *Jpn J Infect Dis* **57,** 137-145.

Kawakami, K., Hossain Qureshi, M., Zhang, T., Koguchi, Y., Xie, Q., Kurimoto, M. and Saito, A. (1999). Interleukin-4 weakens host resistance to pulmonary and disseminated cryptococcal infection caused by combined treatment with interferon-gamma-inducing cytokines. *Cell Immunol* **197,** 55-61.

Kawakami, K., Kinjo, Y., Yara, S., Uezu, K., Koguchi, Y., Tohyama, M.*, et al.* (2001). Enhanced gamma interferon production through activation of Valpha14(+) natural killer T cells by alpha-galactosylceramide in interleukin-18-deficient mice with systemic cryptococcosis. *Infect Immun* **69,** 6643-6650.

Kawakami, K., Kohno, S., Kadota, J., Tohyama, M., Teruya, K., Kudeken, N.*, et al.* (1995). T cell-dependent activation of macrophages and enhancement of their phagocytic activity in the lungs of mice inoculated with heat-killed Cryptococcus neoformans: involvement of IFN-gamma and its protective effect against cryptococcal infection. *Microbiol Immunol* **39,** 135-143.

Kechichian, T.B., Shea, J. and Del Poeta, M. (2007). Depletion of alveolar macrophages decreases the dissemination of a glucosylceramide-deficient mutant of Cryptococcus neoformans in immunodeficient mice. *Infect Immun* **75,** 4792-4798.

Kelly, R.M., Chen, J., Yauch, L.E. and Levitz, S.M. (2005). Opsonic requirements for dendritic cell-mediated responses to Cryptococcus neoformans. *Infect Immun* **73,** 592-598.

Khawcharoenporn, T., Apisarnthanarak, A. and Mundy, L.M. (2007). Non-neoformans cryptococcal infections: a systematic review. *Infection* **35,** 51-58.

Kidd, S.E., Bach, P.J., Hingston, A.O., Mak, S., Chow, Y., MacDougall, L.*, et al.* (2007). Cryptococcus gattii dispersal mechanisms, British Columbia, Canada. *Emerg Infect Dis* **13,** 51-57.

Kidd, S.E., Guo, H., Bartlett, K.H., Xu, J. and Kronstad, J.W. (2005). Comparative gene genealogies indicate that two clonal lineages of Cryptococcus gattii in British Columbia resemble strains from other geographical areas. *Eukaryot Cell* **4,** 1629-1638.

Kidd, S.E., Hagen, F., Tscharke, R.L., Huynh, M., Bartlett, K.H., Fyfe, M.*, et al.* (2004). A rare genotype of Cryptococcus gattii caused the cryptococcosis outbreak on Vancouver Island (British Columbia, Canada). *Proc Natl Acad Sci U S A* **101,** 17258-17263.

Kihara, A., Noda, T., Ishihara, N. and Ohsumi, Y. (2001). Two distinct Vps34 phosphatidylinositol 3-kinase complexes function in autophagy and carboxypeptidase Y sorting in Saccharomyces cerevisiae. *J Cell Biol* **152,** 519-530.

Kleinschek, M.A., Muller, U., Brodie, S.J., Stenzel, W., Kohler, G., Blumenschein, W.M.*, et al.* (2006). IL-23 enhances the inflammatory cell response in Cryptococcus neoformans infection and induces a cytokine pattern distinct from IL-12. *J Immunol* **176,** 1098-1106.

Knodler, L.A., Bestor, A., Ma, C., Hansen-Wester, I., Hensel, M., Vallance, B.A. and Steele-Mortimer, O. (2005). Cloning vectors and fluorescent proteins can significantly inhibit Salmonella enterica virulence in both epithelial cells and macrophages: implications for bacterial pathogenesis studies. *Infect Immun* **73,** 7027-7031.

Koch, G., Tanaka, K., Masuda, T., Yamochi, W., Nonaka, H. and Takai, Y. (1997). Association of the Rho family small GTP-binding proteins with Rho GDP dissociation inhibitor (Rho GDI) in Saccharomyces cerevisiae. *Oncogene* **15,** 417-422.

Koguchi, Y. and Kawakami, K. (2002). Cryptococcal infection and Th1-Th2 cytokine balance. *Int Rev Immunol* **21,** 423-438.

Kozel, T.R. (1993a). Activation of the complement system by the capsule of Cryptococcus neoformans. *Curr Top Med Mycol* **5,** 1-26.

Kozel, T.R. (1993b). Opsonization and phagocytosis of Cryptococcus neoformans. *Arch Med Res* **24,** 211-218.

Kozel, T.R. and Follette, J.L. (1981). Opsonization of encapsulated Cryptococcus neoformans by specific anticapsular antibody. *Infect Immun* **31,** 978-984.

Kozel, T.R., Gulley, W.F. and Cazin, J., Jr. (1977). Immune response to Cryptococcus neoformans soluble polysaccharide: immunological unresponsiveness. *Infect Immun* **18,** 701-707.

Kozel, T.R., Highison, B. and Stratton, C.J. (1984). Localization on encapsulated Cryptococcus neoformans of serum components opsonic for phagocytosis by macrophages and neutrophils. *Infect Immun* **43,** 574-579.

Kozel, T.R. and Pfrommer, G.S. (1986). Activation of the complement system by Cryptococcus neoformans leads to binding of iC3b to the yeast. *Infect Immun* **52,** 1-5.

Kozel, T.R., Pfrommer, G.S., Guerlain, A.S., Highison, B.A. and Highison, G.J. (1988). Strain variation in phagocytosis of Cryptococcus neoformans: dissociation of susceptibility to phagocytosis from activation and binding of opsonic fragments of C3. *Infect Immun* **56,** 2794-2800.

Kozel, T.R., Tabuni, A., Young, B.J. and Levitz, S.M. (1996). Influence of opsonization conditions on C3 deposition and phagocyte binding of large- and small-capsule Cryptococcus neoformans cells. *Infect Immun* **64,** 2336-2338.

Kozel, T.R., Wilson, M.A. and Murphy, J.W. (1991). Early events in initiation of alternative complement pathway activation by the capsule of Cryptococcus neoformans. *Infect Immun* **59,** 3101-3110.

Kozel, T.R., Wilson, M.A., Pfrommer, G.S. and Schlageter, A.M. (1989). Activation and binding of opsonic fragments of C3 on encapsulated Cryptococcus neoformans by using an alternative complement pathway reconstituted from six isolated proteins. *Infect Immun* **57,** 1922-1927.

Kozel, T.R., Wilson, M.A. and Welch, W.H. (1992). Kinetic analysis of the amplification phase for activation and binding of C3 to encapsulated and nonencapsulated Cryptococcus neoformans. *Infect Immun* **60,** 3122-3127.

Kraus, P.R., Boily, M.J., Giles, S.S., Stajich, J.E., Allen, A., Cox, G.M*., et al.* (2004). Identification of Cryptococcus neoformans temperature-regulated genes with a genomic-DNA microarray. *Eukaryot Cell* **3,** 1249-1260.

Krzywinski, M., Schein, J., Birol, I., Connors, J., Gascoyne, R., Horsman, D*., et al.* (2009). Circos: an information aesthetic for comparative genomics. *Genome Res* **19,** 1639-1645.

Kwon-Chung, J., Boekhout, T., Fell, J.W. and Diaz, M. (2002). Proposal to conserve the name *Cryptococcus gattii* against *C. hondurianus* and *C. bacillisporus* (Basidiomycota, Hymenomycetes, Tremellomycetidae). . *Taxon* **51,** 804-806.

Kwon-Chung, K.J., Bennett, J.E. and Rhodes, J.C. (1982). Taxonomic studies on Filobasidiella species and their anamorphs. *Antonie Van Leeuwenhoek* **48,** 25-38.

Kwon-Chung, K.J. and Rhodes, J.C. (1986). Encapsulation and melanin formation as indicators of virulence in Cryptococcus neoformans. *Infect Immun* **51,** 218-223.

La Scolea, L.J., Jr. and Balbinder, E. (1972). Restoration of phosphoribosyl transferase activity by partially deleting the trpB gene in the tryptophan operon of Salmonella typhimurium. *J Bacteriol* **112,** 877-885.

Lambowitz, A.M. and Perlman, P.S. (1990). Involvement of aminoacyl-tRNA synthetases and other proteins in group I and group II intron splicing. *Trends Biochem Sci* **15,** 440-444.

Lang, B.F., Laforest, M.J. and Burger, G. (2007). Mitochondrial introns: a critical view. *Trends Genet* **23,** 119-125.

Larsen, R.A., Pappas, P.G., Perfect, J., Aberg, J.A., Casadevall, A., Cloud, G.A*., et al.* (2005). Phase I evaluation of the safety and pharmacokinetics of murine-

derived anticryptococcal antibody 18B7 in subjects with treated cryptococcal meningitis. *Antimicrob Agents Chemother* **49,** 952-958.

Laxalt, K.A. and Kozel, T.R. (1979). Chemotaxigenesis and activation of the alternative complement pathway by encapsulated and non-encapsulated Cryptococcus neoformans. *Infect Immun* **26,** 435-440.

Lee, H., Bien, C.M., Hughes, A.L., Espenshade, P.J., Kwon-Chung, K.J. and Chang, Y.C. (2007). Cobalt chloride, a hypoxia-mimicking agent, targets sterol synthesis in the pathogenic fungus Cryptococcus neoformans. *Mol Microbiol* **65,** 1018-1033.

Lee, H.-Y., Chou, J.-Y., Cheong, L., Chang, N.-H., Yang, S.-Y. and Leu, J.-Y. (2008). Incompatibility of nuclear and mitochondrial genes causes hybrid sterility between two yeast species. *Cell* **135,** 1065-1073.

Lee, S.C., Kress, Y., Zhao, M.L., Dickson, D.W. and Casadevall, A. (1995). Cryptococcus neoformans survive and replicate in human microglia. *Lab Invest* **73,** 871-879.

Lehrer, R.I. and Ganz, T. (1990). Antimicrobial polypeptides of human neutrophils. *Blood* **76,** 2169-2181.

Levitz, S.M. and DiBenedetto, D.J. (1989). Paradoxical role of capsule in murine bronchoalveolar macrophage-mediated killing of Cryptococcus neoformans. *J Immunol* **142,** 659-665.

Levitz, S.M., Dupont, M.P. and Smail, E.H. (1994). Direct activity of human T lymphocytes and natural killer cells against Cryptococcus neoformans. *Infect Immun* **62,** 194-202.

Levitz, S.M. and Farrell, T.P. (1990). Growth inhibition of Cryptococcus neoformans by cultured human monocytes: role of the capsule, opsonins, the culture surface, and cytokines. *Infect Immun* **58,** 1201-1209.

Levitz, S.M., Harrison, T.S., Tabuni, A. and Liu, X. (1997a). Chloroquine induces human mononuclear phagocytes to inhibit and kill Cryptococcus neoformans by a mechanism independent of iron deprivation. *J Clin Invest* **100,** 1640-1646.

Levitz, S.M., Nong, S.H., Seetoo, K.F., Harrison, T.S., Speizer, R.A. and Simons, E.R. (1999). Cryptococcus neoformans resides in an acidic phagolysosome of human macrophages. *Infect Immun* **67,** 885-890.

Levitz, S.M. and Specht, C.A. (2006). The molecular basis for the immunogenicity of Cryptococcus neoformans mannoproteins. *FEMS Yeast Res* **6,** 513-524.

Levitz, S.M. and Tabuni, A. (1991). Binding of Cryptococcus neoformans by human cultured macrophages. Requirements for multiple complement receptors and actin. *J Clin Invest* **87,** 528-535.

Levitz, S.M., Tabuni, A., Kozel, T.R., MacGill, R.S., Ingalls, R.R. and Golenbock, D.T. (1997b). Binding of Cryptococcus neoformans to heterologously expressed human complement receptors. *Infect Immun* **65,** 931-935.

Lin, X. and Heitman, J. (2006). The biology of the Cryptococcus neoformans species complex. *Annu Rev Microbiol* **60,** 69-105.

Lipovsky, M.M., Gekker, G., Anderson, W.R., Molitor, T.W., Peterson, P.K. and Hoepelman, A.I. (1997). Phagocytosis of nonopsonized Cryptococcus neoformans by swine microglia involves CD14 receptors. *Clin Immunol Immunopathol* **84,** 208-211.

Litvintseva, A.P., Thakur, R., Vilgalys, R. and Mitchell, T.G. (2006). Multilocus sequence typing reveals three genetic subpopulations of Cryptococcus neoformans var. grubii (serotype A), including a unique population in Botswana. *Genetics* **172,** 2223-2238.

Liu, L., Tewari, R.P. and Williamson, P.R. (1999). Laccase protects Cryptococcus neoformans from antifungal activity of alveolar macrophages. *Infect Immun* **67,** 6034-6039.

Liu, X., Hu, G., Panepinto, J. and Williamson, P.R. (2006). Role of a VPS41 homologue in starvation response, intracellular survival and virulence of Cryptococcus neoformans. *Mol Microbiol* **61,** 1132-1146.

Livet, J., Weissman, T.A., Kang, H., Draft, R.W., Lu, J., Bennis, R.A*., et al.* (2007). Transgenic strategies for combinatorial expression of fluorescent proteins in the nervous system. *Nature* **450,** 56-62.

Loftus, B.J., Fung, E., Roncaglia, P., Rowley, D., Amedeo, P., Bruno, D*., et al.* (2005). The genome of the basidiomycetous yeast and human pathogen Cryptococcus neoformans. *Science* **307,** 1321-1324.

Lorenz, M.C. and Heitman, J. (1997). Yeast pseudohyphal growth is regulated by GPA2, a G protein alpha homolog. *EMBO J* **16,** 7008-7018.

Lortholary, O., Poizat, G., Zeller, V., Neuville, S., Boibieux, A., Alvarez, M*., et al.* (2006). Long-term outcome of AIDS-associated cryptococcosis in the era of combination antiretroviral therapy. *AIDS* **20,** 2183-2191.

Lovchik, J.A. and Lipscomb, M.F. (1993). Role for C5 and neutrophils in the pulmonary intravascular clearance of circulating Cryptococcus neoformans. *Am J Respir Cell Mol Biol* **9,** 617-627.

Lovchik, J.A., Lyons, C.R. and Lipscomb, M.F. (1995). A role for gamma interferon-induced nitric oxide in pulmonary clearance of Cryptococcus neoformans. *Am J Respir Cell Mol Biol* **13,** 116-124.

Luberto, C., Martinez-Marino, B., Taraskiewicz, D., Bolanos, B., Chitano, P., Toffaletti, D.L*., et al.* (2003). Identification of App1 as a regulator of phagocytosis and virulence of Cryptococcus neoformans. *J Clin Invest* **112,** 1080-1094.

Luberto, C., Toffaletti, D.L., Wills, E.A., Tucker, S.C., Casadevall, A., Perfect, J.R*., et al.* (2001). Roles for inositol-phosphoryl ceramide synthase 1 (IPC1) in pathogenesis of C. neoformans. *Genes Dev* **15,** 201-212.

Luo, Y., Alvarez, M., Xia, L. and Casadevall, A. (2008). The outcome of phagocytic cell division with infectious cargo depends on single phagosome formation. *PLoS ONE* **3,** e3219.

Luo, Y., Cook, E., Fries, B.C. and Casadevall, A. (2006). Phagocytic efficacy of macrophage-like cells as a function of cell cycle and Fcgamma receptors (FcgammaR) and complement receptor (CR)3 expression. *Clin Exp Immunol* **145,** 380-387.

Lutz, J.E., Clemons, K.V. and Stevens, D.A. (2000). Enhancement of antifungal chemotherapy by interferon-gamma in experimental systemic cryptococcosis. *J Antimicrob Chemother* **46,** 437-442.

Ma, H. (2009) Intracellular parasitism of macrophages by Cryptococcus. In *School of Biosciences*. Birmingham, University of Birmingham, pp. 192.

Ma, H., Croudace, J.E., Lammas, D.A. and May, R.C. (2006). Expulsion of live pathogenic yeast by macrophages. *Curr Biol* **16,** 2156-2160.

Ma, H., Croudace, J.E., Lammas, D.A. and May, R.C. (2007). Direct cell-to-cell spread of a pathogenic yeast. *BMC Immunol* **8,** 15.

Ma, H., Hagen, F., Stekel, D.J., Johnston, S.A., Sionov, E., Falk, R.*, et al.* (2009a). The fatal fungal outbreak on Vancouver Island is characterized by enhanced intracellular parasitism driven by mitochondrial regulation. *Proc Natl Acad Sci U S A* **106,** 12980-12985.

Ma, H. and May, R.C. (2009b). Virulence in Cryptococcus species. *Adv Appl Microbiol* **67,** 131-190.

Ma, L.L., Spurrell, J.C., Wang, J.F., Neely, G.G., Epelman, S., Krensky, A.M. and Mody, C.H. (2002). CD8 T cell-mediated killing of Cryptococcus neoformans requires granulysin and is dependent on CD4 T cells and IL-15. *J Immunol* **169,** 5787-5795.

Ma, L.L., Wang, C.L., Neely, G.G., Epelman, S., Krensky, A.M. and Mody, C.H. (2004). NK cells use perforin rather than granulysin for anticryptococcal activity. *J Immunol* **173,** 3357-3365.

MacDougall, L., Kidd, S.E., Galanis, E., Mak, S., Leslie, M.J., Cieslak, P.R.*, et al.* (2007). Spread of Cryptococcus gattii in British Columbia, Canada, and detection in the Pacific Northwest, USA. *Emerg Infect Dis* **13,** 42-50.

Macher, A.M., Bennett, J.E., Gadek, J.E. and Frank, M.M. (1978). Complement depletion in cryptococcal sepsis. *J Immunol* **120,** 1686-1690.

Maligie, M.A. and Selitrennikoff, C.P. (2005). Cryptococcus neoformans resistance to echinocandins: (1,3)beta-glucan synthase activity is sensitive to echinocandins. *Antimicrob Agents Chemother* **49,** 2851-2856.

Mambula, S.S., Simons, E.R., Hastey, R., Selsted, M.E. and Levitz, S.M. (2000). Human neutrophil-mediated nonoxidative antifungal activity against Cryptococcus neoformans. *Infect Immun* **68,** 6257-6264.

Mansour, M.K., Latz, E. and Levitz, S.M. (2006). Cryptococcus neoformans glycoantigens are captured by multiple lectin receptors and presented by dendritic cells. *J Immunol* **176,** 3053-3061.

Marr, K.J., Jones, G.J., Zheng, C., Huston, S.M., Timm-McCann, M., Islam, A.*, et al.* (2009). Cryptococcus neoformans directly stimulates perforin production and rearms NK cells for enhanced anticryptococcal microbicidal activity. *Infect Immun* **77,** 2436-2446.

May, R.C., Hall, M.E., Higgs, H.N., Pollard, T.D., Chakraborty, T., Wehland, J.*, et al.* (1999). The Arp2/3 complex is essential for the actin-based motility of Listeria monocytogenes. *Curr Biol* **9,** 759-762.

McClelland, C.M., Chang, Y.C. and Kwon-Chung, K.J. (2005). High frequency transformation of Cryptococcus neoformans and Cryptococcus gattii by Agrobacterium tumefaciens. *Fungal Genet Biol* **42,** 904-913.

McGaw, T.G. and Kozel, T.R. (1979). Opsonization of Cryptococcus neoformans by human immunoglobulin G: masking of immunoglobulin G by cryptococcal polysaccharide. *Infect Immun* **25,** 262-267.

Mednick, A.J., Feldmesser, M., Rivera, J. and Casadevall, A. (2003). Neutropenia alters lung cytokine production in mice and reduces their susceptibility to pulmonary cryptococcosis. *Eur J Immunol* **33,** 1744-1753.

Meeusen, S. and Nunnari, J. (2003). Evidence for a two membrane-spanning autonomous mitochondrial DNA replisome. *J Cell Biol* **163,** 503-510.

Mershon, K.L., Vasuthasawat, A., Lawson, G.W., Morrison, S.L. and Beenhouwer, D.O. (2009). Role of complement in protection against Cryptococcus gattii infection. *Infect Immun* **77,** 1061-1070.

Meyer, W., Aanensen, D.M., Boekhout, T., Cogliati, M., Diaz, M.R., Esposto, M.C.*, et al.* (2009). Consensus multi-locus sequence typing scheme for Cryptococcus neoformans and Cryptococcus gattii. *Med Mycol***,** 1-14.

Meyer, W., Castaneda, A., Jackson, S., Huynh, M. and Castaneda, E. (2003). Molecular typing of IberoAmerican Cryptococcus neoformans isolates. *Emerg Infect Dis* **9,** 189-195.

Meyer, W., Marszewska, K., Amirmostofian, M., Igreja, R.P., Hardtke, C., Methling, K.*, et al.* (1999). Molecular typing of global isolates of Cryptococcus neoformans var. neoformans by polymerase chain reaction fingerprinting and randomly amplified polymorphic DNA-a pilot study to standardize techniques on which to base a detailed epidemiological survey. *Electrophoresis* **20,** 1790-1799.

Milam, J.E., Herring-Palmer, A.C., Pandrangi, R., McDonald, R.A., Huffnagle, G.B. and Toews, G.B. (2007). Modulation of the pulmonary type 2 T-cell response to Cryptococcus neoformans by intratracheal delivery of a tumor necrosis factor alpha-expressing adenoviral vector. *Infect Immun* **75,** 4951-4958.

Miller, M.F. and Mitchell, T.G. (1991). Killing of Cryptococcus neoformans strains by human neutrophils and monocytes. *Infect Immun* **59,** 24-28.

Missall, T.A., Pusateri, M.E. and Lodge, J.K. (2004). Thiol peroxidase is critical for virulence and resistance to nitric oxide and peroxide in the fungal pathogen, Cryptococcus neoformans. *Mol Microbiol* **51,** 1447-1458.

Mitchell, A.P. (2006). Cryptococcal virulence: beyond the usual suspects. *J Clin Invest* **116,** 1481-1483.

Mitchell, T.G. and Friedman, L. (1972). In vitro phagocytosis and intracellular fate of variously encapsulated strains of Cryptococcus neoformans. *Infect Immun* **5,** 491-498.

Mitchell, T.G. and Perfect, J.R. (1995). Cryptococcosis in the era of AIDS--100 years after the discovery of Cryptococcus neoformans. *Clin Microbiol Rev* **8,** 515-548.

Monari, C., Casadevall, A., Pietrella, D., Bistoni, F. and Vecchiarelli, A. (1999). Neutrophils from patients with advanced human immunodeficiency virus infection have impaired complement receptor function and preserved Fcgamma receptor function. *J Infect Dis* **180,** 1542-1549.

Monari, C., Retini, C., Casadevall, A., Netski, D., Bistoni, F., Kozel, T.R. and Vecchiarelli, A. (2003). Differences in outcome of the interaction between Cryptococcus neoformans glucuronoxylomannan and human monocytes and neutrophils. *Eur J Immunol* **33,** 1041-1051.

Mondon, P., Petter, R., Amalfitano, G., Luzzati, R., Concia, E., Polacheck, I. and Kwon-Chung, K.J. (1999). Heteroresistance to fluconazole and voriconazole in Cryptococcus neoformans. *Antimicrob Agents Chemother* **43,** 1856-1861.

Mosmann, T.R. and Coffman, R.L. (1989). TH1 and TH2 cells: different patterns of lymphokine secretion lead to different functional properties. *Annu Rev Immunol* **7,** 145-173.

Mucci, A., Varesio, L., Neglia, R., Colombari, B., Pastorino, S. and Blasi, E. (2003). Antifungal activity of macrophages engineered to produce IFNgamma: inducibility by picolinic acid. *Med Microbiol Immunol* **192,** 71-78.

Mukherjee, J., Nussbaum, G., Scharff, M.D. and Casadevall, A. (1995). Protective and nonprotective monoclonal antibodies to Cryptococcus neoformans originating from one B cell. *J Exp Med* **181,** 405-409.

Mukherjee, J., Scharff, M.D. and Casadevall, A. (1992). Protective murine monoclonal antibodies to Cryptococcus neoformans. *Infect Immun* **60,** 4534-4541.

Mukherjee, J., Zuckier, L.S., Scharff, M.D. and Casadevall, A. (1994). Therapeutic efficacy of monoclonal antibodies to Cryptococcus neoformans glucuronoxylomannan alone and in combination with amphotericin B. *Antimicrob Agents Chemother* **38,** 580-587.

Muller, U., Stenzel, W., Kohler, G., Werner, C., Polte, T., Hansen, G.*, et al.* (2007). IL-13 induces disease-promoting type 2 cytokines, alternatively activated macrophages and allergic inflammation during pulmonary infection of mice with Cryptococcus neoformans. *J Immunol* **179,** 5367-5377.

Murray, H.W. and Cartelli, D.M. (1983). Killing of intracellular Leishmania donovani by human mononuclear phagocytes. Evidence for oxygen-dependent and -independent leishmanicidal activity. *J Clin Invest* **72,** 32-44.

Murray, H.W., Spitalny, G.L. and Nathan, C.F. (1985). Activation of mouse peritoneal macrophages in vitro and in vivo by interferon-gamma. *J Immunol* **134,** 1619-1622.

Mwaba, P., Mwansa, J., Chintu, C., Pobee, J., Scarborough, M., Portsmouth, S. and Zumla, A. (2001). Clinical presentation, natural history, and cumulative death rates of 230 adults with primary cryptococcal meningitis in Zambian AIDS patients treated under local conditions. *Postgrad Med J* **77,** 769-773.

Nadrous, H.F., Antonios, V.S., Terrell, C.L. and Ryu, J.H. (2003). Pulmonary cryptococcosis in nonimmunocompromised patients. *Chest* **124,** 2143-2147.

Nakano, K., Mutoh, T., Arai, R. and Mabuchi, I. (2003). The small GTPase Rho4 is involved in controlling cell morphology and septation in fission yeast. *Genes Cells* **8,** 357-370.

Nanno, M., Shiohara, T., Yamamoto, H., Kawakami, K. and Ishikawa, H. (2007). gammadelta T cells: firefighters or fire boosters in the front lines of inflammatory responses. *Immunol Rev* **215,** 103-113.

Nassar, F., Brummer, E. and Stevens, D.A. (1995). Different components in human serum inhibit multiplication of Cryptococcus neoformans and enhance fluconazole activity. *Antimicrob Agents Chemother* **39,** 2490-2493.

Netea, M.G., Brouwer, A.E., Hoogendoorn, E.H., Van der Meer, J.W., Koolen, M., Verweij, P.E. and Kullberg, B.J. (2004). Two patients with cryptococcal meningitis and idiopathic CD4 lymphopenia: defective cytokine production and reversal by recombinant interferon- gamma therapy. *Clin Infect Dis* **39,** e83-87.

Netski, D. and Kozel, T.R. (2002). Fc-dependent and Fc-independent opsonization of Cryptococcus neoformans by anticapsular monoclonal antibodies: importance of epitope specificity. *Infect Immun* **70,** 2812-2819.

Nichols, C.B., Perfect, Z.H. and Alspaugh, J.A. (2007). A Ras1-Cdc24 signal transduction pathway mediates thermotolerance in the fungal pathogen Cryptococcus neoformans. *Mol Microbiol* **63,** 1118-1130.

Noverr, M.C., Cox, G.M., Perfect, J.R. and Huffnagle, G.B. (2003). Role of PLB1 in pulmonary inflammation and cryptococcal eicosanoid production. *Infect Immun* **71,** 1538-1547.

Noverr, M.C., Phare, S.M., Toews, G.B., Coffey, M.J. and Huffnagle, G.B. (2001). Pathogenic yeasts Cryptococcus neoformans and Candida albicans produce immunomodulatory prostaglandins. *Infect Immun* **69,** 2957-2963.

Nussbaum, G., Cleare, W., Casadevall, A., Scharff, M.D. and Valadon, P. (1997). Epitope location in the Cryptococcus neoformans capsule is a determinant of antibody efficacy. *J Exp Med* **185,** 685-694.

Oh-hama, T. (1997). Evolutionary consideration on 5-aminolevulinate synthase in nature. *Orig Life Evol Biosph* **27,** 405-412.

Okagaki, L.H., Strain, A.K., Nielsen, J.N., Charlier, C., Baltes, N.J., Chretien, F.*, et al.* (2010). Cryptococcal cell morphology affects host cell interactions and pathogenicity. *PLoS Pathog* **6,** e1000953.

Okamoto, K. and Shaw, J.M. (2005). Mitochondrial morphology and dynamics in yeast and multicellular eukaryotes. *Annu Rev Genet* **39,** 503-536.

Oliveira, D.L., Freire-de-Lima, C.G., Nosanchuk, J.D., Casadevall, A., Rodrigues, M.L. and Nimrichter, L. (2010). Extracellular vesicles from Cryptococcus neoformans modulate macrophage functions. *Infect Immun* **78,** 1601-1609.

Olson, A. and Stenlid, J. (2001). Plant pathogens. Mitochondrial control of fungal hybrid virulence. *Nature* **411,** 438.

Osterholzer, J.J., Milam, J.E., Chen, G.H., Toews, G.B., Huffnagle, G.B. and Olszewski, M.A. (2009a). Role of dendritic cells and alveolar macrophages in regulating early host defense against pulmonary infection with Cryptococcus neoformans. *Infect Immun* **77,** 3749-3758.

Osterholzer, J.J., Surana, R., Milam, J.E., Montano, G.T., Chen, G.H., Sonstein, J.*, et al.* (2009b). Cryptococcal urease promotes the accumulation of immature dendritic cells and a non-protective T2 immune response within the lung. *Am J Pathol* **174,** 932-943.

Panepinto, J.C., Komperda, K.W., Hacham, M., Shin, S., Liu, X. and Williamson, P.R. (2007). Binding of serum mannan binding lectin to a cell integrity-defective Cryptococcus neoformans ccr4Delta mutant. *Infect Immun* **75,** 4769-4779.

Park, B.J., Wannemuehler, K.A., Marston, B.J., Govender, N., Pappas, P.G. and Chiller, T.M. (2009). Estimation of the current global burden of cryptococcal meningitis among persons living with HIV/AIDS. *AIDS* **23,** 525-530.

Pasko, M.T., Piscitelli, S.C. and Van Slooten, A.D. (1990). Fluconazole: a new triazole antifungal agent. *DICP* **24,** 860-867.

Patton, E.E., Willems, A.R. and Tyers, M. (1998). Combinatorial control in ubiquitin-dependent proteolysis: don't Skp the F-box hypothesis. *Trends Genet* **14,** 236-243.

Perfect, J.R., Dismukes, W.E., Dromer, F., Goldman, D.L., Graybill, J.R., Hamill, R.J.*, et al.* (2010). Clinical practice guidelines for the management of cryptococcal disease: 2010 update by the infectious diseases society of america. *Clin Infect Dis* **50,** 291-322.

Perfect, J.R., Lang, S.D. and Durack, D.T. (1980). Chronic cryptococcal meningitis: a new experimental model in rabbits. *Am J Pathol* **101,** 177-194.

Perlman, P.S. and Butow, R.A. (1989). Mobile introns and intron-encoded proteins. *Science* **246,** 1106-1109.

Pfeiffer, T.J. and Ellis, D.H. (1992). Environmental isolation of Cryptococcus neoformans var. gattii from Eucalyptus tereticornis. *J Med Vet Mycol* **30,** 407-408.

Pfrommer, G.S., Dickens, S.M., Wilson, M.A., Young, B.J. and Kozel, T.R. (1993). Accelerated decay of C3b to iC3b when C3b is bound to the Cryptococcus neoformans capsule. *Infect Immun* **61,** 4360-4366.

Pietrella, D., Corbucci, C., Perito, S., Bistoni, G. and Vecchiarelli, A. (2005). Mannoproteins from Cryptococcus neoformans promote dendritic cell maturation and activation. *Infect Immun* **73,** 820-827.

Portnoy, D.A., Auerbuch, V. and Glomski, I.J. (2002). The cell biology of Listeria monocytogenes infection: the intersection of bacterial pathogenesis and cell-mediated immunity. *J Cell Biol* **158,** 409-414.

Powderly, W.G. (1992). Therapy for cryptococcal meningitis in patients with AIDS. *Clin Infect Dis* **14 Suppl 1,** S54-59.

Powderly, W.G., Cloud, G.A., Dismukes, W.E. and Saag, M.S. (1994). Measurement of cryptococcal antigen in serum and cerebrospinal fluid: value in the management of AIDS-associated cryptococcal meningitis. *Clin Infect Dis* **18,** 789-792.

Price, M.S., Nichols, C.B. and Alspaugh, J.A. (2008). The Cryptococcus neoformans Rho-GDP dissociation inhibitor mediates intracellular survival and virulence. *Infect Immun* **76,** 5729-5737.

Rachini, A., Pietrella, D., Lupo, P., Torosantucci, A., Chiani, P., Bromuro, C.*, et al.* (2007). An anti-beta-glucan monoclonal antibody inhibits growth and capsule formation of Cryptococcus neoformans in vitro and exerts therapeutic, anticryptococcal activity in vivo. *Infect Immun* **75,** 5085-5094.

Radisky, D.C., Snyder, W.B., Emr, S.D. and Kaplan, J. (1997). Characterization of VPS41, a gene required for vacuolar trafficking and high-affinity iron transport in yeast. *Proc Natl Acad Sci U S A* **94,** 5662-5666.

Ralph, P., Prichard, J. and Cohn, M. (1975). Reticulum cell sarcoma: an effector cell in antibody-dependent cell-mediated immunity. *J Immunol* **114,** 898-905.

Rawson, R.B. (2003). The SREBP pathway--insights from Insigs and insects. *Nat Rev Mol Cell Biol* **4,** 631-640.

Reardon, C.C., Kim, S.J., Wagner, R.P. and Kornfeld, H. (1996). Interferon-gamma reduces the capacity of human alveolar macrophages to inhibit growth of Cryptococcus neoformans in vitro. *Am J Respir Cell Mol Biol* **15,** 711-715.

Rhodes, J.C. (1985). Contribution of complement component C5 to the pathogenesis of experimental murine cryptococcosis. *Sabouraudia* **23,** 225-234.

Rhodes, J.C., Wicker, L.S. and Urba, W.J. (1980). Genetic control of susceptibility to Cryptococcus neoformans in mice. *Infect Immun* **29,** 494-499.

Rittershaus, P.C., Kechichian, T.B., Allegood, J.C., Merrill, A.H., Jr., Hennig, M., Luberto, C. and Del Poeta, M. (2006). Glucosylceramide synthase is an essential regulator of pathogenicity of Cryptococcus neoformans. *J Clin Invest* **116,** 1651-1659.

Robbins, J.R., Barth, A.I., Marquis, H., de Hostos, E.L., Nelson, W.J. and Theriot, J.A. (1999). Listeria monocytogenes exploits normal host cell processes to spread from cell to cell. *J Cell Biol* **146,** 1333-1350.

Roilides, E., Dimitriadou-Georgiadou, A., Sein, T., Kadiltsoglou, I. and Walsh, T.J. (1998). Tumor necrosis factor alpha enhances antifungal activities of polymorphonuclear and mononuclear phagocytes against Aspergillus fumigatus. *Infect Immun* **66,** 5999-6003.

Rossier, M.F. (2006). T channels and steroid biosynthesis: in search of a link with mitochondria. *Cell Calcium* **40,** 155-164.

Ruma, P., Chen, S.C., Sorrell, T.C. and Brownlee, A.G. (1996). Characterization of Cryptococcus neoformans by random DNA amplification. *Lett Appl Microbiol* **23,** 312-316.

Sahu, A., Kozel, T.R. and Pangburn, M.K. (1994). Specificity of the thioester-containing reactive site of human C3 and its significance to complement activation. *Biochem J* **302 (Pt 2),** 429-436.

Saldanha, R., Mohr, G., Belfort, M. and Lambowitz, A.M. (1993). Group I and group II introns. *FASEB J* **7,** 15-24.

Santangelo, R., Zoellner, H., Sorrell, T., Wilson, C., Donald, C., Djordjevic, J.*, et al.* (2004). Role of extracellular phospholipases and mononuclear phagocytes in dissemination of cryptococcosis in a murine model. *Infect Immun* **72,** 2229-2239.

Savoy, A.C., Lupan, D.M., Manalo, P.B., Roberts, J.S., Schlageter, A.M., Weinhold, L.C. and Kozel, T.R. (1997). Acute lethal toxicity following passive immunization for treatment of murine cryptococcosis. *Infect Immun* **65,** 1800-1807.

Schaechter, M., Bozeman, F.M. and Smadel, J.E. (1957). Study on the growth of Rickettsiae. II. Morphologic observations of living Rickettsiae in tissue culture cells. *Virology* **3,** 160-172.

Schmiel, D.H. and Miller, V.L. (1999). Bacterial phospholipases and pathogenesis. *Microbes Infect* **1,** 1103-1112.

Sesaki, H. and Jensen, R.E. (1999). Division versus fusion: Dnm1p and Fzo1p antagonistically regulate mitochondrial shape. *J Cell Biol* **147,** 699-706.

Sesaki, H., Southard, S.M., Yaffe, M.P. and Jensen, R.E. (2003). Mgm1p, a dynamin-related GTPase, is essential for fusion of the mitochondrial outer membrane. *Mol Biol Cell* **14,** 2342-2356.

Shaner, N.C., Steinbach, P.A. and Tsien, R.Y. (2005). A guide to choosing fluorescent proteins. *Nat Methods* **2,** 905-909.

Shao, X., Mednick, A., Alvarez, M., van Rooijen, N., Casadevall, A. and Goldman, D.L. (2005). An innate immune system cell is a major determinant of species-related susceptibility differences to fungal pneumonia. *J Immunol* **175,** 3244-3251.

Shapiro, S., Beenhouwer, D.O., Feldmesser, M., Taborda, C., Carroll, M.C., Casadevall, A. and Scharff, M.D. (2002). Immunoglobulin G monoclonal antibodies to Cryptococcus neoformans protect mice deficient in complement component C3. *Infect Immun* **70,** 2598-2604.

Shea, J.M., Kechichian, T.B., Luberto, C. and Del Poeta, M. (2006). The cryptococcal enzyme inositol phosphosphingolipid-phospholipase C confers resistance to the antifungal effects of macrophages and promotes fungal dissemination to the central nervous system. *Infect Immun* **74,** 5977-5988.

Shi, M., Li, S.S., Zheng, C., Jones, G.J., Kim, K.S., Zhou, H.*, et al.* (2010). Real-time imaging of trapping and urease-dependent transmigration of Cryptococcus neoformans in mouse brain. *J Clin Invest* **120,** 1683-1693.

Shoham, S., Huang, C., Chen, J.M., Golenbock, D.T. and Levitz, S.M. (2001). Toll-like receptor 4 mediates intracellular signaling without TNF-alpha release in response to Cryptococcus neoformans polysaccharide capsule. *J Immunol* **166,** 4620-4626.

Shoham, S. and Levitz, S.M. (2005). The immune response to fungal infections. *Br J Haematol* **129,** 569-582.

Siddiqui, A.A., Brouwer, A.E., Wuthiekanun, V., Jaffar, S., Shattock, R., Irving, D.*, et al.* (2005). IFN-gamma at the site of infection determines rate of clearance of infection in cryptococcal meningitis. *J Immunol* **174,** 1746-1750.

Sigler, K. and Hofer, M. (1991). Activation of the plasma membrane H(+)-ATPase of Saccharomyces cerevisiae by addition of hydrogen peroxide. *Biochem Int* **23,** 861-873.

Singh, N., Alexander, B.D., Lortholary, O., Dromer, F., Gupta, K.L., John, G.T.*, et al.* (2008). Pulmonary cryptococcosis in solid organ transplant recipients: clinical relevance of serum cryptococcal antigen. *Clin Infect Dis* **46,** e12-18.

Sionov, E., Chang, Y.C., Garraffo, H.M. and Kwon-Chung, K.J. (2009). Heteroresistance to fluconazole in Cryptococcus neoformans is intrinsic and associated with virulence. *Antimicrob Agents Chemother* **53,** 2804-2815.

Sorrell, T.C. (2001). Cryptococcus neoformans variety gattii. *Med Mycol* **39,** 155-168.

Sorrell, T.C. and Ellis, D.H. (1997). Ecology of Cryptococcus neoformans. *Rev Iberoam Micol* **14,** 42-43.

Soteropoulos, P., Vaz, T., Santangelo, R., Paderu, P., Huang, D.Y., Tamas, M.J. and Perlin, D.S. (2000). Molecular characterization of the plasma membrane H(+)-ATPase, an antifungal target in Cryptococcus neoformans. *Antimicrob Agents Chemother* **44,** 2349-2355.

Southwick, F.S. and Purich, D.L. (1996). Intracellular pathogenesis of listeriosis. *N Engl J Med* **334,** 770-776.

Stadler, N., Hofer, M. and Sigler, K. (2001). Mechanisms of Saccharomyces cerevisiae PMA1 H+-ATPase inactivation by Fe2+, H2O2 and Fenton reagents. *Free Radic Res* **35,** 643-653.

Stano, P., Williams, V., Villani, M., Cymbalyuk, E.S., Qureshi, A., Huang, Y.*, et al.* (2009). App1: an antiphagocytic protein that binds to complement receptors 3 and 2. *J Immunol* **182,** 84-91.

Steenbergen, J.N., Nosanchuk, J.D., Malliaris, S.D. and Casadevall, A. (2003). Cryptococcus neoformans virulence is enhanced after growth in the

genetically malleable host Dictyostelium discoideum. *Infect Immun* **71,** 4862-4872.

Steenbergen, J.N., Shuman, H.A. and Casadevall, A. (2001). Cryptococcus neoformans interactions with amoebae suggest an explanation for its virulence and intracellular pathogenic strategy in macrophages. *Proc Natl Acad Sci U S A* **98,** 15245-15250.

Stephen, C., Lester, S., Black, W., Fyfe, M. and Raverty, S. (2002). Multispecies outbreak of cryptococcosis on southern Vancouver Island, British Columbia. *Can Vet J* **43,** 792-794.

Stevens, J.M., Galyov, E.E. and Stevens, M.P. (2006). Actin-dependent movement of bacterial pathogens. *Nat Rev Microbiol* **4,** 91-101.

Strasser, J.E., Newman, S.L., Ciraolo, G.M., Morris, R.E., Howell, M.L. and Dean, G.E. (1999). Regulation of the macrophage vacuolar ATPase and phagosome-lysosome fusion by Histoplasma capsulatum. *J Immunol* **162,** 6148-6154.

Sturgill-Koszycki, S., Schlesinger, P.H., Chakraborty, P., Haddix, P.L., Collins, H.L., Fok, A.K.*, et al.* (1994). Lack of acidification in Mycobacterium phagosomes produced by exclusion of the vesicular proton-ATPase. *Science* **263,** 678-681.

Sullivan, D., Haynes, K., Moran, G., Shanley, D. and Coleman, D. (1996). Persistence, replacement, and microevolution of Cryptococcus neoformans strains in recurrent meningitis in AIDS patients. *J Clin Microbiol* **34,** 1739-1744.

Supek, F., Supekova, L., Nelson, H. and Nelson, N. (1996). A yeast manganese transporter related to the macrophage protein involved in conferring resistance to mycobacteria. *Proc Natl Acad Sci U S A* **93,** 5105-5110.

Swenson, F.J. and Kozel, T.R. (1978). Phagocytosis of Cryptococcus neoformans by normal and thioglycolate-activated macrophages. *Infect Immun* **21,** 714-720.

Syme, R.M., Spurrell, J.C., Amankwah, E.K., Green, F.H. and Mody, C.H. (2002). Primary dendritic cells phagocytose Cryptococcus neoformans via mannose receptors and Fcgamma receptor II for presentation to T lymphocytes. *Infect Immun* **70,** 5972-5981.

Szilagyi, G., Reiss, F. and Smith, J.C. (1966). The anticryptococcal factor of blood serum. A preliminary report. *J Invest Dermatol* **46,** 306-308.

Taborda, C.P. and Casadevall, A. (2001). Immunoglobulin M efficacy against Cryptococcus neoformans: mechanism, dose dependence, and prozone-like effects in passive protection experiments. *J Immunol* **166,** 2100-2107.

Taborda, C.P. and Casadevall, A. (2002). CR3 (CD11b/CD18) and CR4 (CD11c/CD18) are involved in complement-independent antibody-mediated phagocytosis of Cryptococcus neoformans. *Immunity* **16,** 791-802.

Tacker, J.R., Farhi, F. and Bulmer, G.S. (1972). Intracellular fate of Cryptococcus neoformans. *Infect Immun* **6,** 162-167.

Toffaletti, D.L., Del Poeta, M., Rude, T.H., Dietrich, F. and Perfect, J.R. (2003). Regulation of cytochrome c oxidase subunit 1 (COX1) expression in Cryptococcus neoformans by temperature and host environment. *Microbiology* **149,** 1041-1049.

Toffaletti, D.L., Nielsen, K., Dietrich, F., Heitman, J. and Perfect, J.R. (2004). Cryptococcus neoformans mitochondrial genomes from serotype A and D strains do not influence virulence. *Curr Genet* **46,** 193-204.

Toffaletti, D.L., Rude, T.H., Johnston, S.A., Durack, D.T. and Perfect, J.R. (1993). Gene transfer in Cryptococcus neoformans by use of biolistic delivery of DNA. *J Bacteriol* **175,** 1405-1411.

Torres, M. and Casadevall, A. (2008). The immunoglobulin constant region contributes to affinity and specificity. *Trends Immunol* **29,** 91-97.

Torres, M., Fernandez-Fuentes, N., Fiser, A. and Casadevall, A. (2007). Exchanging murine and human immunoglobulin constant chains affects the kinetics and thermodynamics of antigen binding and chimeric antibody autoreactivity. *PLoS ONE* **2,** e1310.

Truelsen, K., Young, T. and Kozel, T.R. (1992). In vivo complement activation and binding of C3 to encapsulated Cryptococcus neoformans. *Infect Immun* **60,** 3937-3939.

Tucker, S.C. and Casadevall, A. (2002). Replication of Cryptococcus neoformans in macrophages is accompanied by phagosomal permeabilization and accumulation of vesicles containing polysaccharide in the cytoplasm. *Proc Natl Acad Sci U S A* **99,** 3165-3170.

Tuxworth, R.I., Weber, I., Wessels, D., Addicks, G.C., Soll, D.R., Gerisch, G. and Titus, M.A. (2001). A role for myosin VII in dynamic cell adhesion. *Curr Biol* **11,** 318-329.

Uezu, K., Kawakami, K., Miyagi, K., Kinjo, Y., Kinjo, T., Ishikawa, H. and Saito, A. (2004). Accumulation of gammadelta T cells in the lungs and their regulatory roles in Th1 response and host defense against pulmonary infection with Cryptococcus neoformans. *J Immunol* **172,** 7629-7634.

Vallim, M.A., Nichols, C.B., Fernandes, L., Cramer, K.L. and Alspaugh, J.A. (2005). A Rac homolog functions downstream of Ras1 to control hyphal differentiation and high-temperature growth in the pathogenic fungus Cryptococcus neoformans. *Eukaryot Cell* **4,** 1066-1078.

Varma, A., Edman, J.C. and Kwon-Chung, K.J. (1992a). Molecular and genetic analysis of URA5 transformants of Cryptococcus neoformans. *Infect Immun* **60,** 1101-1108.

Varma, A. and Kwon-Chung, K.J. (1992b). DNA probe for strain typing of Cryptococcus neoformans. *J Clin Microbiol* **30,** 2960-2967.

Varma, A. and Kwon-Chung, K.J. (2010). Heteroresistance of Cryptococcus gattii to fluconazole. *Antimicrob Agents Chemother* **54,** 2303-2311.

Vecchiarelli, A., Pietrella, D., Lupo, P., Bistoni, F., McFadden, D.C. and Casadevall, A. (2003). The polysaccharide capsule of Cryptococcus neoformans interferes with human dendritic cell maturation and activation. *J Leukoc Biol* **74,** 370-378.

Velagapudi, R., Hsueh, Y.P., Geunes-Boyer, S., Wright, J.R. and Heitman, J. (2009). Spores as infectious propagules of Cryptococcus neoformans. *Infect Immun* **77,** 4345-4355.

Vermes, A., Guchelaar, H.J. and Dankert, J. (2000). Flucytosine: a review of its pharmacology, clinical indications, pharmacokinetics, toxicity and drug interactions. *J Antimicrob Chemother* **46,** 171-179.

Voelz, K., Johnston, S.A. and May, R.C. (2010a) Intracellular replication and exit strategies. In *Cryptococcus: from human pathogen to model yeast*, J. Heitman, T.R. Kozel, K.J. Kwon-Chung, J.R. Perfect, A. Casadevall (eds.).

Voelz, K., Lammas, D.A. and May, R.C. (2009). Cytokine signaling regulates the outcome of intracellular macrophage parasitism by Cryptococcus neoformans. *Infect Immun*.

Voelz, K. and May, R.C. (2010b). Cryptococcal interactions with the host immune system. *Eukaryot Cell* **9,** 835-846.

Voskoboinik, I., Smyth, M.J. and Trapani, J.A. (2006). Perforin-mediated target-cell death and immune homeostasis. *Nat Rev Immunol* **6,** 940-952.

Wadhwa, A., Kaur, R. and Bhalla, P. (2008). Profile of central nervous system disease in HIV/AIDS patients with special reference to cryptococcal infections. *Neurologist* **14,** 247-251.

Walker, L. and Lowrie, D.B. (1981). Killing of Mycobacterium microti by immunologically activated macrophages. *Nature* **293,** 69-71.

Wang, Y., Aisen, P. and Casadevall, A. (1995). Cryptococcus neoformans melanin and virulence: mechanism of action. *Infect Immun* **63,** 3131-3136.

Wang, Y. and Casadevall, A. (1994). Susceptibility of melanized and nonmelanized Cryptococcus neoformans to nitrogen- and oxygen-derived oxidants. *Infect Immun* **62,** 3004-3007.

Washburn, R.G., Bryant-Varela, B.J., Julian, N.C. and Bennett, J.E. (1991). Differences in Cryptococcus neoformans capsular polysaccharide structure influence assembly of alternative complement pathway C3 convertase on fungal surfaces. *Mol Immunol* **28,** 465-470.

Waugh, M.S., Vallim, M.A., Heitman, J. and Alspaugh, J.A. (2003). Ras1 controls pheromone expression and response during mating in Cryptococcus neoformans. *Fungal Genet Biol* **38,** 110-121.

Weiss, G., Bogdan, C. and Hentze, M.W. (1997). Pathways for the regulation of macrophage iron metabolism by the anti-inflammatory cytokines IL-4 and IL-13. *J Immunol* **158,** 420-425.

Williamson, P.R. (1997). Laccase and melanin in the pathogenesis of Cryptococcus neoformans. *Front Biosci* **2,** e99-107.

Wiseman, J.C., Ma, L.L., Marr, K.J., Jones, G.J. and Mody, C.H. (2007). Perforin-dependent cryptococcal microbicidal activity in NK cells requires PI3K-dependent ERK1/2 signaling. *J Immunol* **178,** 6456-6464.

Witt, M.D., Lewis, R.J., Larsen, R.A., Milefchik, E.N., Leal, M.A., Haubrich, R.H.*, et al.* (1996). Identification of patients with acute AIDS-associated cryptococcal meningitis who can be effectively treated with fluconazole: the role of antifungal susceptibility testing. *Clin Infect Dis* **22,** 322-328.

Wong, E.D., Wagner, J.A., Gorsich, S.W., McCaffery, J.M., Shaw, J.M. and Nunnari, J. (2000). The dynamin-related GTPase, Mgm1p, is an intermembrane space protein required for maintenance of fusion competent mitochondria. *J Cell Biol* **151,** 341-352.

Wood, S.A., Ammann, R.R., Brock, D.A., Li, L., Spann, T. and Gomer, R.H. (1996). RtoA links initial cell type choice to the cell cycle in Dictyostelium. *Development* **122,** 3677-3685.

Wormley, F.L., Jr., Perfect, J.R., Steele, C. and Cox, G.M. (2007). Protection against cryptococcosis by using a murine gamma interferon-producing Cryptococcus neoformans strain. *Infect Immun* **75,** 1453-1462.

Wozniak, K.L., Vyas, J.M. and Levitz, S.M. (2006). In vivo role of dendritic cells in a murine model of pulmonary cryptococcosis. *Infect Immun* **74,** 3817-3824.

Wright, L.C., Santangelo, R.M., Ganendren, R., Payne, J., Djordjevic, J.T. and Sorrell, T.C. (2007). Cryptococcal lipid metabolism: phospholipase B1 is implicated in transcellular metabolism of macrophage-derived lipids. *Eukaryot Cell* **6,** 37-47.

Xu, J., Ali, R.Y., Gregory, D.A., Amick, D., Lambert, S.E., Yoell, H.J.*, et al.* (2000). Uniparental mitochondrial transmission in sexual crosses in Cryptococcus neoformans. *Curr Microbiol* **40,** 269-273.

Xu, J., Yan, Z. and Guo, H. (2009). Divergence, hybridization, and recombination in the mitochondrial genome of the human pathogenic yeast Cryptococcus gattii. *Mol Ecol* **18,** 2628-2642.

Young, B.J. and Kozel, T.R. (1993). Effects of strain variation, serotype, and structural modification on kinetics for activation and binding of C3 to Cryptococcus neoformans. *Infect Immun* **61,** 2966-2972.

Yuan, R.R., Casadevall, A., Oh, J. and Scharff, M.D. (1997). T cells cooperate with passive antibody to modify Cryptococcus neoformans infection in mice. *Proc Natl Acad Sci U S A* **94,** 2483-2488.

Zaragoza, O., Chrisman, C.J., Castelli, M.V., Frases, S., Cuenca-Estrella, M., Rodriguez-Tudela, J.L. and Casadevall, A. (2008). Capsule enlargement in Cryptococcus neoformans confers resistance to oxidative stress suggesting a mechanism for intracellular survival. *Cell Microbiol* **10,** 2043-2057.

Zaragoza, O., Garcia-Rodas, R., Nosanchuk, J.D., Cuenca-Estrella, M., Rodriguez-Tudela, J.L. and Casadevall, A. (2010). Fungal cell gigantism during mammalian infection. *PLoS Pathog* **6,** e1000945.

Zaragoza, O., Rodrigues, M.L., De Jesus, M., Frases, S., Dadachova, E. and Casadevall, A. (2009). The capsule of the fungal pathogen Cryptococcus neoformans. *Adv Appl Microbiol* **68,** 133-216.

Zaragoza, O., Taborda, C.P. and Casadevall, A. (2003). The efficacy of complement-mediated phagocytosis of Cryptococcus neoformans is dependent on the location of C3 in the polysaccharide capsule and involves both direct and indirect C3-mediated interactions. *Eur J Immunol* **33,** 1957-1967.

Zhang, Y., Wang, F., Tompkins, K.C., McNamara, A., Jain, A.V., Moore, B.B.*, et al.* (2009). Robust Th1 and Th17 immunity supports pulmonary clearance but cannot prevent systemic dissemination of highly virulent Cryptococcus neoformans H99. *Am J Pathol* **175,** 2489-2500.

Zhao, L., Zhang, F., Guo, J., Yang, Y., Li, B. and Zhang, L. (2004). Nitric oxide functions as a signal in salt resistance in the calluses from two ecotypes of reed. *Plant Physiol* **134,** 849-857.

Zheng, C.F., Jones, G.J., Shi, M., Wiseman, J.C., Marr, K.J., Berenger, B.M.*, et al.* (2008). Late expression of granulysin by microbicidal CD4+ T cells requires PI3K- and STAT5-dependent expression of IL-2Rbeta that is defective in HIV-infected patients. *J Immunol* **180,** 7221-7229.

Zheng, C.F., Ma, L.L., Jones, G.J., Gill, M.J., Krensky, A.M., Kubes, P. and Mody, C.H. (2007). Cytotoxic CD4+ T cells use granulysin to kill Cryptococcus neoformans, and activation of this pathway is defective in HIV patients. *Blood* **109,** 2049-2057.

APPENDIX